

BACTERIAL EXTRACELLULAR ENZYME ACTIVITY IN A FUTURE OCEAN

Timothy James Burrell

A thesis

submitted to Victoria University of Wellington
in fulfilment of the requirement for the degree of
Doctor of Philosophy
in Marine Biology

Victoria University of Wellington

Te Whare Wananga o te Upoko o te Ika a Maui

2015

Acknowledgements

I would first like to thank my academic supervisors, Dr Els Maas, Dr Cliff Law and Dr Paul Teesdale-Spittle for their guidance, support and patience throughout this research project.

I would like to thank the Royal Society of New Zealand as the primary funding provider and Els Maas and Cliff Law for securing the funding through a successful Marsden grant, for without this I would not have received this unique opportunity or the international travel that it allowed. I feel very fortunate to have had the opportunity to experience multiple international trips and ocean cruises during my time at NIWA.

I would like to thank the staff at NIWA Wellington, particularly Debbie Hulston for technical assistance in the laboratory. At NIWA Hamilton, I would like to thank Marieke van Kooten, Cara Mackle and Karen Thompson, each of whom were invaluable for assistance in sample analysis both during, and after ocean cruises. At the joint NIWA/University of Otago Research Centre for Oceanography, I would like to thank Dr Kim Currie, for her extensive knowledge involving pH and for analysing my seawater carbonate parameters. At Victoria University of Wellington, I would like to thank Dr Dalice Sim for statistical advice and John Van Der Sman for allowing me access to the Victoria University Coastal Ecology Laboratory.

On a personal level, I thank my friends and fellow students at NIWA, Pablo Escobar, Stefan Jendersie, Kyle Morrison and Aitana Forcen. My immediate family for their genuine interest in my research and unconditional support. I would also like to thank my flatmates Thomas Davey, Lily Davey, Kurt Sole and James Kusel.

Lastly, I would like to make special mention to the Fenn family, especially John Gillen Fenn (3 June 1930 – 26 April 2013) who instilled in me the love of the ocean through many summers in the boat on the bay.

Abstract

Heterotrophic bacteria are recognised as vital components in the cycling and regulation of inorganic and organic matter in the ocean. Research to date indicates that future changes in ocean conditions may influence bacterial extracellular enzyme hydrolysis rates, which could affect the strength of the microbial loop and consequently organic matter export. The aim of this thesis was to examine how changes in ocean acidification and warming predicted to occur by the end of the century will affect extracellular enzyme activities in the near-surface ocean and below the surface mixed layer in the South West Pacific.

A series of small-scale seawater incubations were conducted under three different perturbed conditions: elevated temperature (ambient +3°C), low pH (pCO₂ 750 ppmv; pH_T 7.8) and greenhouse conditions (elevated temperature and low pH), with responses compared to ambient control samples. In particular, the response of protease activity (leucine- and arginine-aminopeptidase) and glucosidase activity (β- and α-glucosidase) were examined, as these enzymes are known to degrade the two major components of organic matter in the ocean, namely proteins and carbohydrates. Bacterial secondary production rates (³H-TdR & ³H-Leu incorporation) were also examined as a proxy for carbon turnover.

To investigate spatial variability, parameter responses from near-surface open ocean seawater consisting of different phytoplankton communities were compared with coastal seawater, as well as seawater collected from below the surface mixed layer. To determine temporal variability, both direct and indirect parameter responses were investigated. Finally, responses were determined from a shallow CO₂ vent that provided a natural low pH environment in coastal waters north of New Zealand. By comparing responses derived from vent water and artificially low pH water, vent plumes were also investigated for their utility as proxies for future low pH environments.

Incubation results showed that protease activity increased in response to low pH conditions in each seawater environment tested. However, near-surface open ocean incubations showed variability in the response of protease and glucosidase activity and bacterial cell numbers between different phytoplankton communities and treatments, suggesting that parameter responses were determined by direct and indirect effects. Elevated temperature had an overall positive effect on bacterial secondary production rates between different phytoplankton

communities in the near-surface open ocean. Surprisingly, although elevated temperature and low pH treatments showed independent effects, no clear additive or synergistic effect was detected in any parameter under greenhouse conditions. In contrast to the near-surface ocean, greenhouse conditions had an additive effect on protease activity in seawater collected from below the surface mixed layer (100 m depth). Bacterial secondary production rates and bacterial numbers varied in response to elevated temperature in the subsurface ocean, while bacterial secondary production rates declined under greenhouse conditions. Glucosidase and protease activities were highest in the coastal seawater, with both enzymes responding positively to low pH conditions. Coastal seawater also contained the highest bacterial secondary production rates and bacterial cell numbers, however these parameters were not significantly affected by low pH conditions. Variation in the direct response of enzyme activity to low pH between ocean environments could indicate the synthesis of different extracellular enzymes by surface and subsurface bacteria. Importantly, results from a naturally low pH vent plume indicated that pH was not the only factor influencing the response of extracellular enzymes. Other influential factors could include high concentrations of dissolved nutrients and trace metal ions. Natural low pH vents off Whale Island in the Bay of Plenty were determined not suitable as proxies for future low pH environments based on vent variability and differences in seawater biogeochemistry when compared to the ambient ocean.

Overall, the incubation results show that under conditions predicted for the end of the century, protease activity will increase in open ocean and coastal waters which could accelerate and strengthen the heterotrophic microbial loop. Bacterial secondary production rates are expected to vary in the near-surface ocean, but decline in the subsurface. The resulting increase in surface ocean protease activity could increase heterotrophic metabolic respiration and reduce organic matter export, weaken the biological carbon pump and diminish long-term carbon sequestration. An increased turnover of proteins and amino acids in each environment tested could lead to nitrogen limitation and contribute to an expansion of oligotrophic waters. This future scenario may create a positive inorganic carbon feedback that would further exacerbate acidification of the surface ocean.

Table of Contents

Abstract.....	1
Table of Contents.....	3
List of Figures.....	7
List of Tables.....	12
Abbreviations.....	14
Chapter 1 : General Introduction.....	16
1.1 The world's changing oceans.....	16
1.2 The ocean carbonate system.....	17
1.3 Marine organic matter	20
1.4 Marine carbon cycle and microbial loop.....	24
1.5 Heterotrophic bacteria	27
1.6 Catabolic hydrolysing enzymes	29
1.7 Temperature and pH.....	32
1.8 Research aims.....	34
Chapter 2 : Analytical methods.....	36
2.1 Incubation set up	36
2.2 Incubation sampling protocol.....	42
2.3 Extracellular enzyme activity.....	42
2.4 Bacterial secondary production.....	44
2.5 Cell numbers	46
2.6 Total high molecular weight organic compound concentration.....	46
2.7 Dissolved organic carbon	48
2.8 Chlorophyll <i>a</i> and dissolved nutrients.....	48
2.9 Transparent exopolymer polysaccharides and total carbohydrates.....	49
2.10 Dissolved inorganic carbon and alkalinity	50
2.11 Data analysis	51
Chapter 3 : Methodology optimisation.....	53
3.1 Enzyme assay refinement.....	53
3.1.1 The effect of pH on artificial fluorophore fluorescence	54

3.1.2	The effect of artificial fluorogenic substrate on the pH of seawater.....	55
3.1.3	Fluorescent substrate buffer solution	57
3.1.4	Discussion	60
3.2	Short-term acidification trial	61
3.2.1	Introduction.....	61
3.2.2	Methods.....	62
3.2.3	Results.....	62
3.2.4	Discussion	64
3.3	Seawater acidification methodology	66
3.3.1	Introduction.....	66
3.3.2	Methods.....	68
3.3.3	Results.....	69
3.3.4	Discussion	83
Chapter 4 : The response of enzyme activity to elevated temperature and low pH in near-surface open ocean phytoplankton blooms.....		87
4.1	Introduction	87
4.2	Methods.....	90
4.3	Results	93
4.3.1	Extracellular enzyme activity	95
4.3.2	Cell numbers	109
4.3.3	Bacterial secondary production.....	118
4.3.4	Chlorophyll <i>a</i> concentration	123
4.3.5	Dissolved nutrient concentration	125
4.3.6	Dissolved organic carbon concentration.....	131
4.3.7	Total high molecular weight organic compound concentration	132
4.3.8	Multivariate data analysis	138
4.4	Discussion	142
4.4.1	Effect of low pH.....	143
4.4.2	Effect of elevated temperature	156
4.4.3	Effect of elevated temperature and low pH	161
4.5	Summary	166

Chapter 5 : The response of enzyme activity to elevated temperature and low pH in open ocean subsurface waters167

5.1	Introduction	167
5.2	Methods.....	171
5.3	Results	174
5.3.1	Extracellular enzyme activity	175
5.3.2	Cell numbers	181
5.3.3	Bacterial secondary production.....	184
5.3.4	Chlorophyll <i>a</i> concentration	188
5.3.5	Dissolved nutrient concentration	189
5.3.6	Dissolved organic carbon concentration	191
5.3.7	Total high molecular weight organic compound concentration	192
5.3.8	Multivariate data analysis	194
5.4	Discussion	197
5.4.1	The response of extracellular enzymes in subsurface waters	197
5.4.2	Relationship between bacterial secondary production and bacterial cell numbers	201
5.4.3	Relationship between nutrients and phytoplankton	203
5.5	Summary	204

Chapter 6 : Enzyme activity in a natural low pH marine system206

6.1	Introduction	206
6.2	Methods.....	209
6.3	Results	214
6.3.1	Extracellular enzyme activity	216
6.3.2	Cell numbers	223
6.3.3	Bacterial secondary production.....	228
6.3.4	Dissolved nutrient concentration	231
6.3.5	Dissolved organic carbon concentration	235
6.3.6	Total high molecular weight organic compound concentration	235
6.3.7	TEP & TC	238
6.3.8	Multivariate data analysis	240
6.4	Discussion	243

6.4.1	Coastal water response to low pH.....	243
6.4.2	Vent seawater response.....	250
6.5	Summary	254
Chapter 7 :	Concluding discussion	255
7.1	Influence of low pH.....	255
7.2	Influence of elevated temperature	258
7.3	Influence of low pH and elevated temperature combined.....	260
7.4	Final statement and future research recommendations	264
	Bibliography	266
	Appendix A: Supplementary material	294
	Appendix B: Chapter 3 seawater acidification methodology statistical summary tables....	300
	Appendix C: Chapter 4 sampled parameter statistical summary tables.....	310
	Appendix D: Chapter 5 sampled parameter statistical summary tables	318
	Appendix E: Chapter 6 sampled parameter statistical summary tables	321

List of Figures

Chapter 1

Fig. 1.1.	Partial pressure of dissolved CO ₂ at the ocean surface and <i>in situ</i> pH.....	16
Fig. 1.2.	Organic carbon categorised based on molecular weight	22
Fig. 1.3.	A conceptual diagram of carbon flow in the surface ocean	24

Chapter 2

Fig. 2.1.	Incubation treatment design.....	37
Fig. 2.2.	Custom made nylon screw-cap and valve	37
Fig. 2.3.	Automated pH spectrophotometer.....	39
Fig. 2.4.	External view of an incubation chamber.....	40
Fig. 2.5.	Internal view of an incubation chamber.....	41

Chapter 3

Fig. 3.1.	The effect of pH on MUF and MCA fluorophore fluorescence	55
Fig. 3.2.	pH immediately following and 30 mins after artificial substrate addition	57
Fig. 3.3.	Sample pH following the addition of pH 8.1 Tris/Leu-MCA substrate solution...58	
Fig. 3.4.	Sample pH following the addition of pH 8.1 Tris/Arg-MCA substrate solution. .59	
Fig. 3.5.	Sample pH following the addition of pH 7.8 Tris/Leu-MCA substrate solution. .59	
Fig. 3.6.	Sample pH following the addition of pH 7.8 Tris/Arg-MCA substrate solution...60	
Fig. 3.7.	The direct influence of pH on extracellular enzyme activity	63
Fig. 3.8.	Extracellular enzyme activity throughout trial 1	71
Fig. 3.9.	Cell-specific extracellular enzyme activity throughout trial 1	72
Fig. 3.10.	Extracellular enzyme activity throughout trial 2	74
Fig. 3.11.	Cell-specific extracellular enzyme activity throughout trial 2.....	75
Fig. 3.12.	Bacteria, <i>Synechococcus</i> spp. and total eukaryotic phytoplankton cell numbers throughout trial 1.....	76
Fig. 3.13.	Bacteria, <i>Synechococcus</i> spp. and total eukaryotic phytoplankton cell numbers throughout trial 2.....	77
Fig. 3.14.	BSP throughout trial 1.....	78
Fig. 3.15.	BSP throughout trial 2	79

Fig. 3.16. DIC concentrations per treatment at 24 h and 96 h during trial 1	80
Fig. 3.17. DIC concentrations per treatment at 24 h and 96 h during trial 2	81

Chapter 4

Fig. 4.1. Bulk seawater collection sites for incubation 1 to 4.....	90
Fig. 4.2. Average time-zero phytoplankton composition determined by microscopy from three blooms used in incubations 1, 2 and 3.	93
Fig. 4.3. Extracellular enzyme activities throughout incubation 1	96
Fig. 4.4. Cell-specific extracellular enzyme activities throughout incubation 1	97
Fig. 4.5. Extracellular enzyme activities throughout incubation 2	98
Fig. 4.6. Cell-specific extracellular enzyme activities throughout incubation 2	99
Fig. 4.7. Extracellular enzyme activities throughout incubation 3	101
Fig. 4.8. Cell-specific extracellular enzyme activities throughout incubation 3	102
Fig. 4.9. Extracellular enzyme activities throughout incubation 4	104
Fig. 4.10. Cell-specific extracellular enzyme activities throughout incubation 4	106
Fig. 4.11. Bacterial cell numbers in incubation 1	109
Fig. 4.12. <i>Synechococcus</i> spp., <i>Prochlorococcus</i> spp. and total eukaryotic phytoplankton cell numbers in incubation 1	110
Fig. 4.13. Bacterial cell numbers in incubation 2	111
Fig. 4.14. <i>Synechococcus</i> spp., <i>Prochlorococcus</i> spp. and total eukaryotic phytoplankton cell numbers in incubation 2.....	112
Fig. 4.15. Bacterial cell numbers in incubation 3	113
Fig. 4.16. <i>Synechococcus</i> spp., <i>Prochlorococcus</i> spp. and total eukaryotic phytoplankton cell numbers in incubation 3.....	114
Fig. 4.17. Bacterial cell numbers in incubation 4	115
Fig. 4.18. <i>Synechococcus</i> spp., <i>Prochlorococcus</i> spp. and total eukaryotic phytoplankton cell numbers in incubation 4.....	116
Fig. 4.19. BSP throughout incubation 1	118
Fig. 4.20. BSP throughout incubation 2.....	119
Fig. 4.21. BSP throughout incubation 3.....	120
Fig. 4.22. BSP throughout incubation 4.....	121
Fig. 4.23. Chl <i>a</i> concentrations throughout incubation 1.....	123

Fig. 4.24. Chl <i>a</i> concentrations throughout incubation 4.....	124
Fig. 4.25. Dissolved nutrient concentrations throughout incubation 1	126
Fig. 4.26. Dissolved ammonium concentrations throughout incubation 2	127
Fig. 4.27. Dissolved nutrient concentrations throughout incubation 3	128
Fig. 4.28. DOC concentrations at the beginning and the end of incubation 1	131
Fig. 4.29. DOC concentrations at the beginning and the end of incubation 4	132
Fig. 4.30. Total HMW organic compound concentrations throughout incubation 1	133
Fig. 4.31. Total HMW organic compound concentrations throughout incubation 2	134
Fig. 4.32. Total HMW organic compound concentrations throughout incubation 3	135
Fig. 4.33. Total HMW organic compound concentrations throughout incubation 4	136
Fig. 4.34. MDS plot of sampled parameters collected during incubation 1.	138
Fig. 4.35. MDS plot of sampled parameters collected during incubation 2	139
Fig. 4.36. MDS plot of sampled parameters collected during incubation 3	141
Fig. 4.37. MDS plot of sampled parameters collected during incubation 4	142
Fig. 4.38. Temporal development of selected parameters in the OA treatment in each incubation	147

Chapter 5

Fig. 5.1. Circles mark the location of bulk seawater collection sites in an eddy east of New Zealand.....	171
Fig. 5.2. Extracellular enzyme activities throughout incubation 6	176
Fig. 5.3. Cell-specific extracellular enzyme activities throughout incubation 6	177
Fig. 5.4. Extracellular enzyme activities throughout incubation 7	178
Fig. 5.5. Cell-specific extracellular enzyme activities throughout incubation 7	179
Fig. 5.6. Bacterial cell numbers throughout incubation 6.....	181
Fig. 5.7 <i>Synechococcus</i> spp. and total eukaryotic phytoplankton cell numbers throughout incubation 6.....	182
Fig. 5.8. Bacterial cell numbers throughout incubation 7.....	183
Fig. 5.9. <i>Synechococcus</i> spp. and total eukaryotic phytoplankton cell numbers throughout incubation 7.....	183
Fig. 5.10. BSP throughout incubation 6.....	185
Fig. 5.11. Cell-specific protein synthesis throughout incubation 6	186

Fig. 5.12. BSP throughout incubation 7	187
Fig. 5.13. Chl <i>a</i> concentrations at the beginning and the end of incubation 6.....	188
Fig. 5.14. Dissolved nutrient concentrations at the beginning and the end of incubation 6..	189
Fig. 5.15. Dissolved nutrient concentrations at the beginning and the end of incubation 7 ..	190
Fig. 5.16. DOC concentrations at time-zero and 96 h during incubation 6	192
Fig. 5.17. Total HMW reducing-sugar concentrations throughout incubation 7	193
Fig. 5.18. MDS plot of sampled parameters collected during incubation 6	195
Fig. 5.19. MDS plot of sampled parameters collected during incubation 7	196

Chapter 6

Fig. 6.1. Echogram of the Whale Island vent showing plumes of bubbles.....	209
Fig. 6.2. Incubations 8 and 9 bulk seawater collection sites.....	210
Fig. 6.3. Experimental design	211
Fig. 6.4. Experimental set-up in the temperature controlled container.....	212
Fig. 6.5. Extracellular enzyme activities in incubation 8.....	217
Fig. 6.6. Cell-specific extracellular enzyme activities in incubation 8.....	218
Fig. 6.7. Extracellular enzyme activities in incubation 9.....	220
Fig. 6.8. Cell-specific extracellular enzyme activities in incubation 9.....	221
Fig. 6.9. Bacteria, <i>Synechococcus</i> spp., <i>Prochlorococcus</i> spp. and total eukaryotic phytoplankton cell numbers in incubation 8.....	224
Fig. 6.10. Bacteria, <i>Synechococcus</i> spp., <i>Prochlorococcus</i> spp. and total eukaryotic phytoplankton cell numbers in incubation 9	226
Fig. 6.11. BSP throughout incubation 8.....	228
Fig. 6.12. Cell-specific protein synthesis throughout incubation 8	229
Fig. 6.13. BSP throughout incubation 9.....	230
Fig. 6.14. Cell-specific protein synthesis throughout incubation 9	230
Fig. 6.15. Total HMW organic compound concentrations throughout incubation 8.....	236
Fig. 6.16. Total HMW organic compound concentrations throughout incubation 9.....	237
Fig. 6.17. TEP and TC concentrations throughout incubation 8	238
Fig. 6.18. TEP and TC concentrations throughout incubation 9	239
Fig. 6.19. MDS plot of sampled parameters collected during incubation 8	241
Fig. 6.20. MDS plot of sampled parameters collected during incubation 9	242

Chapter 7

Fig. 7.1. Conceptual diagram of bacterial mediated biological processes in the near-surface and subsurface open ocean under elevated temperature and low pH conditions predicted for the end of the century262

List of Tables

Chapter 3

Table 3.1. Parameter sampling protocol, showing the total number of times a parameter was sampled and its respective sampling frequency	69
Table 3.2. Summary of each parameter response when compared to the ambient control.....	82

Chapter 4

Table 4.1. Parameter sampling protocol for incubations 1 to 4	92
Table 4.2. Average time-zero data for each sampled parameter per incubations	94
Table 4.3. The Leu-aminopeptidase:β-glucosidase activity ratio integrated to 144 h and Leu-aminopeptidase Δ hydrolysis potential integrated to 72 h for each incubation	108
Table 4.4. Summary of extracellular enzyme activity changes in each treatment when compared to the ambient control.....	109
Table 4.5. Summary of cell number changes in each treatment when compared to the ambient control.....	118
Table 4.6. Summary of the DNA and protein synthesis rate responses to treatments compared to the ambient control.....	123
Table 4.7. Summary of dissolved nutrient concentration changes in each treatment when compared to the ambient control.....	131
Table 4.8. Summary of total HMW organic compound concentration changes in each treatment when compared to the ambient control.....	138
Table 4.9. Summary of each parameter response from incubations 1 to 4 when compared to the ambient control.....	149

Chapter 5

Table 5.1. Parameter sampling protocol for incubations 5 to 7	173
Table 5.2. Average time-zero data for each sampled parameter per incubation.....	174
Table 5.3. Summary of extracellular enzyme activity changes in each treatment when compared to the ambient control	180
Table 5.4. Summary of cell number changes in each treatments when compared to the ambient control	184

Table 5.5. Summary of the DNA and protein synthesis rate responses to treatments compared to the ambient control	187
Table 5.6. Summary of dissolved nutrient concentration changes in each treatment when compared to the ambient control at 96 h only.....	191
Table 5.7. Summary of total HMW organic compound concentration changes in each treatment when compared to the ambient control.....	195
Table 5.8. Summary of each parameter response from incubations 6 and 7 when compared to the ambient control.....	199

Chapter 6

Table 6.1. Parameter sampling protocol for incubations 8 and 9	213
Table 6.2. Average time-zero value for each parameter per treatment for both incubations 8 and 9.....	215
Table 6.3. Summary of extracellular enzyme activity changes in each treatment relative to the ambient control over 84 h	222
Table 6.4. Summary of cell number changes in each treatment relative to the ambient control over 84 h	227
Table 6.5. Summary of DNA and protein synthesis rate changes in each treatment relative to the ambient control over 84 h.	231
Table 6.6. Average dissolved nutrient concentrations in each treatment at time-zero and 84 h in incubation 8.....	232
Table 6.7. Average dissolved nutrient concentrations in each treatment at time-zero and 84 h in incubation 9.....	234
Table 6.8. Summary of total HMW organic compound concentration changes in each treatment relative to the ambient control over 84 h.	237
Table 6.9. Summary of TEP concentration changes in each treatment relative to the ambient control over 84 h.....	241
Table 6.10. Summary of each parameter response from incubations 8 and 9 relative to the ambient control over 84 h.....	245

Abbreviations

α -MUF - 4-Methylumbelliferyl α -D-glucopyranoside

Arg-MCA - L-Arginine-7-amido-4-methylcoumarin hydrochloride

β -MUF - 4-Methylumbelliferyl β -D-glucopyranoside

Chl *a* – Chlorophyll *a*

DIC - Dissolved Inorganic Carbon

DOM - Dissolved Organic Matter

DOC - Dissolved Organic Carbon

DON - Dissolved Organic Nitrogen

DRSi - Dissolved Reactive Silica

DRP - Dissolved Reactive Phosphorus

EPOCA - European Project on Ocean Acidification

GH - Greenhouse

h - Hours

HMW – High Molecular Weight

^3H -TdR - ^3H -thymidine

^3H -Leu - ^3H -leucine

HT - High Temperature

IGBP - International Geosphere-Biosphere Programme

IOC - Intergovernmental Oceanographic Commission

IPCC - Intergovernmental Panel on Climate Change

LDPE – Low-Density Polyethylene

Leu-MCA - L-Leucine-7-amido-4-methylcoumarin hydrochloride

LMW – Low Molecular Weight

MCA - 7-amino-4-methylcoumarin

min - Minutes

MUF - 4-methylumbeliferone

NIWA – National Institute of Water & Atmospheric Research Ltd

OA - Ocean Acidification

PAR – Photosynthetic Active Radiation

POC - Particulate Organic Carbon

POM - Particulate Organic Matter

RCP 8.5 - Representative Concentration Pathway 8.5

RDOM - Recalcitrant Dissolved Organic Matter

SCOR - Scientific Committee on Oceanic Research

TCA - Trichloroacetic Acid

TEP - Transparent Exopolymer Particles

T-RF – Terminal-Restriction Fragment

TVZ - Taupo Volcanic Zone

Chapter 1 : General Introduction

1.1 The world's changing oceans

Global atmospheric and oceanic conditions are changing rapidly when compared to the pre-industrial period (IGBP-IOC-SCOR 2013, IPCC 2013). From approximately 24 million years ago up until 1750, the atmospheric CO₂ concentration was relatively stable, remaining below 500 parts per million by volume (ppmv, Pearson & Palmer 2000), equating to an approximate ocean pH of 8.18 to 8.20 (Orr 2011, IGBP-IOC-SCOR 2013, IPCC 2013). Average atmospheric CO₂ concentrations have increased from 280 ppmv in the mid 1700's to 391 ppmv in 2011 (IPCC 2013), a 40% increase since pre-industrial times (Fig. 1.1).

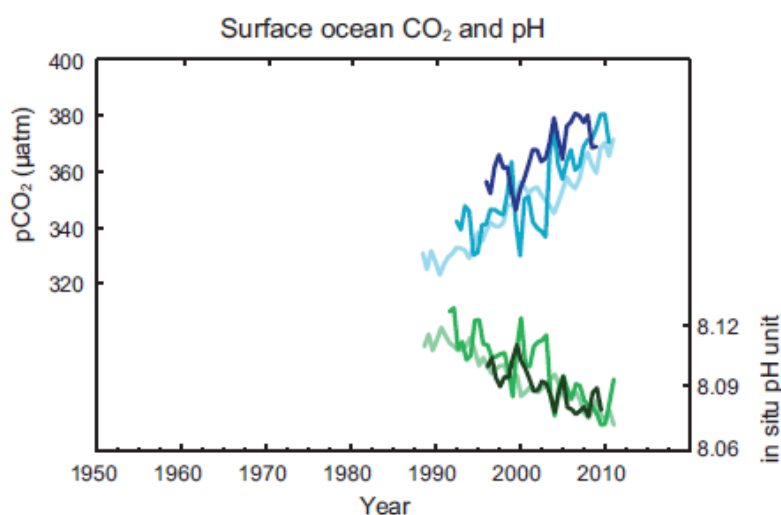


Fig. 1.1. Partial pressure of dissolved CO₂ at the ocean surface (blue curves) and *in situ* pH (green curves). Measurements are from three stations situated in the Atlantic and Pacific Oceans. Source; IPCC 2013: Summary for policymakers

This rapid rise in atmospheric CO₂ is primarily driven by anthropogenic burning of fossil fuels, with forest clearing explaining approximately 20% (Denman et al. 2007, Hannah 2011). Atmospheric CO₂ is freely exchanged with the ocean at the ocean/atmosphere interface, and its absorption directly alters the oceans carbonate chemistry (Zeebe & Wolf-Gladrow 2001). The oceans' uptake of anthropogenic CO₂ is currently estimated at 1 million metric tons per hour (Brewer 2009), and accounts for approximately 48% of anthropogenic CO₂ since

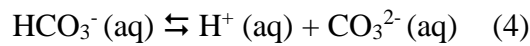
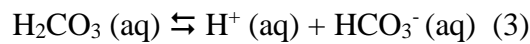
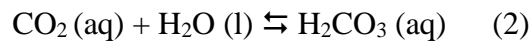
pre-industrial times (Sabine et al. 2004, IGBP-IOC-SCOR 2013, IPCC 2013). The current business as usual emission scenario (Representative Concentration Pathway 8.5, RCP 8.5) predicts that the global average ocean pH could decline to 7.75 by the year 2100, while a decline to 7.76 is predicted for the Chatham Rise region of New Zealand (pers. comm. G. Rickard, NIWA). This decline in global ocean pH is unprecedented in the last 55 million years (IGBP-IOC-SCOR 2013, IPCC 2013).

The Earth's surface and atmosphere receive a significant amount of solar radiation; to balance this incoming energy, it must emit a similar amount of outgoing long-wave radiation (thermal energy). Outgoing radiation is regulated by atmospheric greenhouse gases, the most abundant being water vapour, carbon dioxide and methane. Greenhouse gas concentrations have significantly increased since pre-industrial times (IPCC 2007) leading to the retention of more long-wave solar radiation and thermal energy in our atmosphere (IPCC 2007). This causes atmospheric warming which is transferred to the ocean. Average sea surface temperatures have increased between 0.4 to 0.8°C since the late 19th century (IPCC 2001), with an increase in global surface ocean temperature of 2.0 to 5.4°C predicted by the end of the century under RCP 8.5 (IGBP-IOC-SCOR 2013, IPCC 2013). On a more regional scale, the RCP 8.5 predicts that the offshore Chatham Rise region of New Zealand will increase between 1.4 and 4.3°C (pers. comm. G. Rickard, NIWA). This unprecedented environmental change is expected to have both direct and indirect effects on the biological functioning and large scale biogeochemical cycling in the oceans (IPCC 2001, 2013, Raven et al. 2005, Gattuso & Hansson 2011, IGBP-IOC-SCOR 2013).

1.2 The ocean carbonate system

Carbon dioxide cycles between the atmosphere, ocean and biosphere, and plays a fundamental role in the determination of the oceans' carbonate system, and therefore acidity (Post et al. 1990). The free exchange of atmospheric CO₂ with the ocean surface involves multiple processes, each on a different temporal scale (Zeebe & Wolf-Gladrow 2001, Denman et al. 2007). Little of the exchanged atmospheric CO₂ remains as dissolved CO₂ within the ocean (< 1%); most is converted to HCO₃⁻ (approximately 90%), with the remaining converted to

CO_3^{2-} (approximately 9%, Zeebe & Wolf-Gladrow 2001, Cunha et al. 2010, Gattuso & Hansson 2011). As atmospheric CO_2 enters the surface ocean it reacts with seawater to form a weak acid, carbonic acid (H_2CO_3), which freely dissociates to bicarbonate (HCO_3^-) and free hydrogen ions (H^+). These hydrogen ions react with carbonate to form further bicarbonate (HCO_3^- , Zeebe & Wolf-Gladrow 2001, Riebesell 2004). Importantly, the dissociation constants which determine the rate of each reaction are also affected by temperature, with increasing free hydrogen ions as temperature increases (Dore et al. 2009). The described reactions can be presented as the following equilibria (Stumm & Morgan 1981, DOE 1994, Zeebe & Wolf-Gladrow 2001, Dickson et al. 2007).



(The letters in parentheses refer to the state of the species - gas: g; liquid: l; aqueous: aq)

The oceans carbonate system is described by several different parameters. Dissolved Inorganic Carbon (DIC) represents the sum of the forms, as follows;

$$\text{DIC} = [\text{CO}_2] + [\text{HCO}_3^-] + [\text{CO}_3^{2-}] \quad (5)$$

and the total alkalinity (TA), the sum of negative ions that can be neutralised by adding H^+ ions minus the H^+ already present, and so represents the charge balance of the seawater (Zeebe & Wolf-Gladrow 2001, Emerson & Hedges 2007, see equation 6). Alkalinity is dominated by carbonate and bicarbonate components, however other bases such as borate and hydroxide are also prominent (equation 6).

$$\text{TA} = [\text{HCO}_3^-] + 2[\text{CO}_3^{2-}] + [\text{B}(\text{OH})_4^-] + [\text{OH}^-] - [\text{H}^+] + \text{other minor proton donors} \quad (6)$$

As there is no charge associated with CO_2 , seawater TA does not change when CO_2 enters the ocean by exchange with the atmosphere (Zeebe & Wolf-Gladrow 2001, Emerson & Hedges 2007, Rost et al. 2008). However, the acidity of an aqueous solution, defined by pH as the negative log of the H^+ concentration, increases following an increase in positively charged hydrogen ions (Emerson & Hedges 2007). Importantly, this acidification reaction is naturally buffered by the oceans' carbonate pool (equation 4), neutralising the increased acidity through the formation of bicarbonate (HCO_3^-). This process has successfully regulated the oceans' pH for millions of years (Riebesell et al. 2009). Today however, this natural system is unable to buffer the increase in free hydrogen ions arising from the increasing anthropogenic CO_2 emissions. The natural rate of supply of proton acceptors (bases/ CO_3^{2-}) in the ocean cannot balance the increased concentration of anthropogenic proton donors (acids/ H^+ , Emerson & Hedges 2007); as a result, carbonate levels are declining the oceans natural buffering capacity (Gattuso & Hansson 2011).

The pH of seawater is one of the most influential parameters regulating biological processes in the oceans, determining the rates of biogeochemical reactions as well as individual chemical species distributions and oxidation states (Tipton & Dixon 1979, Hinga 2002). If the natural buffering capacity of the ocean continues to decline, the carbonate system and therefore pH will become less stable. Future changes in ocean pH are predicted to have direct and indirect effects on fundamental biogeochemical reactions which may have a cascade affect onto large scale food-web structures and community shifts.

1.3 Marine organic matter

Carbon is an essential element for biological life (Romankevich 1984) and the oceans are one of the largest reservoirs of organic carbon on the Earth (Post et al. 1990, Benner 2002, Hansell et al. 2009). Carbon in the ocean exists as Dissolved Inorganic Carbon (DIC, Section 1.2), Dissolved Organic Carbon (DOC), Particulate Inorganic Carbon (PIC) and Particulate Organic Carbon (POC, Post et al. 1990), with DOC operationally defined as that which passes through a GF/F filter with a nominal pore size of 0.2 to 0.7 μm , while substrate retained on the filter is termed particulate (Romankevich 1984, Benner 2002, Simon et al. 2002).

The Earth's oceans contain a significantly higher DIC concentration (approximately 37 000 gigatons) than the atmosphere, with a higher proportion found in deep, cold dense waters when compared to surface waters (Post et al. 1990). A significant proportion of the organic carbon in the ocean (> 97%) occurs as DOC (Romankevich 1984), again with the majority residing in the deep ocean (Benner 2002); DOC is the carbon component of Dissolved Organic Matter (DOM, Hopkinson & Vallino 2005), by far the most abundant form of carbon (Azam et al. 1994, Benner 2002, Kirchman 2008, Nagata 2008). As well as DOC, DOM typically consists of dissolved organic nitrogen, dissolved organic phosphorus and dissolved organic sulphur (Kirchman 2008, Wurl & Min Sin 2009, Kujawinski 2011). DOM is highly diverse in physical form, often found as biofilms (Neu & Lawrence 1999), gels (Verdugo et al. 2004), and chromophoric or coloured DOM (Rochelle-Newall et al. 1999, Nelson & Siegel 2002), as well as a range of micro to macro-aggregates such as Extracellular Polymer Substances (EPS, Decho 1990, Neu & Lawrence 1999, Wingender et al. 1999, Bhaskar & Bhosle 2005) and Transparent Exopolymer Particles (TEP, Alldredge et al. 1993, Passow & Alldredge 1994).

DOM is categorised as either labile, semi-labile or recalcitrant, reflecting its nutrient constituents, biological reactivity and therefore its retention time in the water column (Carlson 2002, Church 2008, Hansell et al. 2009, Hansell 2013). The term labile refers to biologically reactive, nutrient rich, fresh organic matter. The majority of new DOM production occurs in the surface ocean, which is therefore the location of the highest concentrations of labile DOM (Benner 2002, Hansell et al. 2009). Labile DOM primarily consists of carbohydrates and simple sugars, and it is a nutrient source for many microbial organisms and therefore rapidly utilised (hours to weeks, Romankevich 1984, Fuhrman & Ferguson 1986, Cherrier et al. 1996, Benner

2002). Demand for labile DOM exceeds supply, creating low surface ocean concentrations (μM range) which further decrease with depth (Williams 1975, Amon & Benner 1996, Benner 2002, Ogawa & Tanoue 2003). Semi-labile organic material is present in the water column for a longer duration (weeks to years, Cherrier et al. 1996), and thus is of lesser nutrient quality having experienced leaching and/or partial degradation. Semi-labile material is composed predominantly of carbohydrates, is often widespread throughout the water column and is a typical subsurface bacterial nutrient source (Benner et al. 1992, Church 2008). Recalcitrant dissolved organic material (RDOM) makes up the largest pool of organic material ($\geq 90\%$) within the ocean (Benner 2002, Church 2008, Jiao et al. 2010, Hansell 2013). Recalcitrant material consists of a range of biologically altered DOM, mainly low bio-reactive waste products (Carlson 2002), resistant material following mortality of an organism (Jiao et al. 2010), or organic substrates that are naturally resistant to microbial degradation (Fry et al. 1996). The majority of RDOM is found in the deep ocean and its biological turnover is very slow, with an average age range anywhere between thousands and millions of years (Hansell et al. 2009, Jiao et al. 2010, Hansell 2013).

The chemical composition of marine organic matter is highly diverse, consisting of hundreds or even thousands of individual monomeric and polymeric units (Azam & Cho 1987, Ducklow 2000). Research shows that the most important substrates for bacterial growth include carbohydrates, proteins, amino acids and lipids (Williams 1975, Azam & Cho 1987, Benner 2002, Church 2008), with glucose also supporting a substantial portion (~ 15 to 45%) of bacterial production and respiration (Rich et al. 1996). The class of organic matter with the highest concentrations of these components is labile DOC. The composition of labile DOC in the surface ocean consists of 10 to 25% carbohydrates, while subsurface DOC consists of approximately 5 to 10% (Pakulski & Benner 1994). Total hydrolysable amino acids make up approximately 1 to 3% of surface ocean DOC and between 0.8 to 1.8% of subsurface DOC, with a range of other organic acid compounds also contributing minor proportions (Romankevich 1984, Benner 2002). Despite many years of research, greater than 80% of surface and subsurface organic carbon is yet to be characterised (Benner 2002).

DOM is categorised based on molecular weight; high molecular weight (HMW) substrate refers to matter which is $> 1 \text{ kDa}$ ($\sim 0.4 \mu\text{m}$, Dalton - atomic mass unit), while low molecular weight (LMW) substrate is $< 1 \text{ kDa}$ (Amon & Benner 1996, Engel et al. 2004, 2014, Fig. 1.2).

To place this in context, phytoplankton releases DOC in the size range 0.5 to > 300 kDa (Chrost & Faust 1983). Monosaccharide and disaccharide compounds are classified as LMW, while oligosaccharides (3 to 10 monomeric units) and polysaccharides (> 10 monomeric units) are HMW (Fig. 1.2).

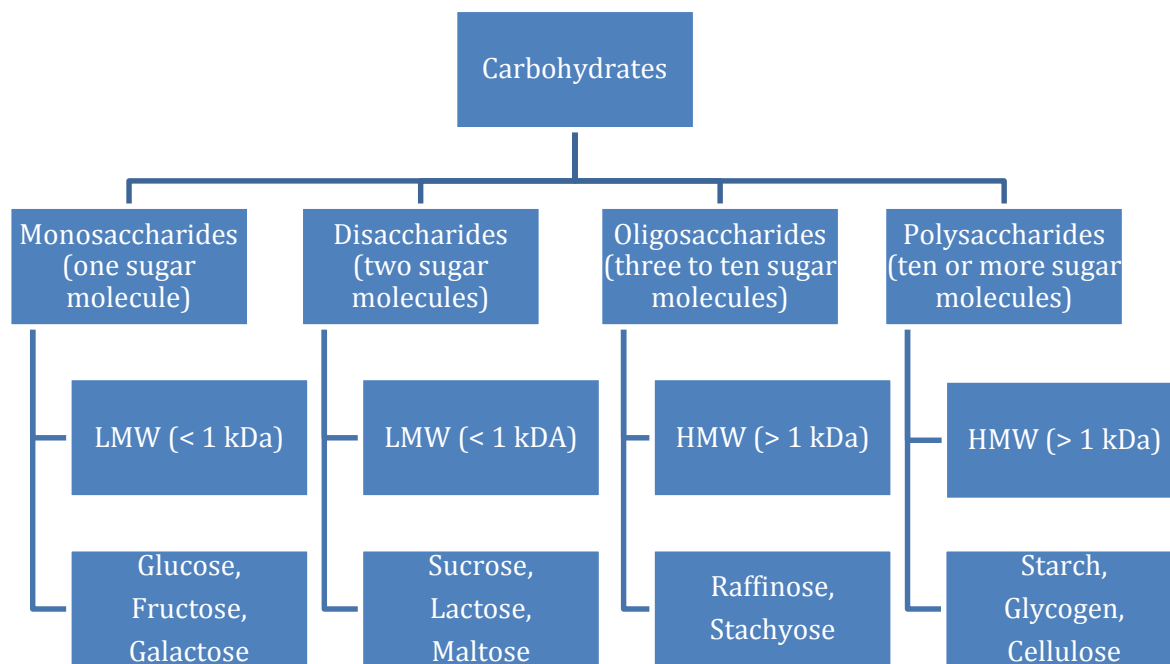


Fig. 1.2. Carbohydrates categorised based on molecular weight. LMW: low molecular weight; HMW: high molecular weight. Figure generated using information derived from Skoog & Benner (1997), Borch & Kirchman (1997) and Benner (2002)

It is accepted that approximately ~65 to 80% of DOM within both surface and subsurface oceans is of LMW (Benner et al. 1992, 1997, Amon & Benner 1994, 1996, Benner 2002), while the remaining component of DOM consists of HMW material, ~20 to 35% > 1 kDa and ~2 to 7% > 10 kDa (Benner et al. 1997, Ogawa & Tanoue 2003). DOM concentrations vary both spatially and temporally, with low concentrations in the open ocean. The availability of HMW organic matter is of great importance to bacterial communities as a carbon rich food source (Amon & Benner 1994, 1996, Benner 2002). In this thesis, the process involving degradation of HMW material to LMW material is referred to as remineralisation. A range of natural aggregates can also occur at much larger particle sizes, for instance Transparent Exopolymer Particles (TEP, 3 to > 100 μm , Alldredge et al. 1993) and marine snow (> 500 μm , Simon et al. 2002). TEP are classed as gels, existing in the medium between dissolved and particulate

matter, operationally described as a particulate ($> 0.4 \mu\text{m}$ in diameter) retained on polycarbonate filters that are stainable with Alcian Blue dye, indicating the presence of polysaccharides (Passow 2002). TEP have a sticky nature due to a large number of cation bridges and hydrogen bond formations between particles (Passow 2002), and as a result they facilitate the production of aggregates that are diverse in composition, while always consisting of an organic polysaccharide component (Passow 2002). TEP form primarily from the products of primary production (Wurl et al. 2011), with highest concentrations occurring in the surface micro layer, ranging from 28 to 5000 particles ml^{-1} (Alldredge et al. 1993), and concentrations decreasing with depth (Wurl et al. 2011). It is constantly recycled in the water column and subject to intensive heterotrophic decomposition (Wurl et al. 2011). TEP are of importance because they promote aggregate formation, transforming DOC into POC, and therefore can significantly influence organic matter export rates (Passow 2002, Engel et al. 2004, Mari 2008). Natural aggregates may also be used by bacteria as attachment sites, thereby altering their spatial distribution and densities when compared to the surrounding environment, as well as providing direct access to hydrolysable organic substrate (Smith et al. 1992, Alldredge et al. 1993, Passow 2002).

Proteins play a vital role in a wide range of microbial processes essential for survival in the ocean (Romankevich 1984), from intracellular growth, to HMW organic compound remineralisation, liberating nutrient rich substrate for cellular assimilation. Microbial proteins make up a large proportion of internal cellular material, which is eventually transferred to the dissolved pool through natural biogeochemical processes (Romankevich 1984). Sources of extracellular proteins include direct liberation by bacteria (Chróst 1989, Hoppe 1993), or indirect release through grazing and cell lysis (Tanoue et al. 1995). Proteinaceous compounds in the ocean make up more than 50% of organic matter (Romankevich 1984), and occur as either individual native extracellular proteins, or peptide chains associated with POM (Tanoue et al. 1995, Saijo & Tanoue 2004). Proteins in the ocean vary in their molecular mass (commonly detected from 14 to 66 kDa) and spatial distribution (Romankevich 1984, Tanoue et al. 1995, Tanoue 1996, Saijo & Tanoue 2004). Native proteins as well as various particulate combined amino acids are highly labile and rapidly degraded by heterotrophic organisms in the surface ocean, however not all extracellular proteins are equally bioavailable, with some more resistant to degradation, such as a porin channel membrane protein derived from Gram-negative bacteria (Tanoue et al. 1995, Tanoue 1996).

1.4 Marine carbon cycle and microbial loop

Carbon in its various states is not found homogeneously throughout the oceans. Rather, its spatial and temporal distribution is largely regulated by the marine carbon cycle (Jiao et al. 2010). This cycle consists of three major component pumps, the biological, carbonate and solubility pumps (Denman et al. 2007, Bowler et al. 2009, Lomas et al. 2010). Of primary interest to this research is the biological pump, also known as the biological carbon pump (Fig. 1.3). This involves the transformation of DIC into particulate organic material (POM) via photosynthesis by phytoplankton, and the eventual export of a small proportion of this through active or passive transport into the oceans' bottom water (Volk & Hoffart 1985, Ducklow et al. 2001, Jiao et al. 2010). Due to the extensive residence time of bottom water (10^3 to 10^4 years), the exported carbon is potentially removed from the atmosphere and trapped for thousands of years (Ducklow et al. 2001, Arrigo 2007, Hansell et al. 2009, Jiao et al. 2010).

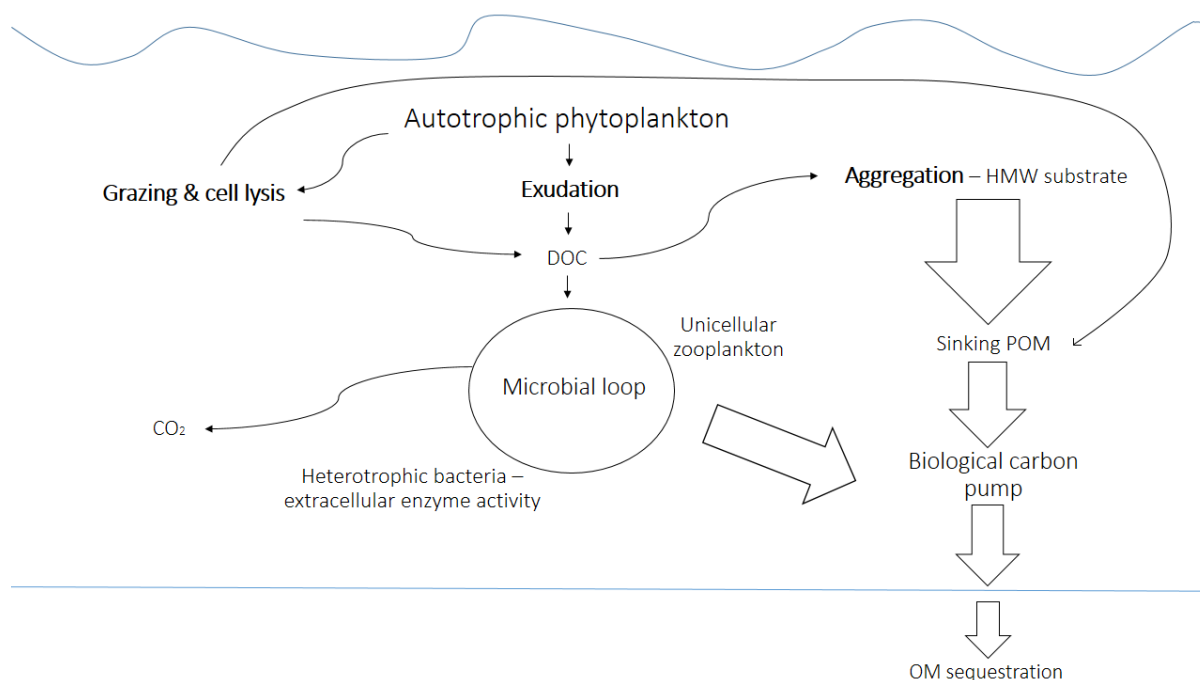
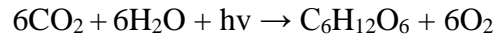


Fig. 1.3. A conceptual diagram of carbon flow in the surface ocean, highlighting two primary drivers, the microbial loop and the biological carbon pump. OM: Organic Matter. Figure generated using information derived from Jiao et al. (2010)

The drawdown of atmospheric CO₂ is largely driven by phytoplankton, including cyanobacteria, fixing inorganic carbon into organic carbon through the use of the sun's radiant energy in a process known as photosynthesis (Sverdrup et al. 1942a, Campbell & Reece 2005), this reaction is presented below:



($h\nu$ represents solar radiation, while C₆H₁₂O₆ is the general formula for organic matter)

Following photosynthesis, a proportion of fixed organic carbon is exuded into the surrounding water column (Saunders 1972, Lancelot & Billen 1985, Fig. 1.3), as not all of the synthesised carbon is incorporated into phytoplankton cellular proteins or lipids (Bell & Mitchell 1972, Williams 1975, Azam et al. 1983, Mykkestad 2000, Church 2008). Significant organic carbon production occurs during a phytoplankton bloom event. The bloom size and therefore the amount of organic carbon produced, its duration and dominant species composition is defined by the *in situ* abiotic and biotic environmental conditions, including dissolved nutrient concentrations, photosynthetic active radiation (PAR), ocean temperature, salinity, pH, and loss processes such as grazing and vertical sinking rates (Sverdrup et al. 1942a, Fehling et al. 2012, McManus & Woodson 2012). Additional processes that influence the DOM pool include zooplankton faecal matter (Jacobsen & Azam 1984, Azam & Cho 1987), grazing of algal and bacterial cell material by zooplankton (Steele 1974, Sharp 1977, Azam et al. 1983, Azam & Cho 1987, Carlson 2002), viral cell lysis (Mykkestad 2000, Kim et al. 2011, Fig. 1.3), natural mortality and marine snow dissolution (Azam & Ammerman 1984, Lancelot & Billen 1985, Suttle 2007).

Organic carbon may be exported from the surface to deep ocean by different pathways. One pathway, referred to as passive transport, involves the natural formation of aggregates via the binding together of LMW organic matter into POM (Fig. 1.3). A small proportion of this aggregate, referred to as marine snow, is exported from the surface ocean (~10%, Bhaskar & Bhosle 2005), with a smaller proportion (< 1%) reaching the ocean floor where it eventually becomes buried and sequestered (Martin et al. 1987, Hedges 1992, Amon et al. 2001, Ducklow

et al. 2001, Fig. 1.3). An alternate pathway, referred to as active transport, involves the direct consumption of surface ocean POM by larger heterotrophic microzooplankton, and its transfer to depth during heterotrophic diurnal migrations with the release of POM in the form of faecal pellets (Ittekkot et al. 1984, Romankevich 1984, Riebesell 2004, Denman et al. 2007).

A portion of organic carbon is channelled through the microbial loop (Azam et al. 1983), involving the consumption of DOC compounds and conversion to inorganic carbon dioxide by heterotrophic bacteria (see equation below);



($\text{C}_6\text{H}_{12}\text{O}_6$ represents the general formula for organic matter)

Heterotrophic bacteria divert a portion of the organic carbon that would otherwise be exported to the ocean floor and eventually sequestered (Legendre & Fèvre 1995, Weinbauer et al. 2011, Fig. 1.3). Nutrients are released following HMW organic matter remineralisation which supports phytoplankton and bacterial growth, and so fuels the heterotrophic food web (Jiao et al. 2010). The microbial loop plays a vital role in recycling of organic carbon; Hedges (2002) reports that it could process the equivalent of 10 to 20 x 10¹⁵ g C per year. Under ocean conditions predicted by the end of the century, these component inputs are likely to change (IPCC 2013), altering the current flow of organic material throughout the water column (Piontek et al. 2010, Riebesell & Tortell 2011, Segschneider & Bendtsen 2013) and directly influencing the efficiency of the ocean as the Earth's largest carbon sink (Gruber et al. 2009).

1.5 Heterotrophic bacteria

Heterotrophic bacteria are amongst the most abundant organisms in the world's oceans (10^7 to 10^9 cells ml^{-1} , Bird & Kalff 1984, Whitman et al. 1998) and are typically most abundant in the surface ocean (Pomeroy & Wiebe 1988, Aristegui et al. 2009, Evans et al. 2011). They also maintain one of the largest biomasses in the ocean (Cho & Azam 1990, Ducklow & Carlson 1992, Kirchman 2008). Marine heterotrophic bacteria are considered part of the microbial community, which refers to organisms smaller than 100 μm (Kirchman 2008). The smallest heterotrophic bacteria range from 0.2 to 0.4 μm in diameter, and are responsible for processing the majority of DOM in the ocean (Andrews & Williams 1971, Kirchman 2008). Azam & Hodson (1977) reported that over 90% of heterotrophic activity in the ocean can be attributed to bacteria $< 1 \mu\text{m}$ in diameter.

Marine heterotrophic bacteria occur as either free-living or particle attached (Hoppe et al. 2002). Free-living bacteria are found in much larger numbers when compared to particle attached bacteria, for example during the development of a phytoplankton bloom. Allgaier et al. (2008) reported that 5 to 6×10^6 cells ml^{-1} were free-living bacteria, while 0.28 to 0.42×10^6 cells ml^{-1} were particle attached bacteria. Also, Cho & Azam (1988) found that $> 95\%$ of the mesopelagic bacteria in their study of the central north Pacific gyre and Santa Monica basin were free-living, while Azam & Hodson (1977) determined that up to 10 to 20% of bacteria may be attached to particles and the remainder exist as free bacterioplankton. Particulate or aggregate formations, such as TEP, have much greater nutrient concentrations when compared to their surrounding seawater (Trent et al. 1978), attracting high concentrations of free-living bacteria which then become particle associated (Azam 1998, Simon et al. 2002, Azam & Malfatti 2007, Grossart et al. 2007). Consequently, although lower in volumetric concentration, particle associated communities have considerably higher metabolic and enzyme activities when compared to free-living bacteria (Kirchman & Mitchell 1982, Hollibaugh & Azam 1983, Smith et al. 1992, Grossart et al. 2007, Piontek et al. 2009), and therefore may contribute proportionately more to organic matter breakdown per cell, when compared to free-living bacteria. However, Jacobsen & Azam (1984) cautioned that this trend may reflect the larger cell size of attached bacteria and their increased organic matter uptake. This trend may be attributed to the increased availability and localised concentration of suitable nutrients associated with organic aggregates (Alldredge 1979). It is also suggested that by attaching to a

solid surface, the bacterium escapes the diffusion boundary layer surrounding the cell, thus increasing the accessibility of nutrients to the bacterial cell (White 1986).

Bacteria are categorised as either Gram-positive or Gram-negative based on their cell structure. Gram-positive bacteria have a simple cell wall which is relatively permeable to HMW molecules (Chróst 1990), whereas Gram-negative bacteria have a more complex cell structure, consisting of a second cell wall membrane (Nikaido & Vaara 1985, Nikaido 2003), thus making the cell less permeable to transport of organic material (Chrost 1990, Nikaido 2003, Weiss et al. 1991). Bacteria efficiently transport nutrients into their cells through both active and passive transport mechanisms (Cohen & Monod 1957, White 1986, Engel et al. 2008). Some bacteria, mostly photosynthetic cyanobacteria, have the ability to directly assimilate CO₂ into cellular biomass (Roslev et al. 2004); however most are heterotrophic and rely on the availability of DOM in the water column to meet their growth requirements (Kujawinski 2011). Because of this dependence on organic matter, bacteria are considered the oceans' dominant consumers (Andrews & Williams 1971, Azam & Hodson 1977, Benner 2002, Kirchman 2008). Bacteria perform two fundamental functions within the marine environment. Firstly, by consuming DOM and respiring (Waksman & Carey 1935) they are a significant producer of CO₂ in the ocean (Pomeroy 1974, Azam et al. 1983, Azam 1998). Secondly, bacteria are responsible for the significant transformation of between 40 to 50% of phytoplankton-derived net primary production in the upper ocean, and account for a significant fraction of the oceans' total metabolism (Pomeroy 1974, Azam et al. 1983, Benner 2002, Azam & Malfatti 2007, Jiao et al. 2010). Bacteria are vital in this particular role as they are one of only a few marine organisms that have the ability to transform both DOM and POM (Chrost 1990, Munster & Chrost 1990), indirectly structuring the distribution of organic matter within the marine environment (Caron et al. 1995, Azam & Malfatti 2007, Kujawinski 2011).

Bacteria are sensitive to environmental conditions due to their large surface area and small volume (Azam et al. 1983, Kawasaki & Benner 2006, Cunha et al. 2010). Temperature and pH can directly affect a range of bacterial activities, including respiration (Iturriaga & Hoppe 1977, Rivkin & Legendre 2001), metabolism (Price & Dixon 1979, Wohlers et al. 2009), and enzyme catalysed hydrolysis rates (Tipton & Dixon 1979, Hoppe 1983, King 1986, Chróst 1989, 1992, Piontek et al. 2009, 2013), as well as bacteria/substrate interactions (Wiebe et al. 1992, Pomeroy & Wiebe 2001). Bacteria possess the ability to modify their surrounding environment

by altering the metabolic products they produce (White 1986). For instance, when exposed to increasing acidic conditions bacteria may target the production of alkaline products, modifying their localised environment to a more optimal pH (White 1986). Furthermore, bacteria may also control their enzyme activity. Grossart et al. (2007) reported that specific bacterial isolates rapidly up- or down-regulate their protease activity based on whether they are attached to an aggregate, or free-living. Individual bacterial communities are known to have species specific environmental sensitivities and stress tolerances (Raven et al. 2005, Passow & Carlson 2012, IPCC 2013), with significant community changes predicted to occur in response to changing ocean conditions.

1.6 Catabolic hydrolysing enzymes

Enzymes are proteins which act as biological catalysts, increasing the speed of a specific chemical reaction without themselves undergoing any permanent change (Segel 1975), while catabolic enzymes break down substances and release energy (Hoppe et al. 2002, Wassenaar 2012). Due to their unique three-dimensional structure, enzymes are highly specific (Kennelly & Krebs 1991, Miller & Agard 1999). Enzymes contain unique active sites which allow specific substrate molecules of a known shape to bind to the enzyme, classically referred to as the 'lock and key mechanism' (Segel 1975, Gottschalk 1985). The catabolic process involves substrate temporarily binding to target enzyme active sites, the cleavage of specific bonds within the substrate molecule, and the subsequent release/liberation of LMW products from the enzyme active site (Segel 1975, Campbell & Reece 2005). Due to enzyme specificity, different enzymes are required to break specific bonds within different substrate (Somville 1984, Kennelly & Krebs 1991, Arnosti 2000); for example, aminopeptidase enzymes target the amino terminus of a peptide based substrate, while β -glucosidase targets the β 1-4 bonds which link two glucose molecules. As each enzyme targets a unique linking bond in an individual substrate molecule, each enzyme produces a unique product (Somville 1984).

In any reaction transforming specific reactants or substrates into one or more products, the reaction's unique activation energy must first be reached (Zeebe & Wolf-Gladrow 2001, Garcia-Viloca et al. 2004). Enzymes act by lowering this initial energy barrier allowing the reaction to proceed at a lower energy requirement, so that each reactant molecule requires less

energy to be converted into the target product (Segel 1975, Garcia-Viloca et al. 2004). At this lower activation energy, a greater number of substrate molecules can be converted into products over a fixed time, increasing the speed of the reaction (Zeebe & Wolf-Gladrow 2001, Garcia-Viloca et al. 2004). Enzymes are highly efficient and maintain substrate hydrolysis even at trace quantities (Zeebe & Wolf-Gladrow 2001, Hoppe et al. 2002).

Catabolic enzymes are frequently termed as endo-, ecto- or exo-, referring to their active location in relation to the host cell that produced it (situated inside, on or outside the host cell, respectively). Another important distinguishing enzyme feature is the location at which the enzyme cleaves substrate polymer bonds (mid-polymer chain or terminal ends). Within marine science, exo-enzymes or extracellular enzymes are referred to as catabolic enzymes which occur outside of the host cell that synthesised it, free in the surrounding environment (Pollock 1962) cleaving substrate polymer bonds at their terminal ends (Chróst et al. 1986, Munster & Chrost 1990, Simon et al. 2002, Cunha et al. 2010). Although a range of aquatic invertebrates have the ability to produce extracellular enzymes (Sala & Gude 1996, Vrba et al. 2004), it is accepted that a significant fraction of catabolic extracellular enzymes are produced by bacteria (Chróst 1989, Hoppe 1993). It is widely considered that there are two primary types of enzymes synthesised by bacteria; constitutive enzymes, those synthesised independent of the ambient substrate concentration; and inducible enzymes, which are synthesised dependent on the concentration of ambient substrate (Cohen & Monod 1957, Rogers 1961, Gottschalk 1985, Arnosti & Jørgensen 2003). The cellular release of extracellular enzymes can occur in response to a number of factors such as the presence of a corresponding HMW substrate (Münster 1991, Boetius 1995), a change in cell permeability (Chróst 1990), and viral lysing and cell rupture (Karner & Rassoulzadegan 1995), as well as through bacterial starvation (Albertson et al. 1990).

Extracellular enzymes are important because a proportion of organic matter consists of insoluble HMW polymeric compounds that are too large for direct transport systems across the bacterial cell membrane (> 600 Da, Rogers 1961, Billen et al. 1980, Munster & Chrost 1990, Chróst & Rai 1993, Nausch et al. 1998). In order for heterotrophic organisms to utilise such nutrient rich substrate, catabolic extracellular enzymes are required to break down the complex polymer structure into smaller sub-units, such as short peptides, amino acids and monomeric sugars (Law 1980, Azam & Ammerman 1984, Azam & Cho 1987, Munster 1991). Proteins and

carbohydrates constitute two of the most common HMW substrates in the ocean (Benner et al. 1992) and both are essential for cellular growth and repair (Azam et al. 1983, Simon & Azam 1989, Section 1.3). Two groups of extracellular enzymes which play a significant role in their respective degradation are aminopeptidases and glucosidases. Aminopeptidases are widely distributed throughout nature, being associated with animals, plants, fungi and bacteria (Matsui et al. 2006). This group of enzymes removes amino acid residues from the termini of peptides, polypeptides and proteins (Burley et al. 1990, Matsui et al. 2006, Bogra et al. 2009). Leucine-aminopeptidase catalyses the hydrolysis of leucine residues from the termini of protein-based substrates (Burley et al. 1990), resulting in a progressively smaller peptide segment. Leucine-aminopeptidase occurs as a single polypeptide chain made up of 87 amino acids and two zinc ions (Burley et al. 1990). Each enzyme has six active sites located in the interior of the enzyme hexamer structure, each including two positively charged amino acid side chains. Potential HMW substrate gains access to the enzyme active sites through specific solvent channels, thereby restricting the peptide length that the enzyme can cleave (Burley et al. 1990). Metal ions play an important role in enzyme activity, determining activation, stability and inhibition (Smith & Spackman 1955). Another common aminopeptidase, arginine, differs from leucine in that it primarily cleaves arginine residues from the N-termini of peptides, polypeptides and proteins (Bogra et al. 2009). Arginine-aminopeptidase is classified as a chloride activated sulfhydryl dependent metalloenzyme (Bogra et al. 2009). Again, as previously described for leucine-aminopeptidase, arginine-aminopeptidase also has two metal binding sites, most likely occupied by Zn^{2+} (Bogra et al. 2009).

Glycosyl hydrolases, which include the group glucosidase, are a large group of enzymes that catalyse the transformation of carbohydrate into glucose (Beguin 1990, Davies & Henrissat 1995, Saha & Bothast 1996). Carbohydrates have extensive stereochemical variation and are subject to hydrolysis by a number of different glycosyl enzymes (Davies & Henrissat 1995, Naumoff 2011). Two particular glycosyl enzymes are β -glucosidase and α -glucosidase. β -glucosidase is an exocellulase that catalyses the hydrolysis of cellulose based substrates at the terminal 1-4 β -glucosidic links, in particular, aryl- β -glucosides and cellobiose substrate (Beguin 1990, Iwashita et al. 1998). β -glucosidases are frequently associated with bacterial activity (Hildebrand & Schroth 1964) and can be inhibited by high concentrations of sugars, as well as activated by glucose, maltose, mannose, lamnose and xylose (Iwashita et al. 1998). Another common glucosidase, α -glucosidase differs from β -glucosidase as it cleaves the

terminal linked 1-4 α -glucose residues, liberating a single alpha-glucose molecule. In contrast to β -glucosidase, α -glucosidase activity is not inhibited by high concentrations of glucose or maltose (Suzuki et al. 1976). Most glucosidases do not require metal ions for hydrolysis, however a small number of enzymes, such as those belonging to the Glycosyl Hydrolase Family 4 (GH4), are dependent on a dinucleotide coenzyme (NAD^+) and Mn^{2+} for catalysis (Varrot et al. 2005).

1.7 Temperature and pH

Extracellular enzyme activity is the initial step in the remineralisation of HMW organic matter which facilitates bacterial cellular uptake of LMW organic matter via diffusion through porin proteins (Billen et al. 1980, Chróst 1989, 1990, 1992, Arnosti & Jørgensen 2003, Delcour 2003, Cunha et al. 2010). As with many biological processes, catabolic hydrolysis is known to have optimal pH and temperature ranges (Segel 1975, Tipton & Dixon 1979, Campbell & Reece 2005). Because extracellular enzymes are by definition free, they are directly susceptible to natural fluctuations in a wide range of variables within their surrounding environment (Cunha et al. 2010).

Temperature has both direct and indirect effects on autotrophic and heterotrophic microbial organisms within the ocean (Waksman & Carey 1935, Haight & Morita 1966, Church 2008, Riebesell et al. 2009). The effect of temperature on metabolic rates is represented by the Q_{10} coefficient which recognises that an increase in temperature of 10°C increases metabolic activity by an approximate factor of two (Sherr & Sherr 1996, Zeebe & Wolf-Gladrow 2001). Similarly, bacterial metabolic activity decreases under reduced temperature environments (Pomeroy & Deibel 1986, Lomas et al. 2002). The increase in bacterial metabolic rates with increasing temperature is reflected by increased bacterial community respiration rates (Pomeroy & Deibel 1986, Lomas et al. 2002, Vázquez-Domínguez et al. 2007, Hoppe et al. 2008), cell numbers (Li & Dickie 1987), total carbon demand (Vázquez-Domínguez et al. 2007), and changes in community composition (Rose et al. 2009). Elevated temperatures may also increase hydrolysis rates for a range of aquatic enzymes (Hollibaugh & Azam 1983, Hoppe 1983, Zeebe & Wolf-Gladrow 2001, Piontek et al. 2009, 2010). The majority of biological and chemical rate processes are driven by enzymatic pathways, and temperature has a significant

effect on these (Eppley 1972, Segel 1975, Pomeroy & Wiebe 2001, Lomas et al. 2002, Brown et al. 2004). All biological reactions have an optimal temperature at which the process of transforming reactants into products is most efficient (Campbell & Reece 2005). A typical reaction rate increases with temperature until a specific maximum temperature is reached. Beyond this, the reaction will plateau and eventually decline (Nedwell 1999). The same principal is true for enzyme catalysed reactions, primarily driven by the increased frequency of substrate collisions with potential enzyme active sites (Campbell & Reece 2005). Beyond an enzyme's optimal temperature, activity will decline as the weak hydrogen bonds between proteins begin to denature (Laidler & Peterman 1979, Nedwell 1999). If the rate of enzyme destruction is greater than repair, the catalysed reactions will decline. Many enzymes have the ability to function at temperatures much higher and lower than found naturally (Thingstad & Martinussen 1991, Arnosti et al. 1998), in some cases in temperatures up to 140°C (Brown & Kelly 1993) or below 0°C (Thingstad & Martinussen 1991). Not only do some enzymes efficiently function under elevated temperatures relative to *in situ*, but particular enzymes actually operate optimally (Yague & Estevez 1988, Arnosti et al. 1998).

As with temperature, bacterial secondary production and cell abundance are also affected by changes in pH, however variation in the response is often reported. For instance, several studies found no significant change in bacterial secondary production rates (Arnosti et al. 2011, Teira et al. 2012) or bacterial cell numbers under low pH conditions (Grossart et al. 2006, Arnosti et al. 2011, Newbold et al. 2012), while others report a significant increase in bacterial cell numbers (Maas et al. 2013, Endres et al. 2014). Similarly, pH is known to significantly influence enzymatic processes (Dixon 1953, Segel 1975, Tipton & Dixon 1979). Catabolic enzymes are typically most active in the pH range from 5 to 9 (Campbell & Reece 2005), as they are made up of a large number of acidic and basic component groups (amino acids, carboxyl and amide termini) that operate under relatively stable intracellular pH. Beyond an enzyme's optimal range, pH has the potential to interfere with the ionisation state of the enzymes component amino acids (Dixon 1953). A significant change in pH can affect the polar and non-polar intramolecular attractive and repulsive forces within an enzyme, potentially altering the shape of the three dimensional structure of the enzyme's active site (Tipton & Dixon 1979). Assuming the reaction does not follow the induced fit hypothesis (Segel 1975), a significant change in active site shape may inhibit the enzyme's ability to breakdown HMW organic matter. Under more extreme pH changes, structural change may lead to irreversible

enzyme conformational change, with the protein unfolding, rendering the enzyme denatured and no longer functional (Segel 1975, Madigan et al. 2000). Overall, changes in the pH of the surrounding environment can affect extracellular enzyme catabolic activity and structural stability (Dixon 1953, Tipton & Dixon 1979). Extracellular enzyme activity may also be indirectly affected by changes in pH, through altering the bacterial cellular membrane fluidity (Jacobs 1940, Ray et al. 1971). As bacteria receive their nutrients through cellular uptake, a pH induced change in cellular permeability would affect cellular diffusion rates for both substrate uptake and extracellular enzyme release (Gould et al. 1975, Vetter & Deming 1994). A change in pH could also alter the activity of enzyme inhibitors, potentially increasing their binding to the enzymes allosteric site (a site other than the enzyme's active site, Hardy et al. 2004), thereby indirectly influencing a specific enzyme activity. Extracellular enzyme activity may also be indirectly affected by changes in the availability of organic substrate driven by changes in phytoplankton composition and biomass in response to pH change (Engel et al. 2014). pH induced changes in bacterial abundance and community composition could also indirectly affect extracellular enzyme activity through change in the number and types of enzyme's synthesised (Endo et al. 2013).

1.8 Research aims

Bacterial extracellular enzymes play a significant role in determining the flux of carbon in the ocean and may be susceptible to future changes in ocean pH and temperature. Two glucosidase and two aminopeptidase enzymes were selected to investigate possible future changes based on their importance in the remineralisation of HMW carbohydrate and protein substrate. The aim of this thesis was to examine how changes in pH and temperature predicted to occur by the end of the century will effect extracellular enzyme activities and bacteria in different water types in the South West Pacific, allowing insight into possible future changes in the ocean carbon flux.

To address this research aim, key questions will be answered, each specifically designed to fill an existing knowledge gap in the literature.

1. Are near-surface ocean extracellular enzyme activities significantly affected by ocean pH and temperature predicted by the end of the century?

To determine this, several different water types (open ocean and coastal) were incubated under different perturbation treatments (a combination of reduced pH and elevated temperature). Following sampling of relevant biotic and abiotic parameters at predetermined time intervals, the community responses were examined.

2. What factors determine spatial and temporal variation in the response of extracellular enzyme activity to decreased pH and elevated temperature?

To determine spatial variability, biotic and abiotic parameter responses from coastal seawater and near-surface open ocean seawater of different phytoplankton communities were compared with seawater collected from below the surface mixed layer. To determine temporal variability, both direct and indirect parameter responses were investigated, including tests on acidification methodology.

3. Do natural high CO₂ shallow water cold vent environments show similar responses?

To examine this, biotic and abiotic parameter responses determined from a naturally high CO₂ cold vent plume were compared to those from artificially acidified ambient seawater. Also, through this treatment comparison pH was investigated as the primary driver for changes, as was whether other confounding variables need to be considered when using vent plume seawater as a proxy environment for a future low pH ocean.

Chapter 2 : Analytical methods

To address the effect of ocean warming and ocean acidification on extracellular enzyme activity and a range of additional abiotic and biotic parameters, a series of perturbation incubations were completed. When designing an incubation experiment multiple factors first need to be considered; for instance, the incubation conditions and the number of treatments should reflect the primary research aim, while the duration of each incubation should reflect the organism or community of interest and its predicted response time. The number of incubated replicates should also be large enough to ensure a representative organism or community response, as well as allow sufficient statistical power for robust interpretation (Riebesell et al. 2010). To address the proposed research aims, a suite of analytical methodologies were used throughout each incubation. Details of the experimental incubation set up and the standard operating procedures of the analytical methods follow.

2.1 Incubation set up

Three perturbation treatments were created to investigate the effect of ocean warming and ocean acidification individually, and also their combined effect under conditions predicted by the end of the century. The high temperature treatment (HT) consisted of ambient pH seawater with an artificially elevated temperature (+3°C); the ocean acidification treatment (OA) consisted of artificially acidified seawater (pH_T 7.8) at ambient seawater temperature; and the greenhouse treatment (GH) consisted of acidified seawater and elevated temperature at the same levels as the individual treatments. Treatment pH values reflect future year 2100 predictions based on an atmospheric CO₂ of 750 µatm (Riebesell et al. 2010, Gattuso & Hansson 2011), while treatment temperatures reflect future year 2100 predictions for the Southern Ocean surrounding New Zealand (Liu & Curry 2010). The three perturbation treatments were compared to an unmodified seawater sample used as an ambient control (Fig. 2.1). Each treatment and ambient control was replicated in triplicate and held in acid washed, milli-Q water rinsed 4.3 l low-density polyethylene (LDPE) cubitainers (Thermo-Fisher Scientific).

Ambient control	OA	HT	GH
<ul style="list-style-type: none"> • Ambient seawater temperature and pH 	<ul style="list-style-type: none"> • Ambient seawater temperature • pH_T 7.8 	<ul style="list-style-type: none"> • Ambient seawater temperature +3⁰C • Ambient sample pH 	<ul style="list-style-type: none"> • Ambient seawater temperature +3⁰C • pH_T 7.8

Fig. 2.1. Incubation treatment design. OA: ocean acidification; HT: high temperature; GH: greenhouse

To achieve the target pH value predicted by the end of the century, different CO₂ gas mixtures were passed through individual gas-permeable tubing loops (Tygon Tubing R-3603; ID 1.6 mm; OD 3.2 mm; Connect 2 Control Ltd, Fig. 2.2) fitted to each 4.3 l cubitainer, as used by Law et al. (2012) and Hoffmann et al. (2013).



Fig. 2.2. Custom made nylon screw-cap and valve, permeable silicon tubing loop hangs below

The OA and GH treatments were acidified through the sequential application of 100% synthetically produced CO₂ gas for 25 min and 10% CO₂ gas for 70 min (in 20.8% O₂ in N₂, BOC Gas Ltd). 742 - 750 μ atm CO₂ gas (also in 20.8% O₂ in N₂) was continuously introduced to maintain the target pH throughout the incubation, whereas the non-acidified treatments (ambient control & HT) received ambient air from aquarium air-pumps. Oxygen concentrations were not measured. Cubitainer headspace was removed to eliminate ambient gas exchange. Before and after each incubation, both cubitainer caps and gas-permeable tubing loops were acid washed and thoroughly rinsed in milli-Q water.

Sample pH values were monitored using a CX-505 laboratory multifunction meter (Elmetron) fitted with a platinum temperature integrated pH electrode (IJ44C-HT enhanced series; accuracy 0.002 pH units) which was regularly cleaned using potassium chloride reference electrolyte gel (RE45-Ionode). Following recommendations from the European Project on Ocean Acidification (Riebesell et al. 2010), all reported pH values in this research reflect the total hydrogen ion scale (pH_T). Using known carbonate parameters and a pCO₂ speciation calculator, CO₂ calc (Hunter 2007), electrode pH measurements calibrated using National Bureau of Standards (NBS) pH buffers (Acorn Scientific Ltd) were converted to pH_T equivalents. The TA values used in this conversion were calculated using a region specific ocean zone algorithm (Lee et al. 2006) and validated against values previously recorded from the respective site. An electrode pH offset was routinely calculated at *in situ* temperature by comparing the pH of artificial Tris buffered seawater determined by the electrode, with that calculated using a formula provided in Dickson et al. (2007). This pH offset was then incorporated into each subsequent electrode pH measurement. Electrode pH measurements were also routinely compared with those attained from a pH spectrophotometer using a thymol blue dye solution (McGraw et al. 2010, Law et al. 2012, Fig. 2.3). Instrument pH agreement to within 0.02 units provided confidence in the continued use of the electrode for routine pH measurements. The pH spectrophotometer was considered for use only when detection of fine scale pH change (< 0.02 units) was predicted, but as the pH difference between the ambient control and high CO₂ treatments was > 0.2 pH_T units, the electrode was used.



Fig. 2.3. Automated pH spectrophotometer taking pH measurements from trial seawater samples, as in Law et al. (2012)

Each cubitainer was housed in one of two identical perspex incubation chambers (1730 mm long, 450 mm high by 325 mm deep). Each chamber was divided into three large internal partitions (325 mm²), each holding two cubitainers (Fig. 2.4). One incubation chamber held the ambient temperature cubitainers (3 x ambient control and 3 x OA), while the other chamber contained the elevated temperature cubitainers (3 x GH and 3 x HT, Fig. 2.4). To ensure a stable incubation temperature, each chamber was externally clad with high density Formathane Rigid Polyurethane Insulation (Forman Building Systems Ltd) and housed in a temperature controlled laboratory. Additional fine temperature control was provided by two manually adjustable temperature controller units (Tropicool - XC4000A; Thermoelectric Refrigeration Unit) installed at both ends of each incubation chamber (Fig. 2.4).



Fig. 2.4. External view of an incubation chamber on board the NIWA research vessel *Tangaroa*. Six empty cubitainers sit ready to be filled. To the right, a temperature controller unit is positioned inside the wall of the incubator

The water sample within each cubitainer was mixed using an inflating diaphragm system of hot water bottles positioned underneath each cubitainer, connected to a time-controlled air-pump programmed at ten second intervals (Fig. 2.5). The inflation and collapse of the hot water bottle under the weight of the sample resulted in continual water displacement and mixing within each cubitainer. To supplement this automated mixing, cubitainers were also manually removed and inverted three times prior to each sampling.

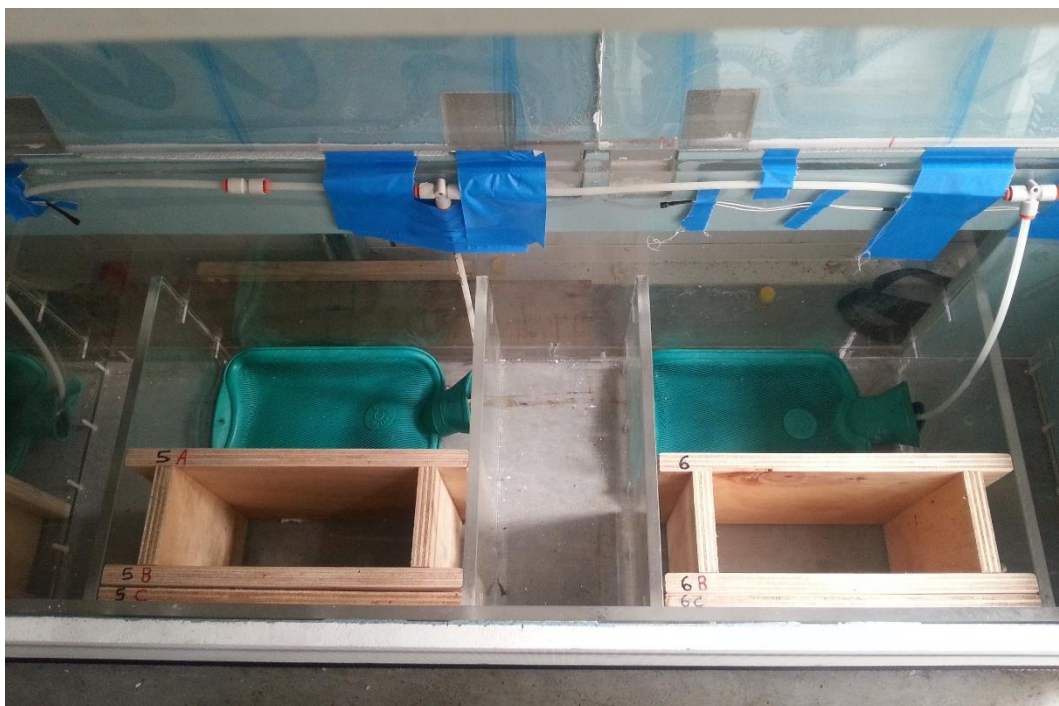


Fig. 2.5. Internal view of an incubation chamber showing wooden spacer blocks and hot water bottles which maintain mixing of water in the overlying cubitainers

Incubated near-surface seawater received artificial photosynthetic light from external fluorescent light banks (Philips TLD 36 W/840). The light intensity at 10 m depth is approximately 10% of surface ocean photosynthetic active radiation (pers. comm. Dr Cliff Law, NIWA). Approximate values were indirectly determined by taking photosynthetic active radiation measurements at sea level on a cloudless Wellington day in November ($350 - 370 \mu\text{E m}^{-2} \text{s}^{-1}$). Neutral density polycarbonate screening (The Light Site Ltd) ensured light intensities were uniform between incubation chambers. Manually adjustable mains timers ensured an automated diurnal 12 h light dark cycle, while black polythene rubbish bags applied to the external viewing windows of each incubator minimised light exposure during the dark cycle.

2.2 Incubation sampling protocol

Three sets of incubation experiments were completed during this research (incubations 1 to 4, 5 to 7 and 8 to 9); each set followed a unique parameter sampling protocol. The original incubation sampling protocol was designed based on information gained from a brief pilot incubation completed during a research cruise in the Southern Ocean during 2011. Results from the pilot incubation revealed that an initial sampling point at 12 h or 24 h would provide a valuable baseline reference point for each parameter sampled. This pilot study also highlighted the importance of incubation duration, with each perturbation treatment requiring incubation for a minimum of 96 h to determine statistically significant responses. Individual samples were collected from each triplicate cubitainer using a sterile disposable pipette. This basic sampling framework was employed for all additional incubations throughout this research.

2.3 Extracellular enzyme activity

Potential extracellular enzyme activity rates were estimated indirectly through the use of artificial fluorescent substrate proxies designed to mimic corresponding natural substrates (Hoppe 1984). Fluorescent substrates consist of an artificial fluorescent molecule bonded (covalently or through peptide binding) to one or more natural monomer molecules (Kim & Hoppe 1984, Arnosti 2011). The molecule is non-fluorescent until it is hydrolysed or cleaved by an extracellular enzyme which triggers the fluorescent response of the fluorophore, allowing it to be detected and quantified (Hoppe 1993). The measured fluorescent intensity is proportional to the amount of substrate analogue hydrolysed by the enzyme (Chróst 1989, 1992).

Two artificial fluorogenic substrate analogues were selected to quantify protease activity; arginine-aminopeptidase activity (Arg-aminopeptidase) was quantified using L-arginine-7-amido-4-methylcoumarin hydrochloride (Arg-MCA, P212121 LLC, USA), and leucine-aminopeptidase activity (Leu-aminopeptidase) was quantified using L-leucine-7-amido-4-methylcoumarin hydrochloride (Leu-MCA, P212121 LLC, USA). Two artificial fluorogenic substrate analogues were selected to quantify glucosidase activity, α -glucosidase activity (α -glucosidase) was quantified using 4-Methylumbelliferyl

α -D-glucopyranoside (α -MUF, P212121 LLC, USA), and β -glucosidase activity (β -glucosidase) was quantified using 4-Methylumbelliferyl β -D-glucopyranoside (β -MUF, P212121 LLC, USA).

A single extracellular enzyme sample was collected from each triplicate cubitainer at each predetermined sampling point using a sterile disposable pipette. Based on preliminary research conducted by E. Maas (NIWA, Wellington, NZ), 5 μ l of 1.6 mM artificial fluorogenic substrate working standard were added to 200 μ l of seawater sample (creating a final artificial substrate assay concentration of 40 μ M) producing saturated enzyme kinetics for greater than 3 h. Each sample was assayed in triplicate and loaded onto a single 96-microwell flat bottom black assay plate (NUNC). An individual enzyme assay was performed for glucosidase and protease activity. Positive glucosidase controls consisted of β -glucosidase from almonds, and α -glucosidase from *Bacillus stearothermophilus* (1×10^{-4} U μ l⁻¹ working standard, Sigma-Aldrich), while the combined protease positive control was proteinase-K (0.2 mg ml⁻¹ working standard, Roche Diagnostics). UltraPure distilled water (Invitrogen™, Life Technologies) was used as the negative control. A four point standard calibration curve of the fluorophore (0 to 8 nmol) was created for each assay using either 4-methylumbelliferone (MUF) for glucosidase activity, or 7-amino-4-methylcoumarin (MCA) for protease activity (Sigma-Aldrich). Each fluorophore working standard (200 μ M) and positive control was made up in autoclaved phosphate buffered saline solution, prepared from commercially produced tablets (Oxoid, UK).

Each assay plate was read at 5 min intervals for a minimum of 3 h using a Modulus microplate reader (Turner Biosystems) at 365 nm excitation and 460 nm emission wavelength. Each enzyme assay was completed inside a temperature controlled laboratory with temperatures reflecting ambient seawater at the site of collection. The maximum enzyme rate (V_{\max} , nmol l⁻¹ h⁻¹, Rudolph & Fromm 1979) was calculated using Michaelis-Menten kinetics (Tipton & Dixon 1979). Triplicate V_{\max} determinations were averaged per sample. To capture optimal linear kinetics, only fluorescence produced between 35 to 180 min was used in the analysis. It must be noted that each assay was run at a higher substrate concentration than typically found in the open ocean to ensure a detectable signal, so average activities reflect potential values unless otherwise specified (Wingender et al. 1999). Extracellular enzyme methodology was optimised based on individual experiment research aims (for details see Section 3.1).

2.4 Bacterial secondary production

Both ^3H -thymidine (^3H -TdR) and ^3H -leucine (^3H -Leu) of high specific activity ($> 80 \text{ Ci mmol}^{-1}$, SciMed Ltd) were used to quantify potential Bacterial Secondary Production (BSP) throughout each incubation. The ^3H -TdR incorporation was used as a proxy for cell division and DNA synthesis (Knap et al. 1996), from hereon referred to as DNA synthesis; while the ^3H -Leu incorporation was used to estimate protein synthesis (Smith & Azam 1992), from hereon referred to as protein synthesis. Total BSP refers to the combination of both DNA and protein synthesis. Both BSP proxies are presented in $\mu\text{g C l}^{-1} \text{ d}^{-1}$, and followed the centrifugation methodology (Smith & Azam 1992, Knap et al. 1996).

Triplicate 1.7 ml samples from each cubitainer were used for the determination of both ^3H -TdR and ^3H -Leu incorporation, including a control sample. Controls were killed by adding 100 μl of 100% cold trichloroacetic acid (TCA, Sigma-Aldrich). Next, 8 μl of 2 nM ^3H -Leu and 2.4 μl of 18 nM ^3H -TdR were added to each respective sample (saturating concentrations were 20 nM and 18 nM respectively) and samples were incubated for a recorded length of time. Following incubation, each sample was killed with 100 μl of 100% cold TCA. Within 36 h of adding TCA, samples were centrifuged at $18\,000 \times g$ for 10 min at 4°C . Each sample supernatant was carefully aspirated under low vacuum pressure ($< 200 \text{ mbar}$), 1 ml of cold 5% TCA was added, and the sample was vortexed and centrifuged as described above. Again the supernatant was carefully aspirated and 1 ml cold 80% ethanol was added. Each sample was vortexed and centrifuged as described above. The supernatant was again aspirated and the sample tube left open to dry for a short period of time. Finally, 1 ml of Optiphase-Highsafe3 (Perkin Elmer) was added to each sample and vortexed. Labelled samples were refrigerated at 4°C until radioassay analysis using liquid scintillation counting (Smith & Azam 1992). The ^3H -Leu incorporation was determined post cruise using a liquid scintillation counter (Tri-Carb 2910 TR). The resulting decay emitted by the radiation source, disintegrations per min (DPM), was calculated based on the duration of sample incubation. Control blanks were subtracted from DPM values, and adjusted for sample volume and ^3H -Leu specific activity. Each value was then multiplied by a known protein constant, according to the following formula (Simon & Azam 1989).

$$\text{Protein synthesis } (\mu\text{g C l}^{-1} \text{ d}^{-1}) = {}^3\text{H-Leu}_{\text{Incorp}} (\text{mol l}^{-1} \text{ h}^{-1}) \times (100/7.3) \times 131.2 \times 0.86 \times 1000000 \times 24$$

The value $100/7.3 = 100/\text{mol\%}$ of leucine in protein, 131.2 is the molar mass of leucine, the bacterial protein production equivalent was converted to bacterial carbon/biomass production by multiplying the value by 0.86 (cellular carbon:protein ratio). Cell-specific protein synthesis was determined for select incubations by dividing the protein synthesis by total bacterial cell numbers, producing an estimate of cell-specific synthesis.

The ${}^3\text{H-TdR}$ incorporation was also determined post cruise using a liquid scintillation counter (Tri-Carb 2910 TR). The DPM output values were adjusted for control blanks, sample volume, incubation duration, the specific activity of ${}^3\text{H-TdR}$ and finally a carbon conversion constant converting mol thymidine into grams of carbon. The selected conversion constant was originally calculated by Fuhrman & Azam (1982) for the Southern Californian Bight, and more recently used by Smith & Hall (1997) in offshore New Zealand research under similar ambient conditions used here. Final productions were then multiplied by a known carbon content per bacterial cell originally derived by Cho & Azam (1988) for use as relevant carbon equivalents.

$$\text{DNA synthesis } (\mu\text{g C l}^{-1} \text{ d}^{-1}) = {}^3\text{H-TdR}_{\text{Incorp}} (\text{mol l}^{-1} \text{ h}^{-1}) \times (2.4 \times 10^{18}) \times (20 \times 10^{-15} \text{ fg C cell}^{-1}) \times 1000000 \times 24$$

The value 2.4×10^{18} refers to the carbon conversion constant, while the value 20×10^{-15} refers to the known carbon content per bacterial cell. Some liquid scintillation counting was performed personally, however the majority was completed by Karen Thompson (NIWA Hamilton).

2.5 Cell numbers

Triplicate samples from each cubitainer were collected in 2 ml cryovials (Raylab Ltd), clearly labelled and frozen in liquid nitrogen (Hall et al. 2004) until post cruise analysis. Cell numbers were determined using a FACS Calibur flow-cytometer (Becton-Dickinson) with photomultipliers set to quantify the red fluorescence from chlorophyll (wavelength 670 nm), the orange fluorescence from phycoerythrin (585 nm), and the green fluorescence from phycourobilin (530 nm). *Synechococcus* spp., *Prochlorococcus* spp. and total eukaryotic phytoplankton (picoplankton < 2 µm and nanoplankton < 20 µm) numbers were determined through fluorescence and forward light-scatter providing an estimate of cell size. Bacterial cell numbers were detected following the addition of 25 µl of SybrGreenII DNA stain (Invitrogen, Lebaron et al. 1998). Once stained, samples were incubated at room temperature in the dark for 20 min, allowing stain uptake prior to analysis. Each 500 µl sample was analysed along with 50 µl of internal reference TruCount™ bead solution (BD Biosciences, Button & Robertson 1989, Lebaron et al. 1998). Cell numbers were calculated based on the ratio of TruCount™ beads detected over a certain time at a standard flow rate. The flow-cytometer was programmed to count 20 000 events. Data were analysed using software CellQuest v3.3 (BD Biosciences) and final count values were recorded as cells ml⁻¹. Some experimental samples were analysed personally, however the majority was analysed by Karen Thompson (NIWA Hamilton).

2.6 Total high molecular weight organic compound concentration

Total High Molecular Weight (HMW) substrate was determined without pre-filtering treatment seawater. Therefore the calculated HMW substrate concentrations include reducing-sugar and protein derived from bacteria and phytoplankton cells trapped on the filter. This cellular content would not have been accessible to extracellular enzymes during the incubation, so the following methodology reflects ‘total’ HMW substrate concentrations.

Total HMW reducing-sugar concentration was quantified using the Somogyi-Nelson detection method in conjunction with filtration (Somogyi 1926). A minimum of 150 ml of sample seawater were filtered through a 25 mm glass-fibre filter (GF/F Whatman). Following filtration

each filter was stored in a 5 ml flat base polypropylene vial (Sarstedt) and frozen at -20°C until post cruise laboratory analysis. GF/Fs are known to absorb and trap particulate organic matter (Karl et al. 1998), and so to avoid rinsing each individual sample filter in an effort to maximise recovery of trapped organic compounds, each filter was directly incorporated into the analysis. This procedure ensured maximum recovery and detection of substrate retained on the filter. During this research, GF/Fs were shown to retain > 50% tetrasaccharide sized substrate (approximately 1231 daltons), consisting of four monomeric units, and therefore according to Fig. 1.2, classed as HMW (refer to Appendix A: 2.1 for substrate size retention trials). Following basic aseptic techniques, each sample filter was defrosted and cut into twelve individual pieces following a standardised cutting pattern. Appropriate reagents were added in accordance with Nelson (1944), and sample filters were then heated in a water bath at 100°C for 15 min. A linear six point glucose calibration curve (0 to 300 $\mu\text{g ml}^{-1}$) incorporating blank GF/Fs was also prepared in triplicate. Final solutions were centrifuged at 13 000 x *g* for 1 min to pellet any loose glass fibre strands, and then a 200 μl aliquot of each sample was placed in a clear flat bottom 96 well tissue culture plate (Sarstedt). Sample absorbance was measured at 520 nm wavelength on a plate reader at 25°C (SpectraMax190-Molecular Devices). Calculated sample concentrations were converted to $\mu\text{g ml}^{-1}$ based on the original volume of seawater filtered. Using the reference glucose standard curve, final HMW reducing-sugar concentrations reflect glucose equivalent values. The methodology has a maximum detection of 0.6 mg and minimum detection of approximately 0.01 mg (Somogyi 1952).

Total HMW protein concentration was quantified using the modified Lowry method in conjunction with filtration (Lowry et al. 1951, Hartree 1972, Thermo-Fisher Scientific 2010). Each sample was collected following the same methodology described for total HMW reducing-sugar detection. Reagent preparation and standard sample analysis protocol were modified from Hartree (1972). A six point linear bovine serum albumin (BSA, Sigma-Aldrich) protein calibration curve (0 to 1000 $\mu\text{g ml}^{-1}$) was run in triplicate with blank GF/Fs directly incorporated. As described for total HMW reducing-sugars, total HMW protein concentration samples were centrifuged at 13 000 x *g* for 1 min prior to absorbance determination at 560 nm wavelength using a 96 well plate reader at 25°C (SpectraMax190-Molecular Devices). This analytical technique is capable of detecting dipeptides, with the detection efficiency increasing with increasing peptide size. The working detection limit is reported to be approximately 5 to 2000 mg ml^{-1} (Hartree 1972, Thermo-Fisher Scientific 2010).

2.7 Dissolved organic carbon

Using a polycarbonate filter holder fitted with a pre-combusted 47 mm GF/F filter, approximately 40 ml of sample filtrate were collected in a triple rinsed pre-combusted 50 ml Schott bottle. Glassware and consumables were pre-combusted by heating in an oven overnight at 550°C. Filtrate samples were double bagged and frozen at -20°C for post cruise laboratory processing.

Using the non-purgable organic carbon method (American Society-Testing & Materials 1994), Dissolved Organic Carbon (DOC) samples were defrosted, 30 ml of sample solution were acidified with 250 µl of 2N HCl and sparged with carbon-free air. This process effectively removed all inorganic carbon, while the residual organic carbon was analysed based on electronic combustion and measured CO₂ output from an infrared detector. The DOC samples were analysed with the assistance of Marieke van Kooten (NIWA Hamilton) using a total organic carbon analyser (TOC-VCSH, Shimadzu Corp., Japan).

2.8 Chlorophyll *a* and dissolved nutrients

Chlorophyll *a* (Chl *a*) and dissolved nutrient concentrations were both determined from a single sample from each cubitainer. Chl *a* was collected by filtering 500 ml of a sample through a 25 mm GF/F. Following filtration, each filter was placed in a secol pocket (Secol Ltd), flash frozen in liquid nitrogen and stored at -80°C until post cruise laboratory processing. Chl *a* detection followed the acidification method described in Strickland & Parsons (1968). Sample filters were first defrosted, soaked in 10 ml of 90% acetone and stored at -20°C overnight. Each sample was analysed and then re-analysed following acidification with three drops of 10% HCl, effectively destroying all chlorophyll pigments. Fluorescence was measured using a luminescent spectrometer (Perkin-Elmer LS55) fitted with a xeno blue light source at 430 nm emission and 670 nm excitation. The Chl *a* pigment was determined by subtracting the un-acidified fluorescence reading from the acidified fluorescence. Resulting values were plotted against a seven point linear calibration curve of known Chl *a* concentration and fluorescence; concentrations are reported in µg ml⁻¹.

Using 200 ml of Chl *a* filtrate from each sample, dissolved reactive phosphate (DRP), nitrate (NO_3^-), ammonia nitrogen ($\text{NH}_4\text{-N}$) and dissolved reactive silicate (DRSi) concentrations were determined. Dissolved nutrient samples were collected in triple rinsed pre-cleaned nutrient bottles, and samples were double bagged and frozen at -20°C until post cruise laboratory processing. Each dissolved nutrient was analysed simultaneously using an Astoria Pacific segmented flow analyser following Astoria-Pacific International protocols (Rev. A 6/00). Each analyte had a detection limit of $1\ \mu\text{g l}^{-1}$. Chl *a* and dissolved nutrient samples were analysed by Marieke van Kooten and Cara Mackle (NIWA Hamilton) using the FASpac II – Flow Analyser Software Package.

2.9 Transparent exopolymer polysaccharides and total carbohydrates

Transparent Exopolymer Polysaccharide (TEP) and Total Carbohydrate (TC) concentrations were determined from a single 600 ml seawater sample collected and stored in a 1 litre screw top bottle spiked with 30 ml of formaldehyde 37% (Sigma-Aldrich). Samples were stored under ambient conditions until post cruise laboratory processing.

TEP concentrations were determined with reference to Arruda Fatibello et al. (2004) with procedural refinement for seawater analysis. A 1 ml aliquot of sample was transferred to a 10 ml centrifuge tube, and to this 0.5 ml of Alcian dye preparation was added and well mixed. Sample tubes were centrifuged at $3\ 500 \times g$ for 25 min, thereby minimising turbidity. Absorbance measurements were made in a spectrophotometer at 602 nm using a 1 cm light path cuvette. The amount of dye taken up was calculated by determining the absorbance difference from a deionised water/Alcian dye blank. A calibration factor was produced from a known concentration of Xanthan standard that was also treated with Alcian dye. The number of equivalent $\mu\text{g ml}^{-1}$ of sample TEP was multiplied by the volume of sample concentrate to provide the final concentration, expressed as $\mu\text{g l}^{-1}$ Xanthan equivalent units.

The TC analysis was determined according to DuBois et al. (1956). A 1 ml subsample was transferred to a 10 ml centrifuge tube, to which 0.5 ml of 5% aqueous phenol solution was added and mixed. Next, 2.5 ml of concentrated sulphuric acid were added to the tube and immediately shaken by hand, ensuring total mixing. An exothermic reaction results with any

carbohydrates present. A deionised water blank and glucose standard were both included in the analysis to provide a direct calibration. Once the tubes had cooled, caps were applied and centrifuged at $3\,500 \times g$ for 25 min. Blanks, standards and sample absorbance were read in a spectrophotometer at 485 nm in a 1 cm light path cuvette. A calibration factor was established from the blanks and standards and applied to the sample absorbances to determine the amount of glucose equivalent per volume of sample concentrate. The number of equivalent $\mu\text{g ml}^{-1}$ of sample was then multiplied by the volume of sample concentrate, providing a final concentration expressed as $\mu\text{g l}^{-1}$ glucose equivalent units. All methodology development and sample analysis was completed by Graham Bryers (NIWA Hamilton).

2.10 Dissolved inorganic carbon and alkalinity

Pre-combusted 12 ml dissolved inorganic carbon (DIC) sample vials (Labco Ltd) were triple rinsed with sample seawater and filled ensuring no air bubbles. One drop of saturated HgCl_2 was added to each sample vial before being capped, labelled and stored at room temperature. Each DIC sample was analysed using evolved CO_2 gas after sample acidification on a Marianda AIRICA system. The accuracy of this method was estimated to be $\pm 5 \mu\text{mol kg}^{-1}$ and determined by analysis of Certified Reference Material provided by Andrew Dickson from Scripps Institution of Oceanography. Alkalinity samples were collected by filling a 1 litre screw top bottle and following the same sample preparation and storage procedures as for DIC above. Sample alkalinity was later analysed by potentiometric titration in a closed cell. The accuracy of this method was estimated to be $\pm 2 \mu\text{mol kg}^{-1}$ and determined by analysis of Certified Reference Material provided by Andrew Dickson from Scripps Institution of Oceanography. Both DIC and alkalinity samples were analysed by Dr Kim Currie (NIWA/University of Otago Research Centre for Oceanography) following methodology from Dickson et al. (2007).

2.11 Data analysis

This research focused on significant differences between perturbation treatments within each incubation, and statistical relationships between incubations were not investigated. All sampled parameter values reported are the means of triplicate samples per treatment; sample outliers were defined as those ± 3 standard deviations and were subsequently removed. Figures with missing data points reflect those removed either because they were below methodology detection limits, were outliers or samples were lost.

Cell-specific β -glucosidase and Leu-aminopeptidase rates were determined by dividing activity by total bacterial cell numbers. β -glucosidase and Leu-aminopeptidase were selected for cell-specific determination because they showed the most consistent measured activity across each ocean environment. The difference between Leu-aminopeptidase activity and the ambient control averaged across 72 h was calculated for each treatment and referred to as Δ hydrolysis potential (as in Piontek et al. 2013). The Δ hydrolysis potential explores the temporal variation in Leu-aminopeptidase activity between treatments; a positive Δ hydrolysis value represents enhanced Leu-aminopeptidase activity, while a negative value represents a lower activity relative to the ambient control. To investigate the effect of temperature on β -glucosidase and Leu-aminopeptidase activity, Q_{10} factors were calculated (for formula see Piontek et al. 2013) for each incubation at 48 h and 96 h.

Statistica v.10 (StatSoft Inc., USA) was used to generate basic graphics and descriptive statistics, including linear-regression, t-test, one-way ANOVA, factorial-ANOVA and repeated-measures ANOVA. Box-plots were used as data exploratory tools, visualising potential parameter responses between treatments at specific sampling points. Line graphs were then generated to illustrate parameter responses within each treatment throughout an incubation. Error bars indicate standard error from triplicate samples for each treatment. Following visual identification of a potentially significant parameter response, data were tested for normality and equality of variance prior to statistical analysis. Due to the small sample size at each sampling point, these assumptions were infrequently met and data were $\log(x+1)$ transformed prior to analysis. A repeated-measures ANOVA (RM-ANOVA) was used when comparing the response of a dependent variable over time throughout an incubation, while a one-way ANOVA was used to investigate a significant treatment response on a selected

dependent variable at a fixed sample point. Standard hypothesis formulations were used for each ANOVA; the alternative hypothesis (H1) tested whether the mean parameter of interest was significantly > 0 , whereas the null hypothesis (H0) was $\mu = 0$. The significance level of each test was $p < 0.05$, unless otherwise specified. If H0 was rejected, a Tukey's HSD posthoc analysis test was run to identify individual variable responses.

PRIMER v.6.1.15 (PRIMER-E Ltd) with the PERMANOVA package was used for multivariate data visualisation and to provide insight into possible parameter interactions. Data collected for six parameters (activities of four extracellular enzymes, DNA synthesis rates and bacterial numbers) sampled at five points during each incubation were $\log(x+1)$ transformed, thereby ensuring both a balanced statistical design as well as a common scale for comparisons (Riebesell et al. 2010). Following the calculation of a Euclidian distance resemblance matrix, a single-linkage cluster analysis was generated to visualise similarities between incubated treatments over time. A similarity profile routine (SIMPROF) was used to test for the presence of patterns between clusters that could have occurred by chance (Clarke et al. 2008). Highlighted clusters were created at a 5% significance level using 1000 random permutations, unless otherwise specified. If the SIMPROF analysis rejected the null hypothesis, that particular sample group had no further identifiable structure (Clarke & Gorley 2006). Using a Euclidian distance resemblance matrix, a series of non-metric Multi-Dimensional Scaling (MDS) plots were also generated. An MDS plot, also known as an ordination plot, orders data based on their similarity or dissimilarity from one another and presents them in dimensional space. The extent to which the multivariate matrices agree is reflected in the stress coefficient (Clarke 1993). An MDS stress < 0.05 gives excellent representation, stress < 0.1 corresponds to a good ordination, while an ordination with a stress > 0.2 has the potential to mislead (Clarke 1993).

Chapter 3 : Methodology optimisation

This chapter describes the optimisation of the methods outlined in Chapter 2 for use in ocean acidification experiments. The following objectives were addressed:

- To investigate the effect of acidification on several fundamental components of the enzyme assay.
- To determine the short term response of enzyme activity to ocean acidification, and whether the method of acidification plays a significant role in the response.

This method optimisation and evaluation is essential for ensuring results collected in field experiments were valid and could be used to address the aims of this thesis.

3.1 Enzyme assay refinement

Introduction

The previously described enzyme kinetic determination technique (Section 2.3) requires the use of several artificial chemical components in order to accurately determine enzyme kinetics. Only limited research has looked at how these individual chemical components respond to changes in pH. If artificial fluorophores are significantly affected by low pH conditions, the proposed enzyme kinetic methodology would be unsuitable for use in ocean acidification experimentation. In this section, the effect of pH on both MUF and MCA artificial fluorophore fluorescence was investigated, after which the effect of artificial fluorogenic substrate on seawater pH was investigated. A buffer solution was trialled in order to mitigate any measured pH effect. Because a buffer solution consists of a weak acid and its conjugate base in equilibrium, the pH of the buffer should remain relatively stable following the addition of an acidic or basic artificial fluorogenic substrate (Riebesell et al. 2010).

3.1.1 The effect of pH on artificial fluorophore fluorescence

Artificial fluorophores are used as reference calibration curves for the determination of enzyme kinetics in response to pH. If pH does have a significant effect on fluorophore fluorescence, the calculated enzyme activity rates may be either under or over estimated. For this reason, the effect of pH was investigated.

Methods

In triplicate, MUF and MCA artificial fluorophore working standards (200 μ M) diluted in 1% 2-methoxyethanol (Sigma-Aldrich) were created at 0.8, 4 and 8 nmol at four pH values (8.2, 8.1, 7.9 and 7.8) using a temperature integrated pH electrode (Section 2.1). To adjust the pH, 0.1 N aqueous NaOH was added. Fluorophores were also added at their respective natural pH. Aliquots of 200 μ l of each sample were placed in a 96-microwell clear flat bottom assay plate (NUNC) and fluorescence determined at 360 nm excitation and 460 nm emission wavelength using a Modulus Nuclear Magnetic Resonance Fluorometer.

Results

The results clearly show that as the pH of the solution containing the MUF and MCA artificial fluorophore decreases, so too does the average fluorophore fluorescence (Fig. 3.1). The MUF fluorescence at pH 7.8 was significantly higher at 8 nmol than the non-adjusted pH 6.22 (t-test, $df = 128$, $p < 0.05$), while MUF fluorescence at pH 8.1 was also significantly higher than fluorescence at pH 7.8 (t-test, $df = 128$, $p < 0.05$, Fig. 3.1). MCA fluorescence at pH 7.8 was not significantly different from the non-adjusted pH 6.42 at 8 nmol (t-test, $df = 128$, $p > 0.05$), while MCA fluorescence at pH 8.1 was also not significantly different from fluorescence at pH 7.8 (t-test, $df = 128$, $p > 0.05$), however fluorescence at pH 8.2 was significantly higher than fluorescence at pH 7.8 (t-test, $df = 128$, $p < 0.05$, Fig. 3.1).

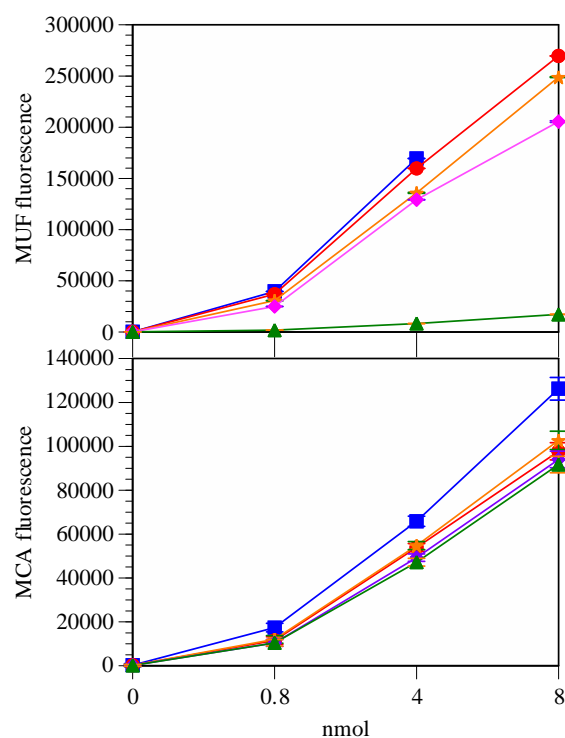


Fig. 3.1. The effect of pH on MUF and MCA fluorophore fluorescence (mean \pm SE, n=3). Treatment legend - pH 8.2: blue squares; pH 8.1: red circles; pH 7.9: orange stars; pH 7.8: pink diamonds; non-adjusted fluorophore control: green triangles. MUF fluorescence at 8 nmol was 3.08×10^5

3.1.2 The effect of artificial fluorogenic substrate on the pH of seawater

To determine basic enzyme kinetics, standard operating procedure only requires the addition of 5 μ l of artificial fluorogenic substrate to 200 μ l of sample (Section 2.3). Following the addition of such a small volume of substrate into seawater which has a high buffering capacity, it was hypothesised that the artificial fluorescent substrate would not have a significant effect on seawater pH.

Methods

To investigate the effect of artificial fluorogenic substrate addition on sample pH, harbour seawater was collected from Evans Bay in Wellington (41°18'06.8"S, 174°48'22.1"E), and the pH of individual seawater samples was adjusted to 7.95 and 7.70 by addition of 0.1 M HCl, including replicates used as controls. All four artificial fluorogenic substrates previously described in Section 2.3 were made up to working standards of 1.6 mM using 1% 2-methoxyethanol (Sigma-Aldrich). A time-zero reference pH was recorded from each seawater sample, and then 650 µl of each substrate at working standard was added to 26 ml of each seawater sample to give a final artificial substrate concentration of 40 µM. Sample pH was recorded immediately following fluorogenic substrate addition, and again 30 min following fluorogenic substrate addition. Each artificial fluorogenic substrate was run in triplicate at each level of pH and compared to a control with no substrate added.

Results

Immediately following the addition of either Leu-MCA or Arg-MCA substrate to sample pH 7.95, pH significantly decreased (ANOVA $F_{1,4}$, $p \leq 0.01$, Fig. 3.2). After 30 mins, both Leu-MCA and Arg-MCA substrates significantly lowered the seawater sample pH when compared to their respective time-zero pH (pH 7.88, ANOVA $F_{1,4} = 13.21$, $p < 0.05$; pH 7.87, ANOVA $F_{1,4} = 16.18$, $p = 0.01$ respectively, Fig. 3.2). Again, immediately following the addition of both Leu-MCA and Arg-MCA substrate to a sample at pH 7.70, pH significantly decreased (pH 7.64, ANOVA $F_{1,4} = 61.16$, $p < 0.01$; pH 7.65, ANOVA $F_{1,4} = 268.83$, $p < 0.001$ respectively, Fig. 3.2). Thirty minutes after the addition of both Leu-MCA and Arg-MCA substrate, sample pH was significantly lower than the time-zero pH (pH 7.66 and pH 7.65, ANOVA $F_{1,4}$, $p < 0.01$ respectively, Fig. 3.2). No statistically significant change in sample pH was recorded immediately following, or 30 mins after the addition of either α -MUF or β -MUF substrate to sample pH 7.95 or 7.70 when compared to the respective controls (Fig. 3.2), suggesting that they are neutral compounds.

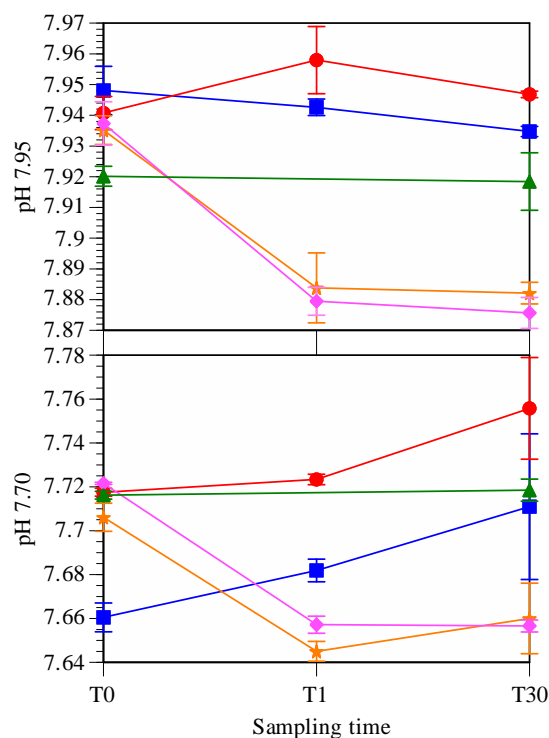


Fig. 3.2. Sample pH immediately following (T1) and 30 mins after artificial fluorescent substrate addition (T30, mean \pm SE, n=3) for samples at initial pH 7.95 (above) and pH 7.70 (below). Treatment legend - α -MUF substrate: blue squares; β -MUF substrate: red circles; Leu-MCA substrate: orange stars; Arg-MCA substrate: pink diamonds; control: green triangles

3.1.3 Fluorescent substrate buffer solution

Methods

Both Leu-MCA and Arg-MCA substrates are hydrochloride salts, and once added they reduce the pH of seawater (average decline of 0.05 and 0.06 pH units respectively) as demonstrated above (Fig. 3.2). To ensure robust application in this research, a buffer solution was required to counteract this. A Tris/HCl buffer was selected as it has been successfully used in the past by researchers using artificial fluorescent molecules (Hoppe 1993).

Tris buffered MCA substrate working standards (1.6 mM) were made by diluting 500 μ l of MCA substrate stock (16 mM) with 4 ml of 0.1 M Tris/HCl buffer. Duplicate Tris buffered substrate working standards were made for both Leu-MCA and Arg-MCA. Using a temperature

integrated pH electrode, duplicate Tris/substrate solutions were adjusted to pH 8.1 and 7.8 through addition of 10% HCl, producing a final volume of 5 ml. Using harbour seawater collected from Evans Bay in Wellington (41°18'06.8"S, 174°48'22.1"E), the pH of duplicate 10 ml aliquots was adjusted using 10% HCl to a target of pH 8.1 and 7.8. For each pH treatment, 250 µl of Tris/MCA substrate solution at the respective pH was added to 10 ml of seawater fixed at the corresponding pH. Duplicate trials were undertaken to determine if sample seawater pH remained stable following the addition of the Tris/MCA substrate solution at working standard concentrations. The pH measurements were recorded at room temperature using a pH electrode (Section 2.1).

Results

Following the addition of Tris/Leu-MCA substrate solution at pH 8.10 to seawater at pH 8.12 (trial 1) and 8.11 (trial 2), pH values were shown to decline by 0.03 and 0.01 pH units respectively (Fig. 3.3).

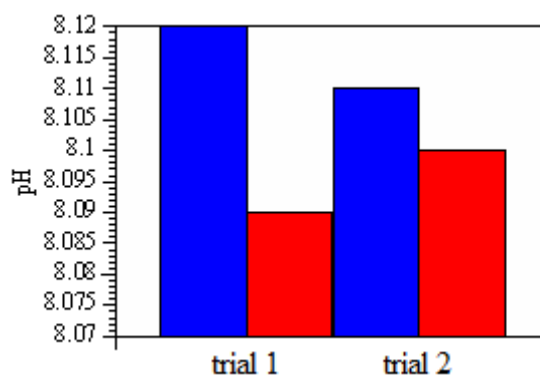


Fig. 3.3. Sample pH following the addition of pH 8.1 Tris/Leu-MCA substrate solution. Duplicate results shown. Treatment legend -sample seawater: blue column; sample seawater and Tris/substrate solution: red column

Similarly, Tris/Arg-MCA substrate solution fixed at pH 8.10 was added to seawater samples at pH 8.10 (trial 1) and pH 8.11 (trial 2). Following substrate addition, sample pH declined by 0.06 and 0.04 units respectively (Fig. 3.4).

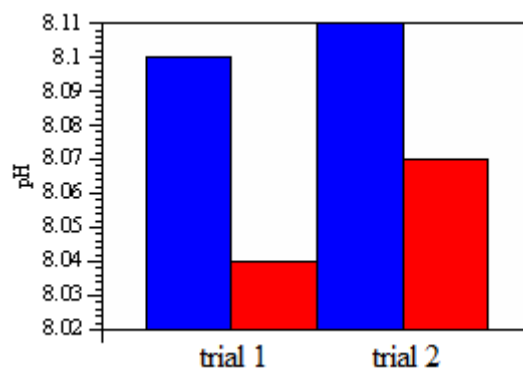


Fig. 3.4. Sample pH following the addition of pH 8.1 Tris/Arg-MCA substrate solution. Duplicate results shown. Treatment legend - sample seawater: blue column; sample seawater and Tris/substrate solution: red column

Tris/Leu-MCA substrate solution fixed at pH 7.80 was then added to seawater samples at pH 7.86 (trial 1) and pH 7.80 (trial 2). Following addition, sample pH declined by 0.03 and 0.08 units respectively (Fig. 3.5).

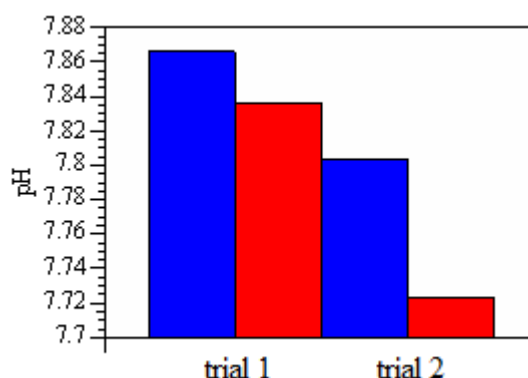


Fig. 3.5. Sample pH following the addition of pH 7.8 Tris/Leu-MCA substrate solution. Duplicate results shown. Treatment legend - sample seawater: blue column; sample seawater and Tris/substrate solution: red column

Tris/Arg-MCA substrate solution fixed at pH 7.80 was then added to seawater samples at pH 7.88 (trial 1) and pH 7.81 (trial 2). Following addition, sample pH declined by 0.01 and 0.03 units respectively (Fig. 3.6).

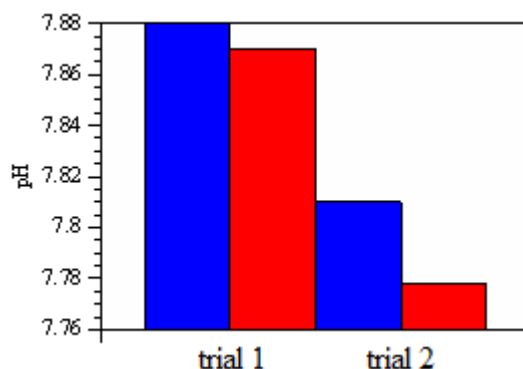


Fig. 3.6. Sample pH following the addition of pH 7.8 Tris/Arg-MCA substrate solution. Duplicate results shown. Treatment legend - sample seawater: blue column; sample seawater and Tris/substrate solution: red column

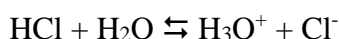
3.1.4 Discussion

The pH had a significant effect on the fluorescence of MUF from pH 8.1 to 7.8, while the MCA fluorescence was significantly affected from pH 8.2 to 7.8. This response supports findings from Belanger et al. (1997), and is of importance because these artificial fluorophores are used to generate fluorescent standard curves for calculating extracellular enzyme kinetics in response to treatment acidification and warming. The pH of seawater declined following the introduction of both Leu-MCA and Arg-MCA artificial substrates. This observation was also reported by Hoppe (1993) who also used a Tris/HCl buffer solution to regulate the acidic effects of MCA substrates, creating an optimal buffer system for enzyme reactions. Acknowledging the sensitivity of the thoroughly cleaned pH electrode (IJ44C-HT enhanced series; accuracy 0.002 pH units), the resulting change in seawater pH following the introduction of buffered Tris/Leu-MCA and Tris/Arg-MCA substrate solutions was determined as acceptable for continued use and so buffered substrate was used routinely. Each artificial fluorogenic substrate stock was diluted to working standards (1.6 mM) using 0.1 M Tris/HCl buffer. The pH of the final solution was adjusted using weak HCl and or NaOH to reflect incubation treatment pH values. Based on the buffering capabilities of Tris/HCl, working standards of both MUF and MCA fluorophores (200 μ M) were also made in 0.1 M Tris/HCl buffer as a substitute for 1% 2-methoxyethanol (Sigma-Aldrich), with the pH adjusted to those of the individual incubation treatments. The resulting enzyme assay standard curve then provides reference fluorophore fluorescence at the same pH as the treatment samples.

3.2 Short-term acidification trial

3.2.1 Introduction

An experiment was designed to investigate whether pH has a direct effect on extracellular enzyme activity by monitoring change in enzyme activity over a short temporal scale. This knowledge is important for interpretation of enzyme kinetics between different experimental perturbation treatments. It is also important to consider the method of seawater acidification because acidification of seawater using acid and CO₂ gas has different effects on the carbonate chemistry. The addition of a strong acid (usually HCl) decreases the sample pH through the formation of hydronium ions (see equation below); this does not alter sample DIC but does modify TA.



The hydronium ions (proton donors) react with available carbonate and form bicarbonate, decreasing sample TA (Emerson & Hedges 2007, equation 4 in Section 1.2), and therefore the resulting carbonate system does not reflect conditions predicted to occur by the end of the century (Iglesias-Rodriguez et al. 2008, Riebesell et al. 2010). Another common method to acidify seawater is using CO₂ gas mixtures. Following the addition of CO₂ gas, DIC increases but does not alter the sample TA (Schulz et al. 2009, Riebesell et al. 2010). Again, as per the equations in Section 1.2, as sample DIC increases, bicarbonate dissociation occurs resulting in an increase in free hydrogen ions and the subsequent decline in sample pH. TA is not subject to change because there is no charge associated with the increased concentration of CO₂ gas. By acidifying individual samples using both acid and CO₂ gas, it was possible to investigate whether the method of acidification played a significant role in any short-term enzyme responses detected.

3.2.2 Methods

Coastal seawater was collected in November 2013 (41°20'53.0"S, 174°45'54.0"E) and pumped through a 15 μm filter, and then a 1 μm inline cartridge filter. Two acidified treatments of 4.3 l were created; the first treatment was acidified to pH 7.8 by adding 4.6 ml of 0.1 M HCl, and was referred to as the acid treatment. The second acidified treatment was referred to as the CO₂ treatment and created by adding CO₂ saturated seawater to ambient coastal seawater. Seawater was saturated (pH 5.97) by bubbling 10% CO₂ gas (in 20.8% O₂ in N₂, BOC Gas Ltd) into 500 ml of ambient coastal seawater, and saturated seawater was added to 4 l of ambient coastal seawater to reach a final pH of 7.77. Following a 30 min equilibration period, β -glucosidase and Leu-aminopeptidase activity was determined (Section 2.3) for each acidified treatment every 2.5 h for a total of 24 h, resulting in a total of five sampling points. Triplicate samples of each treatment were compared to a triplicate ambient coastal seawater control (ambient pH 8.05). Sample DIC and TA were also sampled (Section 2.10) at 3 h following acidification to confirm carbonate chemistry changes following acidification by CO₂ and HCl. Short-term temporal changes in pH were not monitored.

3.2.3 Results

Sample acidification had a significant positive effect on β -glucosidase activity in both the acid treatment (0.05 nmol l⁻¹ h⁻¹) and CO₂ treatment (0.06 nmol l⁻¹ h⁻¹) compared to the ambient control at 0.5 h (0.01 nmol l⁻¹ h⁻¹, ANOVA F_{1, 3}, p < 0.01), however there was no significant difference between the acidified treatments (Fig. 3.7). The β -glucosidase activity across all treatments peaked at 5.5 h (Fig. 3.7), but was significantly higher in the CO₂ treatment at 3 h (0.25 nmol l⁻¹ h⁻¹) and 5.5 h (0.32 nmol l⁻¹ h⁻¹) than the ambient control (0.09 and 0.17 nmol l⁻¹ h⁻¹ respectively, ANOVA F_{1, 4}, p < 0.05, Fig. 3.7). The β -glucosidase activity in the CO₂ treatment (0.25 nmol l⁻¹ h⁻¹) was initially higher than the acid treatment at 3 h (0.11 nmol l⁻¹ h⁻¹, ANOVA F_{1, 3}, p < 0.05, Fig. 3.7), with activity then declining in all treatments from 5.5 h to 8 h (Fig. 3.7). After 24 h, β -glucosidase activity was 35% higher in the CO₂ treatment (0.19 nmol l⁻¹ h⁻¹) than the ambient control (0.14 nmol l⁻¹ h⁻¹, ANOVA F_{1, 2} = 34.22, p < 0.05), but was not significantly different from the acid treatment (0.16 nmol l⁻¹ h⁻¹, Fig. 3.7).

The Leu-aminopeptidase activity was variable between sampling intervals, however in contrast to β -glucosidase activity, acidification did not have a significant effect at 0.5 h (Fig. 3.7). The Leu-aminopeptidase activity in the CO₂ treatment increased from 0.5 h (25.02 nmol l⁻¹ h⁻¹) to 3 h (29.73 nmol l⁻¹ h⁻¹), then declined sharply to 8 h (20.18 nmol l⁻¹ h⁻¹) as was measured for β -glucosidase (Fig. 3.7). Despite Leu-aminopeptidase following a similar activity trend to that of β -glucosidase, there was no overall significant difference between the treatments and control.

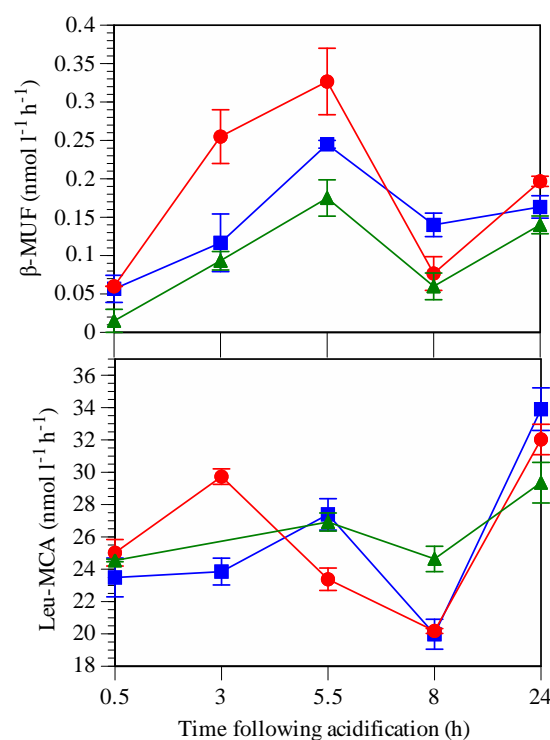


Fig. 3.7. The direct influence of pH on extracellular enzyme activity (mean \pm SE, n=3). Treatment legend - acid treatment: blue squares; CO₂ treatment: red circles; ambient control: green triangles

As expected, sample alkalinity was significantly lower in the acid treatment (2166 μ mol kg⁻¹) when compared to the ambient control at 3 h (2282 μ mol kg⁻¹, ANOVA $F_{1,3} = 10402.12$, $p < 0.0001$) and the CO₂ treatment (2282 μ mol kg⁻¹, ANOVA $F_{1,4} = 28537.53$, $p < 0.0001$). DIC however, was significantly higher in the CO₂ treatment (2152 μ mol kg⁻¹) when compared to the ambient control (2067 μ mol kg⁻¹, ANOVA $F_{1,2} = 2199.81$, $p < 0.01$) and the acid treatment (2066 μ mol kg⁻¹, ANOVA $F_{1,4} = 818.63$, $p < 0.0001$).

3.2.4 Discussion

Extracellular enzyme activity is known to be sensitive to changes in pH (Orsi & Tipton 1979, Tipton & Dixon 1979), however disentangling a direct effect of increased CO₂ from an indirect effect is challenging (Yoshimura et al. 2013). In this study, the results clearly demonstrate an immediate positive β -glucosidase activity response in acidified treatments when compared to the control at 5.5 h, suggesting that there is a direct pH effect on β -glucosidase activity, but that this is not maintained. The β -glucosidase activity increased by a factor of 4.0 in the CO₂ treatment and 3.8 in the acid treatment at 0.5 h after acidification to pH 7.77. In contrast, Leu-aminopeptidase activity in the acidified treatments was not significantly different from the ambient control. Using the same artificial fluorogenic substrates, Piontek et al. (2013) detected a direct response to sample acidification, showing cell-specific β -glucosidase and Leu-aminopeptidase activity increased by a factor of 2.1 and 1.8 respectively at pH 7.79.

Enzymes have different pH optima (Tipton & Dixon 1979), and so a change in pH may be increasingly optimal for some enzymes and less optimal for others. These results, together with those of Piontek et al. (2013) suggest that pH 7.8 was closer to the pH optima of β -glucosidase, while my results suggest that pH 7.8 was further away from the pH optima of protease. The β -glucosidase response is supported by Parham & Deng (2000) who discovered that β -glucosidase activity in soils had an optimal pH of 5.5. The contrasting Leu-aminopeptidase pH response detected by Piontek et al. (2013) could be attributed to a different type of protease. The immediate direct β -glucosidase response could have resulted from a change in H⁺ concentration within the surrounding environment. This could affect the protein tertiary and quaternary structures as these are dependent on charge-charge interactions (Applebury & Coleman 1969). A change in H⁺ concentration could also directly change the charge of key residues in the enzymes' active sites, potentially increasing substrate attraction and active site accessibility. This would result in faster more efficient substrate transformation and turnover (Dixon 1953), in either case modulating the activity of the enzyme. Under more extreme pH changes, a significant increase in H⁺ concentration could result in changes in intramolecular forces, influencing the structural stability of the enzyme and ultimately the exterior three dimensional structure of the enzymes active sites (Tipton & Dixon 1979). If the target substrate molecule can no longer fit into the enzyme's active site, the enzyme would become inhibited with a reduction in activity. Continued structural changes could lead to the enzyme's protein

structures failing, causing the enzyme to unfold and become permanently denatured (Tipton & Dixon 1979). In this short-term acidification trial, the modest pH changes are unlikely to lead to denaturation of the proteins, and indeed, there was no significant decrease in treatment activity relative to controls.

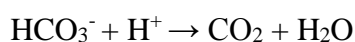
Results from this short-term acidification trial showed that a direct effect of lower pH was not maintained. It is conceivable that the initial increase in activity stimulated feedback inhibition and a decrease in further enzyme synthesis (Berg et al. 2002). The increase in H^+ concentration which stimulated the initial β -glucosidase activity response may have also reduced the bacterial cell membrane permeability, thereby reducing further enzyme release (Jacobs 1940). Differences in seawater carbonate chemistry between the two acidified treatments did not have a significant short-term effect on extracellular enzyme activity, although β -glucosidase activity was initially significantly higher in both treatments. Both treatments and control showed a decline in activity at 8 h, followed by recovery at 24 h, indicating a common response possibly associated with the microbial community. If the elevated β -glucosidase activity is maintained for a longer temporal period, this may have implications for organic matter remineralisation in a future low pH ocean.

In summary, these results show that an increase in seawater acidification either through addition of acid or CO_2 gas has an immediate direct positive effect on β -glucosidase activity, although this was not sustained beyond 6 h, and has no detectable direct effect on Leu-aminopeptidase activity. Although there was a short-term stimulation of the activities of both enzymes to 3 h, there was no significant difference in the response overall. Therefore the differing approaches used, and the resulting differences in alkalinity and DIC did not have differential direct effects.

3.3 Seawater acidification methodology

3.3.1 Introduction

The following experimentation continues on from Section 3.2 to further examine the influence of acidification technique on extracellular enzyme activity in longer incubations. When artificially adjusting the carbonate chemistry of seawater, the acidification method selected needs to be considered in terms of physical and biogeochemical artefacts, as well as the effect on the carbonate chemistry of seawater. Several methods exist to artificially adjust seawater pH (Riebesell et al. 2010). The simplest method involves the addition of a strong acid (typically HCl) to an open system (Section 3.2.1). Another common method of seawater acidification is through the use of CO₂ gas mixtures (Section 3.2.1) which alters the seawater carbonate chemistry in the same way predicted to occur from the uptake of atmospheric CO₂ (Rost et al. 2008, Gattuso & Lavigne 2009, Schulz et al. 2009, Riebesell et al. 2010). Realistic future carbonate system responses can also be achieved by adding equimolar amounts of an acid and a base, HCl and NaHCO₃, to a closed system (Rost et al. 2008, Gattuso & Lavigne 2009, Shi et al. 2009). The addition of the acid reduces pH and maintains the balance of charged species and therefore the sample TA, while the addition of the carbonate species increases the sample DIC (Emerson & Hedges 2007) (equation below).



A review by Hurd et al. (2009) concluded that consideration of the acidification method is vital as the difference in sample carbonate chemistry has the potential to influence phytoplankton photosynthesis and growth rates, as well as POC production per cell. Schulz et al. (2009) suggested that biological organisms are likely to respond to changes in individual carbonate chemistry (e.g. changes in H⁺, CO₂, HCO₃⁻ or CO₃²⁻), rather than changes in overall DIC or TA. For calcifying plankton, the change in carbonate species availability could also affect calcification rates and even dissolution rates (Wolf-Gladrow et al. 1999, Feng et al. 2009, Hendriks et al. 2010). Shi et al. (2009) also reported that acidification methods should be

considered based on the experimental objectives; for instance, they demonstrated that the use of buffers to acidify samples resulted in changes in trace metal availability, suggesting that this method should not be used under trace metal limiting conditions. It is also feasible that changes in carbonate chemistry could significantly alter active and passive cellular transport mechanisms (Jacobs 1940), thereby directly affecting bacterial extracellular enzyme release and also LMW substrate assimilation.

Not only is the method of acidification of importance, but so too is the method of application. One possible method of introducing CO₂ gas into a seawater sample is through bubbling. Although this method is simple to implement and run for extended periods, it is challenging to control the carbonate chemistry due to *in situ* biological activity (Hurd et al. 2009). There is also a mechanical disturbance associated with bubbling CO₂ gas that may influence coagulation of organic matter (Kepkay & Johnson 1989, Zhou et al. 1998, Engel et al. 2004), as well as microbial interactions (Kepkay & Johnson 1989). Because this research concerns the bacterial transformation and processing of HMW organic matter, any artefact on organic matter coagulation may significantly affect experimental findings. Overall, effort should be made to avoid use of mechanical bubbling whenever possible (Riebesell et al. 2010, Weinbauer et al. 2011). An alternative method of introducing CO₂ gas is by gas-permeable silicon tubing, as used in Law et al. (2012) and Hoffmann et al. (2013). A potential downside of this method is the marginal increase in surface area allowing possible bacterial attachment and growth. Although this method of pH adjustment is considerably more time consuming than CO₂ bubbling, the mechanical effect of bubbling is removed as a potential confounding variable yet it still results in realistic carbonate chemistry (Riebesell et al. 2010). Research has been conducted comparing the effect of acid/base acidification with that of CO₂ gas bubbling on phytoplankton growth, with no significant effect detected (Chen & Durbin 1994, Shi et al. 2009, Hoppe et al. 2011). However, no research has been carried out directly comparing the bacterial response to acid/base addition and CO₂ gas aeration with that of CO₂ gas introduced through gas-permeable silicon tubing to determine the most suitable acidification method.

3.3.2 Methods

Two separate OA perturbation incubations were conducted under controlled temperature environments, one in autumn (May 2013 – trial 1) and the other in early spring (October 2013 – trial 2). Coastal seawater was collected and underwent the same two stage filtration as described in Section 3.2.2. Three different acidification methods were selected to acidify seawater to that predicted by the end of the century (pH 7.80, Riebesell et al. (2010)), including acid addition using 0.1 M HCl, referred to as the acid treatment, bubbling CO₂ gas through an acid washed aquarium airstone, referred to as the airstone treatment, and introduction of CO₂ gas through gas-permeable silicon tubing fitted to a custom-made nylon screw-cap (Section 2.1), referred to as the perm-tubing treatment. Each acidification treatment was incubated in triplicate along with an ambient seawater control.

The perm-tubing treatment was acidified through the sequential application of 100% synthetically produced CO₂ gas for 25 min and 10% CO₂ gas (in 20.8% O₂ in N₂, BOC Gas Ltd) for 60 min. The initial use of high concentration CO₂ made it possible to reach the target pH of 7.80 within 3 h. The airstone treatment was acidified by direct bubbling of 742 µatm CO₂ gas (in 20.95% O₂ in N₂, BOC Gas Ltd) for 143 min until the target pH 7.80 was reached. The volume of 0.1 M HCl required to acidify the acid treated sample to pH 7.80 (trial 1; 2.0 ml, trial 2; 3.1 ml) was calculated based on the known sample volume, DIC and TA using a pCO₂ amendment spreadsheet (Dr Kim Currie, NIWA/University of Otago) based on an algorithm from Dickson et al. (2007). Each sample pH was further verified using a pH electrode. The different treatments were acidified at a similar rate over a 150 min period. Each treatment was incubated in acid washed milli-Q water-rinsed 4.3 l LDPE cubitainers (ThermoFisher Scientific), gaseous headspace was removed and no further artificial pH adjustment took place over the 96 h incubation. Each cubitainer was housed in one of the two incubation chambers (Section 2.1), temperature controllers were set at *in situ* ambient seawater temperature and mixing was achieved as described in Section 2.1. Throughout each incubation a range of parameters was sampled every 24 h (or as indicated in Table 3.1) following techniques described in Chapter 2. The initial time-zero sampling occurred after pH was adjusted.

Table 3.1. Parameter sampling protocol, showing the total number of times a parameter was sampled and its respective sampling frequency [in square brackets], following an initial time-zero sampling point. Parameters in bold indicate primary sampling significance

Parameter sampled	Sampling protocol
β-glucosidase and α-glucosidase	4 [24 h]
Leu-aminopeptidase and Arg-aminopeptidase	4 [24 h]
Bacterial numbers	4 [24 h]
<i>Synechococcus</i> spp. numbers	4 [24 h]
Total eukaryotic phytoplankton numbers	4 [24 h]
BSP (DNA & protein synthesis)	4 [24 h]
DIC	2 [48 h]
Alkalinity	1 [96 h]

3.3.3 Results

3.3.3.1 Extracellular enzyme activity

During trial 1, each extracellular enzyme significantly declined in activity across all treatments from time-zero to 96 h (RM-ANOVA, $p < 0.0001$, Fig. 3.8). Time-zero β -glucosidase and α -glucosidase activity was significantly higher in each treatment when compared to the ambient control, with both enzymes declining in a similar trend to 96 h (Fig. 3.8). The β -glucosidase activity was highest in the airstone treatment at each sampling point from 24 h ($11.65 \text{ nmol l}^{-1} \text{ h}^{-1}$) to 96 h ($1.23 \text{ nmol l}^{-1} \text{ h}^{-1}$, Fig. 3.8). Significantly higher β -glucosidase activity was detected in the acid treatment and perm-tubing treatment at 24 h, 48 h and 72 h when compared to the ambient control (Fig. 3.8 & p-values in Appendix B: 3.1). The α -glucosidase activity declined in all treatments throughout trial 1, with the highest activity in the acid treatment from 24 h ($2.62 \text{ nmol l}^{-1} \text{ h}^{-1}$) to 96 h ($0.66 \text{ nmol l}^{-1} \text{ h}^{-1}$), although this was not significantly different from the airstone treatment (Fig. 3.8). The α -glucosidase activity was significantly higher in the perm-tubing treatment compared to the ambient control at each sampling point from time-zero ($1.70 \text{ nmol l}^{-1} \text{ h}^{-1}$) to 72 h ($0.95 \text{ nmol l}^{-1} \text{ h}^{-1}$, Fig. 3.8 & Appendix B: 3.1).

Arg-aminopeptidase activity was highest in the acid treatment at each sampling point from time-zero ($40.58 \text{ nmol l}^{-1} \text{ h}^{-1}$) to 96 h ($24.82 \text{ nmol l}^{-1} \text{ h}^{-1}$, Fig. 3.8), and the only treatment to contain a significantly higher activity than the ambient control (Fig. 3.8 & Appendix B: 3.1). Similarly, Leu-aminopeptidase activity was highest in the acid treatment at each sampling point from 24 h ($71.14 \text{ nmol l}^{-1} \text{ h}^{-1}$) to 96 h ($42.22 \text{ nmol l}^{-1} \text{ h}^{-1}$), with activity significantly higher than the ambient control at each sampling point from time-zero to 96 h (Fig. 3.8 & Appendix B: 3.1). The Leu-aminopeptidase activity was also significantly higher in the airstone treatment and perm-tubing treatment when compared to the ambient control at 48 h and 72 h (Fig. 3.8 & Appendix B: 3.1).

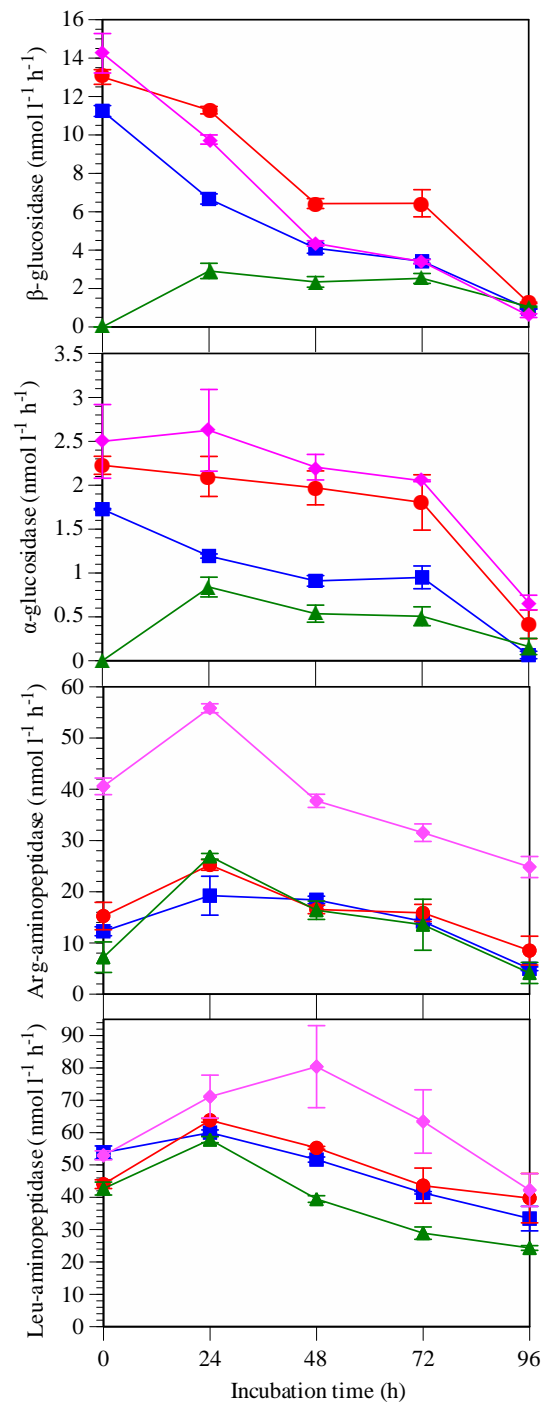


Fig. 3.8. Extracellular enzyme activity throughout trial 1 (mean \pm SE, n=3). Treatment legend – airstone: red circles; acid: pink diamonds; perm-tubing: blue squares; ambient control: green triangles

Total cell-specific β -glucosidase activity in the airstone, perm-tubing and acid treatment declined from time-zero to 96 h (Fig. 3.9). Despite this, a significantly higher cell-specific β -glucosidase activity was measured in each treatment from time-zero to 48 h when compared to the ambient control (ANOVA $F_{1,3}$, $p < 0.05$, Fig. 3.9). Throughout trial 1, the cell-specific β -glucosidase activity in each treatment became increasingly similar to the ambient control, with very similar values at 96 h (Fig. 3.9). Total cell-specific Leu-aminopeptidase activity also declined in each treatment from time-zero ($195.75 \text{ amol l}^{-1} \text{ h}^{-1}$) to 96 h ($56.52 \text{ amol l}^{-1} \text{ h}^{-1}$, Fig. 3.9). A higher cell-specific Leu-aminopeptidase activity was detected in each treatment at selected sampling points from time-zero to 96 h, similar to that detected of Leu-aminopeptidase activity (Fig. 3.8). However, only the acid treatment contained a higher activity throughout much of the incubation (Fig. 3.9).

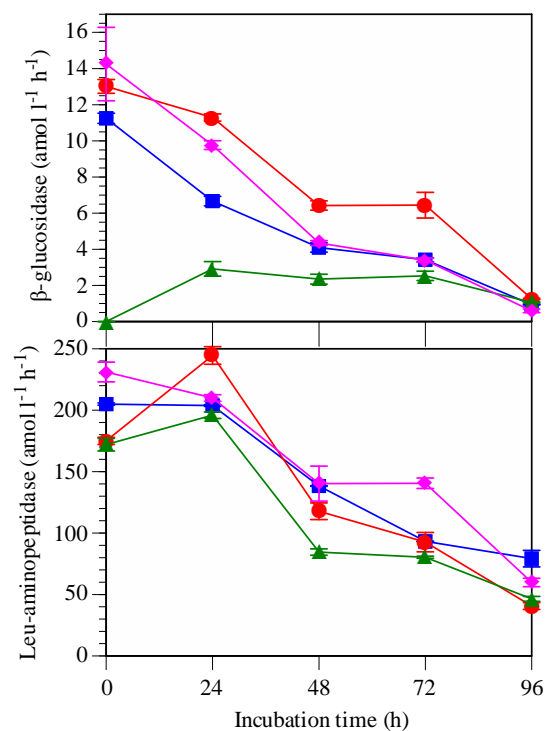


Fig. 3.9. Cell-specific extracellular enzyme activity throughout trial 1 (mean \pm SE, $n=3$). Treatment legend – airstone: red circles; acid: pink diamonds; perm-tubing: blue squares; ambient control: green triangles

In contrast to trial 1, which took place in autumn, β -glucosidase activity more than tripled across all treatments from 24 h to 96 h during trial 2 (RM-ANOVA $F_{3,9} = 42.28$, $p < 0.0001$, Fig. 3.10). The highest β -glucosidase activity was detected in the airstone treatment from 48 h ($0.18 \text{ nmol l}^{-1} \text{ h}^{-1}$) to 96 h ($0.04 \text{ nmol l}^{-1} \text{ h}^{-1}$), with activity significantly higher than the ambient control at each sampling point from 24 h to 96 h. The acid treatment was the only treatment in which α -glucosidase activity was detected. This activity increased from time-zero ($0.07 \text{ nmol l}^{-1} \text{ h}^{-1}$) to 96 h ($0.40 \text{ nmol l}^{-1} \text{ h}^{-1}$, Fig. 3.10). In direct contrast to trial 1, Arg-aminopeptidase activity was significantly lower in the acid treatment than the ambient control from time-zero ($20.69 \text{ nmol l}^{-1} \text{ h}^{-1}$) to 72 h ($14.68 \text{ nmol l}^{-1} \text{ h}^{-1}$, Fig. 3.10 & Appendix B: 3.1). While similar to the trend detected in trial 1, the airstone and perm-tubing treatment followed similar activity profiles as those in the ambient control (Fig. 3.10). In contrast to trial 1, Leu-aminopeptidase activity was significantly lower in the airstone and acid treatment when compared to the ambient control at time-zero (Fig. 3.10 & Appendix B: 3.1), activity increased by 50% across all treatments from time-zero ($20.81 \text{ nmol l}^{-1} \text{ h}^{-1}$) to 96 h ($30.58 \text{ nmol l}^{-1} \text{ h}^{-1}$, RM-ANOVA $F_{4,32} = 65.42$, $p < 0.0001$, Fig. 3.10). The Leu-aminopeptidase activity was significantly higher in the perm-tubing treatment than the ambient control at each sampling point from 24 h ($23.17 \text{ nmol l}^{-1} \text{ h}^{-1}$) to 96 h ($31.74 \text{ nmol l}^{-1} \text{ h}^{-1}$, Fig. 3.10 & Appendix B: 3.1). At the final sampling point, Leu-aminopeptidase activity was significantly higher in each treatment than in ambient control, but activity was significantly higher in the airstone treatment relative to both the perm-tubing treatment and acid treatment (Fig. 3.10 & Appendix B: 3.1).

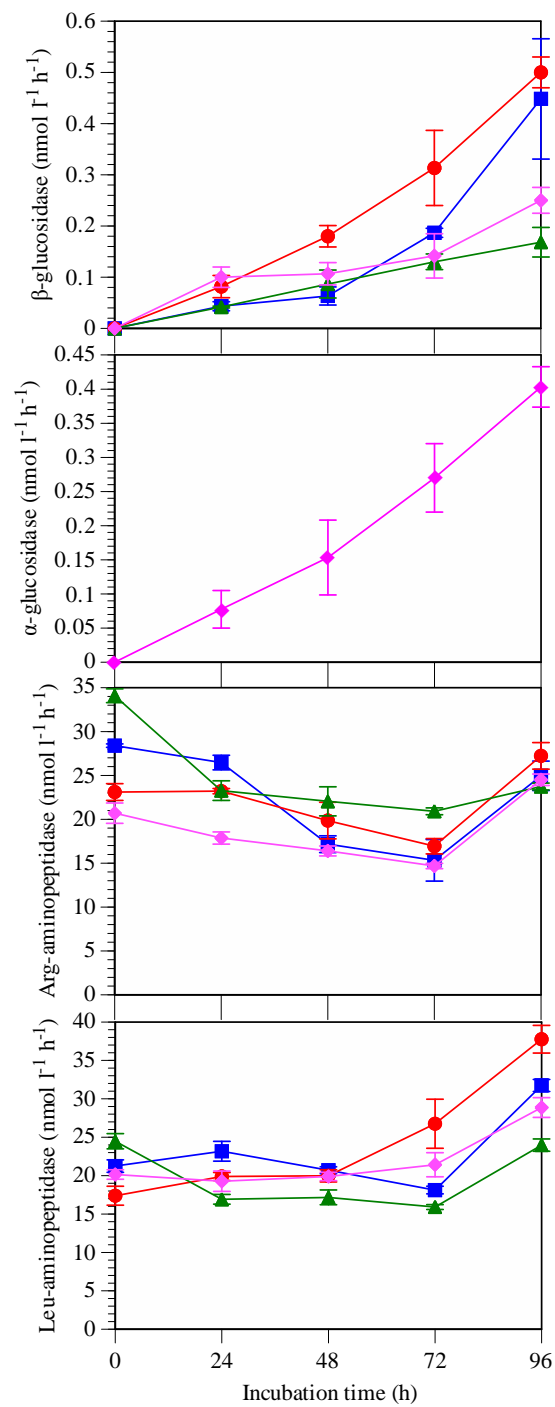


Fig. 3.10. Extracellular enzyme activity throughout trial 2 (mean \pm SE, n=3). Treatment legend – airstone: red circles; acid: pink diamonds; perm-tubing: blue squares; ambient control: green triangles

A very similar treatment response was detected between β -glucosidase activity and cell-specific β -glucosidase activity during trial 2. Cell-specific β -glucosidase activity increased across all treatments from time-zero to 96 h (Fig. 3.11); this trend contrasts that from trial 1. Cell-specific β -glucosidase activity was highest in the acid treatment at 24 h ($0.37 \text{ amol l}^{-1} \text{ h}^{-1}$), while cell-specific activity was highest in the airstone treatment from 48 h to 96 h; each was significantly higher than the ambient control (ANOVA $F_{1,3}$, $p < 0.05$, Fig. 3.11). In contrast to Leu-aminopeptidase activity (Fig. 3.10), cell-specific Leu-aminopeptidase activity declined by 42% across each treatment from time-zero ($93.32 \text{ amol l}^{-1} \text{ h}^{-1}$) to 72 h ($53.72 \text{ amol l}^{-1} \text{ h}^{-1}$, Fig. 3.11). In contrast to trial 1, cell-specific Leu-aminopeptidase activity was also significantly lower in each treatment when compared to the ambient control at time-zero (ANOVA $F_{1,2}$, $p < 0.05$, Fig. 3.11). Cell-specific Leu-aminopeptidase activity was highest in the perm-tubing treatment at 24 h ($78.64 \text{ amol l}^{-1} \text{ h}^{-1}$) and 48 h ($63.97 \text{ amol l}^{-1} \text{ h}^{-1}$), both of which were significantly higher than the ambient control (ANOVA $F_{1,2}$, $p < 0.05$, Fig. 3.11).

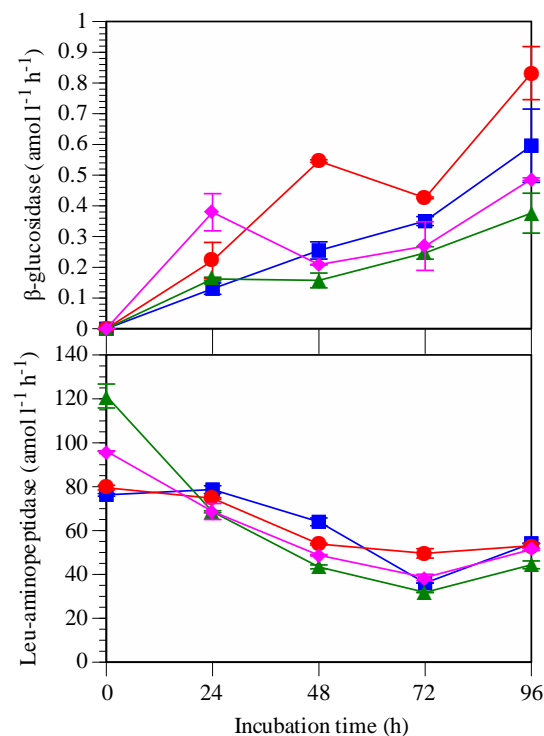


Fig. 3.11. Cell-specific extracellular enzyme activity throughout trial 2 (mean \pm SE, $n=3$). Treatment legend – airstone: red circles; acid: pink diamonds; perm-tubing: blue squares; ambient control: green triangles

3.3.3.2 Cell numbers

Trial 1 bacterial cell numbers increased in each treatment from time-zero to 96 h, while total *Synechococcus* spp. and eukaryotic phytoplankton numbers declined (Fig. 3.12). Total eukaryotic phytoplankton numbers were significantly lower in the perm-tubing treatment and airstone treatment than the ambient control at time-zero (Fig. 3.12 & p-values in Appendix B: 3.2); this trend was also evident within the perm-tubing treatment at 48 h (ANOVA $F_{1,4} = 11.51$, $p < 0.05$, Fig. 3.12). Bacterial cell numbers were significantly higher in the airstone treatment and acid treatment when compared to the ambient control at 96 h (Fig. 3.12 & Appendix B: 3.2).

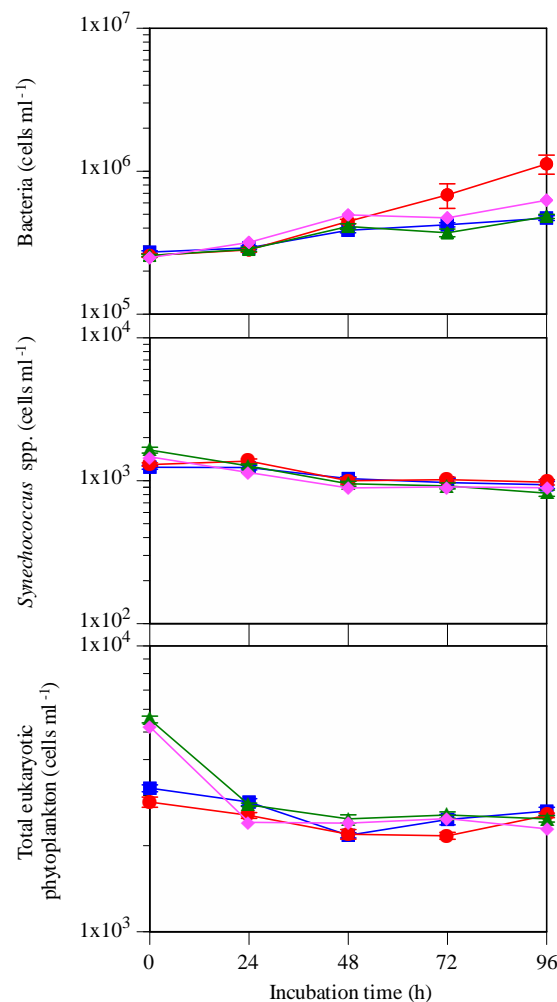


Fig. 3.12. Bacteria, *Synechococcus* spp. and total eukaryotic phytoplankton cell numbers (log scale) throughout trial 1 (mean \pm SE, $n=3$). Treatment legend – airstone: red circles; acid: pink diamonds; perm-tubing: blue squares; ambient control: green triangles

During trial 2, bacterial cell numbers also increased in each treatment from time-zero to 96 h (RM-ANOVA $F_{4, 28} = 1028.3$, $p < 0.0001$), while total *Synechococcus* spp. and eukaryotic phytoplankton numbers declined significantly (RM-ANOVA $F_{4, 32} p < 0.0001$, Fig. 3.13). Bacterial cell numbers were significantly higher in the perm-tubing treatment (3×10^5 cells ml^{-1}) than the ambient control at time-zero (2×10^5 cells ml^{-1} , ANOVA $F_{1, 4} p < 0.01$), but significantly lower (3×10^5 cells ml^{-1}) than the ambient control at 48 h (4×10^5 cells ml^{-1} , ANOVA $F_{1, 4}$, $p < 0.01$). Bacterial cell numbers were significantly higher in each treatment when compared to the ambient control at 96 h (ANOVA $F_{1, 4} p < 0.05$), while total eukaryotic phytoplankton numbers were significantly lower in the airstone treatment than the ambient control at time-zero, 48 h and 96 h (ANOVA $F_{1, 4}$, $p < 0.05$, Fig. 3.13).

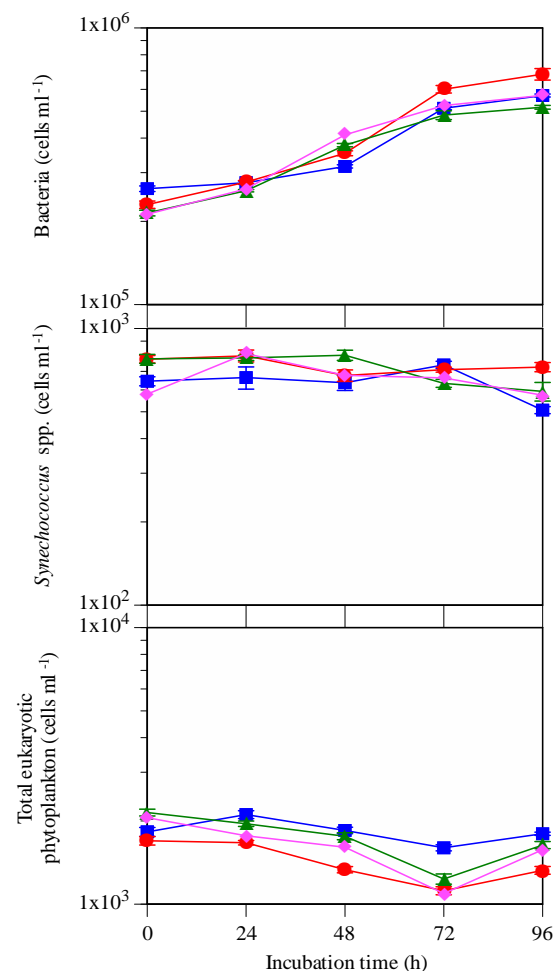


Fig. 3.13. Bacteria, *Synechococcus* spp. and total eukaryotic phytoplankton cell numbers (log scale) throughout trial 2 (mean \pm SE, $n=3$). Treatment legend – airstone: red circles; acid: pink diamonds; perm-tubing: blue squares; ambient control: green triangles

3.3.3.3 Bacterial secondary production

A significant positive relationship was measured between DNA and protein synthesis rates throughout trial 1 (linear regression, $p < 0.01$, $r = 0.52$). DNA synthesis increased in each treatment from time-zero to 96 h (RM-ANOVA $F_{4, 32} = 54.23$, $p < 0.01$, Fig. 3.14). A higher DNA synthesis rate was detected in the airstone treatment at time-zero ($57.01 \mu\text{g C l}^{-1} \text{d}^{-1}$) and 96 h ($141.53 \mu\text{g C l}^{-1} \text{d}^{-1}$) when compared to the ambient control (36.26 & $102.20 \mu\text{g C l}^{-1} \text{d}^{-1}$) respectively, Fig. 3.14 & p-values in Appendix B: 3.3). Protein synthesis also increased in each treatment from time-zero to 96 h (RM-ANOVA $F_{4, 32} = 22.85$, $p < 0.01$, Fig. 3.14). The protein synthesis rate was significantly lower in the airstone treatment ($1.08 \mu\text{g C l}^{-1} \text{d}^{-1}$) than the ambient control at time-zero ($1.22 \mu\text{g C l}^{-1} \text{d}^{-1}$, Fig. 3.14 & Appendix B: 3.3). A higher protein synthesis rate was detected in each treatment at 48 h, 72 h and 96 h when compared to the ambient control, however not all treatments were statistically different from the ambient control (Appendix B: 3.3).

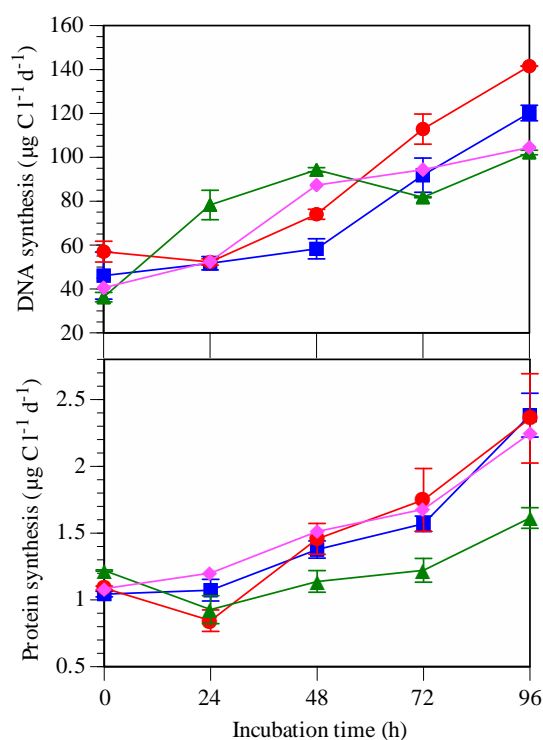


Fig. 3.14. BSP throughout trial 1 (mean \pm SE, $n=3$). Treatment legend – airstone: red circles; acid: pink diamonds; perm-tubing: blue squares; ambient control: green triangles

As in trial 1, a significant positive relationship was also measured between DNA and protein synthesis rates throughout trial 2 (linear regression, $p < 0.0001$, $r = 0.60$). In each treatment, DNA and protein synthesis rates increased from time-zero to 96 h (Fig. 3.15). The rate of DNA synthesis increased significantly in the acid treatment after long-term (> 48 h) exposure (Fig. 3.15 & Appendix B: 3.3), with protein synthesis rates indicating a similar positive long-term response in each treatment (Fig. 3.15 & Appendix B: 3.3).

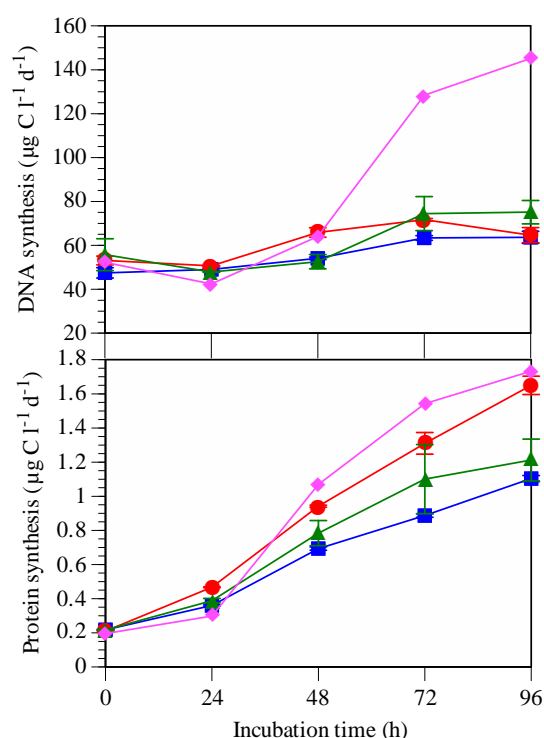


Fig. 3.15. BSP throughout trial 2 (mean \pm SE, $n=3$). Treatment legend – airstone: red circles; acid: pink diamonds; perm-tubing: blue squares; ambient control: green triangles

3.3.3.4 Carbonate chemistry

During trial 1, as expected alkalinity was significantly lower in the acid treatment ($2245 \mu\text{mol kg}^{-1}$) than in the ambient control ($2295 \mu\text{mol kg}^{-1}$, ANOVA $F_{1,4} = 847.12$, $p < 0.01$), the perm-tubing treatment ($2297 \mu\text{mol kg}^{-1}$, ANOVA $F_{1,4} = 663.80$, $p < 0.01$) and the airstone treatment at 96 h ($2300 \mu\text{mol kg}^{-1}$, ANOVA $F_{1,4} = 143.34$, $p < 0.01$). Similarly, during trial 2 alkalinity was again significantly lower in the acid treatment

(2208 $\mu\text{mol kg}^{-1}$) than the ambient control (2285 $\mu\text{mol kg}^{-1}$, ANOVA $F_{1,4} = 8511.45$, $p < 0.01$), the perm-tubing treatment (2285 $\mu\text{mol kg}^{-1}$, ANOVA $F_{1,4} = 32687.38$, $p < 0.01$) and the airstone treatment at 96 h (2285 $\mu\text{mol kg}^{-1}$, ANOVA $F_{1,4} = 15918.32$, $p < 0.01$).

During trial 1, DIC concentrations were significantly higher in the perm-tubing treatment (2139 $\mu\text{mol kg}^{-1}$) and airstone treatment (2137 $\mu\text{mol kg}^{-1}$) than the ambient control at 24 h (2110 $\mu\text{mol kg}^{-1}$, ANOVA $F_{1,3}$, $p < 0.05$, Fig. 3.16), while the same treatment trend was also apparent at 96 h (ANOVA $F_{1,3}$, $p < 0.05$, Fig. 3.16). There was no significant difference in DIC concentrations between the acid treatment (2095 $\mu\text{mol kg}^{-1}$) and the ambient control at 96 h (2094 $\mu\text{mol kg}^{-1}$, ANOVA $F_{1,3} = 8.80$, $p > 0.05$, Fig. 3.16).

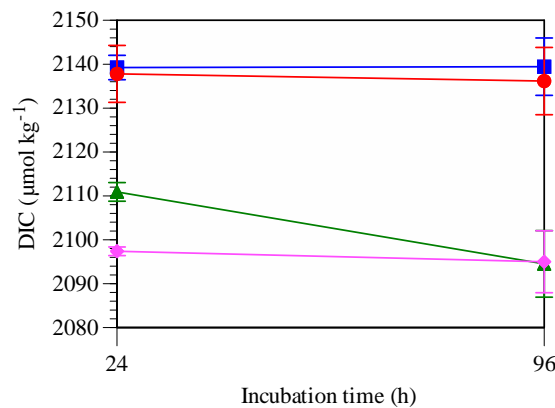


Fig. 3.16. DIC concentrations per treatment at 24 h and 96 h during trial 1 (mean \pm SE, $n=3$).
Treatment legend – airstone: red circles; acid: pink diamonds; perm-tubing: blue squares; ambient control: green triangles

Using the determined sample alkalinity and a pCO_2 speciation calculator, CO_2 calc (Hunter 2007), actual DIC values were validated to within 2% of the predicted DIC values. During trial 2, DIC concentrations were significantly higher in the perm-tubing treatment (2114 $\mu\text{mol kg}^{-1}$) and airstone treatment (2125 $\mu\text{mol kg}^{-1}$) than the ambient control at 24 h (2070 $\mu\text{mol kg}^{-1}$, ANOVA $F_{1,3}$, $p < 0.01$), while the same treatment trend was detected at 96 h (ANOVA $F_{1,2}$, $p < 0.05$, Fig. 3.17). As previously discovered during trial 1, DIC concentrations were not significantly different between the acid treatment (2056 $\mu\text{mol kg}^{-1}$) and ambient control (2080 $\mu\text{mol kg}^{-1}$) at 96 h (Fig. 3.17).

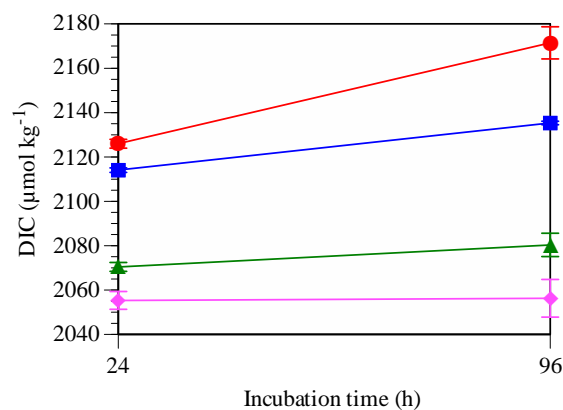


Fig. 3.17. DIC concentrations per treatment at 24 h and 96 h during trial 2 (mean \pm SE, n=3). Treatment legend – airstone: red circles; acid: pink diamonds; perm-tubing: blue squares; ambient control: green triangles

Summary of results

Overall, the results show that β -glucosidase activity was highest in the airstone treatment at 48 h and 96 h in both trials, while α -glucosidase was highest in the acid treatment (Table 3.2). Leu-aminopeptidase and Arg-aminopeptidase activity was highest in the acid treatment at 48 h and 96 h during trial 1. Bacterial cell numbers were highest in the acid treatment at 96 h during trials 1 and 2, while protein synthesis rates were highest in the acid treatment at 48 h during both trials (Table 3.2).

Table 3.2. Summary of each parameter response when compared to the ambient control ($p < 0.05$). Blue shade: significant response at 48 h; no shade: significant response at 96 h. ↑: parameter significantly higher than the ambient control; ↓: significantly lower; empty cell: no significant change was detected. 1: highest numerical response; 2: median numerical response; 3: lowest numerical response; ~: similar numerical values

Parameter	Trial 1 (late summer – May 2013)						Trial 2 (early spring – October 2013)					
	Airstone		Acid		Perm-tubing		Airstone		Acid		Perm-tubing	
β-glucosidase	↑ 1	↑ 1	↑ 2	↑ 2	↑ 3	↑ 3	↑ 1	↑ 1				↑ 2
α-glucosidase	↑ 2	↑ 2	↑ 1	↑ 1	↑ 3				↑ 1	↑ 1		
Arg-aminopeptidase			↑ 1	↑ 1					↓			
Leu-aminopeptidase		↑ ~	↑ 1	↑ 1			↑ ~	↑ 1	↑ ~	↑ ~	↑ 1	↑ ~
Bacterial numbers		↑ 1		↑ 2				↑ 1			↓	
<i>Synechococcus</i> spp. numbers							↓	↑ 1	↓		↓	
Total eukaryotic phytoplankton numbers				↓	↓		↓	↓				↑ 1
BSP (DNA synthesis)	↓	↑ 1			↓	↑ 2				↑ 1		
BSP (protein synthesis)			↑ 1	↑ ~	↑ 2	↑ ~		↑ 2	↑ 1	↑ 1		

3.3.4 Discussion

Temporal enzyme activity responses were different between the two trials, for instance, enzyme activities and cell-specific activities declined in each treatment during trial 1, whereas β -glucosidase activity, cell-specific β -glucosidase activity and Leu-aminopeptidase activity increased during trial 2. This opposing trend may signify differences in substrate concentrations and biological communities associated with the different times of year that each trial was conducted, autumn and early spring. β -glucosidase activity, cell-specific β -glucosidase activity and Leu-aminopeptidase activity was higher in trial 1 when compared to trial 2, possibly corresponding to a higher substrate concentration in trial 1. Vrba et al. (1992) reported a spring glucosidase activity maximum in eutrophic freshwater, while Engel et al. (2014) concluded that extracellular enzyme activity was tightly coupled with the availability of organic matter in the ocean. Total eukaryotic phytoplankton and *Synechococcus* spp. cell numbers were also higher in trial 1 when compared to trial 2, potentially due to the higher light and coastal water temperatures in autumn (Sverdrup et al. 1942a). The higher phytoplankton biomass in trial 1 could have produced a higher concentration of DOC either directly by cellular exudation, or indirectly by cell lysing from phytoplankton grazing (Kim et al. 2011), providing precursor materials for the abiotic formation of HMW organic matter (Zhou et al. 1998, Wurl et al. 2011) and thereby stimulating the higher overall enzyme activity detected. During trial 1, the large immediate difference in β -glucosidase and α -glucosidase activity between each treatment and the ambient control at time-zero supports the findings concluded during the short-term acidification trial (Section 3.2).

Regardless of seasonal differences between the two trials, the different acidification approaches had significantly different effects on enzyme activities and other parameters. The airstone treatment showed the highest β -glucosidase activity and cell-specific β -glucosidase activity in trials 1 and 2 (Table 3.2). The increased β -glucosidase activity may reflect a bubbling effect which could have ruptured phytoplankton cells, releasing labile organic substrates. This is supported by the immediate decline in total eukaryotic phytoplankton cell numbers in the airstone treatment in both trials. The negative phytoplankton response in the airstone treatment contradicts that reported by other researchers. For example, Chen & Durbin (1994) reported no significant difference in the response of the phytoplankton species *Thalassiosira pseudonana*

and *T. oceanica* between acid/base addition and CO₂ gas bubbling from a pH range of 7.0 to 9.4. Hoppe et al. (2011) compared the response of the coccolithophore *Emiliana huxleyi* to seawater media acidified by acid/base addition and CO₂ gas aeration, concluding no significant difference in growth or calcification rates between the methodologies, while Shi et al. (2009) also reported that there was no significant difference in the calcification or growth rate of *Emiliana huxleyi* between acidification using acid/base, buffers or CO₂ gas bubbling. In this thesis research, although the acid treatment was not shown to have a direct effect on phytoplankton cell numbers, the airstone treatment had a direct negative effect on total eukaryotic phytoplankton in both trials.

The acid treatment stimulated the highest α -glucosidase, Arg-aminopeptidase and Leu-aminopeptidase activity during trial 1, although this same response was not detected in trial 2 (Table 3.2). Again, this variation in enzyme response between trials may reflect differences in the availability of enzyme specific substrate. During trial 2, an indirect positive enzyme response was detected in the acid treatment from 72 h to 96 h, which could be explained by the change in carbonate chemistry increasing the rate of substrate coagulation, possibly increasing substrate stickiness (Mari 2008) when compared to the ambient control. The acid treatment also showed the only detectable α -glucosidase activity during trial 2, suggesting that the acid treatment may have differing indirect effects on different enzymes and their specific substrate compositions. Extracellular enzyme activities within the perm-tubing treatment were closest to those detected in the ambient control across all acidified treatments throughout trials 1 and 2.

The increase in enzyme activity would increase the availability of LMW organic matter for bacterial assimilation, supporting the late increase in bacterial cell numbers measured in the airstone treatment in trial 1 and 2 (Table 3.2). A positive bacterial response to physical bubbling was also discovered by Kepkay & Johnson (1989), who suggested that surface DOC coagulation facilitated by bubbling resulted in increased heterotrophic respiration and bacterial numbers. Bubbling may have increased the abiotic coagulation of organic matter and formation of HMW glucose based substrate when compared to the other acidified treatments. This could explain the increased β -glucosidase activity and cell-specific β -glucosidase activity measured, as well as the increase in total BSP. The trend in β -glucosidase activity, however was not detected for any other enzyme in either trial. It is possible that the shape, size or density of aryl-

β -glucosides and cellulose substrate makes these more susceptible to coagulation by bubbling when compared to other organic substrates, resulting in an increase in HMW β -linked glucose substrate relative to the other substrates present.

The airstone treatment also had a positive effect on DNA and protein synthesis rates from 72 h to 96 h during trial 1, while the acid treatment had the same effect in trial 2 (Table 3.2). The initial stimulation of β -glucosidase activity in trial 1 may have increased substrate availability for bacterial growth and assimilation as measured in the later phase of trial 1. As DNA and protein synthesis rates increased in the airstone treatment relative to the ambient control, both metabolic pathways were active in the bacterial community. During the initial stages of trial 2, all treatments showed similar DNA and protein synthesis rates to the ambient control, indicating that BSP was not directly affected by the method of acidification. During trial 1, protein synthesis in the perm-tubing treatment was not significantly different from any other acidified treatment, however during trial 2 protein synthesis in the perm-tubing treatment was significantly lower from 48 h to 96 h when compared to the acid treatment (Table 3.2). Due to the contrasting response between trials, a direct treatment affect is not likely. Importantly, the responses of extracellular enzyme activities, bacterial cell numbers and BSP in the perm-tubing treatment were closest to those measured in the ambient control.

The DNA synthesis response in the airstone treatment correlated well to the late increase in bacterial cell numbers in trial 1, while the high Arg-aminopeptidase and Leu-aminopeptidase activity in the acid treatment corresponded with an increase in protein synthesis and bacterial cell numbers throughout trial 1. These parameter correlations show that total BSP may have been correlated with the catabolic breakdown of HMW organic matter, providing LMW substrate suitable for heterotrophic assimilation and subsequent cellular growth (Alonso & Pernthaler 2006, Allers et al. 2007). Although similar temporal parameter correlations were not as obvious during trial 2, the airstone treatment does show a late increase in Leu-aminopeptidase activity which corresponds well to an increase in protein synthesis and a late increase in bacterial cell numbers. Research suggests that before bacteria can actively assimilate labile substrate into their cells, extracellular enzymes must first transform HMW into LMW products (Law 1980, Azam & Ammerman 1984, Azam & Cho 1987, Munster 1991).

In summary, trial 1 showed that coastal seawater acidified with either acid or CO₂ gas resulted in higher enzyme activities when compared to an ambient control. Variation in the response of extracellular enzymes to the different acidification methods was evident between trials run at different times of the year, most likely reflecting differences in the *in situ* organic matter concentration and bacterial community composition. Significant differences were measured in total glucosidase activity between the airstone treatment and perm-tubing treatment during trial 1, with higher activities detected in the airstone treatment. Total eukaryotic phytoplankton cell numbers declined in the airstone treatment during trial 2, possibly due to the mechanical effect of bubbling causing cell lysing. Significant differences were also measured in protease activity between the acid treatment and the perm-tubing treatment during trial 1, with higher activities detected in the acid treatment. Consequently, the method of acidification has an effect on extracellular enzyme activity. Parameter responses in the perm-tubing treatment were closest to those detected in the ambient control throughout both trials, and, combined with the fact that this method has the least impact on mixing, and also produces the correct species balance in carbonate chemistry, it is the most suitable method of acidification for use in future OA experimentation.

Chapter 4 : The response of enzyme activity to elevated temperature and low pH in near-surface open ocean phytoplankton blooms

4.1 Introduction

The initiation of a phytoplankton bloom requires a combination of suitable photosynthetic active radiation, surface ocean temperatures, dissolved nutrient concentrations, namely nitrogen and phosphorus, trace concentrations of iron and other elements, as well as a low grazing pressure (Sverdrup et al. 1942a). Phytoplankton blooms are characterised by the drawdown of dissolved nutrients and subsequent increase in phytoplankton cell numbers (Sverdrup et al. 1942a, Eppley & Peterson 1979, Finkel et al. 2010). Phytoplankton-derived organic exudation typically increases with increasing phytoplankton numbers until the bloom peaks (Sverdrup et al. 1942b, Engel et al. 2011, 2014). A high concentration of dissolved carbohydrates typically marks the peak in phytoplankton cell numbers (Engel et al. 2011, 2014), followed closely by a decline in numbers due to a combination of nutrient limitation and cell mortality, led by increasing grazing pressure and viral lysis (Engel et al. 2008, Danovaro et al. 2010).

Phytoplankton-derived dissolved organic matter (DOM) typically consists of a range of carbohydrates, proteins, amino acids and lipids (Williams 1975, Azam & Cho 1987, Benner 2002, Church 2008, Engel et al. 2011), the composition and concentration of which varies significantly throughout a bloom, as well as between different phytoplankton blooms (Carlson 2002, Engel et al. 2011, 2014). Some bloom-forming phytoplankton communities produce DOM which consists of a higher carbon or nitrogen component, while other bloom-forming communities may produce more DOM per cell (Engel et al. 2011, 2014). During a phytoplankton bloom, amino acids are often rapidly utilised and therefore typically occur in low concentrations. Complex carbohydrates however, take longer to degrade and often accumulate towards the end of a bloom (Engel et al. 2014).

Heterotrophic bacteria remineralise phytoplankton-derived particulate organic matter (POM) through the use of extracellular enzymes, producing labile low molecular weight (LMW) substrate which drives the microbial loop (Azam et al. 1983, Section 1.6) and supports a substantial portion of bacterial secondary production (Rich et al. 1996, Carlson 2002).

Ocean acidification and warming have a range of direct and indirect effects on bacterial extracellular enzyme activities. For instance, low pH may alter the ionisation state of the enzyme's component amino acids (Dixon 1953), affecting the polar and non-polar intramolecular attractive and repulsive forces within an enzyme, possibly leading to inhibition or altered substrate affinity. A reduction in pH may also change protein amino acid side chains into carbonyl groups (ketones and aldehydes) through oxidation (Suzuki et al. 2010). Low pH conditions could also have several indirect effects on extracellular enzyme activities such as changes in the phytoplankton and bacterioplankton community composition (Riebesell 2004, Engel et al. 2008, Witt et al. 2011, Endo et al. 2013), phytoplankton cell numbers (Riebesell et al. 1993, Schulz et al. 2013) and an increase in phytoplankton-derived carbon rich organic exudation (Engel 2002, Engel et al. 2014).

Temperature plays a key role in the regulation of enzyme kinetics, providing energy to overcome the activation energy of a specific enzyme (Zeebe & Wolf-Gladrow 2001, Daniel & Danson 2010), increasing its turnover rate. Elevated temperature may also have several indirect effects on extracellular enzyme activities, such as increases in bacterial metabolic potential (Sherr & Sherr 1996, Zeebe & Wolf-Gladrow 2001), increased exudation of phytoplankton-derived DOM (Engel et al. 2011) and abiotic coagulation and the formation of high molecular weight (HMW) organic matter (Engel 2002, Piontek et al. 2009), as well as a change in bacterial community composition (Finkel et al. 2010, Huertas et al. 2011). Because surface ocean organic matter composition and concentration are largely determined by the dominant phytoplankton community, a significant change in this community could alter the organic carbon available in the surface ocean (Carlson 2002, Moran et al. 2006, Kim et al. 2011, Tada et al. 2011, Engel et al. 2014). Differences in the composition, concentration and/or aggregation potential of phytoplankton-derived organic matter may affect hydrolysis of bacterial enzymes, as well as how enzyme activity will respond to elevated temperature and low pH conditions predicted to by the end of the century.

Engel et al. (2014) report that future low pH will enhance the production and particulate aggregation of organic matter during coastal phytoplankton bloom events. Similarly, research by Piontek et al. (2009) reported a significantly higher particle aggregation and total POM concentration under elevated temperatures. Engel et al. (2011) however, reported that elevated temperature may have a significant negative effect on the total amount of polysaccharides

produced during a phytoplankton bloom, but state that this is unlikely to affect dissolved amino acid composition. Because polysaccharides make up a significant proportion of DOC released by phytoplankton during a natural bloom formation (Engel et al. 2011, 2014) and are also components of HMW organic matter (Verdugo et al. 2004, Wurl et al. 2011), HMW substrate composition and concentration in the future ocean may depend on the effect of each individual driver on a spatial and temporal scale. Importantly, there is also the potential for interactive effects (additive, synergistic or antagonistic) between the two driving factors, which could also vary on spatial and temporal scales and between different bloom communities.

It is possible that elevated ocean temperature will alter the physical structure of the HMW substrate; its size, shape and/or density (Piontek et al. 2009). These changes could further influence the efficiency with which the substrate is broken down by extracellular enzymes (Münster 1991, Abdullahi et al. 2006). If extracellular enzyme activities differ between phytoplankton communities under elevated temperatures and low pH conditions predicted by the end of the century, variation in the remineralisation rates of surface ocean organic matter is likely to occur. This potential outcome would modify the strength and efficiency of the microbial loop, thereby affecting heterotrophic respiration and the vertical flux of organic matter entering the biological carbon pump. A significant change in the strength of the biological carbon pump could alter the amount of organic carbon sequestered and the overall balance of inorganic and organic carbon in the ocean.

The aim of the following chapter was to investigate potential changes in extracellular enzyme activities in response to elevated temperature and low pH predicted by the end of the century between different near-surface open ocean phytoplankton bloom types.

4.2 Methods

Four perturbation incubations (1 to 4) were completed during two research cruises in 2012. Time-zero bulk seawater for incubations 1, 2 and 3 was collected from a depth of 10 m from independent sites across the Chatham Rise, New Zealand (Fig. 4.1). Time-zero bulk seawater for incubation 4 was collected from a depth of 10 m outside the Cook Strait, South Coast, North Island (Fig. 4.1).

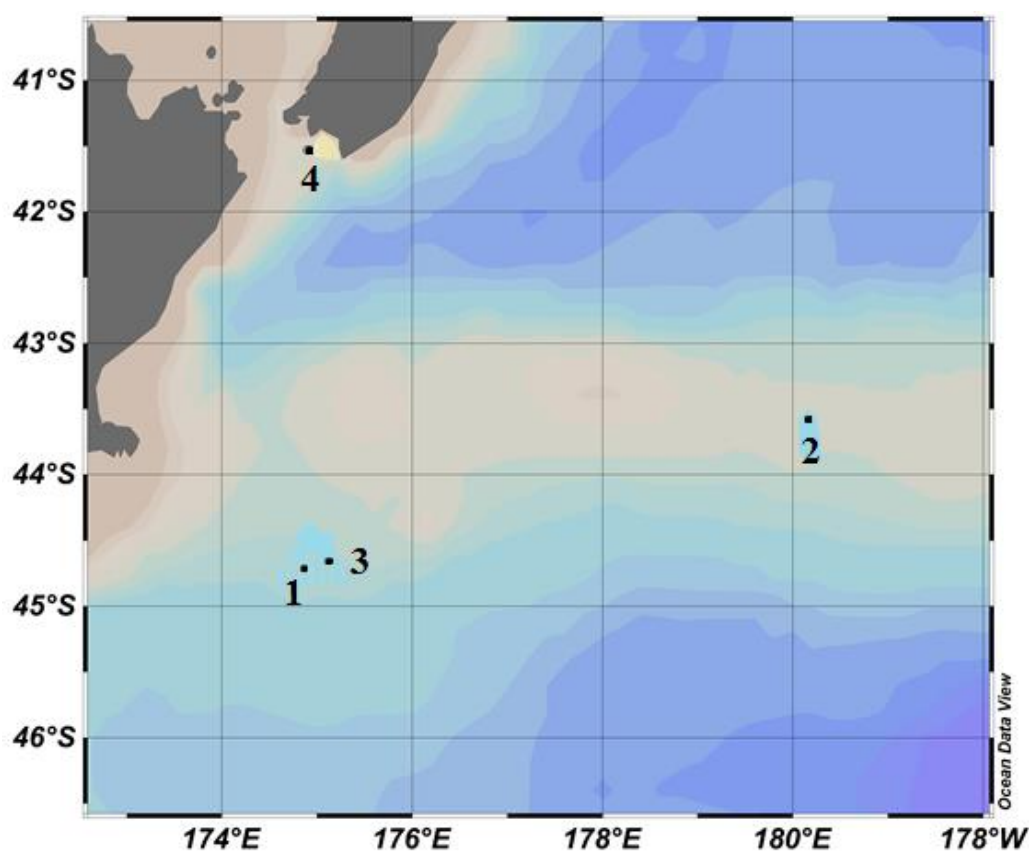


Fig. 4.1. Bulk seawater collection sites for incubations 1 to 4. Colour bathymetry highlights the Chatham Rise off the East Coast of the South Island, New Zealand. Annotated numbers correspond to respective incubation experiments

Seawater was collected from an independent phytoplankton bloom of differing community composition and cell abundance at the four locations. A typical phytoplankton bloom is defined as $> 1 \text{ mg l}^{-1}$ Chl *a*, however in this research, some incubation experiments are referred to as blooms despite not meeting this criterion. Bloom communities used for incubations 1 to 3 were

identified by their optical properties using satellite imagery. For instance, coccolithophore blooms were identified by their characteristic turquoise reflectance, whereas non-calcifying phytoplankton blooms were identified by a green-brown colouration. Once located, the bloom centre was determined by shipboard underway measurements including Chl *a*, pCO₂, dimethyl sulphide concentration and backscatter. Dominant bloom community compositions were determined by Karl Safi (NIWA, Hamilton) using microscopy following sample collection. Bulk seawater was collected using a Seabird Electronics Inc. 32 Carousel water sampler fitted with 24 x 10 l external-spring Niskin-type bottles (Ocean Test Equipment Standard 10 BES). *In situ* water column parameters were monitored and depths acquired using a Seabird Electronics Inc. 911 plus conductivity, temperature and depth sensor (CTD) attached to the carousel water sampler.

Following the protocol in Section 2.1, three treatments (OA, HT and GH) including an ambient control were created. Seawater was not prefiltered. pH and temperature was measured at selected sampling points throughout each incubation (Appendix A: 4.1). Each treatment was incubated and housed in one of the two previously described incubation chambers (Section 2.1). Incubations 1, 2 and 3 were each conducted over a six day period (144 h), with a range of biotic and abiotic parameters sampled at predetermined times (Table 4.1). Cruise logistics dictated incubation periods, with incubation 4 restricted to only five days (120 h). During incubation 4, the same parameters were investigated as in incubations 1 to 3, but were sampled using a different sampling regime (Table 4.1). Enzyme samples collected during incubations 1, 2 and 3 could not be analysed at sea; instead these were frozen at -80°C and processed post cruise. A lower enzyme activity is detected from frozen seawater samples when compared with fresh seawater (pers. comm. Dr Els Maas, NIWA), however previous work conducted by E. Maas suggests that there is no significant difference in enzyme activity if -80°C frozen samples are analysed rapidly post cruise. Land-based enzyme assays were processed using the methodology described in Section 2.3.

Table 4.1. Parameter sampling protocol for incubations 1 to 4. The total number of times a particular parameter was sampled is indicated, followed by its respective sampling frequency [in square brackets], after an initial time-zero sample. Parameters in **bold** indicate primary sampling significance

Incubation	1	2	3	4
Location ($^{\circ}$)	44.61 $^{\circ}$ N 174.77 $^{\circ}$ E	43.59 $^{\circ}$ N 180.17 $^{\circ}$ E	44.54 $^{\circ}$ N 174.88 $^{\circ}$ E	41.53 $^{\circ}$ N 174.90 $^{\circ}$ E
Duration	15.02.13 – 21.02.12	22.02.12 – 28.02.12	29.02.12 – 06.03.12	17.03.12 – 22.03.12
Depth (m)	10	10	10	10
Ambient temperature ($^{\circ}$ C)	11.8	15.8	14.5	14.2
Salinity (psu)	34.46	34.66	34.49	34.68
Phytoplankton community composition at time-zero	Mixed dinoflagellate/diatom	Mixed (dinoflagellate, coccolithophore & small flagellates)	Mixed (dinoflagellate, coccolithophore & small flagellates)	Unidentified
Parameter sampled				
β-glucosidase and α-glucosidase	11 [12 h]	11 [12 h]	11 [12 h]	9 [12 h]
Leu-aminopeptidase and Arg-aminopeptidase	11 [12 h]	11 [12 h]	11 [12 h]	9 [12 h]
Bacterial cell numbers	11 [12 h]	11 [12 h]	11 [12 h]	9 [12 h]
Pico-cyanobacteria cell numbers	2 [72 h]	2 [72 h]	2 [72 h]	2 [60 h]
Total eukaryotic phytoplankton cell numbers	2 [72 h]	2 [72 h]	2 [72 h]	2 [60 h]
BSP DNA synthesis	4 [36 h]	4 [36 h]	4 [36 h]	4 [30 h]
BSP protein synthesis	2 [72 h]	2 [72 h]	2 [72 h]	2 [60 h]
Dissolved nutrients	1 [144 h]	1 [144 h]	1 [144 h]	2 [60 h]
Chl <i>a</i>	1 [144 h]	1 [144 h]	1 [144 h]	2 [60 h]
DOC	1 [144 h]	1 [144 h]	1 [144 h]	1 [120 h]
Total HMW organic compound (reducing-sugar and protein)	2 [72 h]	2 [72 h]	2 [72 h]	2 [60 h]

4.3 Results

Comparison of ambient conditions

Microscopy of bulk seawater samples showed that incubation 1 phytoplankton biomass was dominated by dinoflagellates with a minor diatom component. Bulk seawater collected for incubations 2 and 3 represented a mixed community consisting mainly of coccolithophores, dinoflagellates and a range of silicoflagellates, cryptomonads, and euglenoids, categorised here as ‘other’ (Fig. 4.2). The bulk seawater phytoplankton composition of incubation 4 was not determined.

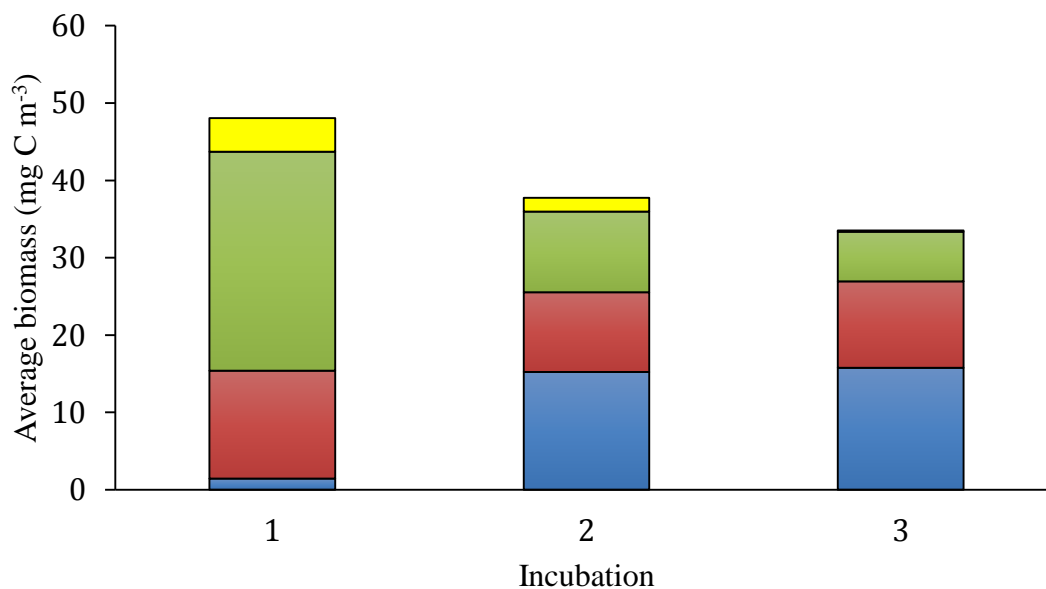


Fig. 4.2. Average time-zero phytoplankton composition determined by microscopy from three blooms used in incubations 1, 2 and 3. Diatoms: yellow; dinoflagellates: green; other: red; coccolithophores: blue (microscopy Karl Safi – NIWA)

As expected from the variation in phytoplankton composition between blooms 1, 2 and 3 (Fig. 4.2), time-zero sampled parameters were different between each incubation (Table 4.2).

Table 4.2. Average time-zero data for each sampled parameter per incubation (\pm SE). Samples were analysed following methodology in Chapter 2. Empty cell: not determined

Parameter	Incubation 1	Incubation 2	Incubation 3	Incubation 4
β -glucosidase (nmol l ⁻¹ h ⁻¹) (n=2)	0	0.04 (\pm 0.01)	0	0.13 (\pm 0.03)
α -glucosidase (nmol l ⁻¹ h ⁻¹) (n=2)	0	0	0	0
Arg-aminopeptidase (nmol l ⁻¹ h ⁻¹) (n=2)	0	3.94 (\pm 0.37)	7.29 (\pm 0.66)	0
Leu-aminopeptidase (nmol l ⁻¹ h ⁻¹) (n=2)	0.84 (\pm 0.21)	6.12 (\pm 0.75)	2.67 (\pm 0.21)	23.13 (\pm 6.48)
Bacterial numbers (cells ml ⁻¹) (n=3)	5 x 10 ⁵ (\pm 4.9 x10 ³)	1 x 10 ⁶ (\pm 2.0 x10 ⁴)	6 x 10 ⁵ (\pm 3.6 x10 ⁶)	5 x 10 ⁵ (\pm 7.8 x10 ³)
<i>Synechococcus</i> spp. numbers (cells ml ⁻¹) (n=3)	3 x 10 ⁴ (\pm 8.7 x10 ³)	4 x 10 ⁴ (\pm 3.0 x10 ³)	1 x 10 ⁴ (\pm 1.0 x10 ³)	1 x 10 ⁴ (\pm 3.2 x10 ²)
<i>Prochlorococcus</i> spp. numbers (cells ml ⁻¹) (n=3)		3 x 10 ³ (\pm 3.0 x10 ²)		6 x 10 ³ (\pm 2.8 x10 ²)
Total eukaryotic phytoplankton numbers (cells ml ⁻¹) (n=3)	9 x 10 ³ (\pm 1.1 x10 ³)	1 x 10 ⁴ (\pm 1.1 x10 ³)	2 x 10 ³ (\pm 1.6 x10 ²)	9 x 10 ³ (\pm 2.1 x10 ²)
BSP DNA synthesis (μ g C l ⁻¹ d ⁻¹) (n=3)	1.56 (\pm 0.02)	3.83 (\pm 0.03)	3.82 (\pm 0.11)	4.25 (\pm 0.19)
BSP protein synthesis (μ g C l ⁻¹ d ⁻¹) (n=3)	1.22 (\pm 0.00)	1.73 (\pm 0.02)	1.19 (\pm 0.05)	1.04 (\pm 0.03)
Nitrate (μ g l ⁻¹) (n=3)	85.37 (\pm 9.11)	35.23 (\pm 0.85)	58.15 (\pm 3.10)	46.07 (\pm 0.46)
DRP (μ g l ⁻¹) (n=3)	51.02 (\pm 0.66)	4.55 (\pm 1.33)	18.36 (\pm 4.87)	50.85 (\pm 0.45)
DRSi (μ g l ⁻¹) (n=3)	5.25 (\pm 0.82)	4.67 (\pm 0.58)	2.90 (\pm 1.42)	50.03 (\pm 0.27)
Ammonium (μ g l ⁻¹) (n=3)	3.28 (\pm 0.82)	2.61 (\pm 0.38)	11.65 (\pm 2.24)	3.05 (\pm 0.75)
Chl <i>a</i> (μ g ml ⁻¹) (n=6)	0.52 (\pm 0.16)	0.54 (\pm 0.02)	0.37 (\pm 0.01)	1.59 (\pm 0.04)
DOC (μ g ml ⁻¹) (n=2)	0.85 (\pm 0.02)	23.43 (\pm 0.42)	20.00 (\pm 0.31)	0.84 (\pm 0.01)
Total HMW reducing-sugar (μ g ml ⁻¹ gluc eq.) (n=2)	0.02 (\pm 0.00)	0.01 (\pm 0.01)	0.02 (\pm 0.01)	0.01 (\pm 0.00)
Total HMW protein (μ g ml ⁻¹ BSA eq.) (n=2)	0.34 (\pm 0.13)	1.17 (\pm 0.01)	0.39 (\pm 0.06)	0.80 (\pm 0.10)

4.3.1 Extracellular enzyme activity

4.3.1.1 Incubation 1

Very little β -glucosidase, α -glucosidase or Arg-aminopeptidase activity was detected throughout incubation 1, and as a result, no clear treatment response was detected. No β -glucosidase activity was detected in the first 72 h of incubation 1 (Fig. 4.3). The β -glucosidase activity was first detected in the OA treatment at 84 h ($0.07 \text{ nmol l}^{-1} \text{ h}^{-1}$), showing highly variable activity within and between treatments; despite this, activity increased across all treatments from 84 h to 144 h (Fig. 4.3). Very little α -glucosidase activity was detected throughout incubation 1, with activity first detected in the OA treatment at 132 h ($0.07 \text{ nmol l}^{-1} \text{ h}^{-1}$). Due to large within treatment variation, α -glucosidase activity in the OA treatment was not significantly different from the ambient control at 144 h. In contrast to α -glucosidase activity, Leu-aminopeptidase activity was detected in each treatment at each sampling point (Fig. 4.3). The Leu-aminopeptidase activity increased throughout the incubation with the highest activities detected in the OA treatment (Fig. 4.3). The Arg-aminopeptidase activity was first detected in the OA treatment at 36 h ($1.23 \text{ nmol l}^{-1} \text{ h}^{-1}$), with activity increasing in each treatment to 144 h (Fig. 4.3). The Arg-aminopeptidase activity in the OA treatment ($12.89 \text{ nmol l}^{-1} \text{ h}^{-1}$) was almost twice as high as that in the GH treatment ($6.89 \text{ nmol l}^{-1} \text{ h}^{-1}$), while activity was significantly higher in both treatments than the ambient control at 144 h ($1.15 \text{ nmol l}^{-1} \text{ h}^{-1}$, Fig. 4.3, p-values in Appendix C: 4.1). The Leu-aminopeptidase activity increased significantly across all treatments from 24 h to 144 h (RM-ANOVA $F_{10, 80} = 38.67$, $p < 0.0001$, Fig. 4.3), however activity was higher in the GH and OA treatments when compared to the HT treatment and ambient control. Q_{10} values for Leu-aminopeptidase activity determined from two sampling points ranged from 10.21 to 11.65 in the HT treatment.

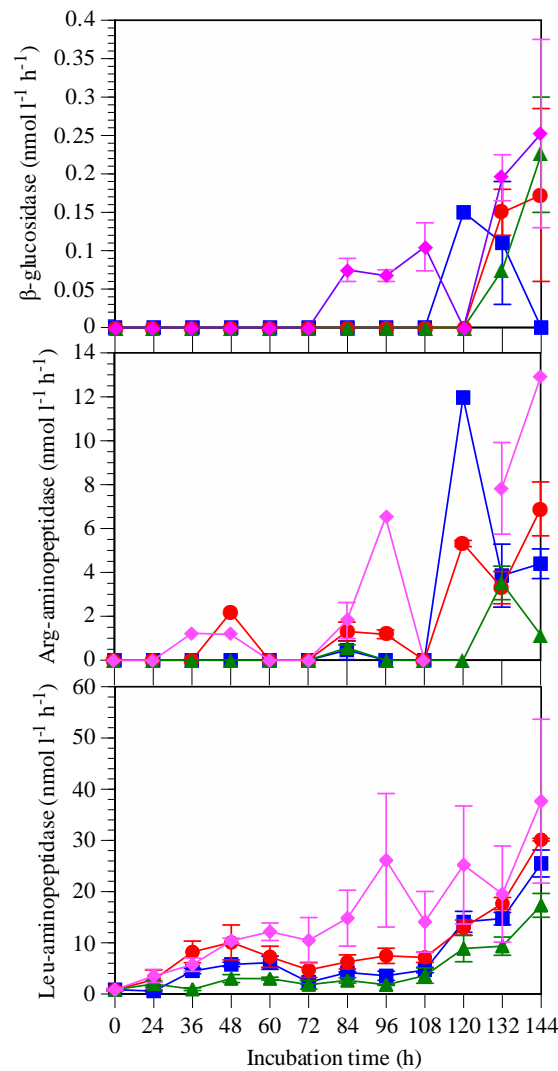


Fig. 4.3. Extracellular enzyme activities throughout incubation 1 (mean \pm SE, $n=3$). Data below detection limits are shown as zero. Treatment legend – HT: blue squares; GH: red circles; OA: pink diamonds; ambient control: green triangles

Due to low β -glucosidase activity during incubation 1, treatment comparisons using cell-specific β -glucosidase activity could not be calculated (Fig. 4.4). Cell-specific Leu-aminopeptidase activity however increased across all treatments from time-zero to 144 h (Fig. 4.4). The only time temperature had an effect was at 36 h, where cell-specific activity in the HT treatment ($4.41 \text{ amol cell}^{-1} \text{h}^{-1}$) was significantly higher than the ambient control ($2.75 \text{ amol cell}^{-1} \text{h}^{-1}$, ANOVA $F_{1,2}$, $p < 0.05$, Fig. 4.4). Cell-specific activity in the OA treatment ($6.33 \text{ amol cell}^{-1} \text{h}^{-1}$) was 30% higher than in the HT treatment ($4.41 \text{ amol cell}^{-1} \text{h}^{-1}$) at 36 h, while at 72 h, cell-specific Leu-aminopeptidase activity was almost three times higher

(9.26 $\text{amol cell}^{-1} \text{h}^{-1}$) than the ambient control (3.42 $\text{amol cell}^{-1} \text{h}^{-1}$, ANOVA $F_{1,2} = 32.43$, $p < 0.05$, Fig. 4.4). Cell-specific Leu-aminopeptidase activity in the GH treatment was not significantly different from the ambient control at any sampling point (Fig. 4.4).

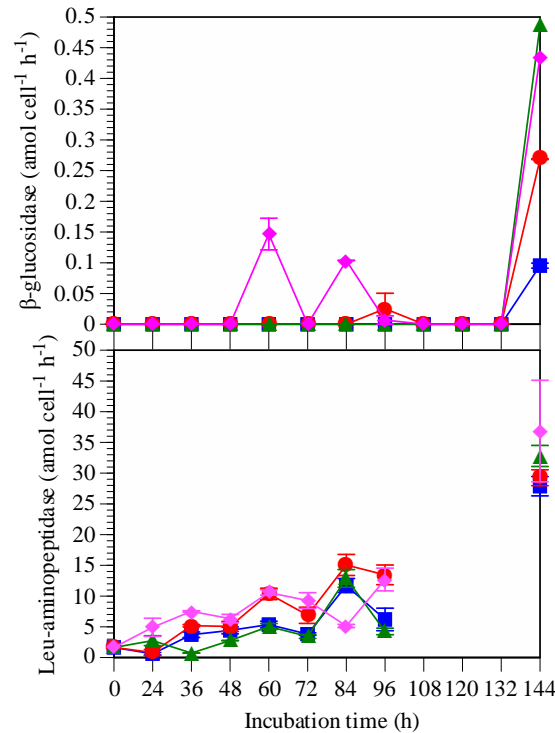


Fig. 4.4. Cell-specific extracellular enzyme activities throughout incubation 1 (mean \pm SE, $n=3$). Data below detection limits are shown as zero. No value indicates missing sample. Treatment legend – HT: blue squares; GH: red circles; OA: pink diamonds; ambient control: green triangles

4.3.1.2 Incubation 2

Throughout incubation 2 enzyme activity was highly variable in the OA treatment. The β -glucosidase and Arg-aminopeptidase activity fluctuated substantially in the OA and GH treatments (Fig. 4.5), while α -glucosidase activity was below detection in each treatment which prevented the interpretation of enzyme response. Overall, the highest β -glucosidase and Leu-aminopeptidase activity was measured in the OA treatment, however due to the large sample variability, activities were only significantly different from the ambient control at selected sampling points. Further analysis of the measured trends showed that β -glucosidase activity

peaked at 36 h in the OA treatment, and then declined from 84 h to 144 h (Fig. 4.5). The β -glucosidase activity was almost three times higher in the OA treatment ($0.26 \text{ nmol l}^{-1} \text{ h}^{-1}$) than the ambient control at 48 h ($0.09 \text{ nmol l}^{-1} \text{ h}^{-1}$, Fig. 4.5 & Appendix C: 4.1), while activity was significantly higher in each treatment when compared to the ambient control at 72 h (Fig. 4.5 & Appendix C: 4.1). Arg-aminopeptidase activity fluctuated substantially across all treatments from 24 h to 144 h with no clear treatment response detected (Fig. 4.5). Leu-aminopeptidase activity in the GH treatment ($13.73 \text{ nmol l}^{-1} \text{ h}^{-1}$) and OA treatment ($17.69 \text{ nmol l}^{-1} \text{ h}^{-1}$) was more than twice that of the ambient control at 48 h ($6.67 \text{ nmol l}^{-1} \text{ h}^{-1}$, Fig. 4.5 & Appendix C: 4.1). The Q_{10} values for Leu-aminopeptidase activity determined from two sampling points ranged from 1.20 to 8.50 in the HT treatment.

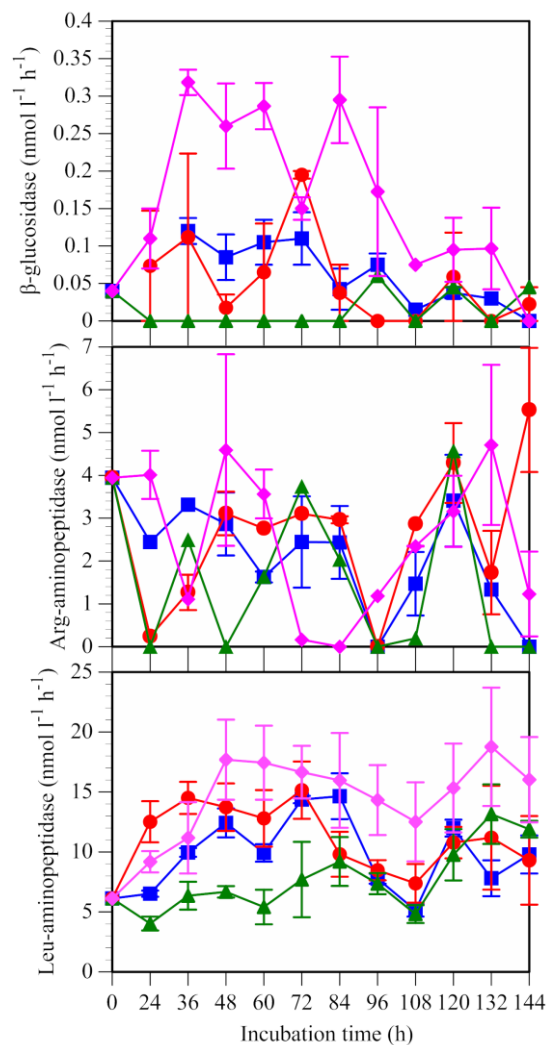


Fig. 4.5. Extracellular enzyme activities throughout incubation 2 (mean \pm SE, $n=3$). Data below detection limits are shown as zero. Treatment legend – HT: blue squares; GH: red circles; OA: pink diamonds; ambient control: green triangles

Cell-specific β -glucosidase activity followed a very similar trend to that of the potential activity, showing very low activity in the ambient control (Fig. 4.6). Cell-specific β -glucosidase activity increased in both the OA and GH treatments from time-zero to 36 h and was significantly higher than the ambient control at 24 h, 48 h, and 72 h (ANOVA $F_{1,3}$, $p < 0.05$, Fig. 4.6). Cell-specific activity in the OA and GH treatments declined from 72 h to 108 h (Fig. 4.6), while activity in the HT treatment was significantly higher than the ambient control at 72 h ($0.02 \text{ amol cell}^{-1} \text{ h}^{-1}$) and 96 h only ($0.03 \text{ amol cell}^{-1} \text{ h}^{-1}$, ANOVA $F_{1,3}$, $p < 0.05$, Fig. 4.6). Cell-specific Leu-aminopeptidase activity was higher in each treatment when compared to the ambient control from 24 h to 72 h (Fig. 4.6), with each treatment significantly higher than the ambient control at 48 h, 72 h and 108 h (ANOVA $F_{1,3}$, $p < 0.05$, Fig. 4.6). There was no clear difference in cell-specific Leu-aminopeptidase activity between each treatment throughout incubation 2 (Fig. 4.6).

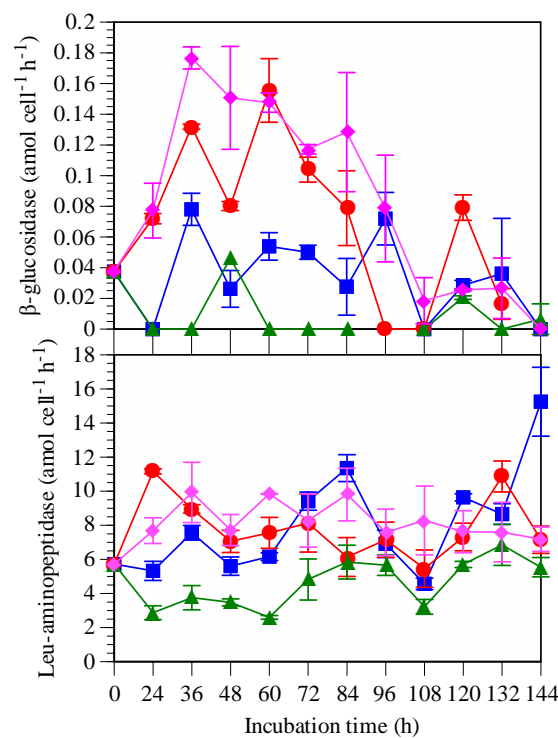


Fig. 4.6. Cell-specific extracellular enzyme activities throughout incubation 2 (mean \pm SE, $n=3$). Data below detection limits are shown as zero. Treatment legend – HT: blue squares; GH: red circles; OA: pink diamonds; ambient control: green triangles

4.3.1.3 Incubation 3

Throughout incubation 3, β - and α -glucosidase activity was higher in each treatment when compared to the ambient control, with the highest activity detected in the HT and GH treatments (Fig. 4.7). Both β - and α -glucosidase activity followed similar activity profiles, with both showing a spike in activity at 72 h (Fig. 4.7). The α -glucosidase activity was significantly different between each perturbation treatment from 96 h to 120 h, but not at 144 h. The α -glucosidase activity in the HT treatment ($0.68 \text{ nmol l}^{-1} \text{ h}^{-1}$) was more than four-fold higher than in the ambient control at 108 h ($0.16 \text{ nmol l}^{-1} \text{ h}^{-1}$, Fig. 4.7 & Appendix C: 4.1) and activity in the GH treatment ($0.42 \text{ nmol l}^{-1} \text{ h}^{-1}$) was almost three-fold higher (Fig. 4.7 & Appendix C: 4.1). The α -glucosidase activity was also 63% higher in the OA treatment ($0.24 \text{ nmol l}^{-1} \text{ h}^{-1}$) when compared to the ambient control at 144 h ($0.09 \text{ nmol l}^{-1} \text{ h}^{-1}$, ANOVA $F_{1,4} = 47.62$, $p < 0.01$, Fig. 4.7 & Appendix C: 4.1). The Arg- and Leu-aminopeptidase activity was higher in each treatment when compared to the ambient control, however in contrast to glucosidase activity, the highest protease activity was detected in the OA treatment (Fig. 4.7). Arg- and Leu-aminopeptidase activity increased significantly across all treatments from 36 h to 144 h. Both Arg- and Leu-aminopeptidase activity were significantly higher in the OA and HT treatment when compared to the ambient control at 72 h and 108 h (Fig. 4.7 & Appendix C: 4.1). Q_{10} values for β -glucosidase and Leu-aminopeptidase activity in the HT treatment determined from two sampling points, ranged from 10.92 to 2687.39 and 5.96 to 20.61 respectively.

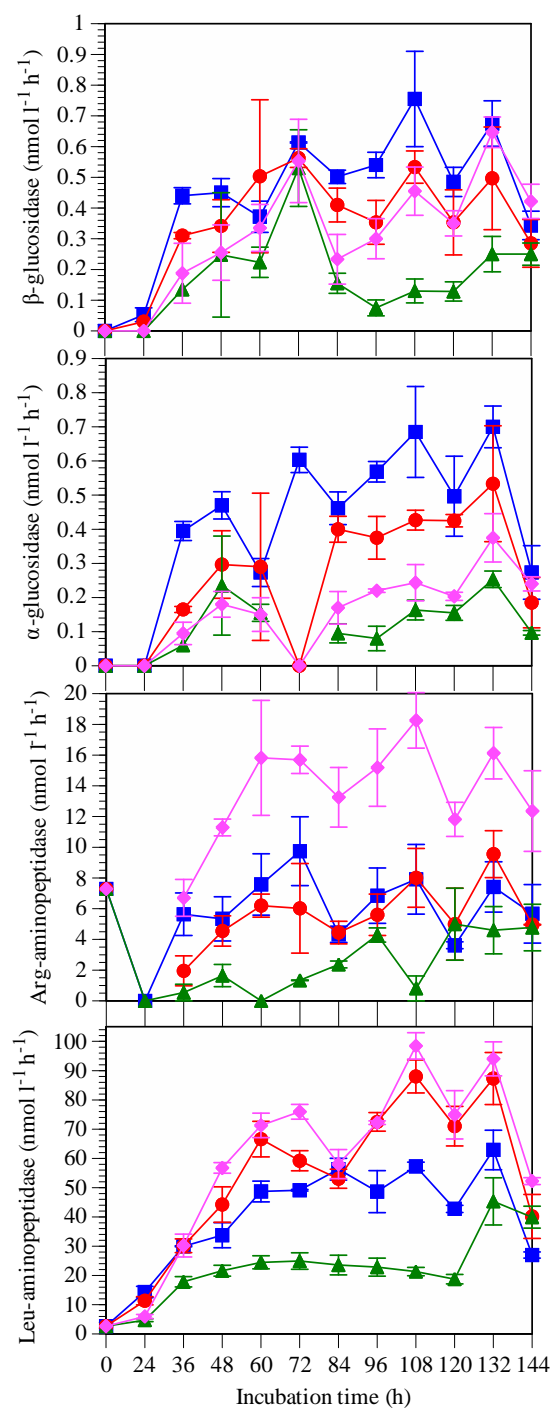


Fig. 4.7. Extracellular enzyme activities throughout incubation 3 (mean \pm SE, n=3). Data below detection limits are shown as zero. Treatment legend – HT: blue squares; GH: red circles; OA: pink diamonds; ambient control: green triangles

Cell-specific β -glucosidase activity was highly variable for the first 72 h of incubation 3, however activity in the GH treatment ($0.24 \text{ amol cell}^{-1} \text{ h}^{-1}$), the HT treatment ($0.25 \text{ amol cell}^{-1} \text{ h}^{-1}$) and the OA treatment ($0.24 \text{ amol cell}^{-1} \text{ h}^{-1}$) were all six-fold higher than the ambient control at 108 h ($0.04 \text{ amol cell}^{-1} \text{ h}^{-1}$, ANOVA $F_{1,2}$, $p < 0.05$, Fig. 4.8). Cell-specific β -glucosidase activity increased in the ambient control from 96 h ($0.03 \text{ amol cell}^{-1}$) to 144 h ($0.15 \text{ amol cell}^{-1}$), with a similar cell-specific activity in each treatment when compared to the ambient control at 144 h (Fig. 4.8). Cell-specific Leu-aminopeptidase activity was higher in each treatment when compared to the ambient control at each sampling point from time-zero to 144 h (Fig. 4.8). Cell-specific Leu-aminopeptidase activity was significantly higher in the GH, HT and the OA treatment when compared to the ambient control at 48 h, 72 h and 108 h (ANOVA $F_{1,3}$, $p < 0.05$, Fig. 4.8). Cell-specific Leu-aminopeptidase activity was statistically higher in the OA treatment when compared to the GH treatment at 48 h and 108 h, with activity in the OA treatment ranging from 31.13 to 44.53 $\text{amol cell}^{-1} \text{ h}^{-1}$ and 33.73 to 43.83 $\text{amol cell}^{-1} \text{ h}^{-1}$ in the GH treatment (ANOVA $F_{1,3}$, $p < 0.05$, Fig. 4.8).

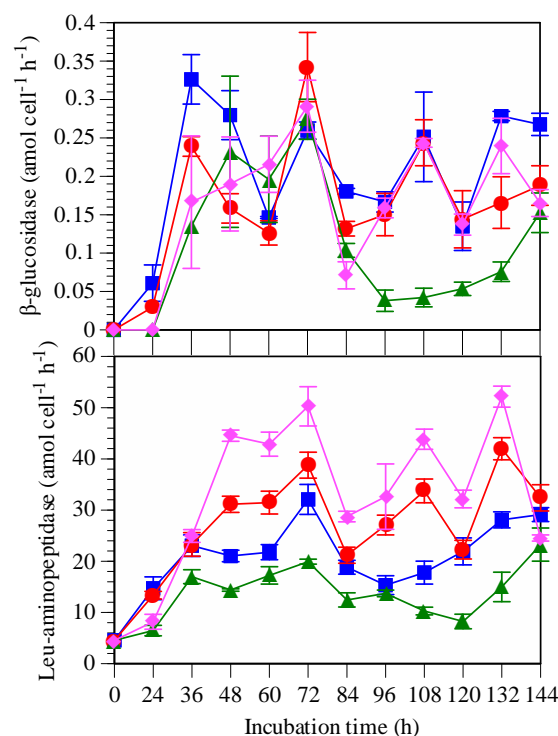


Fig. 4.8. Cell-specific extracellular enzyme activities throughout incubation 3 (mean \pm SE, $n=3$). Data below detection limits are shown as zero. Treatment legend – HT: blue squares; GH: red circles; OA: pink diamonds; ambient control: green triangles

4.3.1.4 Incubation 4

The β -glucosidase, α -glucosidase and Leu-aminopeptidase activity increased in each perturbation treatment from time-zero to 60 h; activity in the GH and HT treatment then declined below the ambient control, however enzyme activity in the OA treatment remained low for the duration of the incubation (Fig. 4.9). In contrast to this trend, Arg-aminopeptidase activity increased in the GH and HT treatments throughout (Fig. 4.9). Similar to incubations 2 and 3, Leu-aminopeptidase activity was higher than β -glucosidase activity in each treatment throughout incubation 4 (Fig. 4.9). Further analysis showed that β -glucosidase activity was almost twice as high in the HT treatment ($4.10 \text{ nmol l}^{-1} \text{ h}^{-1}$) when compared to the ambient control at 36 h ($2.19 \text{ nmol l}^{-1} \text{ h}^{-1}$), while α -glucosidase activity was also significantly higher in the HT treatment ($3.00 \text{ nmol l}^{-1} \text{ h}^{-1}$) than in the ambient control at 36 h ($1.29 \text{ nmol l}^{-1} \text{ h}^{-1}$, Fig. 4.9 & Appendix C: 4.1). However, the β -glucosidase activity ($1.57 \text{ nmol l}^{-1} \text{ h}^{-1}$) and α -glucosidase activity ($0.25 \text{ nmol l}^{-1} \text{ h}^{-1}$) was significantly lower in the HT treatment than in the ambient control at 120 h (4.18 and $2.43 \text{ nmol l}^{-1} \text{ h}^{-1}$ respectively, Fig. 4.9 & Appendix C: 4.1). Q_{10} values for β -glucosidase activity in the HT treatment determined from two sampling points, ranged from 0.01 to 3.39. The Leu-aminopeptidase activity was significantly higher in each treatment when compared to the ambient control at 36 h (Fig. 4.9 & Appendix C: 4.1). At 84 h however, Leu-aminopeptidase activity in both the HT treatment ($231.37 \text{ nmol l}^{-1} \text{ h}^{-1}$) and the GH treatment ($251.16 \text{ nmol l}^{-1} \text{ h}^{-1}$) was two-fold lower than in the ambient control ($448.91 \text{ nmol l}^{-1} \text{ h}^{-1}$, Fig. 4.9 & Appendix C: 4.1). At 96 h, Leu-aminopeptidase activity in the HT treatment ($114.96 \text{ nmol l}^{-1} \text{ h}^{-1}$) was more than four-fold lower than in the ambient control ($490.57 \text{ nmol l}^{-1} \text{ h}^{-1}$, Fig. 4.9 & Appendix C: 4.1). Q_{10} values for Leu-aminopeptidase activity in the HT treatment determined from two sampling points, ranged from 0.005 to 1.67. In contrast to Leu-aminopeptidase activity, Arg-aminopeptidase activity increased significantly across all treatments from 24 h to 120 h (RM-ANOVA $F_{8, 56} = 9.08$, $p < 0.0001$), however due to high within treatment variability, particularly within the ambient control, few statistically significant comparisons could be made.

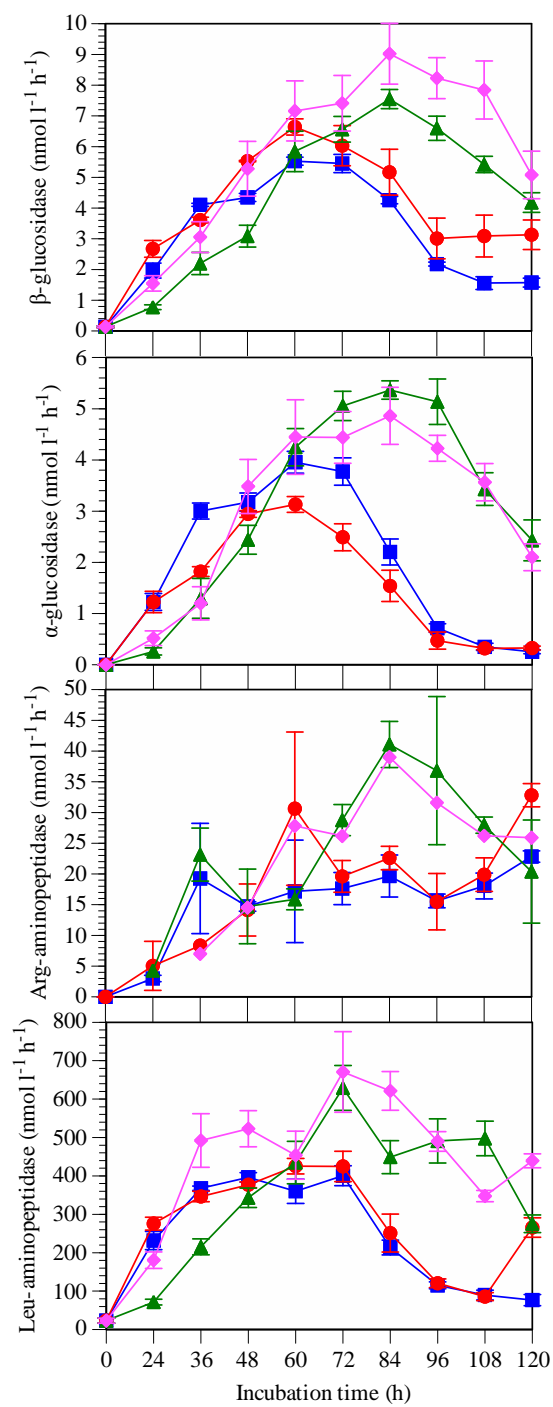


Fig. 4.9. Extracellular enzyme activities throughout incubation 4 (mean \pm SE, n=3). Data below detection limits are shown as zero. Treatment legend – HT: blue squares; GH: red circles; OA: pink diamonds; ambient control: green triangles

Cell-specific β -glucosidase activity increased in each treatment from time-zero to 24 h (Fig. 4.10). Activity was significantly higher in the GH treatment ($2.76 \text{ amol cell}^{-1} \text{ h}^{-1}$), the HT treatment ($2.48 \text{ amol cell}^{-1} \text{ h}^{-1}$) and the OA treatment ($2.57 \text{ amol cell}^{-1} \text{ h}^{-1}$) than in the ambient control at 24 h ($1.31 \text{ amol cell}^{-1} \text{ h}^{-1}$, ANOVA $F_{1, 4}$, $p \leq 0.01$, Fig. 4.10). Cell-specific β -glucosidase activity in each treatment was fairly stable from 36 h to 84 h (Fig. 4.10). At 96 h, activity in the GH treatment ($4.69 \text{ amol cell}^{-1} \text{ h}^{-1}$) increased to double the ambient control ($2.17 \text{ amol cell}^{-1} \text{ h}^{-1}$, ANOVA $F_{1, 2}$, $p < 0.05$, Fig. 4.10), while activity in the OA treatment ($2.87 \text{ amol cell}^{-1} \text{ h}^{-1}$) was 75% higher when compared to the ambient control (ANOVA $F_{1, 2}$, $p < 0.05$, Fig. 4.10). Cell-specific β -glucosidase activity increased in the GH and HT treatments from 96 h to 120 h, with activities significantly higher than in the ambient control at 120 h ($1.99 \text{ amol cell}^{-1} \text{ h}^{-1}$, ANOVA $F_{1, 3}$, $p < 0.01$, Fig. 4.10). Cell-specific Leu-aminopeptidase activity increased in each perturbation treatment from time-zero to 24 h (Fig. 4.10). Activity in each treatment was at least twice as high as the ambient control at 24 h ($134.72 \text{ amol cell}^{-1} \text{ h}^{-1}$, ANOVA $F_{1, 3}$, $p < 0.01$, Fig. 4.10), however activity then declined and was significantly lower in both elevated temperature treatments than the ambient control at 60 h ($177.99 \text{ amol cell}^{-1} \text{ h}^{-1}$, ANOVA $F_{1, 2}$, $p < 0.05$, Fig. 4.10). Cell-specific Leu-aminopeptidase activity in the HT treatment continued to decline from 60 h to 96 h, while activity in the GH treatment increased from 96 h to 120 h, where activity was five-fold higher than in the ambient control at 120 h ($138.98 \text{ amol cell}^{-1} \text{ h}^{-1}$, ANOVA $F_{1, 2}$, $p < 0.05$, Fig. 4.10).

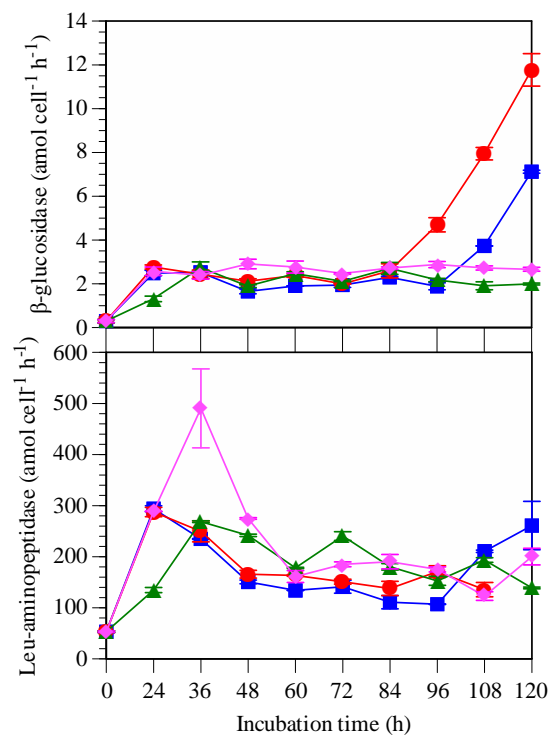


Fig. 4.10. Cell-specific extracellular enzyme activities throughout incubation 4 (mean \pm SE, n=3). Treatment legend – HT: blue squares; GH: red circles; OA: pink diamonds; ambient control: green triangles

The Leu-aminopeptidase to β -glucosidase activity ratio varied between treatments and incubations (Table 4.3). The activity ratio was higher in each treatment when compared to the ambient control during incubation 1, while the activity ratio was lower in the HT treatment when compared to the ambient control during incubations 2, 3 and 4 (Table 4.3). The activity ratio was higher in the OA treatment during incubations 1, 3 and 4 when compared to the HT and GH treatments. The Leu-aminopeptidase Δ hydrolysis potential was highest in the OA treatment and lowest in the HT treatment across each incubation (Table 4.3).

Table 4.3. The Leu-aminopeptidase to β -glucosidase activity ratio averaged across 144 h and the Leu-aminopeptidase Δ hydrolysis potential averaged across 72 h for each incubation

		HT	GH	OA	Control
Incubation 1	Leu-aminopeptidase: β -glucosidase	55.66	59.70	108.19	30.63
	Δ hydrolysis potential	8.52	22.31	31.51	
Incubation 2	Leu-aminopeptidase: β -glucosidase	147.02	150.96	82.62	162.22
	Δ hydrolysis potential	23.02	38.54	41.98	
Incubation 3	Leu-aminopeptidase: β -glucosidase	83.01	137.35	154.45	105.09
	Δ hydrolysis potential	82.36	117.93	146.59	
Incubation 4	Leu-aminopeptidase: β -glucosidase	73.12	66.51	77.45	80.99
	Δ hydrolysis potential	62.55	155.51	626.48	

Summary of results

Overall, glucosidase activity was low and highly variable throughout incubations 1 and 2. The HT temperature treatment had an initial positive effect on β -glucosidase activity at selected sampling points during incubations 2 and 4 (Table 4.4). Leu-aminopeptidase activity was significantly higher in the OA treatment than the ambient control at 72 h in each incubation. β -glucosidase, α -glucosidase and Arg-aminopeptidase activity was negatively affected by both elevated temperature treatments beyond 72 h during incubation 4 (Table 4.4).

Table 4.4. Summary of extracellular enzyme activity changes in each treatment when compared to the ambient control ($p < 0.05$). Blue shaded cells indicate a response at 72 h, neutral shaded cells indicate a response at the final sampling point (incubation 1 to 3 - 144 h, incubation 4 – 120 h). ↑: indicates the parameter was significantly higher than the ambient control; ↓: significantly lower; empty cell: not significantly different

Parameter	Incubation 1			Incubation 2			Incubation 3			Incubation 4		
	OA	HT	GH	OA	HT	GH	OA	HT	GH	OA	HT	GH
β-glucosidase				↑	↑	↑					↑	↓
α-glucosidase								↑			↑	↓
Arg-aminopeptidase				↓			↑	↑	↑		↓	↓
Leu-aminopeptidase	↑	↑	↑	↑	↑	↑	↑	↑	↑	↑	↑	↑

4.3.2 Cell numbers

4.3.2.1 Incubation 1

Bacterial cell numbers peaked at 48 h in each treatment including the ambient control. Cell numbers then declined and reached a minimum at 84 h before increasing again (Fig. 4.11). Bacterial cell numbers were significantly higher in each treatment when compared to the ambient control at 72 h (Fig. 4.11, p-values in Appendix C: 4.2), and significantly higher in the HT treatment (9×10^5 cells ml^{-1}) when compared to the ambient control at 144 h (6×10^5 cells ml^{-1} , ANOVA $F_{1,4} = 20.78$, $p = 0.01$, Fig. 4.11).

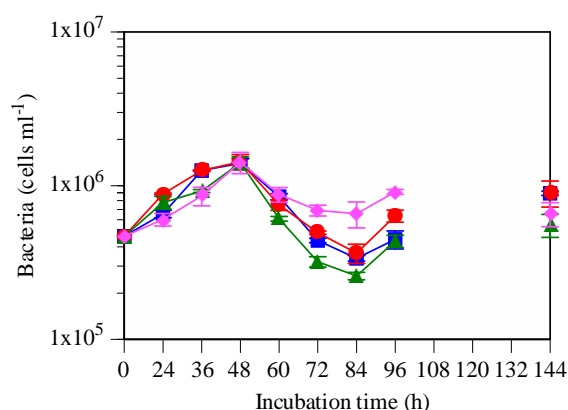


Fig. 4.11. Bacterial cell numbers (log scale) in incubation 1 (mean \pm SE, $n=3$). No value indicates missing sample. Treatment legend – HT: blue squares; GH: red circles; OA: pink diamonds; ambient control: green triangles

Synechococcus spp. cell numbers declined significantly across all treatments from 72 h to 144 h (RM-ANOVA $F_{1,8} = 104.96$, $p < 0.0001$), with cell numbers declining fastest in the OA treatment (Fig. 4.12). In contrast to *Synechococcus* spp., *Prochlorococcus* spp. cell numbers increased from 72 h to 144 h (Fig. 4.12). *Synechococcus* spp. cell numbers were significantly higher in both the HT treatment (7×10^3 cells ml^{-1}) and GH treatment (6×10^3 cells ml^{-1}) when compared to the ambient control at 144 h (3×10^3 cells ml^{-1}). Total eukaryotic phytoplankton cell numbers declined across all treatments from time-zero to 72 h, then increased significantly from 72 h to 144 h (RM-ANOVA $F_{1,8} = 11.98$, $p < 0.01$, Fig. 4.12). Total eukaryotic

phytoplankton cell numbers were significantly higher in the HT treatment when compared to the ambient control at 144 h (Fig. 4.12 & Appendix C: 4.2).

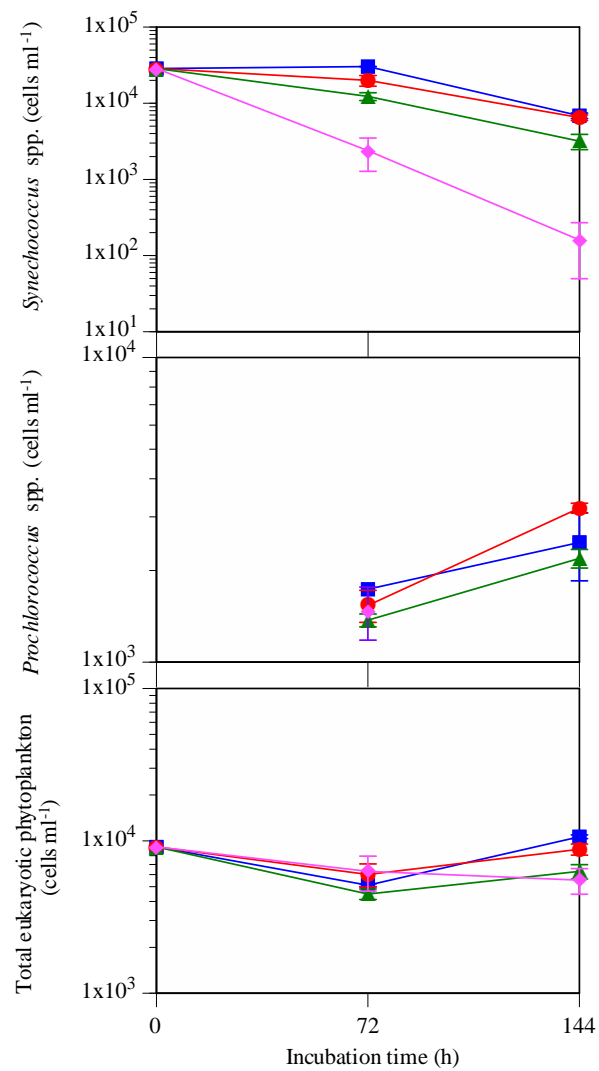


Fig. 4.12. *Synechococcus* spp., *Prochlorococcus* spp. and total eukaryotic phytoplankton cell numbers (log scale) in incubation 1 (mean \pm SE, n=3). No value indicates missing sample. Treatment legend – HT: blue squares; GH: red circles; OA: pink diamonds; ambient control: green triangles

4.3.2.2 Incubation 2

Bacterial cell numbers increased in each treatment including the ambient control from time-zero to 48 h (Fig. 4.13). Bacterial cell numbers declined from 72 h to 144 h in both the HT treatment (2×10^6 to 7×10^5 cells ml^{-1}) and the GH treatment (2×10^6 to 1×10^6 cells ml^{-1}), while cell numbers increased in the ambient control (1.5×10^6 to 2.4×10^6 cells ml^{-1}) and OA treatment (1.6×10^6 to 2.3×10^6 cells ml^{-1} , Fig. 4.13). At 144 h, cell numbers were significantly lower in the GH treatment (1×10^6 cells ml^{-1}) when compared to the ambient control (2×10^6 cells ml^{-1} , ANOVA $F_{1,4} = 10.23$, $p < 0.05$, Fig. 4.13).

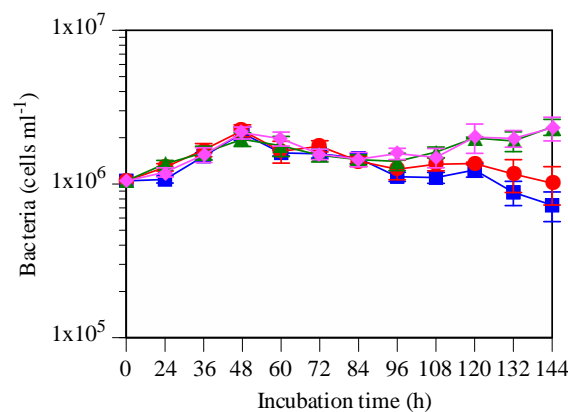


Fig. 4.13. Bacterial cell numbers (log scale) in incubation 2 (mean \pm SE, $n=3$). Treatment legend – HT: blue squares; GH: red circles; OA: pink diamonds; ambient control: green triangles

Synechococcus spp. cell numbers declined in each treatment from time-zero to 72 h, with a significantly higher cell number in the OA treatment when compared to the ambient control at 72 h (ANOVA $F_{1,4} = 40.97$, $p < 0.01$, Fig. 4.14). *Synechococcus* spp. cell numbers continued to decline in the OA treatment until 144 h, at which time cell numbers in the OA and HT treatments were significantly lower than the ambient control (ANOVA $F_{1,2}$, $p < 0.05$, Fig. 4.14). Similar to that determined in incubation 1, the trend in *Prochlorococcus* spp. cell numbers contrasted with *Synechococcus* spp. and increased in all treatments including the ambient control from time-zero to 72 h (Fig. 4.14). At 144 h, *Prochlorococcus* spp. cell numbers were significantly higher in the OA treatment than in the ambient control (ANOVA $F_{1,3} = 10.75$, $p < 0.05$). Total eukaryotic phytoplankton cell numbers declined significantly

across all treatments from 72 h to 144 h (RM-ANOVA $F_{1, 8}$, $p < 0.05$). Total eukaryotic phytoplankton cell numbers were significantly lower in both the HT and GH treatments than in the ambient control at 144 h (ANOVA $F_{1, 2}$, $p < 0.05$, Fig. 4.14).

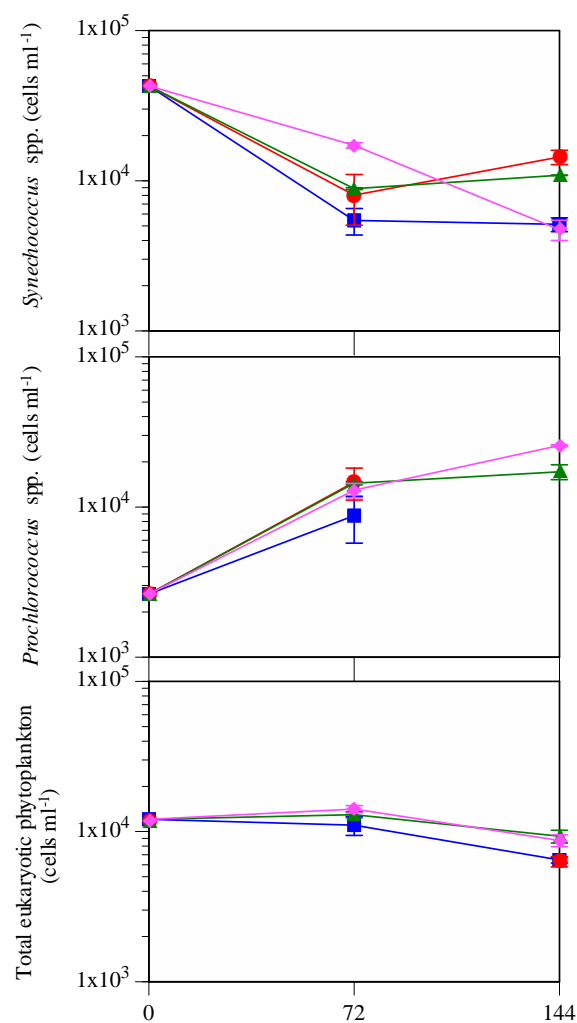


Fig. 4.14. *Synechococcus* spp., *Prochlorococcus* spp. and total eukaryotic phytoplankton cell numbers (log scale) in incubation 2 (mean \pm SE, $n=3$). No value indicates missing sample. Treatment legend – HT: blue squares; GH: red circles; OA: pink diamonds; ambient control: green triangles

4.3.2.3 Incubation 3

Bacterial cell numbers increased significantly across all treatments including the ambient control from 24 h to 144 h (RM-ANOVA $F_{10, 80} = 65.85$, $p < 0.0001$, Fig. 4.15). Although cell numbers remained similar between each treatment for much of the incubation, cell numbers were significantly higher in the HT treatment (2×10^6 cells ml^{-1}) than the ambient control at 72 h (1×10^6 cells ml^{-1} , ANOVA $F_{1, 4} = 20.13$, $p = 0.01$, Fig. 4.15).

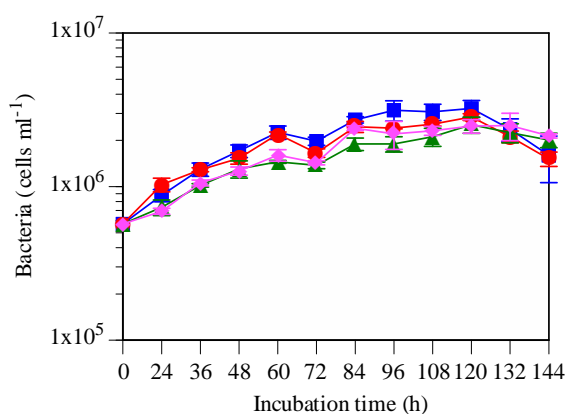


Fig. 4.15. Bacterial cell numbers (log scale) in incubation 3 (mean \pm SE, $n=3$). Treatment legend – HT: blue squares; GH: red circles; OA: pink diamonds; ambient control: green triangles

Synechococcus spp. cell numbers increased in each treatment from time-zero to 72 h, where cell numbers were significantly higher in the HT treatment than the ambient control (ANOVA $F_{1, 2} = 72.15$, $p = 0.01$, Fig. 4.16). *Prochlorococcus* spp. cell numbers increased in all but the HT treatment from 72 h to 144 h (Fig. 4.16). Total eukaryotic phytoplankton cell numbers increased significantly in each treatment from time-zero to 144 h (RM-ANOVA $F_{1, 8}$, $p < 0.01$, Fig. 4.16), while cell numbers were significantly higher in the HT treatment (2×10^4 cells ml^{-1}) than in the ambient control at 144 h (1×10^4 cells ml^{-1} , ANOVA $F_{1, 4} = 9.60$, $p < 0.05$, Fig. 4.16).

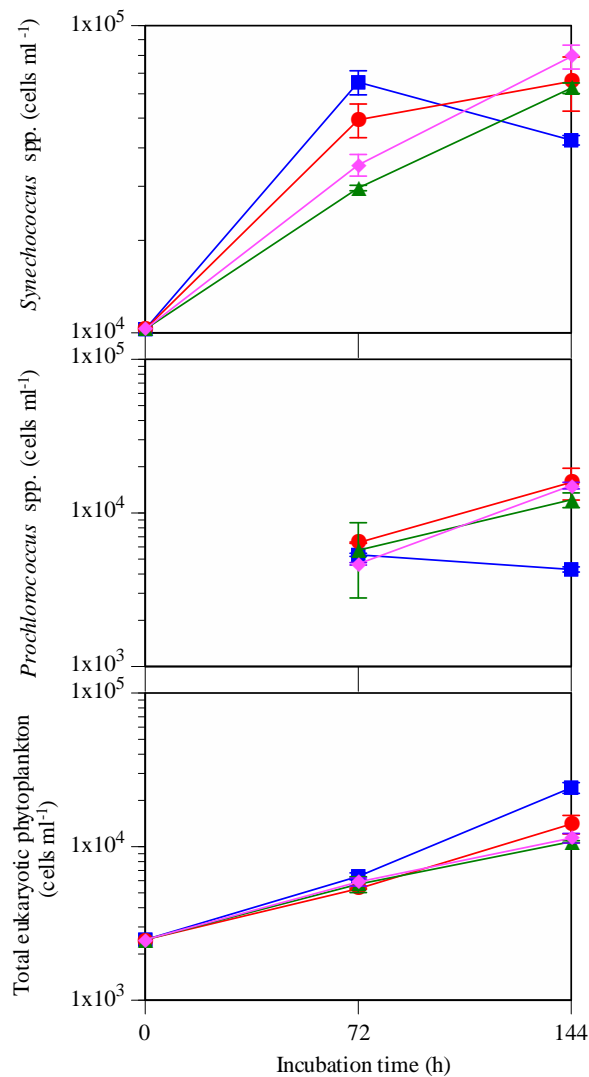


Fig. 4.16. *Synechococcus* spp., *Prochlorococcus* spp. and total eukaryotic phytoplankton cell numbers (log scale) in incubation 3 (mean \pm SE, n=3). No value indicates missing sample. Treatment legend – HT: blue squares; GH: red circles; OA: pink diamonds; ambient control: green triangles

4.3.2.4 Incubation 4

Bacterial cell numbers varied significantly across all treatments from 24 h to 120 h (RM-ANOVA $F_{8, 64} = 103.14$, $p < 0.0001$, Fig. 4.17). Bacterial cell numbers increased to 72 h in each treatment and were significantly higher in each treatment at 36 h compared to the ambient control (Fig. 4.17 & Appendix C: 4.2). Bacterial cell numbers declined in the HT and GH treatment beyond 72 h, while numbers in the ambient control and OA treatment continued

to increase; as a result of this trend, bacterial numbers were significantly lower in the HT and GH treatments when compared to the ambient control at both 96 h and 120 h (Fig. 4.17).

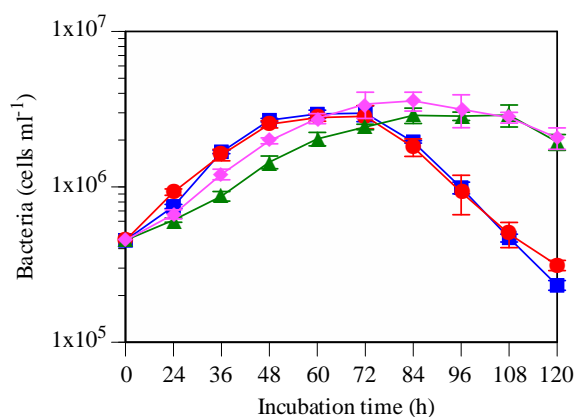


Fig. 4.17. Bacterial cell numbers (log scale) in incubation 4 (mean \pm SE, $n=3$). Treatment legend – HT: blue squares; GH: red circles; OA: pink diamonds; ambient control: green triangles

Synechococcus spp. cell numbers declined significantly in all treatments from 48 h to 120 h (RM-ANOVA $F_{1,8} = 220.18$, $p < 0.0001$, Fig. 4.18), with significantly lower cell numbers detected in the HT and GH treatments than in the ambient control at 120 h (Fig. 4.18 & Appendix C: 4.2). *Prochlorococcus* spp. cell numbers declined in the ambient control, HT and OA treatments from time-zero to 48 h, and then recovered. There was no significant difference in cell numbers between treatments and the ambient control at 120 h (Fig. 4.18). Total eukaryotic phytoplankton numbers increased across all treatments from time-zero to 48 h, then declined significantly from 48 h to 120 h (RM-ANOVA $F_{1,8} = 424.89$, $p < 0.0001$). Similar to bacterial cell numbers, total eukaryotic phytoplankton numbers began to decline in both the HT and GH treatments from 48 h, while numbers in the ambient control and OA treatment remained stable (Fig. 4.18). As a result of this trend, total eukaryotic phytoplankton numbers were significantly lower in the HT and GH treatments when compared to the ambient control at 120 h (Fig. 4.18 & Appendix C: 4.2).

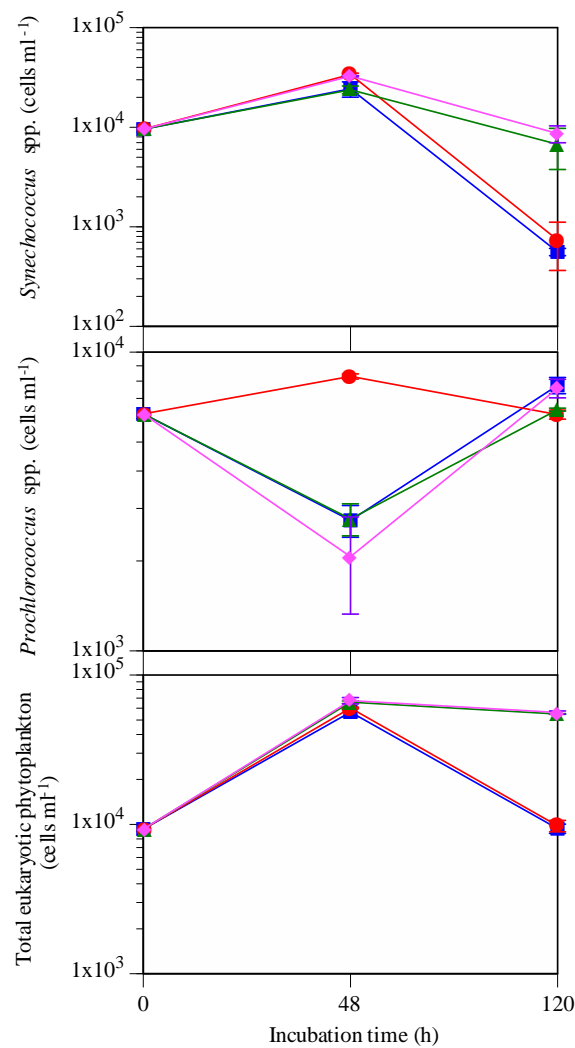


Fig. 4.18. *Synechococcus* spp., *Prochlorococcus* spp. and total eukaryotic phytoplankton cell numbers (log scale) in incubation 4 (mean \pm SE, n=3). Treatment legend – HT: blue squares; GH: red circles; OA: pink diamonds; ambient control: green triangles

Summary of results

Overall, bacterial, *Synechococcus* spp. and total eukaryotic phytoplankton numbers had similar treatment responses in incubations 2 and 4 (Table 4.5). Bacterial and *Synechococcus* spp. cell numbers were significantly higher in the HT treatment at 72 h when compared to the ambient control in incubations 1 and 3 (Table 4.5). Bacterial, *Synechococcus* spp. and total eukaryotic phytoplankton numbers were significantly lower in the HT and GH treatments at the final sampling point in incubation 2 and 4 when compared to the ambient control. The OA treatment did not have a consistent effect on bacterial or phytoplankton cell numbers in any incubation (Table 4.5).

Table 4.5. Summary of cell number changes in each treatment when compared to the ambient control ($p < 0.05$). Blue shaded cells indicate a response at 72 h, neutral shaded cells indicate a response at the final sampling point (incubation 1 to 3 - 144 h, incubation 4 – 120 h). ↑: indicates the parameter was significantly higher than the ambient control; ↓: significantly lower; empty cell: not significantly different; n.s: indicates the parameter was not sampled at 72 h

Parameter	Incubation 1			Incubation 2			Incubation 3			Incubation 4		
	OA	HT	GH	OA	HT	GH	OA	HT	GH	OA	HT	GH
Bacterial	↑	↑	↑	↑	↓	↓	↑	↓	↓	n.s	n.s	↓
<i>Synechococcus</i> spp.	↓	↑	↑	↑	↓	↓	↑	↓	↓	n.s	n.s	↓
<i>Prochlorococcus</i> spp.		↑	↑	↑				↓	↓	n.s	n.s	n.s
Total eukaryotic phytoplankton cells			↑		↓	↓		↑		n.s	↓	↓

4.3.3 Bacterial secondary production

4.3.3.1 Incubation 1

A significant positive relationship was detected between DNA and protein synthesis rates (linear regression, $p < 0.0001$, $r = 0.89$). DNA synthesis rates increased significantly in all treatments from 36 h to 144 h (RM-ANOVA $F_{3, 24} = 67.24$, $p < 0.0001$, Fig. 4.19). The rate of DNA synthesis was significantly higher in the GH treatment at 36 h ($6.19 \mu\text{g C l}^{-1} \text{d}^{-1}$), 72 h ($17.20 \mu\text{g C l}^{-1} \text{d}^{-1}$) and 108 h ($22.98 \mu\text{g C l}^{-1} \text{d}^{-1}$) when compared to the respective ambient controls (4.04 , 8.31 and $11.57 \mu\text{g C l}^{-1} \text{d}^{-1}$ respectively, Fig. 4.19, p-values in Appendix C: 4.3). DNA synthesis rates in the HT treatment ($23.80 \mu\text{g C l}^{-1} \text{d}^{-1}$) were double rates in the ambient control at 108 h ($11.57 \mu\text{g C l}^{-1} \text{d}^{-1}$, ANOVA $F_{1, 4} = 9.04$, $p < 0.05$), and also significantly higher than the ambient control at 144 h (ANOVA $F_{1, 4} = 9.02$, $p < 0.05$). The rate of protein synthesis also increased in all the treatments from time-zero to 144 h (Fig. 4.19). Protein synthesis was significantly higher in the OA treatment ($5.90 \mu\text{g C l}^{-1} \text{d}^{-1}$) compared to the ambient control at 72 h ($3.78 \mu\text{g C l}^{-1} \text{d}^{-1}$, ANOVA $F_{1, 4} = 13.71$, $p < 0.05$, Fig. 4.19), while protein synthesis in the HT treatment ($10.60 \mu\text{g C l}^{-1} \text{d}^{-1}$) was 75% higher than the ambient control at 144 h ($7.90 \mu\text{g C l}^{-1} \text{d}^{-1}$, ANOVA $F_{1, 4} = 17.95$, $p = 0.01$, Fig. 4.19). No significant GH treatment effect was apparent.

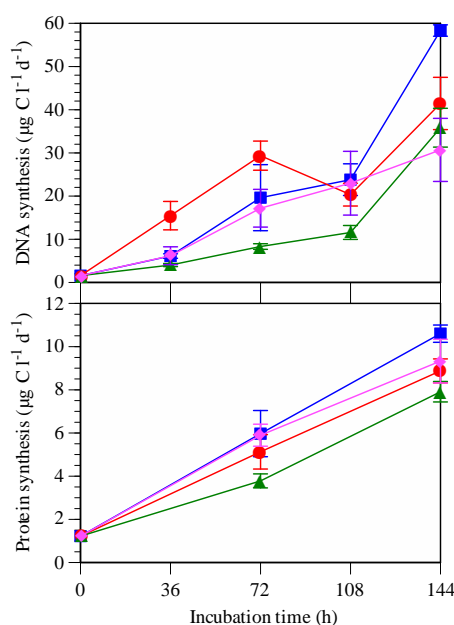


Fig. 4.19. BSP throughout incubation 1 (mean \pm SE, $n=3$). Treatment legend – HT: blue squares; GH: red circles; OA: pink diamonds; ambient control: green triangles

4.3.3.2 Incubation 2

A significant positive relationship was also detected between DNA and protein synthesis rates throughout incubation 2 (linear regression, $p < 0.0001$, $r = 0.75$). DNA synthesis rates increased in the HT and GH treatment from time-zero to 36 h, then steadily declined from 36 h to 144 h (Fig 4.20). Protein synthesis rates also increased in all treatments from time-zero to 72 h (Fig. 4.20). Protein synthesis was significantly higher in both the HT treatment ($6.85 \mu\text{g C l}^{-1} \text{d}^{-1}$) and GH treatment ($6.17 \mu\text{g C l}^{-1} \text{d}^{-1}$) when compared to the ambient control at 72 h ($3.69 \mu\text{g C l}^{-1} \text{d}^{-1}$, Fig. 4.20 & Appendix C: 4.3). Synthesis rates then declined from 72 h to 144 h in the HT treatment (6.85 to $6.67 \mu\text{g C l}^{-1} \text{d}^{-1}$) and GH treatment (6.17 to $4.61 \mu\text{g C l}^{-1} \text{d}^{-1}$, Fig. 4.20).

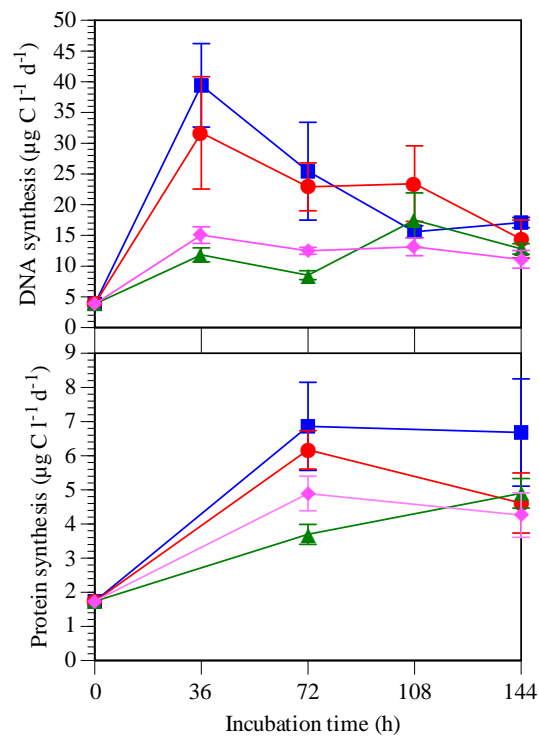


Fig. 4.20. BSP throughout incubation 2 (mean \pm SE, $n=3$). Treatment legend – HT: blue squares; GH: red circles; OA: pink diamonds; ambient control: green triangles

4.3.3.3 Incubation 3

A significant positive relationship was detected between DNA and protein synthesis rates throughout incubation 3 (linear regression, $p = 0.0001$, $r = 0.71$). DNA synthesis rates increased significantly in the HT and GH treatment from time-zero to 36 h when compared to the ambient control, and were also significantly higher at 72 h and 108 h (Fig. 4.21 & Appendix C: 4.3). At 144 h, DNA synthesis rates were twice as high in the HT treatment ($142.91 \mu\text{g C l}^{-1} \text{d}^{-1}$) when compared to the ambient control ($70.28 \mu\text{g C l}^{-1} \text{d}^{-1}$), however synthesis in the OA treatment ($59.94 \mu\text{g C l}^{-1} \text{d}^{-1}$) was 10% lower than the ambient control (Fig. 4.21 & Appendix C: 4.3). Protein synthesis rates increased in each treatment from time-zero to 144 h, with synthesis almost doubling across all treatments from 72 h to 144 h (RM-ANOVA $F_{1,8} = 221.12$, $p < 0.0001$, Fig. 4.21). Protein synthesis was significantly higher in the HT treatment ($6.39 \mu\text{g C l}^{-1} \text{d}^{-1}$) and GH treatment ($5.87 \mu\text{g C l}^{-1} \text{d}^{-1}$) when compared to the ambient control at 72 h ($2.60 \mu\text{g C l}^{-1} \text{d}^{-1}$, Fig. 4.21 & Appendix C: 4.3), and also significantly higher in the HT treatment ($9.87 \mu\text{g C l}^{-1} \text{d}^{-1}$) than in the ambient control at 144 h ($8.25 \mu\text{g C l}^{-1} \text{d}^{-1}$, Fig. 4.21 & Appendix C: 4.3).

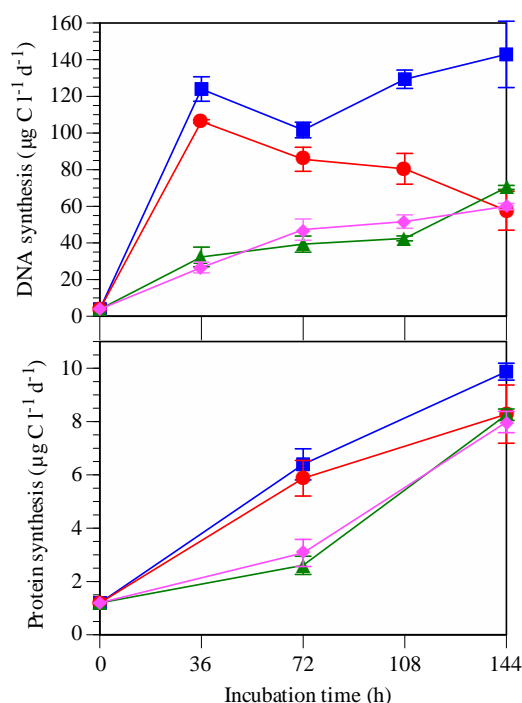


Fig. 4.21. BSP throughout incubation 3 (mean \pm SE, $n=3$). Treatment legend – HT: blue squares; GH: red circles; OA: pink diamonds; ambient control: green triangles

4.3.3.4 Incubation 4

In contrast to previous incubations, there was no significant relationship between DNA and protein synthesis rates throughout incubation 4 (linear regression, $p > 0.05$, $r = 0.16$). DNA synthesis rates increased across all treatments from time-zero to 60 h, with a higher rate detected in the HT and GH treatments (Fig. 4.22). DNA synthesis responded positively in both elevated temperature treatments at 36 h and 60 h when compared to the ambient control, however DNA synthesis rates began to decline in both treatments from 60 h onward (Fig. 4.22 & Appendix C: 4.3). In contrast to the elevated temperature treatments, DNA synthesis increased in the OA treatment from 60 h ($37.40 \mu\text{g C l}^{-1} \text{d}^{-1}$) to 120 h ($45.99 \mu\text{g C l}^{-1} \text{d}^{-1}$), while synthesis in the ambient control increased by 10% from 60 h ($36.91 \mu\text{g C l}^{-1} \text{d}^{-1}$) to 120 h ($46.09 \mu\text{g C l}^{-1} \text{d}^{-1}$, Fig. 4.22). The rate of protein synthesis also increased across all treatments and the ambient control from time-zero to 60 h, however synthesis then declined significantly from 60 h to 120 h (RM-ANOVA $F_{1, 8} = 305.83$, $p < 0.0001$, Fig 4.22). Protein synthesis was significantly lower in the HT treatment ($30.76 \mu\text{g C l}^{-1} \text{d}^{-1}$) and GH treatment ($27.30 \mu\text{g C l}^{-1} \text{d}^{-1}$) compared to the ambient control at 120 h ($46.09 \mu\text{g C l}^{-1} \text{d}^{-1}$, Fig. 4.22 & Appendix C: 4.3), similar to that measured for DNA synthesis.

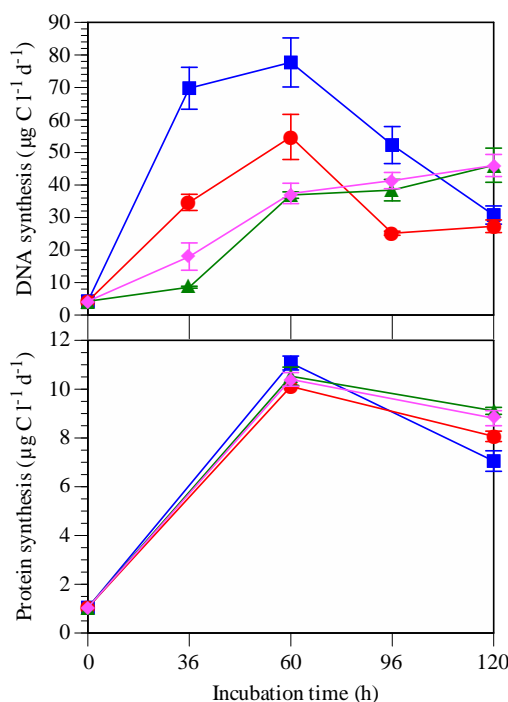


Fig. 4.22. BSP throughout incubation 4 (mean \pm SE, $n=3$). Treatment legend – HT: blue squares; GH: red circles; OA: pink diamonds; ambient control: green triangles

Summary of results

Overall, elevated temperature (HT and GH treatments) had a significant positive effect on DNA synthesis at 72 h and/or 60 h in incubations 2, 3 and 4, while the same response was measured for protein synthesis in incubations 2 and 3 (Table 4.6). BSP values measured in the OA treatment were very similar to the ambient control (Table 4.6). BSP values were not significantly affected by the OA treatment at 144 h and/or 120 h in any incubation (Table 4.6).

Table 4.6. Summary of the DNA and protein synthesis rate responses to treatments compared to the ambient control ($p < 0.05$). Blue shaded cells indicate a response halfway through the incubation (incubation 1 to 3 - 72 h, incubation 4 - 60 h), neutral shaded cells indicate a response at the final sampling point (incubation 1 to 3 - 144 h, incubation 4 - 120 h). ↑: indicates the parameter was significantly higher than the ambient control; ↓: significantly lower; empty cell: not significantly different

Parameter	Incubation 1			Incubation 2			Incubation 3			Incubation 4		
	OA	HT	GH	OA	HT	GH	OA	HT	GH	OA	HT	GH
DNA			↑	↑	↑	↑		↑	↑	↑	↑	↓
Protein	↑	↑		↑	↑	↑		↑	↑	↑	↓	↓

4.3.4 Chlorophyll *a* concentration

4.3.4.1 Incubation 1

Chlorophyll *a* (Chl *a*) concentrations increased across all treatments from time-zero to 144 h (RM-ANOVA $F_{1,8} = 25.64$, $p < 0.01$, Fig. 4.23). Chl *a* concentrations were highest in the OA treatment at each sampling point and statistically higher ($0.87 \mu\text{g ml}^{-1}$) than the ambient control at 72 h ($0.63 \mu\text{g ml}^{-1}$, ANOVA $F_{1,4} = 47.74$, $p < 0.01$). Chl *a* concentrations were also significantly higher in both the GH treatment ($0.96 \mu\text{g ml}^{-1}$) and OA treatment ($1.12 \mu\text{g ml}^{-1}$) when compared to the ambient control at 144 h ($0.72 \mu\text{g ml}^{-1}$, ANOVA $F_{1,4}$, $p < 0.05$, Fig. 4.23).

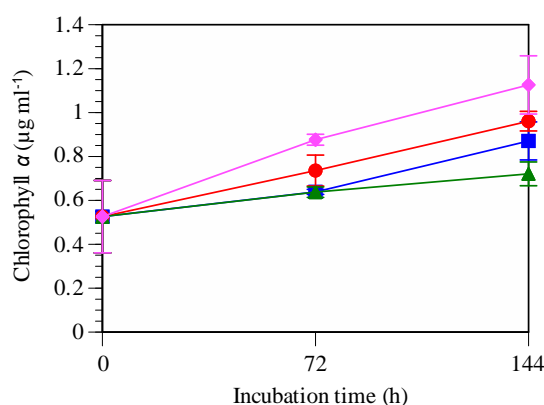


Fig. 4.23. Chl *a* concentrations throughout incubation 1 (mean \pm SE, $n=3$). Treatment legend – HT: blue squares; GH: red circles; OA: pink diamonds; ambient control: green triangles

4.3.4.2 Incubation 2

Chl *a* concentrations declined in each treatment including the ambient control from time-zero ($0.54 \mu\text{g ml}^{-1}$) to 144 h (HT; $0.38 \mu\text{g ml}^{-1}$, GH; $0.29 \mu\text{g ml}^{-1}$, OA; $0.24 \mu\text{g ml}^{-1}$ and ambient control; $0.32 \mu\text{g ml}^{-1}$). Chl *a* concentrations did not change significantly within or between each treatment throughout incubation 2 (ANOVA $F_{1,4}$, $p > 0.05$).

4.3.4.3 Incubation 3

Chl *a* concentrations did not change significantly from time-zero to 72 h in any treatment, however concentrations significantly increased in each treatment from 72 h to 144 h (RM-ANOVA $F_{1, 6} = 92.86$, $p < 0.01$). There was no significant difference in Chl *a* concentration between the different treatments and the ambient control at 72 h or 144 h (ANOVA $F_{1, 4}$, $p > 0.05$).

4.3.4.4 Incubation 4

Chl *a* concentrations declined significantly in the HT treatment from time-zero ($1.59 \mu\text{g ml}^{-1}$) to 120 h ($1.05 \mu\text{g ml}^{-1}$, RM-ANOVA $F_{1, 4}$, $p < 0.05$), while concentrations also declined in the GH treatment from time-zero ($1.59 \mu\text{g ml}^{-1}$) to 120 h ($0.98 \mu\text{g ml}^{-1}$, Fig. 4.24). Chl *a* concentrations were significantly lower in both the HT and GH treatment when compared to the ambient control at 120 h ($1.55 \mu\text{g ml}^{-1}$, ANOVA $F_{1, 4}$, $p < 0.05$, Fig. 4.24), whereas concentrations in the OA treatment were not significantly different from the ambient control (Fig. 4.24).

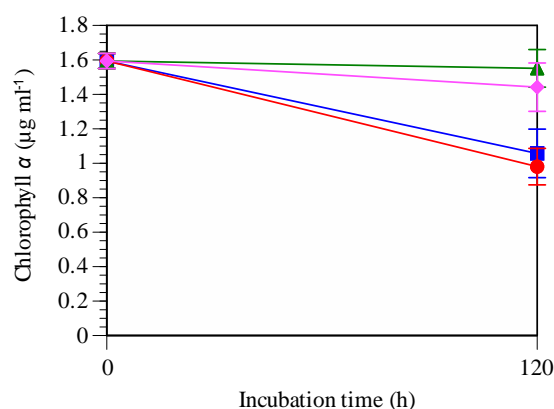


Fig. 4.24. Chl *a* concentrations throughout incubation 4 (mean \pm SE, $n=3$). Treatment legend – HT: blue squares; GH: red circles; OA: pink diamonds; ambient control: green triangles

4.3.5 Dissolved nutrient concentration

4.3.5.1 Incubation 1

Dissolved nitrate and DRP concentrations declined throughout incubation 1, while DRSi concentrations increased (Fig. 4.25). Dissolved nitrate concentrations were significantly lower in the OA treatment ($37.40 \mu\text{g l}^{-1}$) and HT treatment ($51.63 \mu\text{g l}^{-1}$) when compared to the ambient control at 72 h ($75.85 \mu\text{g l}^{-1}$), while the concentrations in each treatment were significantly lower than the ambient control at 144 h ($40.00 \mu\text{g l}^{-1}$, Fig. 4.25). DRP concentrations in the OA treatment ($7.83 \mu\text{g l}^{-1}$) were half that of the ambient control at 72 h ($14.03 \mu\text{g l}^{-1}$, ANOVA $F_{1,4} = 15.85$, $p = 0.01$, Fig. 4.25), while concentrations in each treatment were significantly lower than in the ambient control at 144 h ($9.63 \mu\text{g l}^{-1}$, ANOVA $F_{1,4}$, $p < 0.05$, Fig. 4.25). DRSi concentrations were lower in both elevated temperature treatments when compared to the ambient treatments at 72 h and 144 h (Fig. 4.25). DRSi concentrations in the HT treatment were significantly lower ($4.71 \mu\text{g l}^{-1}$) than in the ambient control at 72 h ($7.43 \mu\text{g l}^{-1}$, ANOVA $F_{1,4} = 9.55$, $p < 0.05$, Fig. 4.25), while concentrations in the GH treatment ($6.83 \mu\text{g l}^{-1}$) were also significantly lower than in the ambient control at 144 h ($11.90 \mu\text{g l}^{-1}$, ANOVA $F_{1,4} = 16.58$, $p < 0.05$, Fig. 4.25). Dissolved ammonium concentrations in each treatment were not significantly different from the ambient control at 72 h ($4.17 \mu\text{g l}^{-1}$) or 144 h ($4.10 \mu\text{g l}^{-1}$).

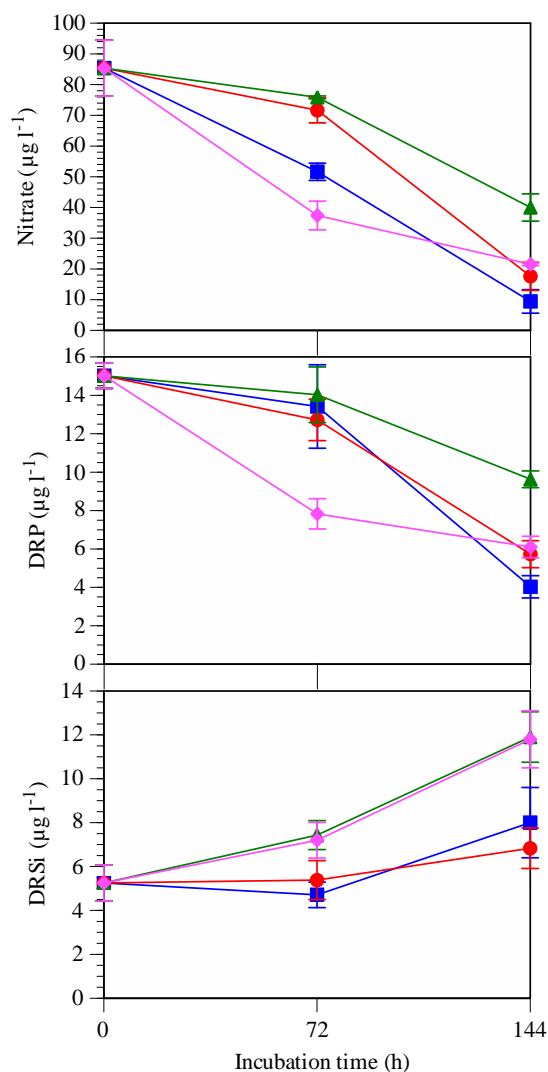


Fig. 4.25. Dissolved nutrient concentrations throughout incubation 1 (mean \pm SE, $n=3$). Treatment legend – HT: blue squares; GH: red circles; OA: pink diamonds; ambient control: green triangles

4.3.5.2 Incubation 2

Of the dissolved nutrient concentrations measured, only dissolved ammonium differed significantly from the ambient control, with concentrations in the HT treatment ($9.28 \mu\text{g l}^{-1}$) and GH treatment ($7.98 \mu\text{g l}^{-1}$) higher than the ambient control at 72 h ($2.34 \mu\text{g l}^{-1}$, Fig. 4.26), and concentrations in the HT treatment ($4.73 \mu\text{g l}^{-1}$), more than six times higher than the ambient control at 144 h ($0.71 \mu\text{g l}^{-1}$, ANOVA $F_{1,4} = 15.60$, $p < 0.05$, Fig. 4.26).

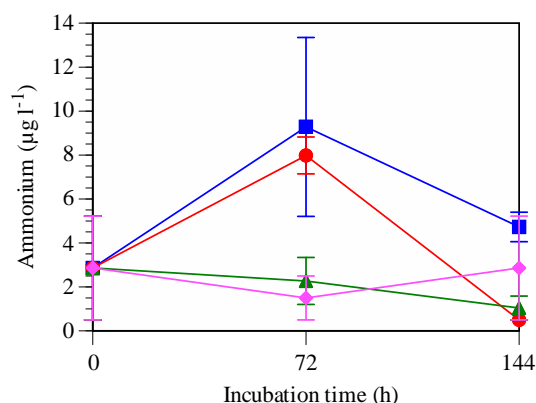


Fig. 4.26. Dissolved ammonium concentrations throughout incubation 2 (mean \pm SE, $n=3$).
Treatment legend – HT: blue squares; GH: red circles; OA: pink diamonds;
ambient control: green triangles

4.3.5.3 Incubation 3

Dissolved nitrate and ammonium concentrations declined in each treatment from time-zero to 144 h (Fig. 4.27). Dissolved nitrate concentrations were significantly lower in both the HT treatment ($0 \mu\text{g l}^{-1}$) and GH treatment ($0 \mu\text{g l}^{-1}$) compared to the ambient control at 144 h ($12.87 \mu\text{g l}^{-1}$, ANOVA $F_{1, 3}$, $p < 0.01$). Dissolved ammonium concentrations were also significantly lower in the HT treatment ($1.18 \mu\text{g l}^{-1}$) than the ambient control at 144 h ($3.45 \mu\text{g l}^{-1}$, ANOVA $F_{1, 3}$, $p < 0.05$, Fig. 4.27). DRP concentrations were highly variable between treatments with concentrations in the OA treatment and ambient control declining from 72 h to 144 h (Fig. 4.27). DRP concentrations in the HT treatment increased from 72 h ($105.55 \mu\text{g l}^{-1}$) and were more than fifty times higher than the ambient control at 144 h ($4.82 \mu\text{g l}^{-1}$, ANOVA $F_{1, 4} = 39.34$, $p < 0.01$, Fig. 4.27). DRSi concentrations increased in each treatment from time-zero to 144 h, however concentrations were not significantly different than the ambient control at 72 h ($11.57 \mu\text{g l}^{-1}$) or 144 h ($7.61 \mu\text{g l}^{-1}$).

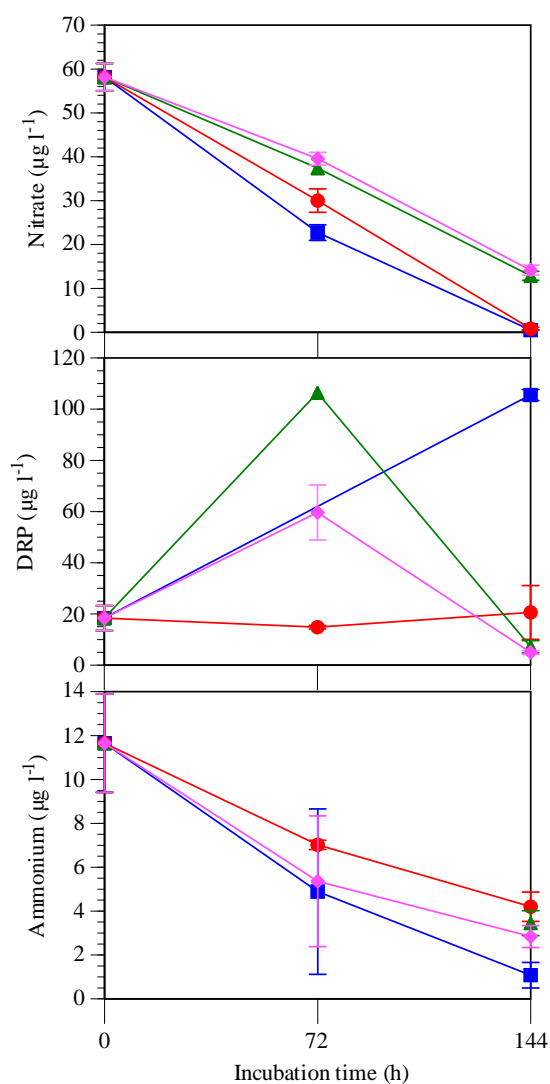


Fig. 4.27. Dissolved nutrient concentrations throughout incubation 3 (mean \pm SE, n=3).
 Treatment legend – HT: blue squares; GH: red circles; OA: pink diamonds;
 ambient control: green triangles

4.3.5.4 Incubation 4

Each measured dissolved nutrient concentration declined across all treatments from time-zero to 120 h. Nutrient concentrations in each perturbation treatment were not significantly different from the ambient control at 120 h (Dissolved nitrate: $0.81 \mu\text{g l}^{-1}$; ammonium: $1.23 \mu\text{g l}^{-1}$; DRP: $9.30 \mu\text{g l}^{-1}$; DRSi: $5.95 \mu\text{g l}^{-1}$).

Summary of results

Overall, dissolved nutrient concentrations varied in response to each treatment in each incubation, with no consistent treatment response apparent (Table 4.7). Dissolved nitrate and DRP concentrations typically declined in each treatment throughout each incubation, while DRSi concentrations increased in incubations 1 and 3. Dissolved ammonium concentrations increased in the elevated temperature treatments from time-zero to 72 h in incubation 2 (Table 4.7).

4.3.6 Dissolved organic carbon concentration

4.3.6.1 Incubation 1

Dissolved organic carbon (DOC) concentrations increased across all treatments from time-zero to 144 h (Fig. 4.28). DOC concentrations were significantly higher in the HT treatment ($1.21 \mu\text{g ml}^{-1}$) when compared to the ambient control at 144 h ($1.06 \mu\text{g ml}^{-1}$, ANOVA $F_{1,3} = 10.54$, $p < 0.05$, Fig. 4.28). The DOC concentration in the OA treatment at 144 h was removed as an extreme outlier ($26.63 \mu\text{g ml}^{-1}$) because similar concentrations have not been measured in these waters (pers. comm. Dr Cliff Law, NIWA). The high value in the OA treatment may have resulted from contamination either during sample collection or analysis.

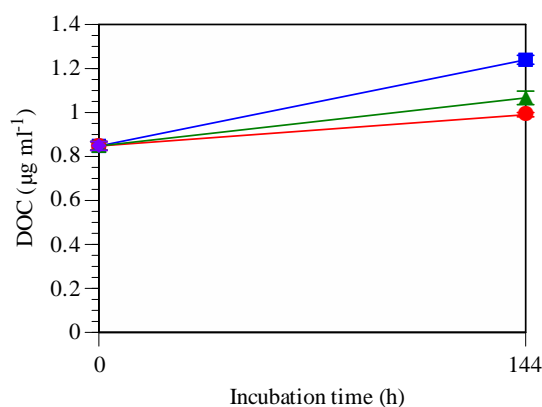


Fig. 4.28. DOC concentrations at the beginning and the end of incubation 1 (mean \pm SE, $n=3$). Treatment legend – HT: blue squares; GH: red circles; OA: pink diamonds; ambient control: green triangles

4.3.6.2 Incubations 2 & 3

DOC concentrations declined across all treatments from time-zero to 144 h in incubations 2 and 3. DOC concentrations in each treatment were not significantly different from the ambient control at 144 h (Incubation 2: $22.89 \mu\text{g ml}^{-1}$; Incubation 3: $1.03 \mu\text{g ml}^{-1}$).

4.3.6.3 Incubation 4

DOC concentrations increased in each treatment from time-zero to 120 h, except for the OA treatment (Fig. 4.29). Concentrations were significantly higher in the HT treatment ($1.20 \mu\text{g ml}^{-1}$) and GH treatment ($0.96 \mu\text{g ml}^{-1}$) compared to the ambient control at 120 h ($0.89 \mu\text{g ml}^{-1}$, ANOVA $F_{1,3}$, $p < 0.05$, Fig. 4.29).

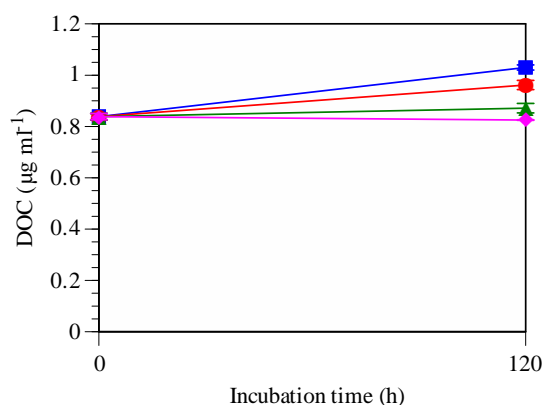


Fig. 4.29. DOC concentrations at the beginning and the end of incubation 4 (mean \pm SE, $n=3$). Treatment legend – HT: blue squares; GH: red circles; OA: pink diamonds; ambient control: green triangles

4.3.7 Total high molecular weight organic compound concentration

4.3.7.1 Incubation 1

Total High Molecular Weight (HMW) reducing-sugar concentrations declined in the HT and OA treatments from time-zero to 72 h (HT: $0.007 \mu\text{g ml}^{-1}$; OA: $0.003 \mu\text{g ml}^{-1}$), but increased in the GH treatment and ambient control (GH: $0.052 \mu\text{g ml}^{-1}$; ambient control: $0.075 \mu\text{g ml}^{-1}$, Fig. 4.30). Total HMW reducing-sugar concentrations declined in the GH treatment and ambient control from 72 h to 144 h, and were significantly lower in the OA treatment ($0.001 \mu\text{g ml}^{-1}$) than in the ambient control at 144 h ($0.034 \mu\text{g ml}^{-1}$, ANOVA $F_{1,3} = 21.81$, $p < 0.05$, Fig. 4.30). Total HMW protein concentrations declined in the OA treatment from time-zero ($0.66 \mu\text{g ml}^{-1}$) to 72 h ($0.45 \mu\text{g ml}^{-1}$), while concentrations increased in the other treatments (Fig. 4.30). Concentrations declined in each treatment from 72 h to 144 h, but were significantly

higher in the HT treatment ($0.45 \mu\text{g ml}^{-1}$) and GH treatment ($0.37 \mu\text{g ml}^{-1}$) when compared to the ambient control at 144 h ($0.17 \mu\text{g ml}^{-1}$, Fig. 4.30, p-values in Appendix C: 4.4).

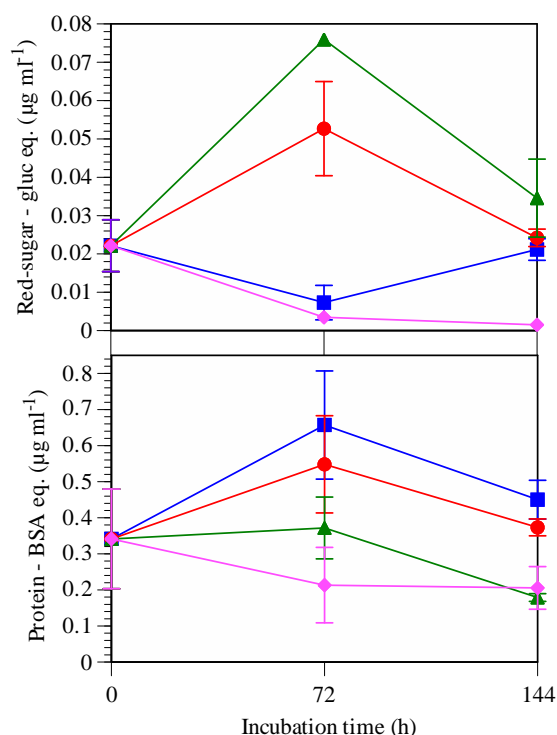


Fig. 4.30. Total HMW organic compound concentrations throughout incubation 1 (mean \pm SE, $n=3$). Red-sugar refers to reducing-sugar. Treatment legend – HT: blue squares; GH: red circles; OA: pink diamonds; ambient control: green triangles

4.3.7.2 Incubation 2

Total HMW reducing-sugar concentrations increased in each treatment from time-zero to 72 h, concentrations in the ambient control declined from 72 h to 144 h, while concentrations increased significantly in the HT treatment (Fig. 4.31 & Appendix C: 4.4). Total HMW reducing-sugar concentrations in the HT treatment were five-fold higher ($0.50 \mu\text{g ml}^{-1}$) than in the ambient control at 144 h ($0.10 \mu\text{g ml}^{-1}$). Total HMW protein concentrations declined in each treatment from time-zero to 72 h (Fig. 4.31). HMW protein concentrations in the HT treatment increased significantly from 72 h and were twice as high ($2.25 \mu\text{g ml}^{-1}$) as the ambient control at 144 h ($0.88 \mu\text{g ml}^{-1}$, Fig. 4.31 & Appendix C: 4.4).

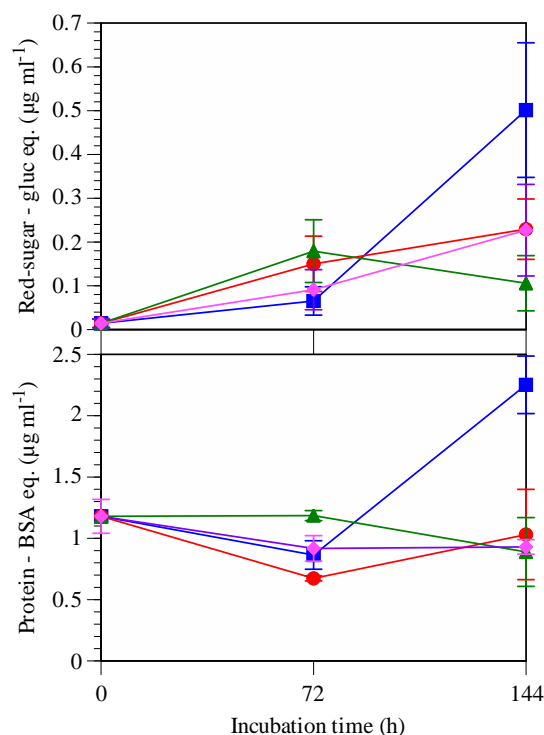


Fig. 4.31. Total HMW organic compound concentrations throughout incubation 2 (mean \pm SE, $n=3$). Red-sugar refers to reducing-sugar. Treatment legend – HT: blue squares; GH: red circles; OA: pink diamonds; ambient control: green triangles

4.3.7.3 Incubation 3

Total HMW reducing-sugar concentrations increased in each treatment from time-zero to 72 h, with the highest concentrations in the HT treatment and ambient control (Fig. 4.32). HMW reducing-sugar concentrations declined sharply in the HT and GH treatment from 72 h to 144 h (HT: 0.52 to 0.21 $\mu\text{g ml}^{-1}$; GH: 0.37 to 0.06 $\mu\text{g ml}^{-1}$), but increased in the OA and GH treatment from 72 h to 144 h (Fig. 4.32). Total HMW reducing-sugar concentrations were significantly higher in the HT treatment (0.21 $\mu\text{g ml}^{-1}$) and the OA treatment (0.17 $\mu\text{g ml}^{-1}$) when compared to the ambient control at 144 h (0.06 $\mu\text{g ml}^{-1}$, Fig. 4.32 & Appendix C: 4.4). Total HMW protein concentrations increased in the HT and OA treatments from time-zero to 72 h, with a significantly higher concentration detected in the OA treatment when compared to the ambient control at 72 h (1.04 $\mu\text{g ml}^{-1}$, ANOVA $F_{1,4} = 29.24$, $p < 0.01$, Fig. 4.32). Concentrations in the GH treatment declined from time-zero to 72 h, with concentrations significantly lower (0.34 $\mu\text{g ml}^{-1}$) than in the ambient control at 72 h (0.60 $\mu\text{g ml}^{-1}$, ANOVA

$F_{1,4} = 30.26$, $p < 0.01$). HMW protein concentrations declined in the OA treatment from 72 h ($1.04 \mu\text{g ml}^{-1}$) to 144 h ($0.74 \mu\text{g ml}^{-1}$), while concentrations increased in all other treatments (Fig. 4.32). At 144 h, HMW protein concentrations were significantly higher in the HT treatment ($1.53 \mu\text{g ml}^{-1}$) than the ambient control ($0.92 \mu\text{g ml}^{-1}$, ANOVA $F_{1,4} = 11.02$, $p < 0.05$, Fig. 4.32).

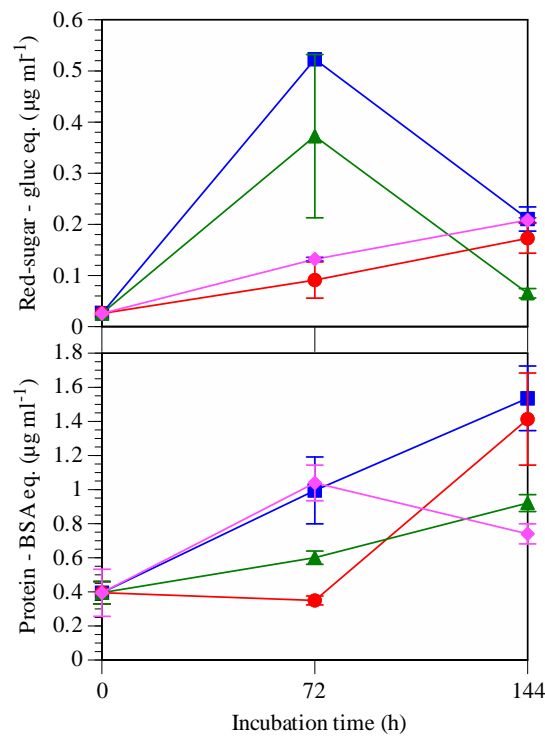


Fig. 4.32. Total HMW organic compound concentrations throughout incubation 3 (mean \pm SE, $n=3$). Red-sugar refers to reducing-sugar. Treatment legend – HT: blue squares; GH: red circles; OA: pink diamonds; ambient control: green triangles

4.3.7.4 Incubation 4

Total HMW reducing-sugar concentrations increased in each treatment from time-zero to 60 h (Fig. 4.33). Concentrations remained constant in the GH treatment from 60 h to 120 h, while concentrations continued to increase in all other treatments, peaking at 120 h (Fig. 4.33). Total HMW reducing-sugar concentrations were significantly higher in the HT treatment ($0.21 \mu\text{g ml}^{-1}$) than the ambient control at 120 h ($0.14 \mu\text{g ml}^{-1}$, ANOVA $F_{1,3} = 24.85$, $p = 0.01$, Fig. 4.33). Total HMW protein concentrations also increased in each treatment from time-zero to

60 h (Fig. 4.33). Concentrations in the ambient control and OA treatment declined from 60 h to 120 h, while concentrations in the GH and HT treatments increased. At 120 h, total HMW protein concentrations were significantly higher in the HT treatment ($1.26 \mu\text{g ml}^{-1}$) and the GH treatment ($1.25 \mu\text{g ml}^{-1}$) than the ambient control ($0.95 \mu\text{g ml}^{-1}$, ANOVA $F_{1,3}$, $p < 0.05$, Fig. 4.33).

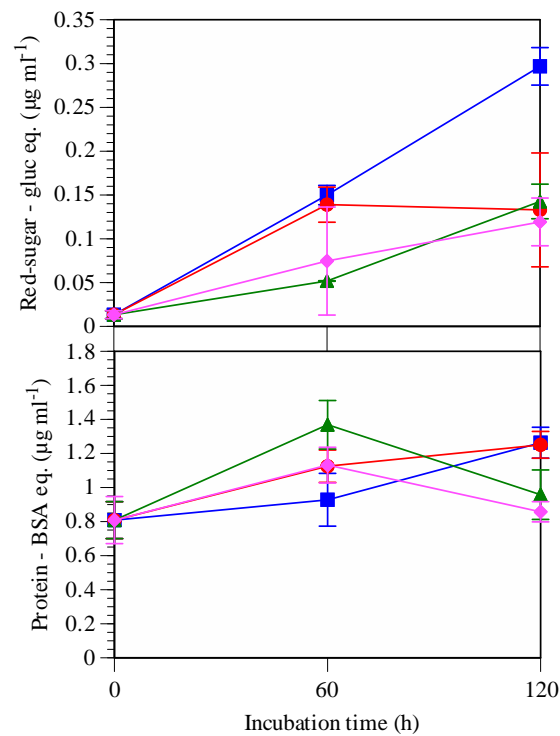


Fig. 4.33. Total HMW organic compound concentrations throughout incubation 4 (mean \pm SE, $n=3$). Red-sugar refers to reducing-sugar. Treatment legend – HT: blue squares; GH: red circles; OA: pink diamonds; ambient control: green triangles

Summary of results

Overall, total HMW protein concentrations were higher than reducing-sugar concentrations in each incubation. Total HMW protein concentrations increased in the HT treatment relative to the ambient control at the final sampling point of each incubation (Table 4.8). The GH treatment had a negative effect on total HMW protein synthesis at 72 h in incubations 2 and 3 (Table 4.8), while the OA treatment had a variable response (Table 4.8).

Table 4.8. Summary of total HMW organic compound concentration changes in each treatment when compared to the ambient control ($p < 0.05$). Blue shaded cells indicate a response halfway through the incubation (incubation 1 to 3 - 72 h, incubation 4 – 60 h), neutral shaded cells indicate a response at the final sampling point (incubation 1 to 3 - 144 h, incubation 4 – 120 h). ↑: indicates the parameter was significantly higher than the ambient control; ↓: significantly lower; empty cell: not significantly different; n.s: indicates the parameter was not sampled at 72 h

Parameter	Incubation 1			Incubation 2			Incubation 3			Incubation 4		
	OA	HT	GH	OA	HT	GH	OA	HT	GH	OA	HT	GH
Total HMW reducing-sugar	↓				↑		↑	↑		n.s	n.s	n.s
Total HMW protein		↑	↑	↓	↑	↓	↑	↓	↑	n.s	n.s	↑

4.3.8 Multivariate data analysis

The following section will investigate similarity and dissimilarity of multivariate data from each treatment simultaneously. Multivariate data will be presented visually for each phytoplankton community, allowing identification of treatment affects at selected sampling times. Statistical difference is based on a SIMPROF analysis at 5% significance taking into account all data points simultaneously. Each incubation MDS plot has a stress coefficient ≤ 0.05 which indicates the multivariate matrices are represented extremely well by the 2D ordination plot (Section 2.11).

4.3.8.1 Incubation 1

Multivariate analysis of incubation 1 data showed that each treatment was tightly clustered with the ambient control for the initial 108 h, and that no treatment could be separated using the primary sampled parameters (Fig. 4.34). Although ANOVA analyses of individual parameters detected significant differences from the ambient control at specific sampling points, the multivariate analysis using all primary parameter data and sample points simultaneously, did not detect a significant difference between treatments until 144 h (Fig 4.34). At 144 h, each treatment was significantly different from the ambient control, as well as each other (Fig. 4.34).

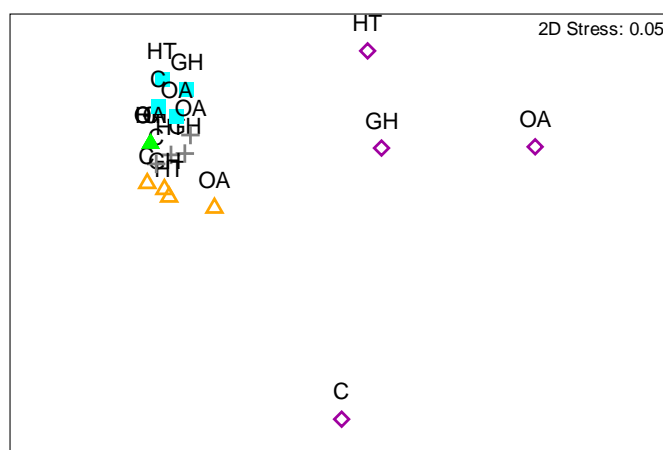


Fig. 4.34. MDS plot of six sampled biotic and abiotic parameters collected during incubation 1. Abbreviations are as previously described in Section 2.1. Incubation treatments are labelled per sampling point - 0 h: ▲; 36 h: ■; 72 h: +; 108 h: △; 144 h: ◆

4.3.8.2 Incubation 2

Multivariate analysis of incubation 2 data revealed that the HT and GH treatment were significantly different from the ambient control at 36 h (solid line cluster, Fig. 4.35), while the OA treatment was not. Although ANOVA analyses of individual parameters in the OA treatment did detect significant differences from the ambient control at 72 h, the multivariate analysis using all primary parameter data and sample points simultaneously did not (Fig. 4.35). At 144 h, the HT and GH treatments were significantly different from the ambient control (broken line cluster, Fig. 4.35), while the OA treatment was not.

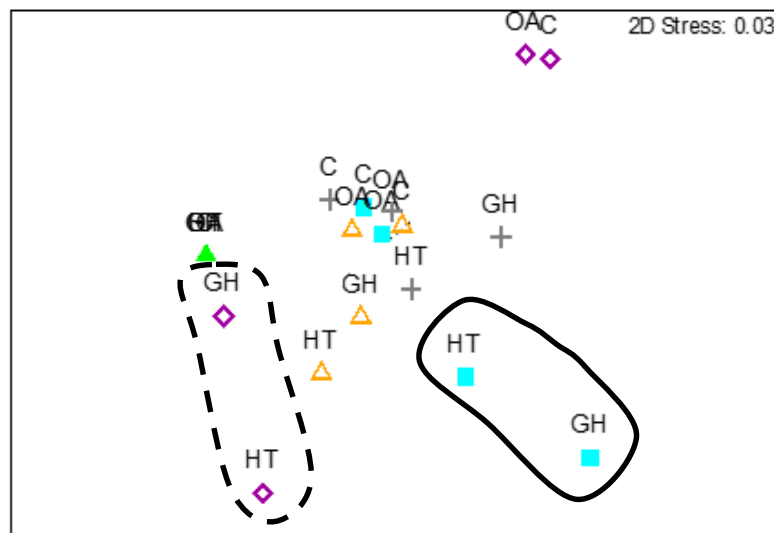


Fig. 4.35. MDS plot of six sampled biotic and abiotic parameters collected during incubation 2. Highlighted clusters are based on a SIMPROF analysis at 5% significance. Abbreviations are as previously described in Section 2.1. Incubation treatments are labelled per sampling point - 0 h: ▲; 36 h: ■; 72 h: +; 108 h: △; 144 h: ◆

4.3.8.3 Incubation 3

Multivariate analysis of incubation 3 data showed that the primary sampled parameters changed significantly from time-zero to 36 h (Fig. 4.36). Each treatment including the ambient control diverged from time-zero, while sampled parameters in the HT treatment were significantly different for all other treatments at 36 h, 72 h, 108 h and 144 h (broken line cluster, Fig. 4.36).

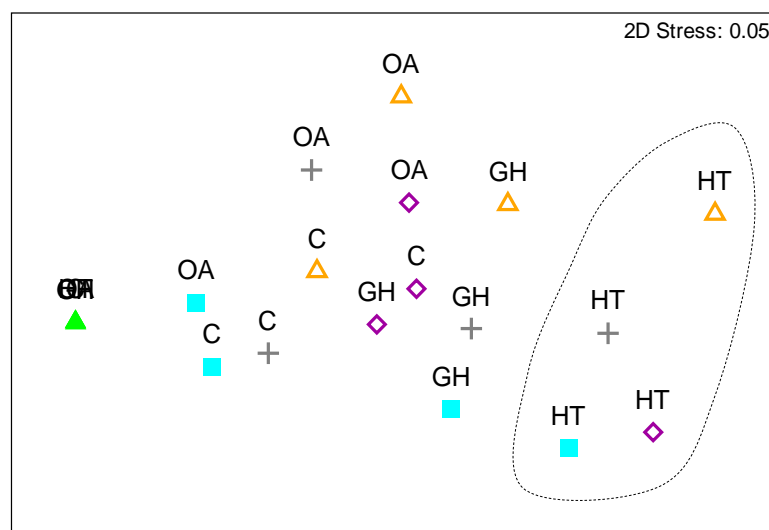


Fig. 4.36. MDS plot of six sampled biotic and abiotic parameters collected during incubation 3. Highlighted clusters are based on a SIMPROF analysis at 5% significance. Abbreviations are as previously described in Section 2.1. Incubation treatments are labelled per sampling point - 0 h: ▲; 36 h: ■; 72 h: +; 108 h: ▲; 144 h: ◆

4.3.8.4 Incubation 4

The primary sampled parameter data from incubation 4 changed significantly from time-zero to 120 h (Fig. 4.37). Multivariate data from the HT treatment diverged away from their respective ambient control at 60 h, 96 h and 120 h, while the GH treatment showed the same trend at 96 h and 120 h only (Fig. 4.37). The OA treatment was not significantly different from the respective ambient control at 60 h, 96 h or 120 h (Fig. 4.37).

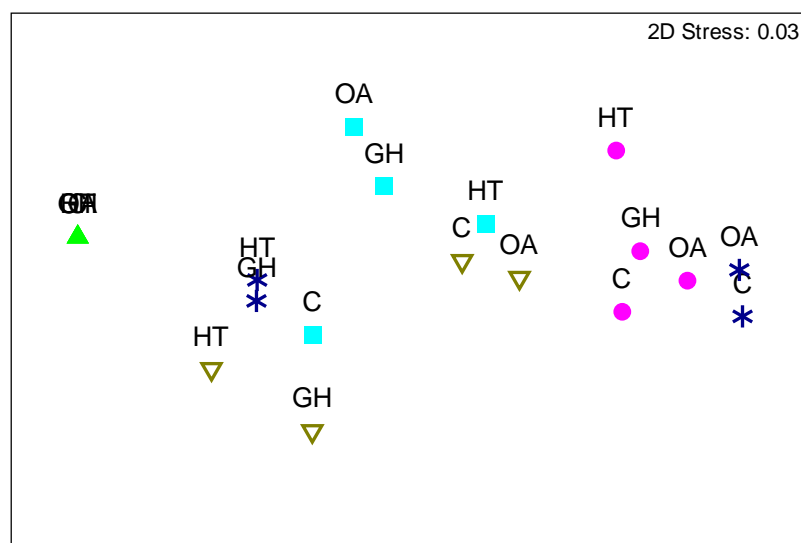


Fig. 4.37. MDS plot of six sampled biotic and abiotic parameters collected during incubation 4. Abbreviations are as previously described in Section 2.1. Incubation treatments are labelled per sampling point - 0 h: ▲; 36 h: ■; 60 h: ●; 96 h: ★; 120 h: ▼

4.4 Discussion

Average time-zero values provide insight into the phase of the phytoplankton bloom at time of bulk seawater collection. For instance, bulk seawater collected for incubation 1 was colder and contained high dissolved nutrient concentrations and lower DOC concentrations (Table 4.2). Based on these measurements, it is likely incubation 1 water was of Sub-Antarctic origin. Bulk seawater collected for incubation 3 was collected eight days after incubation 1 from a similar spatial location (Fig. 4.1), and contained lower dissolved nutrient concentrations but higher dissolved ammonium concentration, indicative of heterotrophic grazing (pers. comm. Dr Cliff Law, NIWA). It is possible that the bulk seawater collected for incubation 3 was a different bloom advected into the region, or the same original bloom that had undergone community changes (Fig. 4.2). Bulk seawater collected for incubation 2 contained the highest *Synechococcus* spp. and total eukaryotic phytoplankton biomass, which is thought to be responsible for the lowest nitrate and DRP concentrations of any bulk seawater. Seawater collected for incubation 2 also contained the highest DOC concentration as well as the highest protein synthesis, bacterial cell numbers and HMW organic compound concentrations (Table 4.2). These trends may be indicative of enhanced phytoplankton exudation, organic matter aggregation and bacterial assimilation and growth, characteristic of bloom peak (Engel et al. 2014). Considering the higher temperature and salinity when compared to the other bloom water masses, incubation 2 seawater may have consisted of sub-tropical water. Bulk seawater collected for incubation 4 contained surprisingly high dissolved nutrient concentrations considering the high Chl *a* and phytoplankton cell numbers (Table 4.2), and may have been coastal seawater or Sub-Antarctic water transported into the Cook Strait.

Time-zero bacterial cell numbers in each phytoplankton community were similar to those collected from the same depth by other researchers during each respective cruise (data courtesy of NIWA), and also similar to those of a coastal ecosystem (Karner & Rassoulzadegan 1995), nutrient depleted surface waters (Yoshimura et al. 2009), a Bergen fjord (Grossart et al. 2006) and the Baltic Sea (Lindh et al. 2013). However, numbers were lower than many other values cited within the literature (Allgaier et al. 2008, Teira et al. 2012, Newbold et al. 2012, Piontek et al. 2013), including those reported from Antarctic waters (Rivkin 1991, Maas et al. 2013). Time-zero BSP values were slightly higher in each phytoplankton community when compared to samples collected from the same depth by other researchers during each respective cruise

(data courtesy of NIWA), and also higher relative to existing Southern Ocean research (Maas et al. 2013). However, time-zero BSP values were lower when compared to bacteria isolated from the Mediterranean Sea (Teira et al. 2012), and an Arctic glacial fjord system (Piontek et al. 2013). Protease activity was within the range typically found in the near surface ocean (5 to 80 nmol l⁻¹ h⁻¹, Arnosti 2003, 2011 and references therein), while glucosidase activity was within the range found in the Southern Ocean and Pacific Subtropical gyre (0.02 to 0.03 nmol l⁻¹ h⁻¹, Christian & Karl 1995).

This discussion will address several key questions, firstly, do extracellular enzyme activities change significantly under low pH conditions, elevated temperature conditions and the combined effect of low pH and elevated temperature conditions predicted by the end of the century? And if enzyme activities are significantly affected, which perturbation treatment is driving this change? Secondly, does the measured treatment response differ between different mixed phytoplankton communities?

4.4.1 Effect of low pH

4.4.1.1 Temporal trends and related parameters

The purpose of this section is to analyse the temporal change between sampled parameters and to investigate how parameter correlations differ between different phytoplankton communities. This analysis will provide insight into parameter interactions throughout each incubation. During incubation 1, dissolved nitrate and DRP concentrations declined significantly from time-zero to 144 h, while Chl *a* concentrations increased. Surprisingly, no correlation was detected between Chl *a* concentrations and total eukaryotic phytoplankton or *Synechococcus* spp. cell numbers, most likely due to differences in sampling frequencies (Table 4.1). Planktonic cell numbers declined from time-zero to 144 h (Fig. 4.38) and may reflect increased grazing pressure (Deason 1980, Riemann et al. 2000), while the presence of an additional undetected phytoplankton group could have supplemented the Chl *a* concentration. Organic matter derived from phytoplankton exudation and lysed cells from grazing, could have stimulated abiotic coagulation and the formation of labile total HMW organic matter (Engel et al. 2014), thereby stimulating an increase in Leu-aminopeptidase activity (Fig. 4.38). A positive

correlation was detected between Leu-aminopeptidase activity, BSP (DNA and protein synthesis) and bacterial cell numbers (Fig. 4.38), showing that active degradation of HMW substrate and subsequent assimilation of LMW organic matter may have contributed to an increase in bacterial cell numbers. Throughout incubation 1, bacterial cell numbers increased steadily, declined and appeared to stabilise after 96 h which is likely to reflect temporal changes in top down control through viral lysing (Proctor & Fuhrman 1990) or protozoan grazing (Sherr et al. 1987). Very little β - and α -glucosidase activity was detected during incubation 1, suggesting that there was insufficient substrate available, enzyme inhibition was prevalent or that the substrate was too recalcitrant for bacteria to synthesise glucosidase (Rogers 1961, Gottschalk 1985, Arrieta & Herndl 2002). This is further supported by the low HMW reducing-sugar concentration in incubation 1 when compared to the other incubations. It is possible that the bulk seawater used in incubation 1 was collected during a very early bloom development phase, as HMW substrate concentrations typically become more abundant toward the bloom peak and decline phase (Cloern 1996, Münster & Chrost 1990, Sverdrup 1942a).

During incubation 2, dissolved nitrate and DRSi concentrations increased from time-zero to 72 h, while ammonium and DRP concentrations did not change significantly. This result suggests a net regeneration of nutrients with bacterial remineralisation exceeding phytoplankton uptake. Phytoplankton dissolved nutrient uptake rates may have declined in response to a decline in *Synechococcus* spp. cell numbers from time-zero to 144 h, however Chl *a* concentrations and total eukaryotic phytoplankton cell numbers did not change significantly (Fig. 4.38). The measured increase in DRSi concentration during incubation 2 could indicate remineralisation of diatoms (Martin-Jézéquel et al. 2000), however as diatoms were not a dominant component of the mixed community (Fig. 4.2), this originated from an unknown source. β -glucosidase activity initially increased but declined beyond 84 h, with cell-specific β -glucosidase activity showing a similar short-term positive response. Under low pH conditions, Arnosti et al. (2011) recorded differences in laminarinase and xylanase activities during the development of a natural phytoplankton bloom, showing that the activity of different enzymes can vary throughout a bloom, with some more active in the early developmental phase, and others more active in the later post-bloom phase. As measured in incubation 1, Arg-aminopeptidase activity showed high levels of within-sample variation during incubation 2, and consequently, no clear temporal trend was evident. This large variation in activity may

reflect increased diversity of bacterioplankton species and their associated enzymes, or an increased diversity in HMW organic compounds (Arrieta & Herndl 2002, Fig. 4.38). Total HMW reducing-sugar concentrations increased from time-zero to 144 h while phytoplankton and bacterial cell numbers remained stable; this result qualitatively suggests that reducing-sugar concentrations may have increased through abiotic coagulation. As detected in incubation 1, there was a positive correlation between Leu-aminopeptidase activity, DNA and protein synthesis rates and bacterial cell numbers, indicating HMW substrate remineralisation, active assimilation and subsequent bacterial growth (Fig. 4.38). The temporal trend of Leu-aminopeptidase activity and bacterial cell numbers was not linear, instead showing an initial peak, decline and recovery period (Fig. 4.38). This trend could reflect diauxic growth as bacterial metabolism switches between different substrates. Alternatively, the fluctuating bacterial cell numbers and enzyme activity may indicate top-down control from viral lysis (Proctor & Fuhrman 1990) and/or protozoan grazing (Sherr et al. 1987).

During incubation 3, dissolved nitrate and ammonium concentrations declined from time-zero to 144 h. As dissolved nutrient concentrations declined, a significant positive correlation was measured between Chl *a* concentration and total eukaryotic phytoplankton cell numbers, suggesting biological uptake of dissolved nutrients and phytoplankton growth. DOC concentrations declined throughout the incubation despite an increase in phytoplankton cell numbers and potential DOM production. This trend suggests that DOC was being degraded faster than it was being produced, a trend most likely driven by heterotrophic consumption (Wright & Hobbie 1966). Cell-specific β -glucosidase activity, as well as β -glucosidase and α -glucosidase activity were positively correlated with an increasing concentration of total HMW reducing-sugar from 84 h to 132 h, qualitatively suggesting substrate induced glucosidase activity. Similarly, Leu-aminopeptidase activity was positively correlated with total HMW protein concentration throughout the incubation, potentially stimulating the initial increase in protease activity measured from time-zero to 96 h (Fig. 4.38). However, because both phytoplankton and bacterial numbers also increased from time-zero to 144 h, an unknown proportion of the detected total HMW substrate may have been intracellular during the incubation and not accessible to extracellular enzymes. A positive correlation was also measured between BSP (DNA and protein synthesis) and bacterial cell numbers during

incubation 3 (Fig. 4.38), again suggesting active assimilation of LMW organic matter and bacterial growth.

During incubation 4, total dissolved nutrient concentrations declined from time-zero to 120 h, while *Synechococcus* spp. and total eukaryotic phytoplankton cell numbers increased from time-zero to 48 h (Fig. 4.38). As measured in incubations 1 and 3, the drawdown of dissolved nutrients and the initial increase in phytoplankton cell numbers are indicative of active biological growth. DOC concentrations declined slightly from time-zero to 120 h, potentially resulting from increased heterotrophic consumption (Wright & Hobbie 1966). β -glucosidase and α -glucosidase activity followed very similar trends throughout incubation 4; both enzyme activities increased from time-zero to 84 h, after which activity declined. In contrast to this, cell-specific β -glucosidase activity remained the same from 24 h to 120 h, suggesting that relative activity per bacterial cell did not increase over time, but rather an increase in bacterial numbers resulted in the synthesis of more enzymes (Arnosti 2003). The decline in glucosidase activity is most likely in response to a decline in bacterial numbers (Fig. 4.38) potentially from viral lysis (Proctor & Fuhrman 1990, Danovaro et al. 2010) and/or protozoan grazing (Sherr et al. 1987). As previously measured in each phytoplankton bloom community, DNA and protein synthesis rates were also positively correlated with bacterial cell numbers. Bacterial numbers and protein synthesis both peaked at 72 h, then declined slowly from 72 h to 120 h (Fig. 4.38).

In each incubation, a strong correlation between Leu-aminopeptidase activity, DNA and protein synthesis rates and bacterial cell numbers was measured in the OA treatment (Fig. 4.38). However, variation in the magnitude of change of select parameters was evident between incubations. For instance, during incubation 3, Leu-aminopeptidase activity was approximately three-fold higher from 72 h to 144 h when compared to incubations 1 and 2, while activity was approximately 400% higher in incubation 4 over the same time period (Fig. 4.38). This variation between incubations may reflect a different bloom phase or phytoplankton and bacterial community composition.

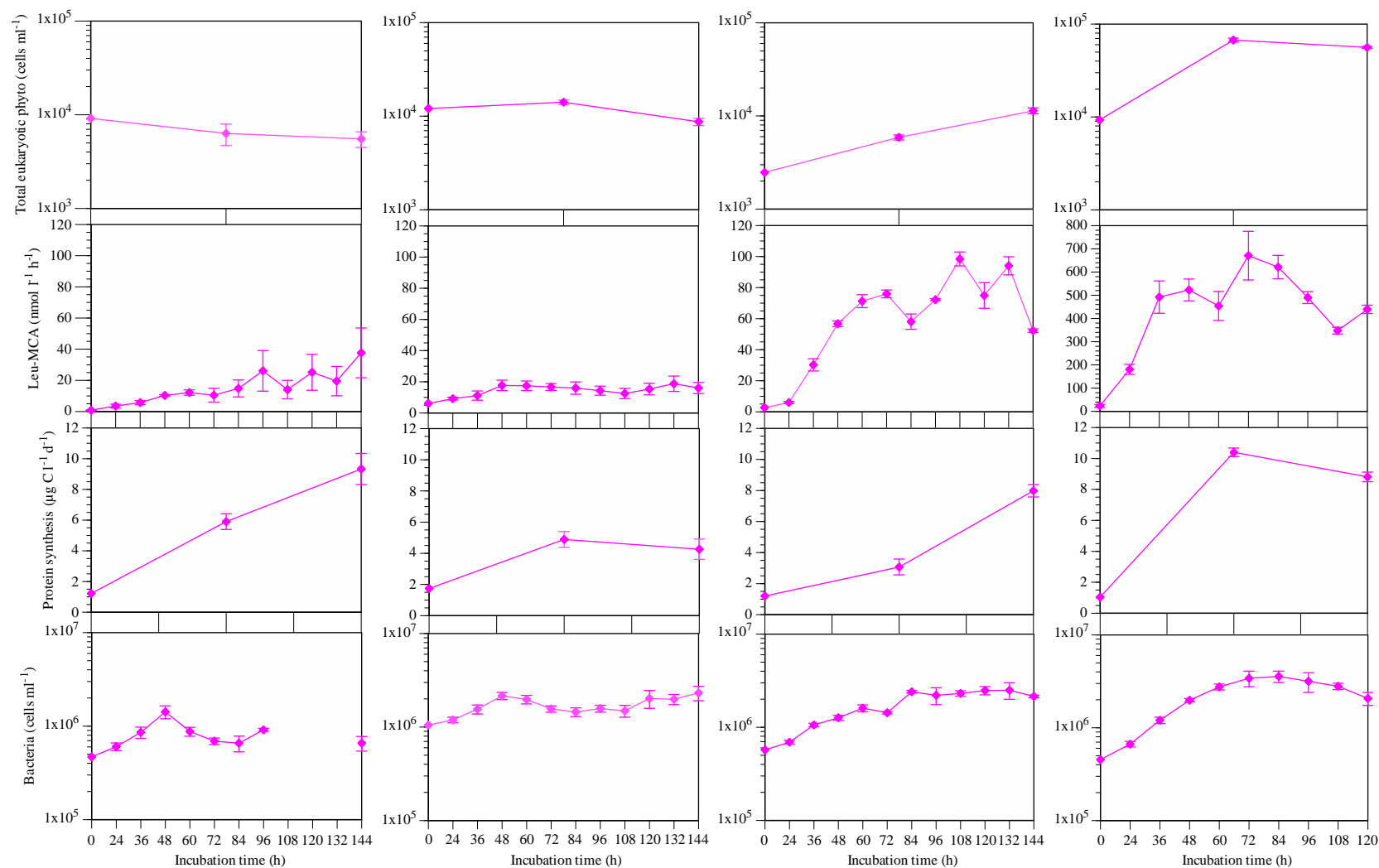


Fig. 4.38. Temporal development of selected parameters in the OA treatment in each incubation. Arranged in sequential order with incubation 1 on the far left, and incubation 4 on the far right. Missing value indicates sample was not determined

4.4.1.2 The response of extracellular enzyme activities to low pH conditions

The OA treatment had a variable effect on extracellular enzyme activities when compared to the ambient control between the different phytoplankton bloom communities. The OA treatment had a significant negative effect on Arg-aminopeptidase activity at 72 h during incubation 2, while a significant positive response was measured in incubation 3 (Table 4.9). Variation was also measured in the Leu-aminopeptidase Δ hydrolysis potential integrated to 72 h across each incubation, with activities ranging from 31.51 to 626.48 nmol l⁻¹ (Table 4.3). This trend indicates that Leu-aminopeptidase activity was positively affected by low pH but varied between incubations relative to the ambient control.

Variation in β - and α -glucosidase activity between the mixed phytoplankton communities under low pH conditions may indicate differences in the glucosidase diversity throughout each bloom community and their respective pH sensitivities. Arrieta & Herndl (2002) detected up to eight different β -glucosidases at the peak of a coastal *Phaeocystis* phytoplankton bloom. It is possible that in this thesis research, each mixed bloom community contained a different assemblage of glucosidase, each with a different pH optimum (Tipton & Dixon 1979), potentially explaining the measured variation in the response to low pH conditions. The variation in extracellular enzyme activity between phytoplankton communities could also result from bacterial specific responses to changes in seawater pH. Takeuchi et al. (1997) discovered that *Alteromonas rubra* was more sensitive to acidification at pH 5.5 than ten other bacterial strains. Maas et al. (2013) and Witt et al. (2011) also discovered variation in bacterial pH sensitivities with high CO₂ concentrations resulting in changes in bacterial diversity, while Teira et al. (2012) discovered that low pH conditions increased the growth efficiency of *Cytophaga* spp. when compared to *Roseobacter* spp.

Table 4.9. Summary of each parameter response from incubations 1 to 4 when compared to the ambient control ($p < 0.05$). Blue shaded cells indicate a response at 72 h, neutral shaded cells indicate a response at the final sampling point (incubation 1 to 3 - 144 h, incubation 4 – 120 h). ↑: indicates the parameter was significantly higher than the ambient control; ↓: significantly lower; empty cell: not significantly different; n.s: indicates the parameter was not sampled at 72 h

Parameter	Incubation 1			Incubation 2			Incubation 3			Incubation 4		
	OA	HT	GH	OA	HT	GH	OA	HT	GH	OA	HT	GH
β-glucosidase				↑	↑	↑					↑	↓
α-glucosidase											↑	↓
Arg-aminopeptidase		↑		↓			↑	↑	↑	↑	↓	↓
Leu-aminopeptidase	↑		↑	↑	↑	↑	↑	↑	↑	↑		↑
Bacterial numbers	↑		↑	↑				↑	↑		↓	↓
<i>Synechococcus</i> spp. numbers	↓	↓	↑	↑				↑	↓	n.s	n.s	↓
<i>Prochlorococcus</i> spp. numbers				↑	↓				↓	n.s	n.s	n.s
Total eukaryotic phytoplankton numbers			↑		↓	↓		↑		n.s	n.s	↓
BSP DNA synthesis			↑	↑	↑	↑		↑	↑		↑	↓
BSP protein synthesis	↑		↑	↑	↑	↑		↑	↑		↓	↓
Chl <i>a</i>	↑	↑		↑						n.s	n.s	↓
Nitrate	↓	↓	↓	↓					↓	n.s	n.s	n.s
DRP	↓	↓	↓	↓				↑		n.s	n.s	n.s
DRSi		↓	↓	↓						n.s	n.s	n.s
Ammonium					↑	↑	↑		↓	n.s	n.s	n.s
DOC	n.s	n.s	↑	n.s	n.s	n.s	n.s	n.s	n.s	n.s	n.s	↑
Total HMW reducing-sugar		↓			↑	↑		↑	↑	n.s	n.s	↑
Total HMW protein			↑	↓	↑	↓	↑	↓	↓	n.s	n.s	↑

The increase in β -glucosidase activity under low pH conditions lasted longer than 24 h in incubation 2. This response was not detected during the short-term acidification trial (Section 3.2). An increase in β -glucosidase activity under low pH conditions has also been detected in laboratory cultures (Yague & Estevez 1988), perturbation incubations using seawater collected from the Bay of Biscay (Piontek et al. 2010), from an Arctic glacial fjord system (Piontek et al. 2013) and seawater from the Ross Sea (Maas et al. 2013). Grossart et al. (2006) also reported elevated β -glucosidase, α -glucosidase and protease activity under acidified conditions in a large outdoor mesocosm experiment, however statistically significant responses were only detected for protease activity. Large variations in Arg-aminopeptidase and Leu-aminopeptidase activity were measured in the OA treatment during incubation 2. This variation could signify instability of the enzyme under low pH conditions. Leu- and Arg-aminopeptidase are metalloenzymes (Burley et al. 1990, Bogra et al. 2009) which contain metal ions that assist in enzyme activity (McCall et al. 2000). Smith & Spackman (1955) report that acidic conditions may remove the metal ions in the enzymes through ion exchange processes thereby increasing their instability. An alternate explanation for the variation in aminopeptidase activity as previously described for glucosidase by Tipton & Dixon (1979), is that proteases may also display high activity variability in response to low pH.

The initial positive response of Leu-aminopeptidase activity to low pH conditions was the same across each mixed phytoplankton community, although the magnitude of each response was different. Leu-aminopeptidase activity was positively affected by acidification independent of the dominant phytoplankton community; this result was also reported by Piontek et al. (2010, 2013). The uniform Leu-aminopeptidase activity trend between different phytoplankton communities is in contrast to the variation measured in total glucosidase and Arg-aminopeptidase activity. Because the time-zero bacterial community compositions were significantly different between the different phytoplankton communities in incubations 1 to 4 (pers. comm. Dr Els Maas, NIWA), it is possible that near-surface bacterial communities possess similar Leu-aminopeptidase degradation capabilities (Martinez et al. 1996, Arnosti 2003), while greater variation exists for carbohydrate degradation. During incubation 3, a positive correlation was detected between total HMW reducing-sugar concentration and β -glucosidase activity in the ambient control. This trend suggests that substrate inducible enzymes were activated under ambient conditions (Rogers 1961, Gottschalk 1985, Münster

1991, Arrieta & Herndl 2002). A similar positive correlation was also detected in the OA treatment during incubations 2 and 3, as well as for total HMW protein concentration and protease activity during incubation 4. However, the concentration of HMW substrate in the OA treatment was not consistently higher than the ambient control (Table 4.9), therefore substrate concentration alone does not explain the significantly higher Leu-aminopeptidase activity measured in each phytoplankton community in the OA treatment. Because an unknown proportion of the HMW substrate could have originated from phytoplankton and bacterial cells during sample analysis, this interpretation is only qualitative. pH is known to have several direct effects on enzyme activities (reviewed in Section 1.7 & 3.2.4) which could explain the trend in Leu-aminopeptidase activity between each incubation. Not only can pH directly affect catabolic enzyme activity, but it may also influence potential substrates and coenzymes, thereby indirectly affecting enzyme activity (Dixon 1953).

Throughout the present study, higher Leu-aminopeptidase activity was detected across all phytoplankton bloom types relative to β -glucosidase activity (Table 4.3), demonstrating that bacteria preferentially degrade peptide based HMW substrate relative to carbohydrate based substrate (Skopinstev 1981, Smith et al. 1992, Skoog & Benner 1997). An alternative explanation however is that a disproportionate concentration of HMW protein substrate relative to polysaccharides was present in each incubation, or the proportion of the bacterial community expressing Leu-aminopeptidase was larger than that expressing β -glucosidase (Arnosti 2011). The ratio between Leu-aminopeptidase and β -glucosidase can be used as an indicator of the quality of the carbon pool (Christian & Karl 1995): a high ratio indicates higher Leu-aminopeptidase activity relative to β -glucosidase, potentially in response to nitrogen limitation, whereas a low ratio value indicates increased carbohydrate degradation potentially reflecting lower protein availability or nitrogen replete conditions, and a nutrient rich carbon pool (Christian & Karl 1992, 1995). In this study, the Leu-aminopeptidase to β -glucosidase ratio in the OA treatment for each incubation ranged from 77.45 to 154.45 (Table 4.3). These activity ratios were much higher than those reported from Southern Ocean seawater (Maas et al. unpublished, ratios ranged from 0.64 to 3.18), implying increased Leu-aminopeptidase activity in response to a shortage of inorganic nitrogen (Piontek et al. 2013). Activity ratios in this study were lower than those reported from non-acidified polar environments (Christian & Karl 1995, ratios ranged from 339 to 1052), but consistent with ratio values from an Arctic Fjord (Piontek

et al. 2013, ratios ranged from 2 to 32). Activity ratios in the OA treatment were higher in incubations 1 and 3 relative to the ambient control (Table 4.3), suggesting that low pH conditions had a positive effect on Leu-aminopeptidase activity relative to β -glucosidase activity and that Leu-aminopeptidase is potentially more susceptible to direct pH effects (Section 1.7). Because a higher Leu-aminopeptidase activity was detected relative to β -glucosidase in the OA treatment across all phytoplankton bloom types, it is possible that protease degradation is of greater importance for bacterial metabolism than glucosidase. Using analysis of coastal bacterial community genes, Poretsky et al. (2010) experimentally showed that bacterioplankton exposed to phytoplankton-derived labile DOC, expressed more genes associated with the transport of amino acids than those for the transport of carbohydrates. Alternatively, it is also possible that the calculated activity ratios reflect the bioavailability of the dominant carbohydrate substrates in the ocean, i.e. cellulose (Benner et al. 1992), which tends to be more recalcitrant than protein-based substrates (Arnosti 2003). The calculated activity ratios could also reflect the dominant bacterial community composition in each incubation. For instance, Poretsky et al. (2010) observed variation in substrate transporter expression between bacterial species, suggesting that some bacterial species focus less on carbohydrate degradation or scavenging than other species.

4.4.1.3 Relationship between bacterial secondary production and bacterial cell numbers

In this research, the OA treatment had a significant positive effect on total BSP rates (DNA and protein synthesis) at selected sampling points during incubations 1 and 2 only (Table 4.9). Existing literature reports variable BSP responses to different acidified environments. For example, Arnosti et al. (2011) reported that high CO₂ had no significant effect on BSP rates in a developing phytoplankton bloom, as did Teira et al. (2012) who focused on the response of two bacterial isolates to high CO₂. Grossart et al. (2006) however, detected an increase in BSP rates with increasing CO₂ in a Norwegian mesocosm study, while Maas et al. (2013) and Siu et al. (2014) recorded a decrease in BSP rates with increasing CO₂ in Southern Ocean and Salish seawater respectively. These contrasting responses suggest that BSP in this thesis research may have been indirectly affected by OA and consequently, the changes detected may

signify variability in substrate availability and bacterial cell mortality. A strong positive correlation was however recorded between BSP and bacterial cell numbers in each incubation, implying that the active assimilation of LMW organic matter stimulated an increase in bacterial growth and cell numbers.

The OA treatment also had a variable effect on bacterial cell numbers between each incubation. Several acidification studies report no significant change in bacterial cell numbers (Grossart et al. 2006, Allgaier et al. 2008, Yoshimura et al. 2009, Arnosti 2011, Krause et al. 2012, Teira et al. 2012, Newbold et al. 2012, Roy et al. 2013), while others report a significant increase in bacterial numbers (Maas et al. 2013, Endres et al. 2014, Engel et al. 2014). Throughout incubations 2 and 3, bacterial cell numbers in the OA treatment were not significantly different from the ambient control, while numbers were positively affected at specific sampling points during incubation 1. Results show that bacterial numbers in incubation 1 increased concurrently with protein synthesis rates at 72 h. It is possible that bacterial cells associated with a dinoflagellate community are more sensitive to changes in pH. From these results, as well as the contrasting reports in the literature, it is clear that the response of BSP and bacterial cell numbers to low pH, is dependent on more than just pH. Although not clear from these incubations, it is likely that phytoplankton-derived organic matter composition and concentration, and its response to low pH will significantly affect bacterial growth and community structure in a future ocean (Tada et al. 2011).

4.4.1.4 Relationship between nutrients and phytoplankton

A positive correlation between low pH, Chl *a* concentration, phytoplankton cell numbers and DOC production has been extensively reported in surface ocean planktonic communities (Raven 1991, Chen & Durbin 1994, Hein & Sand-Jensen 1997, Tortell et al. 2008, Egge et al. 2009, Lomas et al. 2012, Maas et al. 2013). However, a correlation between dissolved nutrient drawdown, Chl *a* concentration and phytoplankton cell numbers was not detected in the OA treatment during incubations 1, 2 or 4; a correlation was measured in incubation 3 but this was not significantly affected by the OA treatment. A possible explanation for this contrasting response when compared to the literature may relate to differences in phytoplankton community responses when subject to low pH conditions. This hypothesis is supported by Endo

et al. (2013) and Engel et al. (2008) who suggest that different phytoplankton species have different carbon concentrating efficiencies. Depending on the efficiency of membrane transport and diffusion of HCO_3^- , those species which are not currently saturated under ambient inorganic carbon conditions may increase in numbers in a future low pH environment due to an increase in the inorganic carbon delivered to the carboxylation site (Kaplan & Reinhold 1999). Reports suggest that small eukaryotic phytoplankton ($< 10 \mu\text{m}$), such as *Micromonas* spp., may increase in numbers in a future low pH ocean (Engel et al. 2008, Endo et al. 2013).

An increase in total eukaryotic phytoplankton cell numbers should correspond to a more rapid drawdown of dissolved nutrients, indicating biological uptake and cell growth (Sverdrup et al. 1942c, Murray et al. 2007, Engel et al. 2014). In the OA treatment, nutrient concentrations declined across all phytoplankton bloom types, however this trend was not significantly different from the ambient control in three of the four phytoplankton communities. This result shows that the dissolved nutrient drawdown was not directly affected by low pH conditions, but rather the *in situ* phytoplankton community (Yoshimura et al. 2013). Yoshimura et al. (2009) reported that the response of nutrient-deplete plankton communities to high CO_2 treatments was significantly different from that of planktonic communities under nutrient-replete conditions. In this research, incubation 2 contained the lowest dissolved nutrient concentrations and was the only incubation in which *Synechococcus* spp. cell numbers significantly increased relative to the ambient control at 72 h. Under future low pH ocean conditions, Thornton (2014) hypothesised that DOM released by phytoplankton will increase based on the change in ocean chemistry creating a more stressful environment for phytoplankton growth. Although DOC concentrations were not significantly affected by low pH conditions in incubations 1 to 4 (Table 4.9), Kim et al. (2011) measured a 20% increase in DOC production under low pH mesocosm conditions, while Engel et al. (2014) experimentally showed that low pH conditions resulted in an increased production and exudation of organic matter during a coastal phytoplankton bloom.

Overall, low pH conditions predicted by the end of the century may have a significant effect on individual parameters sampled between different mixed phytoplankton communities, with these individual responses indirectly affecting the strength of parameter correlations. Low pH conditions had a positive effect on β -glucosidase and Leu-aminopeptidase activity, and although variation in the magnitude of enzyme response was apparent between incubations, a

clear preferential degradation of labile peptide substrates over carbohydrate substrates was detected. A potential increase in the availability of labile LMW protein substrate under low pH conditions could result in an increased BSP rate and bacterial cell numbers. A future increase in phytoplankton derived DOM could increase the availability of labile protein substrate to the microbial food web, potentially strengthening the microbial loop. An increase in protease remineralisation will also increase bacterial respiration, and potentially diminish the ocean's capacity to act as a carbon sink (Endres et al. 2014). Based on the preferential degradation of labile peptide substrate however, this could ultimately lead to an accumulation of carbohydrate relative to protein substrate and the possibility of increased carbon export (Arístegui et al. 2009).

4.4.2 Effect of elevated temperature

This section will discuss the response of extracellular enzyme activities to elevated temperature conditions. The analysis of additional sampled parameter responses will provide insight into possible indirect affects resulting from parameter interactions. The measured treatment response will also be compared between different phytoplankton communities.

4.4.2.1 The response of extracellular enzyme activities to elevated temperature conditions

Enzyme kinetics were determined under ambient seawater temperatures and therefore any significant change in enzyme activity reflects changes in the amount of enzymes synthesised during each incubation. Enzymes are considered to have optimal operating temperatures at which hydrolysis of substrate occurs most efficiently (Nedwell 1999). It is possible that glucosidase and protease activity sampled in incubations 2, 3 and 4 operate more optimally at elevated temperatures (+3°C) and bacteria respond by synthesising more to compensate. This is supported by the positive Leu-aminopeptidase Δ hydrolysis potentials (Table 4.3) as well as the increase in β -glucosidase cell-specific activity in incubation 3, and Leu-aminopeptidase cell-specific activity in incubations 2 and 3. According to the Q_{10} coefficient which suggests that biological metabolic processes double with an increase of 10°C (Sherr & Sherr 1996, Zeebe & Wolf-Gladrow 2001), extracellular enzyme synthesis may have occurred at a faster rate in the HT treatment relative to the ambient temperature treatments. In each incubation during this study, β -glucosidase Q_{10} values calculated from two sample points over 96 h ranged from 0.01 to 10.92, which are consistent with those reported by Piontek et al. (2013). However, in contrast to Piontek et al. (2013), Leu-aminopeptidase activity was more temperature dependent, with Q_{10} values ranging from 1.2 to 20.61. Assuming the same enzymes were measured, these findings suggest that although enzyme activities increased with temperature, the change in activity may depend on additional factors, such as the availability of labile aggregate substrate (Piontek et al. 2009).

Within the HT treatment, higher Leu-aminopeptidase activity was detected in each phytoplankton community relative to β -glucosidase activity (Table 4.3). The Leu-

aminopeptidase to β -glucosidase ratio in incubation 1, 2, 3 and 4 was 55.66, 147.02, 83.02 and 73.12 respectively. These ratio values are higher than values derived from oligotrophic equatorial waters (Christian & Karl 1995, ratios ranged from 0.12 to 0.27), as well as Southern Ocean seawater (Maas et al. unpublished, ratios ranged from 0.64 to 3.18), suggesting high organic nitrogen demand and enhanced enzymatic protein hydrolysis (Piontek et al. 2013). However, ratio values were also lower than those derived from Antarctic seawater (Christian & Karl 1995, ratios ranged from 339 to 1052). Elevated temperature did not have a significant effect on the preferential degradation of peptides over polysaccharides throughout incubations 2, 3 or 4, but the dinoflagellate and diatom dominated community of incubation 1 did have a higher ratio value than the ambient control (30.63). This enhanced Leu-aminopeptidase activity relative to β -glucosidase under elevated temperature is supported by Piontek et al. (2009), who reported a ratio value of 7.30 at 2.5°C and 23.12 at 8.5°C.

Trends identified from the Q_{10} coefficient and Leu-aminopeptidase to β -glucosidase ratio suggest that elevated temperature may not be the only factor effecting enzyme activity in the HT treatment. The production of aggregates from HMW substrate is primarily driven by abiotic particle collisions associated with differential settling (Simon et al. 2002). Piontek et al. (2009) hypothesised that particle aggregation is influenced by temperature, reporting an increase in aggregate formation with an increase in seawater temperature of only 2.5°C. Organic aggregates not only provide labile substrate for enzyme remineralisation, but also physical attachment sites for free-living bacteria, often leading to increased cell numbers and enzyme activity (Sutherland 1972, Decho 1990, Passow 2002). Findings from this thesis research showed that total HMW organic compound concentrations increased in incubations 2 and 3 under elevated temperature, while bacterial and phytoplankton cell numbers declined. This trend is consistent with an increase in aggregate concentration, potentially increasing bacterial attachment sites and stimulating the production and activation of inducible glucosidase and protease activity during incubations 2 and 3. However, it is apparent that when total HMW substrate concentrations are high, such as during incubations 2 and 3, elevated temperature is not shown to affect the preferential degradation of peptides over carbohydrates.

During incubation 3, β - and α -glucosidase activity was high in the HT treatment from 72 h to 120 h, while activity declined in incubation 4. The trend measured in incubation 3 is supported by a high cell-specific β -glucosidase activity which may reflect the Q_{10} coefficient (Sherr &

Sherr 1996, Zeebe & Wolf-Gladrow 2001) as well as an increase in enzyme synthesis. However, the decline in β - and α -glucosidase activity in incubation 4 corresponded to a significant increase in cell-specific β -glucosidase activity from 96 h to 120 h. This trend may indicate a reduction in the number of enzymes synthesised due to the rapid decline in bacterial cell numbers. This late decline in bacterial numbers could signify an increase in viral lysis (Proctor & Fuhrman 1990, Danovaro et al. 2010) and/or protozoan grazing (Sherr et al. 1987), which would also explain the significant increase in DOC concentrations detected during incubation 4 (Weinbauer et al. 2011, Weitz & Wilhelm 2012). This hypothesis is further supported by a similar declining trend in bacterial cell numbers, β -glucosidase and Leu-aminopeptidase activity during incubation 2.

Overall, variation in extracellular enzyme activity was detected between each mixed phytoplankton community, particularly incubation 4. An increase in aggregate concentrations and total glucosidase and Leu-aminopeptidase activity under elevated temperature would increase the strength of the microbial loop, increasing the concentration of LMW labile substrate in the near-surface open ocean. This process could temporarily reduce the vertical flux of organic matter and therefore the efficiency of the biological carbon pump.

4.4.2.2 Relationship between bacterial secondary production and bacterial cell numbers

Total BSP rates (DNA and protein synthesis) increased in the HT treatment across all phytoplankton communities for the first 60 h. This was not surprising as BSP is a function of metabolism and according to the Q_{10} coefficient is expected to increase with increasing temperature (Tibbles 1996, Shiah & Ducklow 1997, Rivkin & Legendre 2001, Vázquez-Domínguez et al. 2007, 2012). The initial positive BSP response in incubations 2 and 3 represents a direct increase in metabolic processes as predicted by the Q_{10} coefficient (Sherr & Sherr 1996, Zeebe & Wolf-Gladrow 2001, Brown et al. 2004), while the positive responses recorded in incubations 1 and 3 from 108 h to 144 h are likely to signify an indirect community interaction, such as low bacterial mortality and high LMW substrate concentrations. A positive correlation was detected between total BSP rates and bacterial cell numbers in the HT treatment during incubations 2, 3 and 4. During incubations 2 and 4, both parameters show an initial positive response, followed by a negative response at the final sampling point. This negative response was likely due to intensive grazing (Sherr et al. 1987), as *Synechococcus* spp. and total eukaryotic phytoplankton numbers also decline.

4.4.2.3 Relationship between nutrients and phytoplankton

Phytoplankton communities in incubations 2 and 3 showed an inverse correlation between dissolved nutrient drawdown, increased planktonic cell numbers and DOC production. Surface ocean DOC production occurs through both autotrophic and heterotrophic processes (Hansell 2002, Hopkinson & Vallino 2005), with autotrophic production the most significant source of organic matter (Lefevre et al. 1996, Karl et al. 1998, Thornton 2014). Mesocosm experiments provide evidence for increased phytoplankton release of DOM under elevated temperature conditions (Engel et al. 2011, Wohlers et al. 2009, 2011), while a short-term (6 h) warming experiment using a natural Southern Ocean phytoplankton community resulted in a 54% increase in organic extracellular release (Moran et al. 2006). The HT treatment had a positive effect on DOC concentrations during incubations 1 and 4, both thought to be dominated by dinoflagellates. It is possible that dinoflagellates favour warmer conditions (Chen et al. 2011) and in accordance to the Q_{10} coefficient increase DOC

production and exudation in the HT treatment relative to ambient temperature treatments. Alternatively, the elevated DOC concentrations in the HT treatment during incubation 4 may indicate increased grazing and viral lysis (Proctor & Fuhrman 1990). This hypothesis would also explain the sudden decline in total eukaryotic phytoplankton, *Synechococcus* spp. and bacterial cell numbers measured throughout incubation 4, however it would not explain the significant increase in DOC concentration shown in incubation 1, as phytoplankton and bacterial cell numbers did not show the same rapid decline.

Overall, the HT treatment had variable effects on sampled parameters across mixed phytoplankton communities. This significant HT response is supported by the MDS plots of incubations 3 & 4 which show divergence away from the ambient control (Section 4.3.8). The HT treatment had a positive effect on total glucosidase and protease activity throughout incubations 3 and 4, in accordance with the Q_{10} coefficient. The results suggest that near-surface extracellular enzyme activities will vary between phytoplankton communities in a future warming ocean, and that total BSP, metabolic respiration and bacterial cell numbers may respond positively across phytoplankton blooms of different community compositions. The findings suggest that heterotrophy may increase in a future warming ocean, resulting in the strengthening of the microbial loop and a decrease in the efficiency of the biological carbon pump following a reduction in carbon export.

4.4.3 Effect of elevated temperature and low pH

This section will discuss the response of extracellular enzyme activities under elevated temperature and low pH conditions predicted by the end of the century, as well as determine which perturbation treatment is driving this change. The analysis of additional sampled parameter responses will provide insight into possible indirect affects resulting from parameter interactions. The measured treatment response will be compared between different phytoplankton communities.

4.4.3.1 The response of extracellular enzyme activities to elevated temperature and low pH conditions

The GH treatment simulates realistic elevated temperature and low pH conditions predicted by the end of the century. Consequently the direct and indirect effects of both low pH (Section 4.4.1) and elevated temperature (Section 4.4.2) may be expected, although these may be altered by additive, synergistic or antagonistic interactions between the two stressors.

Extracellular enzyme activity in the GH treatment was significantly different between each incubation. In the ‘unidentified’ phytoplankton community (incubation 4), β -glucosidase, α -glucosidase and Leu-aminopeptidase activity followed a very similar trend to that measured in the HT treatment (Section 4.4.2). It was hypothesised in Section 4.4.2 that a decline in enzyme activity may have resulted from a decline in total enzyme synthesis and overall enzyme abundance due to bacterial mortality from viral lysing (Proctor & Fuhrman 1990, Danovaro et al. 2010) and/or protozoan grazing (Sherr et al. 1987). As cell-specific β -glucosidase and Leu-aminopeptidase activity was not significantly affected under GH conditions from 36 h to 96 h during incubation 4, this same hypothesis is viable for explaining the decline in total glucosidase activity and Leu-aminopeptidase activity during incubation 4, as well as the decline in Leu-aminopeptidase activity from 72 h to 144 h during incubation 2. This significant GH response is supported by the MDS plot of incubations 2 and 4 which showed divergence away from the ambient control by the final sampling point (Section 4.3.8). In contrast to the other sampled enzymes, Arg-aminopeptidase activity did not decline beyond 60 h in incubation 4 and could result from a unique enzyme response (Arnosti et al. 2011), rather than a specific

treatment response. Münster (1991) reports that extracellular enzyme activity and their regulation is not only controlled by *in situ* environmental conditions (pH and temperature), but rather a combination of environmental, metabolic and genetic controls. This hypothesis suggests that extracellular enzyme activities are also subject to *in situ* substrate availability as well as the community composition. The variation in enzyme responses measured between the different phytoplankton communities supports this hypothesis.

The dominant phytoplankton community in a bloom can significantly affect the composition and concentration of available DOM (Passow et al. 2007, Tada et al. 2011), and potentially the tendency of the substrate to coagulate (Passow et al. 2007). Therefore, it is possible that the organic components contributing to the formation of HMW compounds were significantly different between the incubated phytoplankton communities, thereby explaining the variable HMW protein concentrations measured. The GH treatment may have directly altered the chemical and physical composition of the HMW protein substrate, increasing its accessibility to protease active sites and indirectly stimulating the significantly higher Leu-aminopeptidase activity. As measured in both the OA and HT treatments, significantly higher Leu-aminopeptidase activity was detected when compared to β -glucosidase activity in all incubations. The Leu-aminopeptidase to β -glucosidase ratio in the GH treatment during incubation 1, 2, 3 and 4 was 59.70, 150.96, 137.35 and 66.51 respectively, with ratio values in incubations 1 and 3 higher than their respective ambient controls (Table 4.3), suggesting that GH conditions increased the degradation of peptide substrates relative to carbohydrates. Ratio values were higher in the OA treatment relative to the GH treatment during incubations 1, 3 and 4, while the HT treatment had lower values than the GH treatment during incubations 1 and 3. Both acidified treatments had higher values than the ambient control during incubations 1 and 3 (Table 4.3). This trend suggests that an antagonistic effect occurred between elevated temperature and low pH and that low pH was the driving factor behind the elevated ratio values in the GH treatment. This hypothesis is further supported by the Leu-aminopeptidase Δ hydrolysis potential values which were highest in the OA treatment and lowest in the HT treatment (Table 4.3).

Overall, both elevated temperature and low pH treatments show independent effects on extracellular enzyme activities, however no clear additive or synergistic treatment effect was detected in the GH treatment. This finding indicates that when both treatments are combined,

the OA effect is reduced or that the effect of temperature dominates the overall response. During incubation 3, Leu-aminopeptidase activity in the GH treatment was more similar to activity in the OA treatment than the HT treatment, in contrast to incubations 1, 2 and 4. Although no additive or synergistic effect was detected, the OA effect in the GH treatment did not appear to be reduced by elevated temperature. In contrast, total HMW organic compound concentrations increased in the HT treatment but not in the GH treatment. This suggests that the effect of elevated temperature was reduced when combined with low pH.

4.4.3.2 Relationship between bacterial secondary production and bacterial cell numbers

A positive correlation was detected between total BSP and bacterial cell number in the GH treatment in each phytoplankton community, similar to the OA and HT treatments. The GH conditions had a significant positive effect on DNA synthesis rates in each incubation for the first 72 h, resembling a very similar rate to the HT treatment. Protein synthesis rates also increased in each incubation from time-zero to 72 h, however rates were similar to the ambient control. Bacterial cell numbers in the GH treatment increased in each incubation for the first 48 h, and then began to decline, correlating strongly with a decline in DNA synthesis. Overall, these findings suggest that temperature initially drove both cell growth and division, however beyond 72 h, DNA synthesis rates and cell numbers rapidly declined. This decline could indicate a low temporal tolerance to GH conditions, a reduction in available labile substrate following the initial growth period or an increase in viral cell lysing (Proctor & Fuhrman 1990) and/or protozoan grazing (Sherr et al. 1987) corresponding to increases in their respective metabolism. During incubation 1, the same rapid decline in DNA synthesis and bacterial cell numbers was not detected from 72 h to 144 h. It is possible that incubation 1 contained a bacterial community that was more tolerant to elevated temperature and/or low pH when compared to communities in incubations 2 or 4. Lindh et al. (2013) showed that temperature is a major driver in structuring a bacterial community; it is possible that the bacterial community composition in incubation 1 changed under GH conditions to a more temperature or pH tolerant community. Alternatively, the bacterial community within incubation 1 may indicate different nutrient or organic matter preferences or increased resistance to viral lysing and/or protozoan grazing.

Both DNA and protein synthesis initially increased in the GH treatment during incubation 3, however DNA synthesis began to decline following 36 h, while protein synthesis continued to increase. This trend suggests that the bacterial community invested metabolic energy in different pathways at different temporal stages throughout the incubation. An increase in protein synthesis may show an increase in metabolic activity, perhaps contributing towards synthesis of new extracellular enzymes, or alternatively, expressed in response to adverse environmental conditions, in which the bacteria would focus on protein based cellular repair (Lenhart et al. 2012). Bacterial cell numbers were typically higher in the GH treatment than in the ambient control throughout incubation 3, indicating that bacteria were not experiencing adverse conditions, but rather may reflect an increase in metabolism and bacterial community growth under GH conditions. Once again, no obvious additive or synergistic treatment effect was measured for BSP or bacterial cell numbers in the GH treatment.

It appears that temperature effects on BSP may override the influence of low pH when combined in the GH treatment (Table 4.9), which is in accordance to the Q_{10} coefficient (Sherr & Sherr 1996, Zeebe & Wolf-Gladrow 2001). Similarly, elevated temperature is likely to be responsible for the positive short-term effect on bacterial numbers, which was also reported by Piontek et al. (2009) and Lindh et al. (2013) from Baltic Sea incubation experiments.

4.4.3.3 Relationship between nutrients and phytoplankton

Variation in the response of each phytoplankton community was measured in the GH treatment. This response is supported by Feng et al. (2009) who concluded that temperature and CO_2 had different effects on different phytoplankton groups during the North Atlantic spring bloom. During incubation 1, the dinoflagellate and diatom dominated community showed a strong correlation between dissolved nutrient concentrations, Chl *a* concentrations and planktonic cell numbers, with the GH treatment showing a significant positive effect. Photosynthetic phytoplankton use the enzyme RuBisCo to fix organic carbon. RuBisCo is naturally under-saturated at current CO_2 levels (~380 ppmv) and therefore expected to increase under high CO_2 /low pH conditions predicted by the end of the century (Descolas-Gros & Billy 1987, Engel et al. 2008, Hannah 2011). The increase in Chl *a* concentrations and planktonic cell numbers measured in incubation 1 may signify an increase in photosynthetic activity driven

by RuBisCo under GH conditions. It is equally plausible that the elevated temperature associated with the GH treatment increased the metabolic potential of the phytoplankton community in accordance to the Q_{10} coefficient, thereby increasing planktonic cell numbers and Chl *a* concentrations. Although the GH treatment had a positive effect, a clear additive or synergistic affect was not detected.

During incubations 2 and 3, the GH treatment did not have a significant effect on dissolved nutrient concentrations, Chl *a* concentrations, total eukaryotic phytoplankton cell numbers or DOC concentrations. During incubation 4, *Synechococcus* spp., total eukaryotic phytoplankton cell numbers and Chl *a* concentrations were negatively affected by the GH treatment. Because dissolved nutrient concentrations in the GH treatment were not significantly different from the ambient control, the recorded decline in plankton cell numbers may signify increased grazing pressure (Deason 1980). *Prochlorococcus* spp. and *Synechococcus* spp. cell numbers responded to the GH treatment differently, with *Synechococcus* spp. appearing more sensitive to changes in temperature and pH. This trend is supported by Fu et al. (2007) who reported very different responses between cyanobacteria when exposed to pH and temperature predicted by the year 2100. Fu et al. (2007) reported that *Synechococcus* spp. showed a different photosynthetic response to increasing CO₂ depending on temperature, concluding that *Synechococcus* spp. and *Prochlorococcus* spp. may have different mechanisms of carbon uptake.

Overall, the GH treatment showed strong parameter correlations during incubations 2 and 4. Each mixed planktonic community showed a broad range of sensitivities and responses under GH conditions, similar to that reported by Feng et al. (2009). Ocean warming is expected to drive changes in bacterial community composition (Lindh et al. 2013) and consequently variation in substrate degradation and cell growth. No clear additive or synergistic effect was apparent in any sampled parameters within the GH treatment, however antagonistic effects were detected. Dissolved nutrient concentrations, total phytoplankton cell numbers and Chl *a* concentrations in the GH treatment were more similar to those in the HT treatment when compared to the OA treatment, and therefore the elevated temperature in the GH treatment may have reduced the effect of low pH.

4.5 Summary

In these near-surface open ocean incubations, a positive Leu-aminopeptidase activity response was recorded in each treatment of the different phytoplankton communities. Each incubation also highlighted temporal variability in extracellular enzyme activities and bacterial cell numbers between different phytoplankton communities and perturbation treatments, suggesting that parameter responses were determined by direct and indirect effects. Within the GH treatment, the individual factor driving a particular parameter response was not the same between different phytoplankton communities, and no clear additive or synergistic effect was detected for any sampled parameter in any mixed phytoplankton community.

These incubations suggest that by the end of the century, Leu-aminopeptidase activity will increase. An increase in peptide substrate remineralisation could accelerate and strengthen the heterotrophic microbial loop (Piontek et al. 2010, Passow & Carlson 2012), increasing transfer of organic carbon to higher trophic levels. This future scenario may increase heterotrophic metabolic activity in the near-surface ocean, thereby creating a positive inorganic carbon feedback (Feng et al. 2009, Wohlers et al. 2009, Piontek et al. 2010) likely to contribute to/and further exacerbate surface OA conditions. However, the results suggest that this increased heterotrophic activity will not be sustained, reflected by the eventual decline in bacterial numbers and secondary production.

Chapter 5 : The response of enzyme activity to elevated temperature and low pH in open ocean subsurface waters

5.1 Introduction

From the ocean surface a vertical gradient exists for a wide range of abiotic oceanographic parameters, including pH, temperature, pressure, salinity, photosynthetic active radiation (PAR), and dissolved nutrient and organic carbon concentrations (Sverdrup et al. 1942b, Hansell & Carlson 2001, Pukate & Rim-Rukeh 2008, Stewart 2008, Wohlers-Zöllner et al. 2011). These factors directly and indirectly affect a range of microbial processes below the ocean surface, for instance, bacterial metabolism, primary and secondary production (Tamburini et al. 2002, Baltar et al. 2010), heterotrophic respiration (Baltar et al. 2009), heterotrophic community composition (Davey et al. 2001, Hewson et al. 2006) and bacterial extracellular enzyme activities (Aristegui et al. 2009, Baltar et al. 2009, 2010). Maximum extracellular enzyme activities typically occur near the ocean surface (Rosso & Azam 1987, Davey et al. 2001, Tamburini et al. 2002), and decline with depth (Karner & Rassoulzadegan 1995, Hoppe & Ullrich 1999, Baltar & Aristegui 2009). Although enzyme activities may be influenced by hydrostatic pressure (Takata et al. 1995, Tamburini et al. 2002), depth is not the primary factor regulating activity. Instead subsurface extracellular enzyme activities are thought to be controlled by the availability of labile organic matter (Rosso & Azam 1987, Davey et al. 2001, Baltar et al. 2010). The majority of subsurface labile organic matter is produced near the ocean surface through autotrophic primary production (Sverdrup et al. 1942a, Aristegui et al. 2009), and as PAR diminishes with depth (Cullen 1982) so too does the number of autotrophic organisms and the production of labile organic carbon (Williams 1975, Benner 2002, Ogawa & Tanoue 2003). Surface ocean labile organic matter undergoes a range of abiotic and biotic processes, transforming its physical shape and size. The abiotic coagulation and formation of POM is one such process (Kjørboe et al. 2001, Engel 2002). Labile POM is subject to intensive remineralisation in the near-surface ocean, resulting in declining abundance with depth (Williams 1975, Haake et al. 1993, Amon & Benner 1996, Benner 2002, Ogawa & Tanoue 2003). Despite intensive remineralisation, a small proportion (~10%) escapes the surface ocean and sinks below the surface mixed layer (Martin et al. 1987, Hansell 2002, Hoppe et al. 2002, Tamburini et al. 2003, Bhaskar & Bhosle 2005). The rate at

which the organic matter sinks is a function of size, varying with substrate composition and density (Smayda 1969, Simon et al. 2002). As particles sink they are continuously degraded through extracellular enzyme hydrolysis (Aristegui et al. 2009, Baltar et al. 2009), becoming increasingly recalcitrant with depth (Carlson & Ducklow 1995). The dominant organic matter at depth consists of recalcitrant semi-labile material (Benner et al. 1992), mainly low bio-reactive waste products (Carlson 2002), resistant material following mortality of an organism (Jiao et al. 2010), or organic substrates that are naturally resistant to microbial degradation (Fry et al. 1996), such as silicate frustules of diatoms (Alldredge 1998).

There are several pathways through which labile organic material is exported from near-surface waters into subsurface waters, thereby providing potential substrate for heterotrophic enzyme activity and bacterial growth. One such pathway is referred to as passive flux, involving non-assisted sinking of labile organic matter from the ocean surface (Hansell & Carlson 2001, Aristegui et al. 2009, Passow & Carlson 2012). Passive flux typically occurs following the seasonal occurrence of a near-surface phytoplankton bloom event (Sverdrup et al. 1942a) when high concentrations of nutrient rich labile organic matter are produced, ensuring that an increased proportion of POM escapes near-surface heterotrophic remineralisation and sinks. An alternate pathway through which labile organic material is exported to subsurface waters is referred to as active flux. This pathway involves the direct consumption of surface-derived labile DOM by larger heterotrophic microzooplankton which is actively exported to greater depths during diurnal migrations and excreted as particulate faecal pellets (Riebesell 2004, Denman et al. 2007, Passow & Carlson 2012). An additional pathway involves export by ocean entrainment and detrainment of the surface mixed layer (Levy et al. 2013), which can extend to deep-water upwelling and down-welling in some regions (Hansell & Carlson 2001, Baltar et al. 2009, 2010).

The availability of labile DOM in the subsurface open ocean is far lower than that of the near-surface, with bacterial communities forced to gain their energy requirements from bulk organic matter of a semi-labile nature (Tamburini et al. 2002, 2003, Aristegui et al. 2009). Labile organic matter typically consists of carbohydrates, proteins, amino acids and lipids at higher concentrations relative to surrounding bulk DOM (Section 1.4). Heterotrophic bacteria are known to preferentially degrade protein based organic compounds over polysaccharides (Smith et al. 1992, Skoog & Benner 1997, Baltar et al. 2009, and results in Chapter 4), which

is thought to reflect the importance of proteins for cell growth as well as being less recalcitrant compared to polysaccharide substrate (Arnosti 2003). This preferential degradation increases the compositional ratio of carbohydrate within subsurface organic matter (Haake et al. 1993). Because labile organic matter concentration, composition and size declines with depth, bacterial secondary production rates (BSP), bacterial numbers and extracellular enzyme activities also decline with depth when compared to the near-surface open ocean (Hoppe & Ullrich 1999, Davey et al. 2001, Baltar et al. 2009, 2010).

The subsurface bacterial community is often distinct from the surface mixed layer community, reflecting a different community composition with specific adaptive strategies for survival in low light and nutrient conditions (Field et al. 1997, Davey et al. 2001, Tamburini et al. 2002). Importantly, not only do bacterial communities change vertically within the water column, but they also change between water masses (Ghiglione et al. 2012), reflecting differences in climatic conditions around the world and their influence on regional oceanography (Stewart 2008). Predicted future changes in ocean pH and temperature will not only affect a range of biological processes, but also alter a series of oceanographic processes which could also indirectly affect bacterial extracellular enzyme activity in the subsurface ocean. For example, *in situ* temperature, pressure and conductivity combine to determine the density of seawater (Stewart 2008). Differences in seawater density between two water masses can lead to increased ocean stratification (Stewart 2008). The subsurface ocean is less susceptible to changes in temperature arising from solar insolation and stratification, whereas the near-surface ocean experiences regular temporal variation (Lau & Sui 1997, Kaiser et al. 2011). With surface ocean temperatures predicted to increase in the future (Section 1.1), the ocean is predicted to become more stratified, increasing the stability of the surface mixed layer (Sarmiento et al. 2010, Passow & Carlson 2012). An increase in ocean stratification can influence light regimes and the segregation of organic and inorganic nutrients throughout the water column (Rost et al. 2008, Sarmiento et al. 2010, Engel et al. 2011).

Seasonal phytoplankton blooms in oligotrophic open ocean waters require dissolved nutrients brought to the surface through mixing during winter. If the surface ocean becomes increasingly stratified, dissolved nutrients required to initiate and maintain a phytoplankton bloom will not reach the surface where sufficient PAR is available. Increased ocean stratification could therefore impact negatively on phytoplankton primary production and organic matter

production, with further decreases in available growth-limiting nutrients resulting in phytoplankton population declines (Taylor 1995, Sarmiento et al. 2010). A decline in phytoplankton-derived organic matter as well as the establishment or strengthening of a stratified layer, is also expected to reduce the export of labile POM into the subsurface ocean (Doval & Hansell 2000), thereby negatively affecting heterotrophic extracellular enzyme activities and bacterial secondary production rates. Current literature suggests that the effects of temperature and pH on the abiotic coagulation and formation of organic aggregates are antagonistic. Mari (2008) reported that increased ocean acidification could lead to a decrease in organic matter coagulation and aggregate formation, negatively affecting POM export to the subsurface, while Piontek et al. (2009) reported that aggregate formation may increase in a warming ocean, increasing organic matter export.

Not only are heterotrophic organisms expected to be negatively affected by a future stratified ocean, but a significant decline in organic carbon export would also affect the efficiency of the biological carbon pump (Hopkinson & Vallino 2005), reducing the amount of active organic carbon entering the deep ocean and eventually becoming sequestered (Laws et al. 2000, Bopp et al. 2001, Bhaskar & Bhosle 2005, Wohlers et al. 2009, Piontek et al. 2010, Weinbauer et al. 2011). Moreover, because the subsurface ocean is characterised as a low oxygen high respiration environment, coupled with low mixing and ventilation, CO₂ will be retained and ultimately contribute to a positive feedback of inorganic carbon and an increasingly acidic subsurface ocean. Current OA perturbation research is typically conducted using surface ocean seawater, however as a large proportion of microbial heterotrophic activity occurs in/or below the surface mixed layer (Gasol et al. 1997, Arístegui et al. 2009), determining how this microbial community will respond to future ocean conditions predicted by the end of the century is vital for understanding the future flow of inorganic and organic carbon within the ocean's interior. Considering the oceanographic differences between the near-surface and subsurface ocean, the response of subsurface extracellular enzymes could be very different from those of the near-surface ocean.

The aim of this chapter was to investigate potential differences in the response of extracellular enzyme activities to ocean conditions predicted by the end of the century sampled from below the surface mixed layer.

5.2 Methods

Three perturbation incubations were conducted to ascertain the effect of low pH and elevated temperature on microbial processes below the surface mixed layer. Bulk seawater for each incubation was collected from within an open ocean eddy circulating off the east coast of the North Island, New Zealand (Fig. 5.1). The Spring Bloom voyage followed the eddy circulation using drifter buoys to determine phytoplankton bloom development in a semi-isolated body of water.

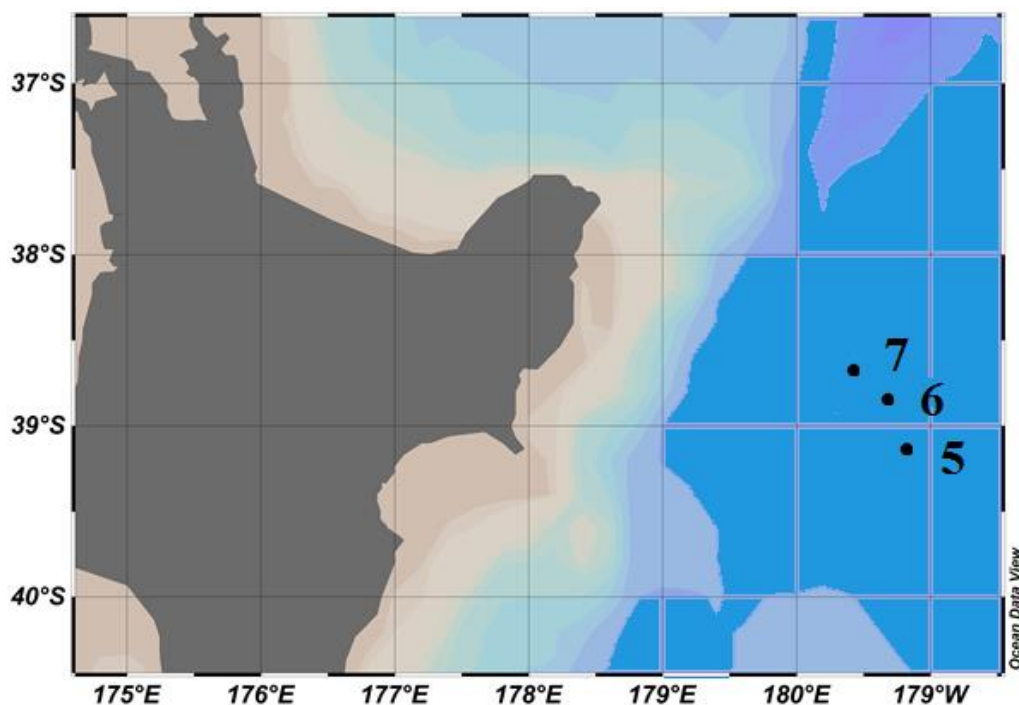


Fig. 5.1. Circles mark the location of bulk seawater collection sites in an eddy east of New Zealand. Annotated numbers correspond to the three individual subsurface incubations completed, numbering continues on from the near-surface incubations (Chapter 4)

Bulk seawater for each incubation was collected from below the base of the surface mixed layer (~100 to 200 m depth). Each incubation employed the same seawater collection equipment as described in Section 4.2 and the same experimental perturbation treatments as described in Section 2.1, with ambient incubation temperatures reflecting the bulk seawater

collected. Treatment pH and temperature were measured at selected sampling points throughout each incubation (Appendix A: 5.1). Light availability at the seawater collection depth was not measured but was likely to be very low (pers. comm. Dr Cliff Law), so incubated seawater was maintained in the dark. Further to this, each cubitainer viewing window was covered with a black polythene bag, to minimise ambient light exposure during sub-sampling. Based on preliminary findings gained from incubations 1 to 4 (Chapter 4), the experimental sampling protocol used for the following incubations was modified to emphasise identified parameter interactions. Modifications included reducing the frequency of primary parameter sampling from 12 h to 24 h, as each incubation had a duration of 96 h. This produced a total of five sampling points. Also, total HMW organic compound concentrations were upgraded to primary parameter status, with sampling frequency intensified to every 24 h (Table 5.1).

Table 5.1. Parameter sampling protocol for incubations 5 to 7. The total number of times and frequency each parameter was sampled is indicated, followed by its respective sampling frequency [in square brackets], after an initial time-zero sample. Parameters in **bold** indicate parameters of primary significance

Incubation	5	6	7
Location ($^{\circ}$)	39.16 $^{\circ}$ N 180.76 $^{\circ}$ E	38.93 $^{\circ}$ N 180.56 $^{\circ}$ E	38.79 $^{\circ}$ N 180.34 $^{\circ}$ E
Duration	19.9.12 – 23.9.12	25.9.12 – 29.9.12	1.10.12 – 5.10.12
Depth (m)	200	100	100
Ambient temperature ($^{\circ}$ C)	13.00	13.38	13.36
Salinity (psu)	35.24	35.23	35.22
β-glucosidase and α-glucosidase	4 [24 h]	4 [24 h]	4 [24 h]
Leu-aminopeptidase and Arg-aminopeptidase	4 [24 h]	4 [24 h]	4 [24 h]
Bacterial numbers	4 [24 h]	4 [24 h]	4 [24 h]
Pico-cyanobacteria numbers	2 [48 h]	2 [48 h]	2 [48 h]
Total eukaryotic phytoplankton numbers	2 [48 h]	2 [48 h]	2 [48 h]
BSP DNA synthesis	4 [24 h]	4 [24 h]	4 [24 h]
BSP protein synthesis	2 [48 h]	2 [48 h]	2 [48 h]
Dissolved nutrients	1 [96 h]	1 [96 h]	1 [96 h]
Chl <i>a</i>	1 [96 h]	1 [96 h]	1 [96 h]
DOC	1 [96 h]	1 [96 h]	1 [96 h]
Total HMW organic compound (reducing-sugar and protein)	4 [24 h]	4 [24 h]	4 [24 h]

5.3 Results

Comparison of ambient conditions

Bulk seawater used in incubations 6 and 7 was collected from 100 m depth, resulting in similar time-zero parameter samples (Table 5.2). For instance, time-zero dissolved nutrient, Chl *a* and DOC concentrations were very similar, as was protein synthesis. Bulk seawater collected for incubation 5 was collected from 200 m depth within the same eddy. At this greater depth, DNA synthesis rates, dissolved ammonium and DOC concentrations were lower when compared to bulk seawater collected from 100 m depth (Table 5.2). Incubations 6 and 7 time-zero protein synthesis rates and bacterial cell numbers were within the range reported from 100 m depth in the NW Mediterranean (Tamburini et al. 2002), while cell numbers were also similar to those reported from a similar depth in the North Atlantic (Davey et al. 2001) as well as the Santa Monica Basin (Rosso & Azam 1987).

Table 5.2. Average time-zero data for each sampled parameter per incubation (\pm SE). Samples were analysed following methodology in Chapter 2

Parameter	Incubation 5	Incubation 6	Incubation 7
β -glucosidase (nmol l ⁻¹ h ⁻¹) (n=2)	0	0	0
α -glucosidase (nmol l ⁻¹ h ⁻¹) (n=2)	0	0	0
Arg-aminopeptidase (nmol l ⁻¹ h ⁻¹) (n=2)	2.91 (\pm 0.80)	0	3.21 (\pm 0.31)
Leu-aminopeptidase (nmol l ⁻¹ h ⁻¹) (n=2)	5.01 (\pm 0.48)	0	0
Bacterial numbers (cells ml ⁻¹) (n=3)	3 x 10 ⁵ (\pm 1.6 x10 ⁴)	2 x 10 ⁵ (\pm 2.4 x10 ²)	4 x 10 ⁵ (\pm 1.5 x10 ³)
<i>Synechococcus</i> spp. numbers (cells ml ⁻¹) (n=3)	4 x 10 ³ (\pm 1.0 x10 ²)	1 x 10 ³ (\pm 1.7 x10 ¹)	3 x 10 ³ (\pm 8.5 x10 ¹)
Total eukaryotic phytoplankton numbers (cells ml ⁻¹) (n=3)	9 x 10 ³ (\pm 1.5 x10 ²)	8 x 10 ³ (\pm 3.0 x10 ²)	1 x 10 ⁴ (\pm 1.1 x10 ²)
BSP DNA synthesis (μ g C l ⁻¹ day) (n=3)	0.13 (\pm 0.00)	0.56 (\pm 0.06)	1.05 (\pm 0.25)
BSP protein synthesis (μ g C l ⁻¹ day) (n=3)	0.10 (\pm 0.00)	0.13 (\pm 0.00)	0.14 (\pm 0.00)
Nitrate (μ g l ⁻¹) (n=4)	64.89 (\pm 0.48)	68.84 (\pm 0.12)	66.45 (\pm 0.07)
DRP (μ g l ⁻¹) (n=4)	14.29 (\pm 0.22)	15.41 (\pm 0.17)	14.49 (\pm 0.12)
Ammonium (μ g l ⁻¹) (n=4)	2.69 (\pm 0.16)	5.09 (\pm 0.24)	4.67 (\pm 0.14)
Chl <i>a</i> (ng ml ⁻¹) (n=4)	0.12 (\pm 0.00)	0.16 (\pm 0.00)	0.11 (\pm 0.00)
DOC (μ g ml ⁻¹) (n=2)	0.56 (\pm 0.02)	0.71 (\pm 0.09)	0.75 (\pm 0.06)
Total HMW reducing-sugar (μ g ml ⁻¹ gluc eq.) (n=4)	0	0	0
Total HMW protein (μ g ml ⁻¹ BSA eq.) (n=4)	0.008 (\pm 0.00)	0	0

Preliminary analysis of data from incubation 5 revealed patchy and sporadic biological responses, making interpretation of treatment responses and parameter coupling very challenging. Due to this, it was decided not to include incubation 5 in the following results and interpretation. This section therefore presents findings from incubations 6 and 7 only.

5.3.1 Extracellular enzyme activity

5.3.1.1 Incubation 6

Total β -glucosidase activity increased across all treatments from 24 h to 96 h (RM-ANOVA $F_{3, 18} = 36.58$, $p < 0.0001$, Fig. 5.2). The β -glucosidase activity was first detected in the OA and GH treatment at 24 h, while activity was significantly higher in the ambient control than each treatment at 96 h ($1.3 \text{ nmol l}^{-1} \text{ h}^{-1}$, Fig. 5.2, p-values in Appendix D: 5.1). The β -glucosidase activity in the OA treatment ($0.47 \text{ nmol l}^{-1} \text{ h}^{-1}$) was double that of the HT treatment ($0.25 \text{ nmol l}^{-1} \text{ h}^{-1}$) at 96 h. Low α -glucosidase activity was detected within and between incubated treatments, with activity first detected in the OA treatment at 48 h, and then in the ambient control at 72 h ($0.05 \text{ nmol l}^{-1} \text{ h}^{-1}$). Insufficient α -glucosidase activity was detected within each treatment for any robust comparison. The Arg-aminopeptidase activity was also low and variable throughout incubation 6. Despite this, activity was significantly higher in the OA treatment ($14.08 \text{ nmol l}^{-1} \text{ h}^{-1}$) than in the ambient control at 96 h ($3.81 \text{ nmol l}^{-1} \text{ h}^{-1}$, ANOVA $F_{1, 3} = 1068.38$, $p < 0.0001$, Fig 5.2). The Leu-aminopeptidase activity increased in each treatment from 24 h to 96 h (RM-ANOVA $F_{3, 24} = 245.16$, $p < 0.0001$, Fig. 5.2), and was significantly higher in the OA treatment ($3.11 \text{ nmol l}^{-1} \text{ h}^{-1}$) when compared to the ambient control at 24 h ($0.43 \text{ nmol l}^{-1} \text{ h}^{-1}$, ANOVA $F_{1, 4} = 30.79$, $p < 0.01$). The Leu-aminopeptidase activity was also significantly higher in the GH treatment at 24 h, 48 h and 96 h when compared to the ambient control, with respective activity ranging from 5.71 to $25.23 \text{ nmol l}^{-1} \text{ h}^{-1}$ (Fig. 5.2 & Appendix D: 5.1).

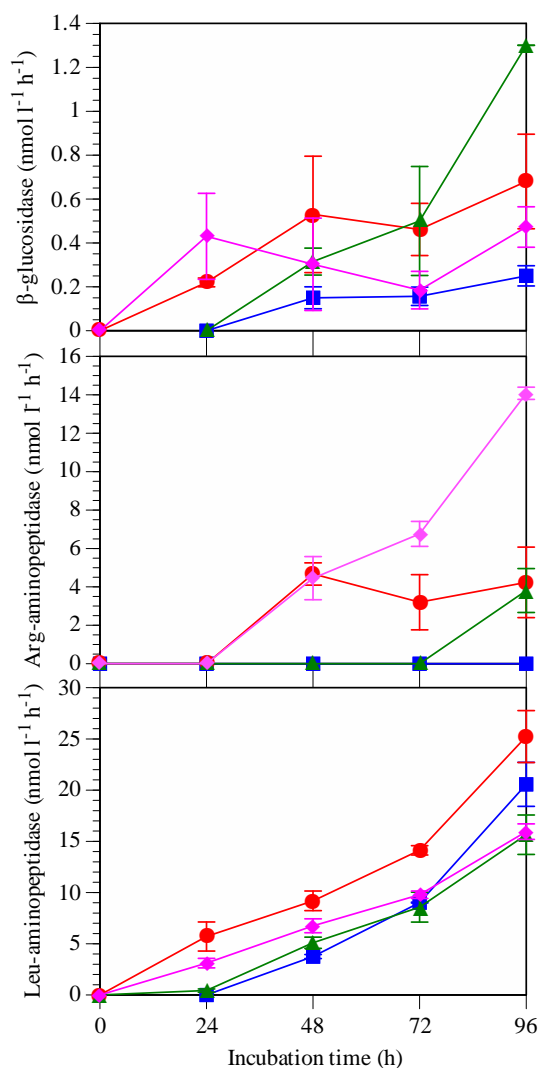


Fig. 5.2. Extracellular enzyme activities throughout incubation 6 (mean \pm SE, $n=3$). Data below detection limits are shown as zero. Treatment legend – HT: blue squares; GH: red circles; OA: pink diamonds; ambient control: green triangles

Cell-specific β -glucosidase activity was first detected at 24 h in the GH treatment, OA treatment and the ambient control, however activities were highly variable (Fig. 5.3). Cell-specific β -glucosidase activity in the GH treatment increased three-fold from 24 h ($0.32 \text{ amol cell}^{-1} \text{ h}^{-1}$) to 96 h ($1.13 \text{ amol cell}^{-1} \text{ h}^{-1}$), and was significantly higher when compared to the ambient control at 72 h ($0.81 \text{ amol cell}^{-1} \text{ h}^{-1}$, ANOVA $F_{1,2} = 169.21$, $p = 0.05$, Fig. 5.3). Cell-specific β -glucosidase activity remained low in the HT treatment resulting in a significantly lower activity ($0.25 \text{ amol cell}^{-1} \text{ h}^{-1}$) compared to the ambient control at 96 h ($1.16 \text{ amol cell}^{-1} \text{ h}^{-1}$, ANOVA $F_{1,2} = 183.70$, $p < 0.01$, Fig. 5.3).

Cell-specific Leu-aminopeptidase activity was also first detected at 24 h, increasing across all treatments from 24 h to 96 h (Fig. 5.3). Cell-specific Leu-aminopeptidase activity was significantly higher in the GH treatment at 24 h, 72 h and 96 h when compared to the ambient control, with respective activities ranging from 7.62 to 30.17 $\text{amol cell}^{-1} \text{h}^{-1}$ (ANOVA $F_{1,3}$, $p < 0.05$, Fig. 5.3). Cell-specific Leu-aminopeptidase activity was also significantly higher in the HT treatment (24.32 $\text{amol cell}^{-1} \text{h}^{-1}$) and OA treatment (23.07 $\text{amol cell}^{-1} \text{h}^{-1}$) than in the ambient control at 96 h (13.94 $\text{amol cell}^{-1} \text{h}^{-1}$, ANOVA $F_{1,4}$, $p < 0.05$, Fig. 5.3).

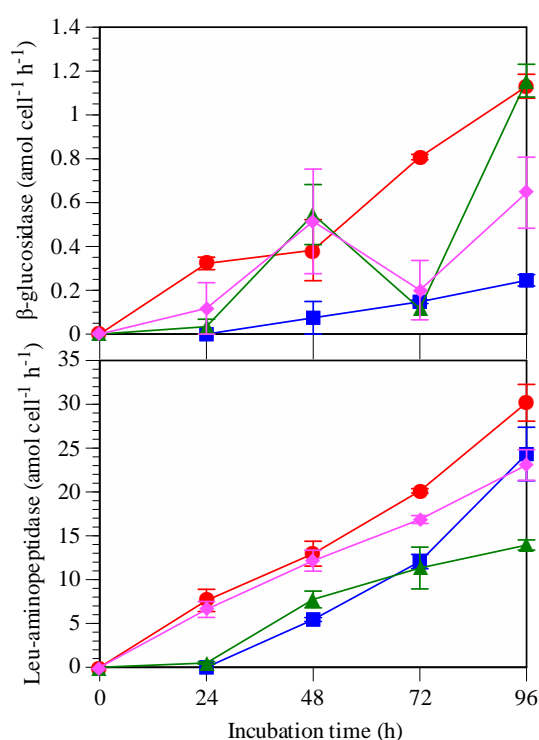


Fig. 5.3. Cell-specific extracellular enzyme activities throughout incubation 6 (mean \pm SE, $n=3$). Data below detection limits are shown as zero. Treatment legend – HT: blue squares; GH: red circles; OA: pink diamonds; ambient control: green triangles

5.3.1.2 Incubation 7

Low β -glucosidase activity was detected throughout incubation 7, with no clear treatment response. Despite this, total activity increased across all treatments from 24 h to 96 h (RM-ANOVA $F_{3,18} = 9.89$, $p < 0.0001$, Fig. 5.4). As previously measured in incubation 6, very low α -glucosidase activity (0.06 – 1.00 $\text{nmol l}^{-1} \text{h}^{-1}$) and Arg-aminopeptidase activity (2.10 –

21.09 nmol l⁻¹ h⁻¹) was detected within each treatment during incubation 7. Due to within treatment variation, statistical comparisons could not be made. In contrast to this, Leu-aminopeptidase activity increased in each treatment from 24 h to 96 h (RM-ANOVA $F_{3,24} = 9.83$, $p < 0.01$), however activity was similar between each treatment. The Leu-aminopeptidase activity in the GH treatment increased by 63% from 24 h (6.05 nmol l⁻¹ h⁻¹) to 48 h (9.55 nmol l⁻¹ h⁻¹), with activity significantly higher than in the ambient control at both time points (1.88 and 6.63 nmol l⁻¹ h⁻¹ respectively, Fig. 5.4 & Appendix D: 5.1). The Leu-aminopeptidase activity in the HT treatment (3.27 nmol l⁻¹ h⁻¹) was half that of the ambient control at 48 h (6.63 nmol l⁻¹ h⁻¹, ANOVA $F_{1,3} = 30.37$, $p = 0.01$), while activity in the OA treatment (42.59 nmol l⁻¹ h⁻¹) was more than double that in the ambient control at 96 h (20.78 nmol l⁻¹ h⁻¹, ANOVA $F_{1,4} = 160.94$, $p < 0.001$, Fig. 5.4).

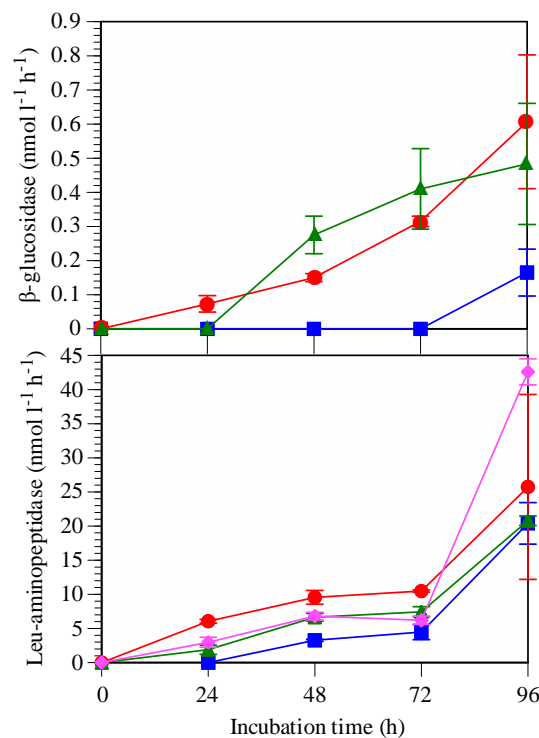


Fig. 5.4. Extracellular enzyme activities throughout incubation 7 (mean \pm SE, $n=3$). Data below detection limits are shown as zero. Treatment legend – HT: blue squares; GH: red circles; OA: pink diamonds; ambient control: green triangles

Cell-specific β -glucosidase activity was also very low (Fig. 5.5). In the GH treatment, cell-specific β -glucosidase activity increased six-fold from 24 h (0.16 amol cell⁻¹ h⁻¹) to 96 h

(0.97 $\text{amol cell}^{-1} \text{h}^{-1}$), however, activity was 63% lower than the ambient control at 72 h (0.54 $\text{amol cell}^{-1} \text{h}^{-1}$, ANOVA $F_{1,2} p = 0.05$, Fig. 5.5). Cell-specific Leu-aminopeptidase activity was similar between each perturbation treatment and remained relatively stable from 24 h to 72 h (Fig. 5.5). Cell-specific activity was higher in the GH treatment at 24 h, 48 h and 72 h when compared to the ambient control, with respective activity ranging from 13.82 to 17.58 $\text{amol cell}^{-1} \text{h}^{-1}$, ANOVA $F_{1,3}, p < 0.05$, Fig. 5.5). Cell-specific Leu-aminopeptidase activity increased in the ambient control from 24 h (2.77 $\text{amol cell}^{-1} \text{h}^{-1}$) to 96 h (24.27 $\text{amol cell}^{-1} \text{h}^{-1}$), while activity in the HT treatment also increased from 48 h (4.91 $\text{amol cell}^{-1} \text{h}^{-1}$) to 96 h (22.79 $\text{amol cell}^{-1} \text{h}^{-1}$, Fig. 5.5). Cell-specific Leu-aminopeptidase activity increased more than five-fold in the OA treatment from 72 h (11.28 $\text{amol cell}^{-1} \text{h}^{-1}$) to 96 h (58.71 $\text{amol cell}^{-1} \text{h}^{-1}$), with an activity twice as high as the ambient control at 96 h (24.27 $\text{amol cell}^{-1} \text{h}^{-1}$, ANOVA $F_{1,4} = 553.04, p < 0.01$, Fig. 5.5).

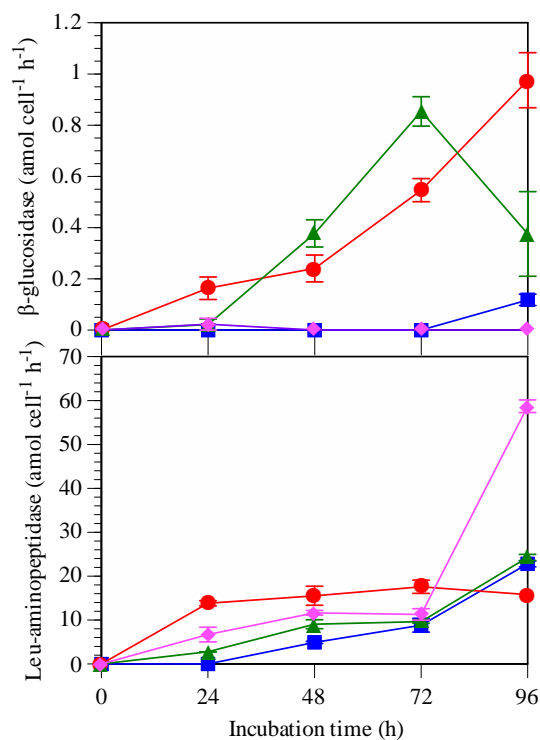


Fig. 5.5. Cell-specific extracellular enzyme activities throughout incubation 7 (mean \pm SE, $n=3$). Data below detection limits are shown as zero. Treatment legend – HT: blue squares; GH: red circles; OA: pink diamonds; ambient control: green triangles

Summary of results

Overall, β -glucosidase activity was significantly lower in the OA treatment than the ambient control at 48 h and 96 h in incubations 6 and 7, while activity was also significantly lower in the HT treatment at 48 h in both incubations (Table 5.3). Insufficient α -glucosidase activity was detected in each incubation for a significant treatment response to be measured. The Leu-aminopeptidase activity was significantly higher in the GH treatment when compared to the ambient control at 48 h in incubations 6 and 7 (Table 5.3), while also significantly higher in the OA treatment at 96 h (Table 5.3).

Table 5.3. Summary of extracellular enzyme activity changes in each treatment when compared to the ambient control ($p < 0.05$). Blue shaded cells indicate a response at 48 h, neutral shaded cells indicate a response at 96 h. \uparrow : indicates the parameter was significantly higher than the ambient control; \downarrow : significantly lower; empty cell: not significantly different

Parameter	Incubation 6						Incubation 7			
	OA		HT		GH		OA		HT	GH
β -glucosidase	↓	↓	↓	↓			↓	↓	↓	
α -glucosidase										
Arg-aminopeptidase		↑								
Leu-aminopeptidase		↑			↑	↑	↑	↓		↑

5.3.2 Cell numbers

5.3.2.1 Incubation 6

Total bacterial cell numbers increased across all treatments from 24 h to 96 h (RM-ANOVA $F_{3, 24} = 31.66$, $p < 0.0001$), however there was no clear treatment response (Fig. 5.6). Bacterial cell numbers were higher in the GH treatment (7×10^5 cells ml^{-1}) than in the ambient control at 48 h (5×10^5 cells ml^{-1} , ANOVA $F_{1, 4} = 35.96$, $p < 0.01$, Fig. 5.6), and fewer bacteria were detected in each treatment when compared to the ambient control at 96 h (Fig. 5.6, p-values in Appendix D: 5.2).

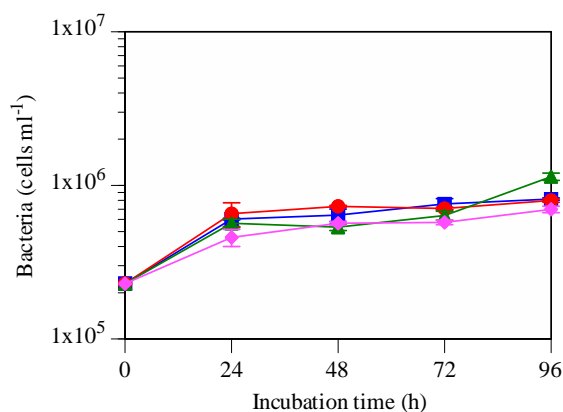


Fig. 5.6. Bacterial cell numbers (log scale) throughout incubation 6 (mean \pm SE, $n=3$). Treatment legend – HT: blue squares; GH: red circles; OA: pink diamonds; ambient control: green triangles

During incubation 6, there was no clear treatment response in *Synechococcus* spp. cell numbers or total eukaryotic phytoplankton cell numbers (Fig. 5.7). *Synechococcus* spp. cell numbers were lower in the GH treatment (1.1×10^3 cells ml^{-1}) when compared to the ambient control at 96 h (1.4×10^3 cells ml^{-1} , ANOVA $F_{1, 2} = 100.10$, $p < 0.009$, Fig. 5.7), while total eukaryotic phytoplankton cell numbers declined in each treatment from 48 h to 96 h (RM-ANOVA $F_{1, 8} = 51.91$, $p < 0.0001$, Fig. 5.7). Total eukaryotic phytoplankton numbers were significantly lower in the GH treatment (8×10^3 cells ml^{-1}) and OA treatment (7×10^3 cells ml^{-1}) than in the ambient control at 96 h (9×10^3 cells ml^{-1} , Fig. 5.7 & Appendix D: 5.2).

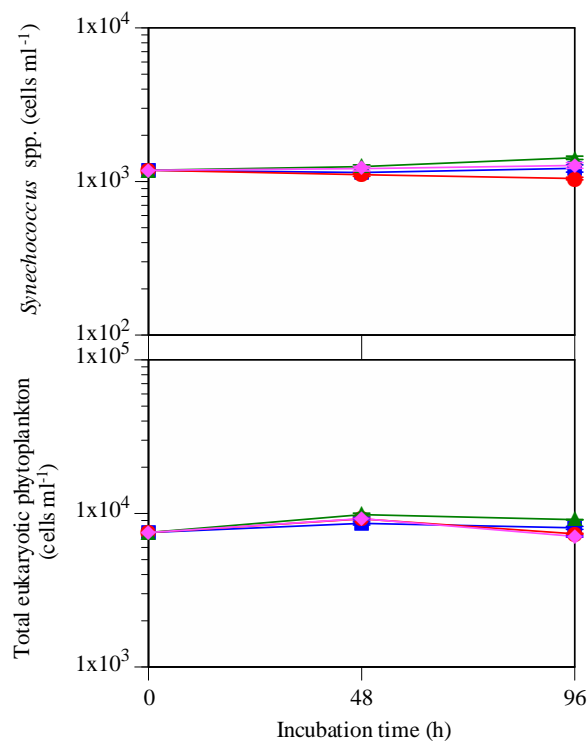


Fig. 5.7 *Synechococcus* spp. and total eukaryotic phytoplankton cell numbers (log scale) throughout incubation 6 (mean \pm SE, n=3). Treatment legend – HT: blue squares; GH: red circles; OA: pink diamonds; ambient control: green triangles

5.3.2.2 Incubation 7

During incubation 7, total bacterial cell numbers increased across all treatments from 24 h to 96 h (RM-ANOVA $F_{3, 24} = 88.31$, $p < 0.0001$, Fig. 5.8), however as measured in incubation 6, there was no clear treatment response (Fig. 5.8). Bacterial cell numbers were higher in the HT treatment (5.2×10^5 cells ml⁻¹) than the ambient control at 24 h (4.5×10^5 cells ml⁻¹, ANOVA $F_{1, 4} = 17.46$, $p = 0.01$, Fig. 5.8), while numbers were lower in both the GH treatment (6.1×10^5 cells ml⁻¹) and OA treatment (6.0×10^5 cells ml⁻¹) when compared to the ambient control at 48 h (7.4×10^5 cells ml⁻¹, Fig. 5.8 & Appendix D: 5.2).

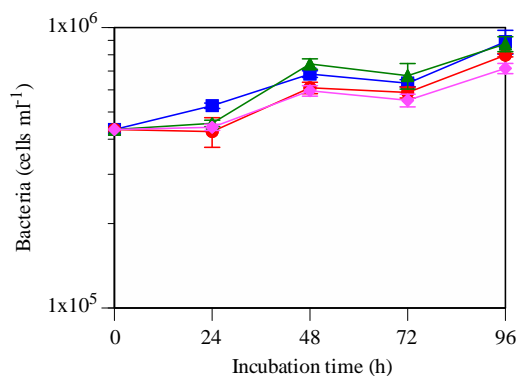


Fig. 5.8. Bacterial cell numbers (log scale) throughout incubation 7 (mean \pm SE, $n=3$). Treatment legend – HT: blue squares; GH: red circles; OA: pink diamonds; ambient control: green triangles

During incubation 7, there was no clear perturbation treatment response in *Synechococcus* spp. cell numbers or total eukaryotic phytoplankton cell numbers (Fig. 5.9). Total *Synechococcus* spp. cell numbers and total eukaryotic phytoplankton cell numbers declined from 48 h to 96 h (Fig. 5.9). Total eukaryotic phytoplankton cell numbers were 12.5% higher in the OA treatment (8×10^3 cells ml^{-1}) than in the ambient control at 48 h (7×10^3 cells ml^{-1} , ANOVA $F_{1,4} = 8.32$, $p < 0.05$, Fig. 5.9).

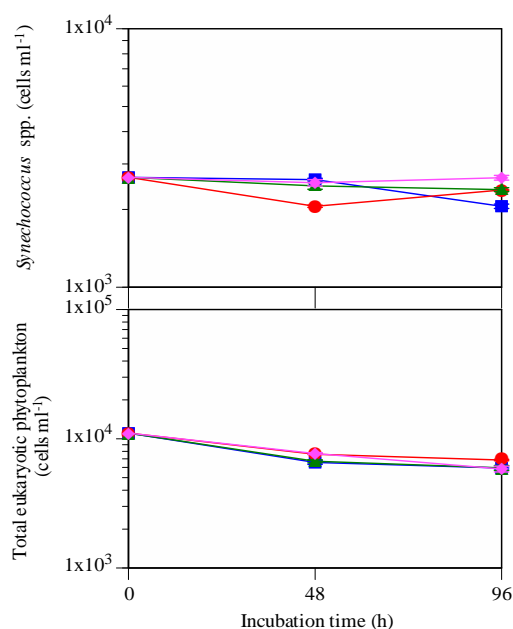


Fig. 5.9. *Synechococcus* spp. and total eukaryotic phytoplankton cell numbers (log scale) throughout incubation 7 (mean \pm SE, $n=3$). Treatment legend – HT: blue squares; GH: red circles; OA: pink diamonds; ambient control: green triangles

Summary of results

Overall, cell number responses varied between treatments and incubations (Table 5.4). Bacterial cell numbers were significantly lower in the OA treatment when compared to the ambient control at 96 h in incubations 6 and 7 (Table 5.4). Bacterial, *Synechococcus* spp. and total eukaryotic phytoplankton numbers were significantly lower in the GH treatment when compared to the ambient control at 96 h in incubation 6, however this same response was not detected in incubation 7 (Table 5.4).

Table 5.4. Summary of cell number changes in each treatments when compared to the ambient control ($p < 0.05$). Blue shaded cells indicate a response at 48 h, neutral shaded cells indicate a response at 96 h. ↑: indicates the parameter was significantly higher than the ambient control; ↓: significantly lower; empty cell: not significantly different

Parameter	Incubation 6			Incubation 7		
	OA	HT	GH	OA	HT	GH
Bacterial	↓	↓	↑	↓		↓
<i>Synechococcus</i> spp.			↓	↓		
Total eukaryotic phytoplankton cells	↓		↓	↑		

5.3.3 Bacterial secondary production

5.3.3.1 Incubation 6

A significant positive relationship was measured between DNA and protein synthesis rates throughout incubation 6 (linear regression, $p < 0.0001$, $r = 0.86$). DNA synthesis rates increased in all treatments from 24 h to 96 h (RM-ANOVA $F_{3, 24} = 68.21$, $p < 0.0001$), however a significant treatment response was not detected (Fig. 5.10). DNA synthesis was at least twice as high in the HT treatment at both 24 h ($3.68 \mu\text{g C l}^{-1} \text{d}^{-1}$) and 48 h ($8.54 \mu\text{g C l}^{-1} \text{d}^{-1}$) when compared to the ambient control (1.24 and $4.60 \mu\text{g C l}^{-1} \text{d}^{-1}$ respectively, Fig. 5.10, p-values in Appendix D: 5.3). DNA synthesis in the OA treatment ($3.76 \mu\text{g C l}^{-1} \text{d}^{-1}$) was half that detected in the ambient control at 72 h ($7.72 \mu\text{g C l}^{-1} \text{d}^{-1}$, ANOVA $F_{1, 4} = 11.97$, $p < 0.05$), while synthesis in the GH, OA and HT treatments was also lower when compared to the ambient control at 96 h (Fig. 5.10 & Appendix D: 5.3). Protein synthesis rates also increased in all treatments from 48 h to 96 h (RM-ANOVA $F_{1, 8} = 15.47$, $p < 0.01$, Fig. 5.10) and reflected a very similar trend to DNA synthesis. The only distinguishable trend was that the OA treatment had a

significantly lower protein synthesis rate than the ambient control at 48 h ($1.62 \mu\text{g C l}^{-1} \text{ d}^{-1}$) and 96 h ($2.63 \mu\text{g C l}^{-1} \text{ d}^{-1}$, Fig. 5.10, Appendix D: 5.3).

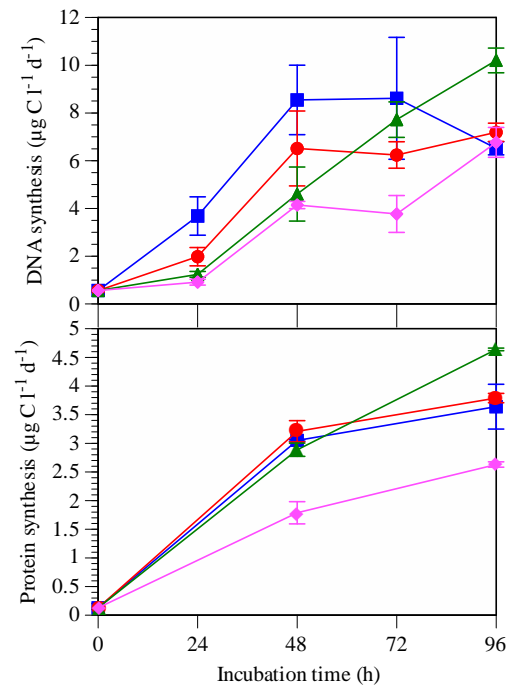


Fig. 5.10. BSP throughout incubation 6 (mean \pm SE, $n=3$). Treatment legend – HT: blue squares; GH: red circles; OA: pink diamonds; ambient control: green triangles

Cell-specific protein synthesis rates increased ten-fold in the GH treatment from time-zero ($0.31 \text{ fg C cell}^{-1} \text{ d}^{-1}$) to 96 h ($3.69 \text{ fg C cell}^{-1} \text{ d}^{-1}$) in incubation 6, while synthesis in all other treatments peaked at 48 h (Fig. 5.11). Cell-specific protein synthesis was 33% lower in the OA treatment ($3.50 \text{ fg C cell}^{-1} \text{ d}^{-1}$) than in the ambient control at 96 h ($4.67 \text{ fg C cell}^{-1} \text{ d}^{-1}$, ANOVA $F_{1,3} = 31.87$, $p = 0.01$, Fig. 5.11).

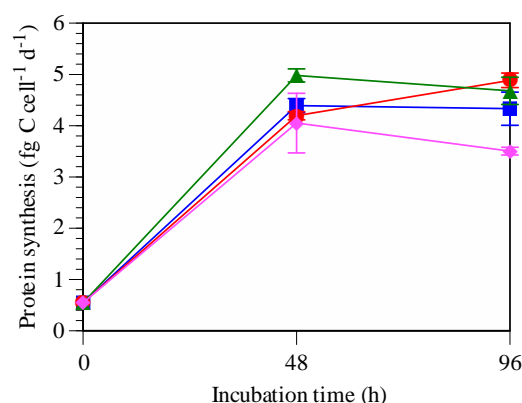


Fig. 5.11. Cell-specific protein synthesis throughout incubation 6 (mean \pm SE, $n=3$). Treatment legend – HT: blue squares; GH: red circles; OA: pink diamonds; ambient control: green triangles

5.3.3.2 Incubation 7

A significant positive relationship was also measured between DNA and protein synthesis rates throughout incubation 7 (linear regression, $p < 0.0001$, $r = 0.85$). DNA synthesis rates increased significantly in all treatments from 24 h to 96 h (RM-ANOVA $F_{3, 21} = 54.27$, $p < 0.0001$), however no definitive treatment response was detected (Fig. 5.12). DNA synthesis was higher in the GH treatment ($3.74 \mu\text{g C l}^{-1} \text{d}^{-1}$) and HT treatment ($5.23 \mu\text{g C l}^{-1} \text{d}^{-1}$) when compared to the ambient control at 24 h ($1.63 \mu\text{g C l}^{-1} \text{d}^{-1}$), while synthesis was significantly lower in the OA treatment ($0.001 \mu\text{g C l}^{-1} \text{d}^{-1}$, Fig. 5.12 & Appendix D: 5.3). DNA synthesis rates were also significantly lower in the OA treatment at 48 h ($2.54 \mu\text{g C l}^{-1} \text{d}^{-1}$) and 96 h ($5.25 \mu\text{g C l}^{-1} \text{d}^{-1}$) when compared to the ambient control (6.37 and $7.76 \mu\text{g C l}^{-1} \text{d}^{-1}$ respectively, Fig. 5.12 & Appendix D: 5.3). Protein synthesis rates increased across all treatments from 48 h to 96 h (RM-ANOVA $F_{1, 8} = 42.63$, $p < 0.0001$, Fig. 5.12). Protein synthesis was significantly lower in the OA treatment ($1.38 \mu\text{g C l}^{-1} \text{d}^{-1}$), the GH treatment ($2.59 \mu\text{g C l}^{-1} \text{d}^{-1}$) and the HT treatment ($1.60 \mu\text{g C l}^{-1} \text{d}^{-1}$) when compared to the ambient control at 48 h ($3.43 \mu\text{g C l}^{-1} \text{d}^{-1}$, Fig. 5.12 & Appendix D: 5.3). Protein synthesis was also 42% lower in the OA treatment ($2.42 \mu\text{g C l}^{-1} \text{d}^{-1}$) than the ambient control at 96 h ($3.45 \mu\text{g C l}^{-1} \text{d}^{-1}$, ANOVA $F_{1, 4} = 57.60$, $p < 0.01$, Fig. 5.12), similar to that measured during incubation 6.

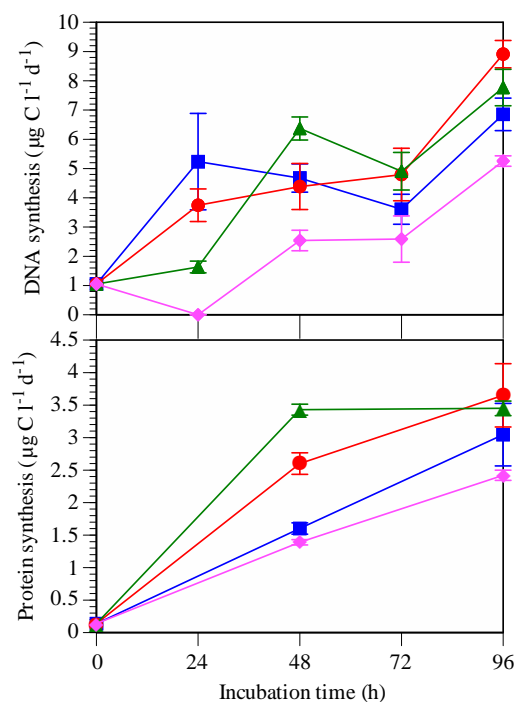


Fig. 5.12. BSP throughout incubation 7 (mean \pm SE, n=3). Treatment legend – HT: blue squares; GH: red circles; OA: pink diamonds; ambient control: green triangles

During incubation 7, cell-specific protein synthesis rates showed exactly the same treatment responses as protein synthesis at 48 h and 96 h (Fig. 5.12).

Summary of results

Overall, protein synthesis was significantly lower in the OA treatment when compared to the ambient control at 48 h and 96 h in incubations 6 and 7 (Table 5.5). DNA and protein synthesis had variable responses in the HT treatment between incubations. Synthesis rates were significantly lower in the GH treatment when compared to the ambient control at 96 h in incubation 6, while the same response was recorded in incubation 7 at 48 h only (Table 5.5).

Table 5.5. Summary of the DNA and protein synthesis rate responses to treatments compared to the ambient control. Blue shaded cells indicate a response at 48 h, neutral shaded cells indicate a response at 96 h. \uparrow : indicates the parameter was significantly higher than the ambient control; \downarrow : significantly lower; empty cell: not significantly different

Parameter	Incubation 6			Incubation 7		
	OA	HT	GH	OA	HT	GH
BSP DNA synthesis	\downarrow	\uparrow	\downarrow	\downarrow	\downarrow	\downarrow
BSP protein synthesis	\downarrow	\downarrow	\downarrow	\downarrow	\downarrow	\downarrow

5.3.4 Chlorophyll *a* concentration

5.3.4.1 Incubation 6

During incubation 6, chlorophyll *a* (Chl *a*) concentrations declined in each treatment from time-zero to 96 h. Concentrations were 17% lower in the GH treatment (0.10 ng ml^{-1}) than the ambient control at 96 h (0.12 ng ml^{-1} , ANOVA $F_{1,4} = 12.34$, $p < 0.05$, Fig. 5.13).

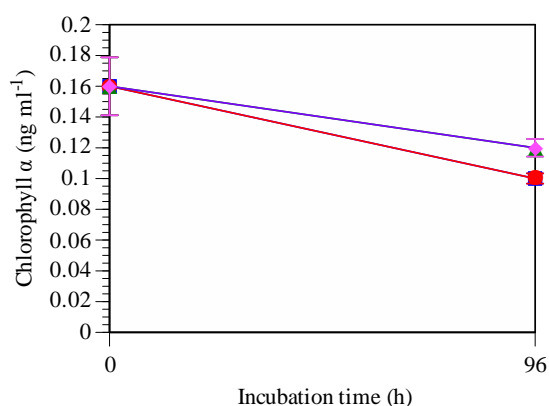


Fig. 5.13. Chl *a* concentrations at the beginning and the end of incubation 6 (mean \pm SE, $n=3$). Treatment legend – HT: blue squares; GH: red circles; OA: pink diamonds; ambient control: green triangles

5.3.4.2 Incubation 7

During incubation 7, Chl *a* concentrations also declined in each treatment from time-zero (0.10 ng ml^{-1}) to 96 h (range from $0.06 - 0.07 \text{ ng ml}^{-1}$). Chl *a* concentrations in the HT treatment (0.06 ng ml^{-1}), the GH treatment (0.07 ng ml^{-1}) and the OA treatment (0.08 ng ml^{-1}) were not significantly different from the ambient control at 96 h (0.07 ng ml^{-1} , ANOVA $F_{1,4}$, $p > 0.05$).

5.3.5 Dissolved nutrient concentration

5.3.5.1 Incubation 6

Dissolved nitrate, DRP and dissolved ammonium concentrations declined in each treatment from time-zero to 96 h (Fig. 5.14). Dissolved nitrate and DRP concentrations were significantly higher in the OA treatment than the ambient control at 96 h (ANOVA $F_{1,4}$, $p < 0.05$, Fig. 5.14). Total dissolved ammonium concentrations declined across all treatments from time-zero to 96 h; no treatment concentration was statistically different from the ambient control at 96 h (Fig. 5.14).

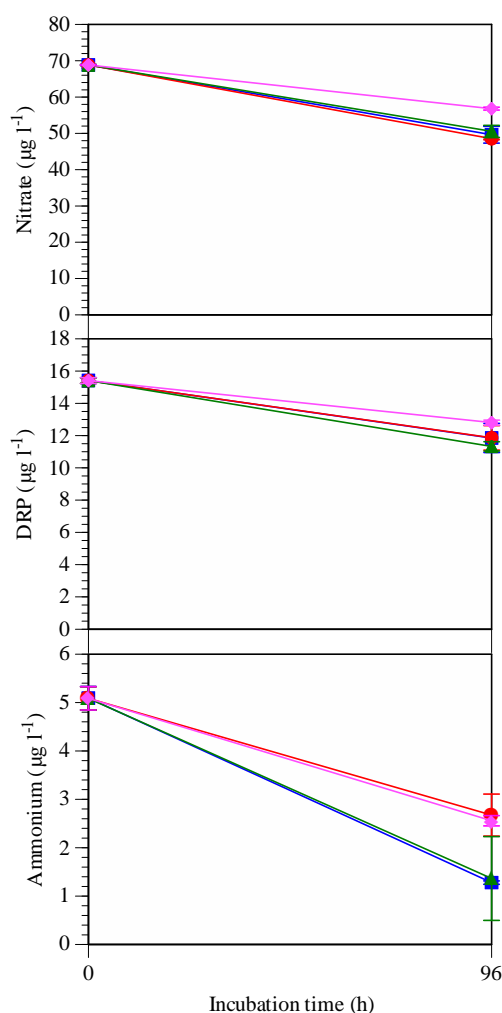


Fig. 5.14. Dissolved nutrient concentrations at the beginning and the end of incubation 6 (mean \pm SE, $n=3$). Treatment legend – HT: blue squares; GH: red circles; OA: pink diamonds; ambient control: green triangles

5.3.5.2 Incubation 7

Dissolved nitrate concentrations were significantly higher in the GH treatment (44.59 $\mu\text{g l}^{-1}$) and OA treatment (47.01 $\mu\text{g l}^{-1}$) when compared to the ambient control at 96 h (31.06 $\mu\text{g l}^{-1}$, ANOVA $F_{1,4}$, $p < 0.05$, Fig. 5.15), while DRP concentrations were also significantly higher in the GH treatment (10.89 $\mu\text{g l}^{-1}$) and OA treatment (11.36 $\mu\text{g l}^{-1}$, ANOVA $F_{1,3}$, $p < 0.05$, Fig. 5.15). In contrast to these trends, dissolved ammonium concentrations were significantly lower in the OA treatment (2.53 $\mu\text{g l}^{-1}$) when compared to the ambient control at 96 h (4.94 $\mu\text{g l}^{-1}$, ANOVA $F_{1,2} = 69.39$, $p = 0.01$, Fig. 5.15).

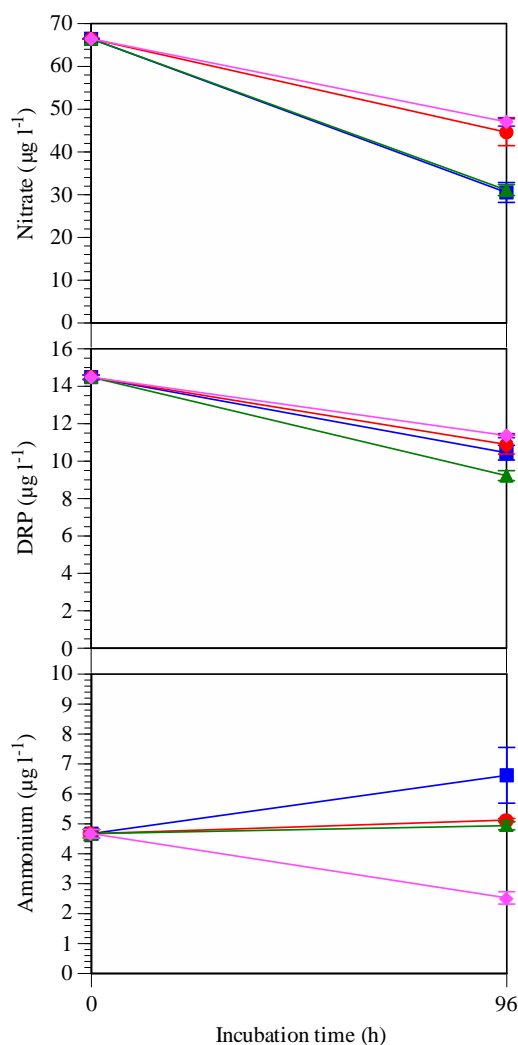


Fig. 5.15. Dissolved nutrient concentrations at the beginning and the end of incubation 7 (mean \pm SE, $n=3$). Treatment legend – HT: blue squares; GH: red circles; OA: pink diamonds; ambient control: green triangles

Summary of results

Overall, dissolved nitrate and DRP concentrations were significantly higher in the OA treatment than in the ambient control at 96 h in incubations 6 and 7 (Table 5.6). Dissolved nutrient concentrations were not significantly affected by the HT treatment at 96 h in either incubation (Table 5.6). Similarly, dissolved ammonium concentrations were not affected by the GH treatment at 96 h in either incubation, while nitrate and DRP concentrations were significantly higher in the GH treatment when compared to the ambient control at 96 h in incubation 7 only (Table 5.6).

Table 5.6. Summary of dissolved nutrient concentration changes in each treatment when compared to the ambient control at 96 h only ($p < 0.05$). ↑: indicates the parameter was significantly higher than the ambient control; ↓: significantly lower; empty cell: not significantly different

Parameter	Incubation 6			Incubation 7		
	OA	HT	GH	OA	HT	GH
Nitrate	↑			↑		↑
DRP	↑			↑		↑
Ammonium				↓		

5.3.6 Dissolved organic carbon concentration

5.3.6.1 Incubation 6

Dissolved organic carbon (DOC) concentrations increased in each treatment from time-zero to 96 h (Fig. 5.16), however no clear perturbation treatment response was evident. DOC concentrations were 15% lower in the GH treatment ($0.75 \mu\text{g ml}^{-1}$) than in the ambient control at 96 h ($0.88 \mu\text{g ml}^{-1}$, ANOVA $F_{1,4} = 25.13$, $p < 0.01$, Fig. 5.16).

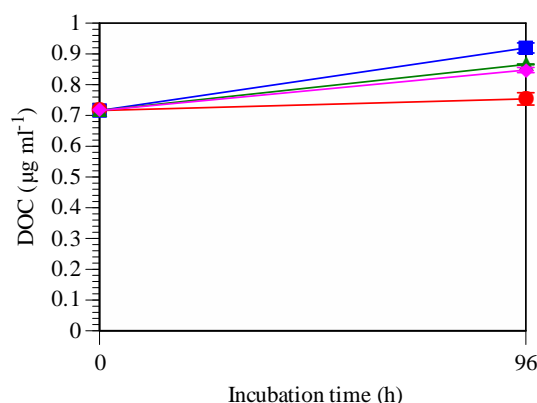


Fig. 5.16. DOC concentrations at time-zero and 96 h during incubation 6 (mean \pm SE, $n=3$). Treatment legend – HT: blue squares; GH: red circles; OA: pink diamonds; ambient control: green triangles

5.3.6.2 Incubation 7

DOC concentrations did not change significantly across all treatments from time-zero ($0.71 \mu\text{g ml}^{-1}$) to 96 h (range from $0.75 - 0.91 \mu\text{g ml}^{-1}$). DOC concentrations in the GH treatment ($0.79 \mu\text{g ml}^{-1}$), the HT treatment ($0.72 \mu\text{g ml}^{-1}$) and the OA treatment ($0.81 \mu\text{g ml}^{-1}$) were not statistically different from the ambient control at 96 h ($0.80 \mu\text{g ml}^{-1}$, ANOVA $F_{1,4}$, $p > 0.05$).

5.3.7 Total high molecular weight organic compound concentration

5.3.7.1 Incubation 6

Very low total high molecular weight (HMW) reducing-sugar concentrations were detected throughout incubation 6. Several analysed samples per treatment were below the methodology detection limit, producing high within-treatment variation. Consequently no treatment concentration was statistically different from the ambient control (ANOVA $F_{2,16}$, $p > 0.05$). The total HMW protein concentrations throughout incubation 6 were also frequently below the detection limit and consequently no statistical comparisons were possible.

5.3.7.2 Incubation 7

During incubation 7, total HMW reducing-sugar concentrations increased across all treatments from 48 h onwards (RM-ANOVA $F_{2, 16} = 8.53$, $p < 0.01$), however no clear treatment effect was measured (Fig. 5.17). Total HMW reducing-sugar concentrations were higher in the HT treatment ($0.025 \mu\text{g ml}^{-1}$) and OA treatment ($0.029 \mu\text{g ml}^{-1}$) than in the ambient control at 48 h ($0.022 \mu\text{g ml}^{-1}$, Fig. 5.17, p-values in Appendix D: 5.4).

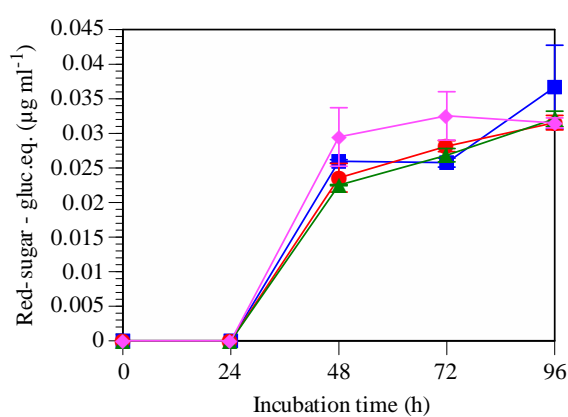


Fig. 5.17. Total HMW reducing-sugar concentrations throughout incubation 7 (mean \pm SE, $n=3$). Data below detection limits are shown as zero. Treatment legend – HT: blue squares; GH: red circles; OA: pink diamonds; ambient control: green triangles

During incubation 7, total HMW protein concentrations were below the detection limit in each treatment and at each sampling point. Due to this, no statistical comparisons were possible.

Summary of results

Overall, total HMW organic compound concentrations were often below methodology detection during incubation 6, and therefore no clear treatment response was detected (Table 5.7). In incubation 7 however, total HMW reducing-sugar concentrations were significantly higher in the OA and HT treatments than the ambient control at 48 h (Table 5.7). As measured during incubation 6, total HMW protein concentrations were again below methodology detection during incubation 7 (Table 5.7).

Table 5.7. Summary of total HMW organic compound concentration changes in each treatment when compared to the ambient control ($p < 0.05$). Blue shaded cells indicate a response at 48 h, neutral shaded cells indicate a response at 96 h. ↑: indicates the parameter was significantly higher than the ambient control; ↓: significantly lower; empty cell: not significantly different

Parameter	Incubation 6			Incubation 7		
	OA	HT	GH	OA	HT	GH
Total HMW reducing-sugar				↑	↑	
Total HMW protein						

5.3.8 Multivariate data analysis

The following section will investigate multivariate data collected from each treatment including the control, at selected sampling times for each incubation. Differences in multivariate data between treatments will be presented visually, allowing identification of change over time. Statistical difference is based on a SIMPROF analysis at 5% significance. Both incubation MDS plots have a stress coefficient ≤ 0.05 which indicates the multivariate matrices are represented extremely well by the 2D ordination plot (Section 2.11).

5.3.8.1 Incubation 6

Multivariate analysis of incubation 6 data showed that the six primary sampled parameters significantly changed from time-zero to 96 h (Fig. 5.18). Analysed parameters from the OA treatment were significantly different from all other treatments at 48 h and 72 h (solid line cluster, Fig. 5.18). Analysed parameters for the HT and GH treatments were also significantly different from the ambient control at 72 h, however they were not significantly different from each other (broken line cluster, Fig. 5.18). By the end of the incubation (96 h), each treatment was significantly different from the ambient control, as well as from each other (Fig. 5.18).

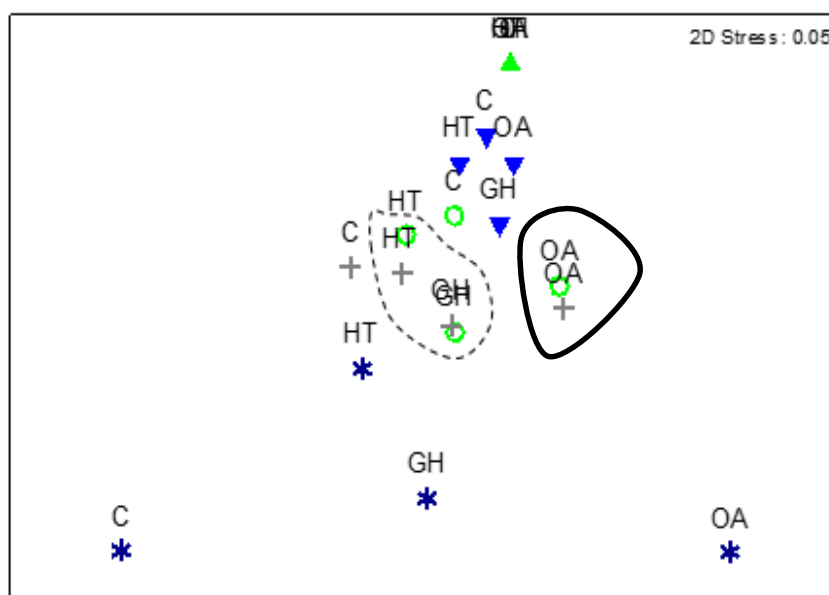


Fig. 5.18. MDS plot of six sampled biotic and abiotic parameters collected during incubation 6. Highlighted clusters are based on a SIMPROF analysis at 5% significance. Abbreviations are as previously described in Section 2.1 Incubation treatments are labelled per sampling point - 0 h: ▲; 24 h: ▼; 48 h: ○; 72 h: +; 96 h: *

5.3.8.2 Incubation 7

Multivariate analysis of incubation 7 data showed that the six sampled parameters changed significantly in each treatment from time-zero to 96 h (Fig. 5.19). Again, the analysis showed that at 48 h and 72 h, the OA treatments were significantly different from the ambient control (solid line cluster, Fig. 5.19). At the final sampling point (96 h), the HT and OA treatments were significantly different from the ambient control, while there was no significant difference between the GH treatment and the ambient control (broken line cluster, Fig. 5.19).

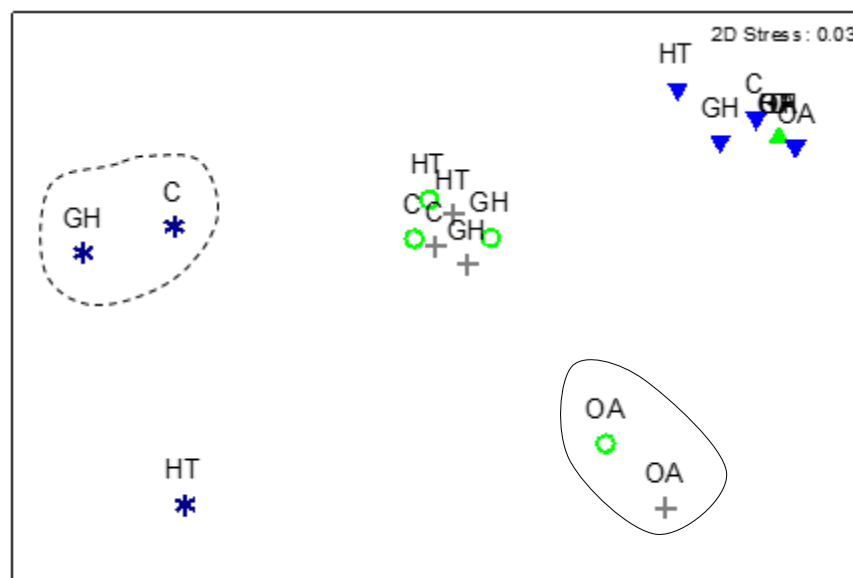


Fig. 5.19. MDS plot of six sampled biotic and abiotic parameters collected during incubation 7. Highlighted clusters are based on a SIMPROF analysis at 5% significance. Abbreviations are as previously described in Section 2.1. The OA value at 96 h was treated as an extreme outlier and removed. Incubation treatments are labelled per sampling point - 0 h: ▲; 24 h: ▼; 48 h: ○; 72 h: +; 96 h: *

5.4 Discussion

The following discussion is divided into three key sections, each focused on a principal parameter interaction. Each section will discuss parameter responses in each treatment to gain a better understanding of which factor is driving potential change. In this study, measured responses in the GH treatment show those expected to occur in a realistic future ocean.

5.4.1 The response of extracellular enzymes in subsurface waters

Very similar enzyme activity profiles were measured between incubations 6 and 7, especially for β -glucosidase and Leu-aminopeptidase activity (Table 5.8). This was surprising as the time-zero bacterial community compositions were significantly different between each incubation (pers. comm. Dr Els Maas, NIWA). Grossart et al. (2007) discovered significantly different cell-specific protease activity between different bacterial strains. My findings however, suggest that different subsurface bacterial communities may have similar peptide hydrolysis capabilities. The β -glucosidase and α -glucosidase activities were very low across all treatments, with α -glucosidase activity largely undetectable in both incubations (Table 5.8). Non-detectable glucosidase activities were reported by Davey et al. (2001) at 200 m depth in the north-eastern North Atlantic Ocean, while the β -glucosidase and Leu-aminopeptidase activities detected in these incubations were similar to those reported from approximately 100 m depth in the Sub-Tropical and Central Atlantic Ocean (Baltar et al. 2009, 2010). This low extracellular activity is likely to reflect the lower concentration of HMW substrate in each incubation, as well as its potential recalcitrant nature (Karner & Rassoulzadegan 1995, Nagata et al. 2000, Aristegui et al. 2009). Subsurface total HMW substrate concentrations were approximately ten-fold lower than those detected from 10 m depth off the Chatham Rise (Chapter 4), and due to the detection method, this also suggests a decline in bacterial and phytoplankton numbers with depth. Similar declines in HMW carbohydrate concentrations with depth are also reported from different oceans around the world (Smith et al. 1992, Pakulski & Benner 1994, Skoog & Benner 1997, Baltar et al. 2009). Surprisingly, despite the very low total HMW organic substrate concentrations, β -glucosidase and α -glucosidase activities increased throughout both incubations and across each treatment.

Table 5.8. Summary of each parameter response from incubations 6 and 7 when compared to the ambient control ($p < 0.05$). Blue shaded cells indicate a response at 48 h, neutral shaded cells indicate a response at 96 h. \uparrow : indicates the parameter was significantly higher than the ambient control; \downarrow : significantly lower; empty cell: not significantly different

Parameter	Incubation 6			Incubation 7		
	OA	HT	GH	OA	HT	GH
β -glucosidase	\downarrow	\downarrow		\downarrow	\downarrow	
α -glucosidase						
Arg-aminopeptidase		\uparrow				
Leu-aminopeptidase		\uparrow	\uparrow	\uparrow	\downarrow	\uparrow
Bacterial numbers	\downarrow	\downarrow	\uparrow	\downarrow	\downarrow	\downarrow
<i>Synechococcus</i> spp. numbers			\downarrow			
Total eukaryotic phytoplankton numbers	\downarrow		\downarrow	\uparrow		
BSP DNA synthesis	\downarrow	\uparrow	\downarrow	\downarrow	\downarrow	\downarrow
BSP protein synthesis	\downarrow		\downarrow	\downarrow	\downarrow	\downarrow
Chl <i>a</i>			\downarrow			
Nitrate	\uparrow			\uparrow		\uparrow
DRP	\uparrow			\uparrow		\uparrow
Ammonium				\downarrow		
DOC			\downarrow			
Total HMW reducing-sugar				\uparrow	\uparrow	
Total HMW protein						

The deep ocean is typically a thermally stable environment, and according to the Q_{10} coefficient bacterial metabolic rates are slower by approximately one order of magnitude relative to the surface ocean (Tamburini et al. 2002). An increase in treatment temperature, like that in the HT treatment, should result in an increase in bacterial metabolic activity (Brown et al. 2004, Campbell & Reece 2005), and reflect an increase in extracellular enzyme production and activity. In accordance with the Q_{10} coefficient, β -glucosidase Q_{10} values calculated from two time points throughout each incubation ranged from 0.001 to 0.05, while Leu-aminopeptidase values ranged from 0.30 to 2.83. These Q_{10} values suggest that temperature had a positive effect on enzyme activity, however the increase in activity was not significantly different from the ambient control. It is possible that under elevated temperature conditions, subsurface bacterial communities subject to low HMW substrate availability may invest metabolic energy into alternative pathways other than catabolism, potentially explaining the low glucosidase and protease activity detected in the HT treatment.

During incubation 7, a positive correlation was detected between total HMW reducing-sugar concentrations and both potential and cell-specific β -glucosidase activity. Baltar et al. (2010)

also discovered a positive correlation between β -glucosidase, α -glucosidase, Leu-aminopeptidase activity, bacterial metabolism and POM concentrations at depth, while Nagata et al. (2000) concluded that subsurface bacterial biomass and production were strongly correlated with POM availability at depth. This evidence suggests that subsurface bacterial extracellular enzyme activity is dependent on the availability of HMW organic substrate (Davey et al. 2001, Baltar et al. 2010). Total HMW protein substrate concentrations were below methodology detection in all treatments (Table 5.8), yet Leu-aminopeptidase activity increased throughout both incubations. This trend may indicate one of several possible scenarios: that sufficient HMW protein substrate was available to induce protease synthesis but was remineralised before it could be detected; that HMW protein substrate was present but not detected due to the sensitivity of the methodology used; that Leu-aminopeptidase was cleaving a HMW substrate which was not detected. If subsurface extracellular enzyme activity was dependent on HMW substrate availability, this does not explain the absence of β -glucosidase and α -glucosidase activity in the OA treatment following the detection of total HMW reducing-sugar in incubation 7 (Table 5.8).

It is possible that this decoupling of substrate availability and enzyme activity was due to the recalcitrant nature of the subsurface HMW substrate, however because the labile fraction of the measured total HMW organic compound was not determined, this is only speculation. Alternatively, the lack of glucosidase activity could result from a preference to remineralise protein based substrate over carbohydrates (Chapter 4.0), thereby supporting the Leu-aminopeptidase activity detected in each treatment in both incubations 6 and 7. The total Leu-aminopeptidase to β -glucosidase ratio across all treatments for incubations 6 and 7 was 23.13 and 34.92 respectively, indicating a poor nutritional carbon pool (Section 4.4). According to Poretsky et al. (2000), certain near-surface bacterial species show a higher number of genes coding for amino acid transport than carbohydrates, suggesting that this pathway is of greater biological importance. A very similar discovery was also made from bacteria at 3000 m deep in the Mediterranean (Martín-Cuadrado et al. 2007). Although samples for this thesis research were collected from a comparatively shallow 100 m depth, this could explain the far higher Leu-aminopeptidase activity detected when compared to β -glucosidase activity across all treatments in both incubations. Interestingly, these activity ratios are lower than those from near-surface seawater (10 m depth) discussed in Section 4.4, potentially reflecting the increasingly recalcitrant nature of the HMW organic substrate at depth, or that a

large proportion of the protein based substrate has been degraded and only carbohydrate substrate remains. Similar activity ratios to those detected during this research were also reported under ambient pH conditions from a range of oceans and depths from 0 - 800 m (Hoppe & Ullrich 1999). As a protein based substrate preference was also measured in the near-surface ocean (Section 4.4), sinking POM would already have a higher carbohydrate composition relative to protein when it reaches the subsurface, so continued protein degradation would likely result in further accumulation of carbohydrate based substrate in the subsurface ocean, potentially increasing the efficiency of active carbon export (Arístegui et al. 2009).

Cell-specific enzyme activities are often used as a proxy for bacterial remineralisation efficiency (Davey et al. 2001). In this research, temporal trends in potential and cell-specific enzyme activities were in close agreement between both incubations. This is consistent with observations of Davey et al. (2001) who identified similar trends in Leu-aminopeptidase activity at 200 m depth. A rapid increase in Leu-aminopeptidase activity occurred in the GH treatment from 24 h to 96 h during each incubation, while the same trend was also shown by cell-specific activity in incubation 6, but not in incubation 7. As cell-specific Leu-aminopeptidase activity was relatively stable in the GH treatment throughout incubation 7, the increase in potential activity indicates that sufficient HMW substrate was available for hydrolysis to occur. This finding suggests that the bacterial community of incubation 7 increased the total production of Leu-aminopeptidase or the enzyme had a faster turnover of substrate. Under ambient conditions, Baltar et al. (2009) and Tamburini et al. (2002) reported an increase in cell-specific enzyme activities with increasing depth. Both authors hypothesised that this may reflect an increase in hydrolytic efficiency at depth, and possible active ecological adaptation to the increased refractory nature and reduced availability of organic matter. This hypothesis suggests that deep-sea bacteria are more adapted to HMW organic compound degradation than bacteria from the near-surface ocean. By comparing cell-specific Leu-aminopeptidase activity from 200 m depth in incubation 5, with that calculated from 100 m depth in incubations 6 and 7, each from a similar spatial location (Fig. 5.1), no consistent increase in cell-specific activity was apparent with depth, suggesting that the theoretical hydrolytic efficiency did not change with depth. This finding was not overly surprising due to the comparatively shallow depth at which cell-specific activities were determined, with both Tamburini et al. (2002) and Baltar et al. (2009) determining cell-specific activities from 200

≥ 2000 m deep. In contrast to the near-surface ocean incubations (Chapter 4), subsurface responses in the GH treatment provide evidence of an additive effect on potential and cell-specific Leu-aminopeptidase activity during incubation 6, as well during the initial stages of incubation 7. This subsurface additive treatment effect suggests that the HT treatment, as well as the OA treatment may have different effects on enzyme activities in different ocean environments.

5.4.2 Relationship between bacterial secondary production and bacterial cell numbers

The pH of the ocean typically declines with increasing depth (Ben-Yaakov & Kaplan 1968, Pukate & Rim-Rukeh 2008). Due to this, subsurface bacterial processes are reportedly adapted to low pH conditions (Tamburini et al. 2002, Baltar et al. 2009). However, as seawater used in this subsurface research was only sampled from below the surface mixed layer (100 m depth), bacterial communities would experience similar pH conditions to the ocean surface and therefore it is not surprising that the OA treatment had a significant negative effect on total BSP as well as bacterial numbers across both incubations (Table 5.8). This significant OA response is supported by the MDS plots of incubations 6 and 7 which show a divergence away from the ambient control at 48 h and 72 h (Section 5.3.8). Surface seawater incubations from a variety of spatial locations show that BSP responds positively (Grossart et al. 2006), or negatively (Maas et al. 2013), or shows no significant response to elevated CO₂ (Arnosti 2011, Teira et al. 2012). These variable responses suggest that increasing CO₂ may not have a direct effect on BSP synthesis, and that additional factors may indirectly influence the portion of the bacterial community that is actively assimilating labile LMW organic matter in the ocean.

In ambient near-surface water, BSP is often positively correlated with bacterial cell numbers, with both parameters regulated by primary production and labile organic matter concentrations (Smith & Hall 1997, Ducklow 2000). In this thesis research, a positive correlation was also recorded in the subsurface ocean during incubation 6. However, the OA treatment had a negative effect on total BSP and bacterial cell numbers when compared to the control in both incubations (Table 5.8). This treatment effect cannot be explained by lower numbers of bacterial cells because cell-specific protein synthesis rates in the OA treatment were also lower than in the ambient control (Fig. 5.11). Instead this trend is likely to reflect a lower

concentration of labile LMW substrate available for bacterial assimilation. It is possible that bacterial membrane fluidity and passive cellular transport pathways were negatively affected when incubated under surface pressure (Kamimura et al. 1992) and OA conditions, resulting in reduced LMW substrate assimilation and BSP. Further to this, literature shows that not all living bacteria within the ocean are actively metabolising and respiring at any one time (Hoppe 1976, Kjelleberg et al. 1987, Sherr & Sherr 1996). Following exposure to low pH and low nutrient conditions, it is possible that a portion of active bacteria became inactive, resulting in a reduction in BSP.

In the HT treatment, both incubations 6 and 7 show a short-term (< 48 h) positive correlation between DNA synthesis rates and bacterial cell numbers. This short-term increase in DNA synthesis signifies not only an increase in metabolically active heterotrophic bacteria in accordance with the Q_{10} coefficient, but also suggests that the subsurface bacteria were focusing their energy towards cell division and new DNA synthesis, as opposed to protein production (Shiah & Ducklow 1997). This positive trend could also indicate the activation of a previously inactive portion of the existing bacterial community. Hoppe (1978) compared the metabolically active bacterial populations in summer and winter months from a range of aquatic environments, concluding that water temperature could have an effect on bacterial active states. Similar to that measured in both the OA and HT treatments, a weak positive correlation was apparent between BSP and bacterial cell number in the GH treatment of both incubations. However, BSP showed contrasting responses in each incubation at 48 h, with incubation 6 showing an initial positive response and incubation 7 showing a negative response, which is further supported by cell-specific protein synthesis. This temporal variation in BSP between incubations is likely a result of changes in LMW substrate availability at different times throughout the incubation, rather than a direct GH effect on the active bacterial community. The decline in BSP detected toward the end of incubation 6 is likely to reflect the concurrent decline in bacterial cell numbers, possibly resulting from viral lysis stimulated by the elevated temperature in the GH treatment (Danovaro et al. 2010). This research shows that future GH subsurface BSP and bacterial cell numbers may vary temporally, dependent on a combination of labile substrate availability and bacterial cell mortality. Changes in bacterial cell numbers may have a direct effect on the number of extracellular enzymes synthesised and therefore subsurface substrate remineralisation and the efficiency of the biological carbon pump.

Although water samples from incubations 6 and 7 were collected from the same depth within the same eddy circulation, time-zero bacterial diversity was significantly different (SIMPROF at 5% significance), likely reflecting temporal change between incubations. During incubations 6 and 7, bacterial diversity in the GH and HT treatments continued to change and were significantly different from the ambient control and each other at 96 h (pers. comm. Dr Els Maas, NIWA). Interestingly, Lindh et al. (2013) reported a similar bacterial diversity change in near-surface seawater under GH conditions, and concluded that although the GH treatment had an additive effect on community diversity, elevated temperature was the primary driver of change rather than pH. In this thesis research, no additive or synergistic effect was evident for total BSP rates or bacterial cell numbers. Across both parameters, the response to the GH treatment was similar to that of the HT treatment as opposed to the OA treatment, suggesting that elevated temperature was a stronger driver, thereby supporting the conclusion made by Lindh et al. (2013).

5.4.3 Relationship between nutrients and phytoplankton

Dissolved nitrate and DRP concentrations declined in each treatment across both incubations, however, in contrast to that of the near-surface ocean, concentrations in the OA treatment were significantly higher than in the ambient control at 96 h (Table 5.8). Due to the absence of light at 100 m depth, photosynthetic phytoplankton are typically found at lower numbers when compared to near-surface communities (Marra 1978), as shown by the low Chl *a* concentrations in each incubation when compared to near-surface ocean concentrations (Chapter 4). As a result, this nutrient trend is not thought to reflect phytoplankton processes but instead reflect utilisation by bacteria who require nutrients to carry out heterotrophic metabolism.

The HT treatment had very little effect on nutrient drawdown and organic matter production during incubations 6 and 7 (Table 5.8). Although a weak coupling was evident between dissolved nutrient concentrations and phytoplankton cell numbers in both incubations, the HT treatment did not have a significant effect. This weak correlation was expected due to the low phytoplankton cell numbers and low PAR available during each incubation. What was surprising however, was that despite the low phytoplankton cell numbers, DOC concentrations increased in each incubation, in all but the HT treatment. This increase in DOC is not likely in

response to a significant increase in phytoplankton production and DOC exudation, but rather an increase in grazing and subsequent release of organic carbon (Kim et al. 2011). The decline in total eukaryotic phytoplankton numbers in incubation 7 is likely to indicate senescence in the absence of light and top-down control by grazing (Engel et al. 2008). Because elevated temperature has a positive effect on metabolic potential, it would also have a positive effect on potential grazing pressure (Deason 1980). An increased grazing pressure in the GH treatment may have led to the decline in phytoplankton cell numbers when compared to the ambient control. Time-zero sampled parameters show that both incubations had very similar dissolved nutrient and DOC concentrations (Table 5.2), yet despite this, both reflected significantly different parameter correlations and responses to GH conditions. Overall, a lower number of photosynthetic planktonic cells was detected in the subsurface ocean when compared to the near-surface ocean, with a weak correlation between cell numbers, dissolved nutrients and DOC thought to reflect the low PAR available at the sampling depth. Elevated temperature and/or low pH did not have a clear effect on planktonic cells numbers in either incubation.

5.5 Summary

These results suggest that in contrast to the near-surface ocean, elevated temperature and low pH will have an additive effect on Leu-aminopeptidase activity below the surface mixed layer (100 m depth), with activity maintained even at very low total HMW substrate concentrations. Although the Leu-aminopeptidase to β -glucosidase activity ratios were lower in the subsurface ocean relative to the near-surface ocean (Chapter 4), an overall preferential degradation of peptide substrate in the subsurface ocean may result in the accumulation of carbohydrate substrates, potentially increasing carbon export. The possibility of ocean stratification in a future GH ocean may reduce the vertical flux and input of HMW substrate into the subsurface ocean but also prevent subsurface de-gassing, potentially trapping respired CO₂ and reducing the replenishment of oxygen through mixing events. An increasingly anoxic subsurface ocean may alter the dominant bacterial community and because different bacteria have different degradation capabilities (Fukami et al. 1981), could further effect substrate remineralisation. The overall organic/inorganic carbon balance below the ocean surface is likely to vary depending on the strength of future ocean stratification and the episodic organic matter input

from the surface ocean, thereby altering the biological carbon pump and the ocean's overall ability to buffer future changes in acidification.

Chapter 6 : Enzyme activity in a natural low pH marine system

6.1 Introduction

There is more than one way to investigate the effect of low pH on a microbial community. The most frequently used methods include laboratory based culture experiments, artificial perturbation incubations, and *in situ* field mesocosm experiments. The experimental method selected should be based on the proposed research aim. For example, if the research is focused on the response of an individual species, a simple laboratory culture experiment would be suitable. Alternatively, if a community based response is the aim, then a larger seawater incubation experiment would be more practical. A field based mesocosm experiment is often used if the research aim requires natural diurnal light/dark cycles and/or physical factors such as currents and particle export. If however, the aim is to investigate a microbial community exposed to long-term low pH conditions on larger spatial scales, laboratory based artificial perturbation experiments become impractical due to the resources required for long-term experimental monitoring and maintenance (Riebesell et al. 2010, Doney et al. 2012). An alternative approach is to use a natural ecosystem that is subject to elevated CO₂.

Volcanically active regions around the world often have submarine cold water vents or seeps which discharge large volumes of CO₂ gas, producing naturally low pH conditions in localised areas. These geological features have typically been active for prolonged periods of time thereby providing a natural proxy for predicted future OA conditions. The use of vent water as a natural OA proxy has two key experimental advantages when compared to typical OA experimentation undertaken in a laboratory. Firstly, depending on the residence time of seawater surrounding the vent plume, the *in situ* microbial community and wider ecosystem may have been exposed to a low pH for an extended period of time, allowing adaptive evolution to occur (Riebesell et al. 2010, Form & Riebesell 2012). This provides the opportunity to investigate a biological community potentially adapted to low pH conditions. The second advantage is the inclusion of all elements of the ecosystem (Riebesell et al. 2010). For example, the inclusion of complete food-web interactions, physical-biogeochemical interactions (vertical nutrient cycling, diffusion and advection), and water column-benthic interactions (substrate sedimentation and burial), each of which is not easily replicated in a laboratory.

Based on these experimental strengths, active vents have been used to investigate low pH effects on reef fish behaviour (Munday et al. 2014), dissolution and calcification of bryozoans (Rodolfo-Metalpa et al. 2010), effects on benthic microalgae (Johnson et al. 2013) and early stages of algal colonisation (Porzio et al. 2013), changes in microplankton biomass and diversity (Sorokin et al. 1998, Ziveri et al. 2014), potential adaptation strategies in polychaete species (Calosi et al. 2013) and invertebrate settlement success (Cigliano et al. 2010). As with any experimental approach, there are limitations and assumptions that need to be considered when using natural CO₂ vent sites for low pH studies. Firstly, volcanic vent sites can be highly dynamic environments with seawater pH often highly variable and unpredictable, making replication challenging (Riebesell et al. 2010). In addition, active vent plumes discharge gas and liquids of diverse composition typically consisting of minerals, trace metals and gases at much higher concentrations than the surrounding seawater (Glasby 1971, Tarasov 2006). These emissions are often highly localised and site specific, confounding interpretation of the effects of high CO₂ (Riebesell et al. 2010).

The active vents in the Bay of Plenty, New Zealand occur along an offshore extension of the Taupo Volcanic Zone (TVZ) which extends 300 km from the Tongariro and Ruapehu volcanic zone in the North Island of New Zealand, up to White Island volcano, 50 km offshore (Stoffers et al. 1999, Hocking et al. 2010). One particular active vent field within the TVZ is named the Calypso field (Sarano et al. 1989) and discharges both gas and liquid (Hocking et al. 2010). Gas is released through active bubbling and is dominated by CO₂ (45 to 84% volume, Stoffers et al. 1999, Botz et al. 2002), with smaller contributions of methane (6 to 10% volume) and hydrogen sulphide (0.8 to 1.0% volume, Botz et al. 2002, Tarasov 2006). Dissolved iron, zinc, lead, copper and manganese are also released from localised vents (Tarasov 2006), with adjacent benthic geology consisting of extensive silica and sulphur deposits, with mercuric sulphide also detected (Stoffers et al. 1999). Gas and liquid discharged from vents have a different biogeochemical composition when compared to the surrounding non-vent seawater; the possibility of high concentrations of dissolved inorganic nutrients such as nitrate and ammonium as well as growth limiting trace metals, such as iron, could affect vent water chemoautotrophic bacterial communities which derive energy from dissolved nutrients but synthesise organic compounds from CO₂ (Buck et al. 2000). Elevated trace metal concentrations could also influence extracellular enzyme activity as Leu-aminopeptidase and Arg-aminopeptidase are both metalloenzymes, and are thought to utilise trace metal cofactors

to assist in hydrolysis (Burley et al. 1990, Bogra et al. 2009). Another active vent site within the TVZ is situated in coastal waters off Whale Island in the Bay of Plenty, only 5 to 10 km from the Whakatane coast (Duncan & Pantin 1969). Coastal seawater is typically characterised by elevated concentrations of dissolved nutrients when compared to open ocean seawater, owing largely to localised river input and land runoff (Morris & Foster 1971, Romankevich 1984, Retamal et al. 2007). High organic matter concentrations often support large bacterial communities and elevated extracellular enzyme activities (del Giorgio et al. 2011), and so a coastal bacterial community response to low pH may differ from those determined from open ocean seawater (Chapters 4 & 5).

The aim of the following chapter was to investigate whether extracellular enzymes from coastal seawater show the same activity response to low pH as those from open ocean seawater. This chapter will also investigate whether extracellular enzyme activities in a naturally low pH coastal vent environment are significantly different from ambient coastal seawater, and if so, determine whether pH is the key driver of this variation. Comparing extracellular enzyme activities in a low pH treatment, as in previous open ocean water experiments (Chapters 4 & 5), with that of naturally low pH vent plume water, will determine whether low pH is the key determinant of bacterial substrate degradation, and the value of naturally low pH vent systems as proxy environments for a future low pH ocean.

6.2 Methods

Two short-term incubations (84 h) were completed on-board the research vessel *Kaharoa* during a research cruise centred off Whale Island in the Bay of Plenty, North Island, New Zealand from the 04.03.2013 to 15.03.2013. To investigate the response of extracellular enzyme activity in a naturally low pH environment, subsurface seawater from a vent plume was collected from a depth of 45 to 50 m. Using an on-board depth sonar (ES60 Echosounder), as in Glasby (1971) and Sarano et al. (1989), active vent plumes were identified as large streams of gas bubbles originating from the ocean floor (Fig. 6.1).

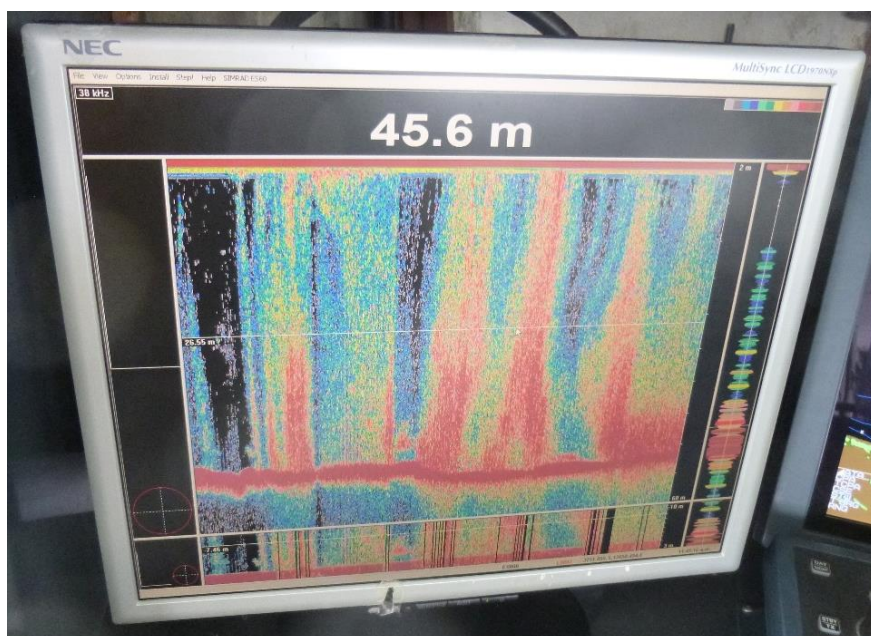


Fig. 6.1. Echogram of backscatter data from repeated crossing of the Whale Island vent at 46 m depth, showing plumes of bubbles emanating from the seafloor (photo E. Maas)

Bulk seawater was collected using the same techniques described in Section 4.2, however a smaller Seabird Electronics Inc. 32 Carousel water sampler fitted with 12 x 10 l external-spring Niskin-type bottles (Ocean Test Equipment Standard 10 BES) was employed. Incubations 8 and 9 were carried out using seawater collected from the Whale Island vent site (Fig. 6.2), and ambient coastal seawater used as the control was collected from a similar depth, 18 km upstream of the vent site (Fig. 6.2). In addition, an artificially acidified low pH treatment,

consisting of upstream coastal control seawater acidified to the same pH as the vent water, was compared with the control and vent plume water. No elevated temperature treatment was carried out in incubations 8 and 9.

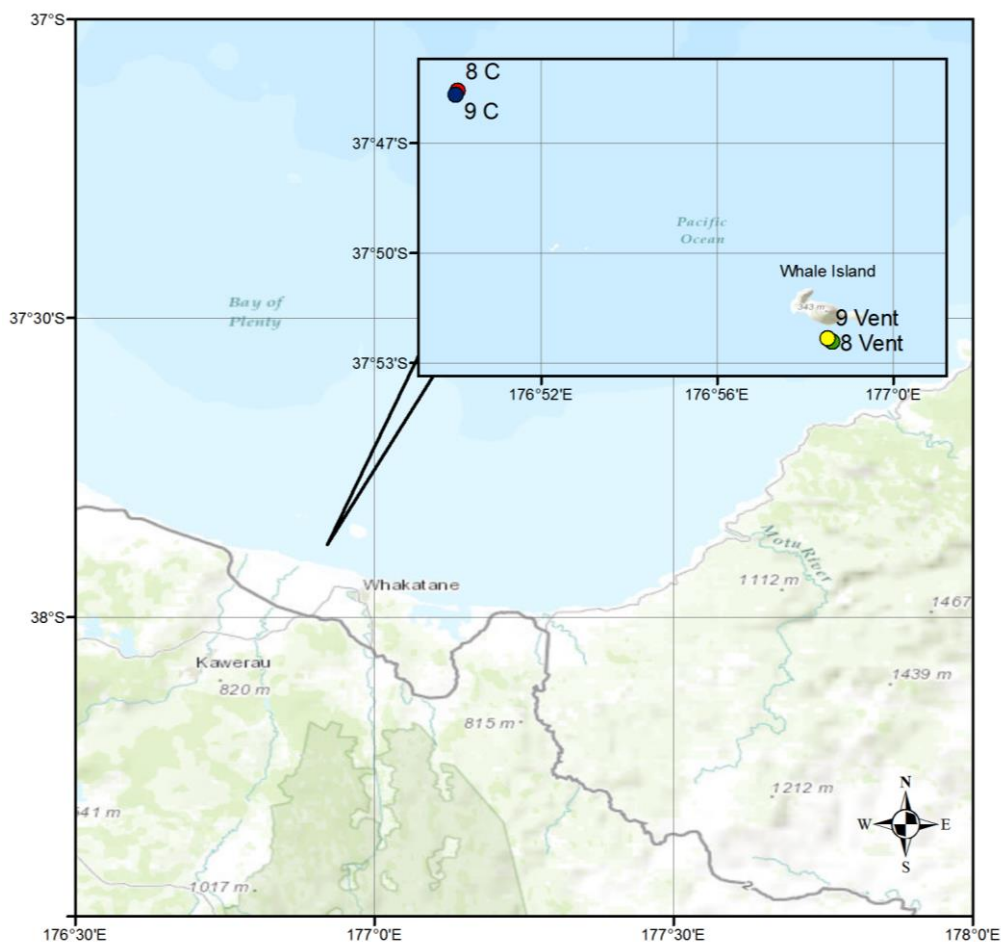


Fig. 6.2. Incubations 8 and 9 bulk seawater collection sites. Inset magnified view: 8 & 9 C mark the location of the upstream control site, and 8 & 9 Vent mark the vent seawater collection sites

The artificially low pH treatment was created by saturating 1.5 l of ambient upstream coastal control seawater with 10% CO₂ gas (in 20.8% O₂ in N₂, BOC Gas Ltd) for 90 mins. Between 200 and 300 ml of the saturated seawater (pH_T 5.82) was added to 4 l of upstream coastal control seawater, with pH measured to ensure this matched that of the vent seawater (Fig. 6.3). Each treatment and ambient control was replicated in triplicate and held in acid washed, milli-Q water rinsed 4.3 l LDPE cubitainers (Thermo-Fisher Scientific), as described

in Section 2.1. The headspace was removed from each cubitainer and no further artificial pH alteration occurred.

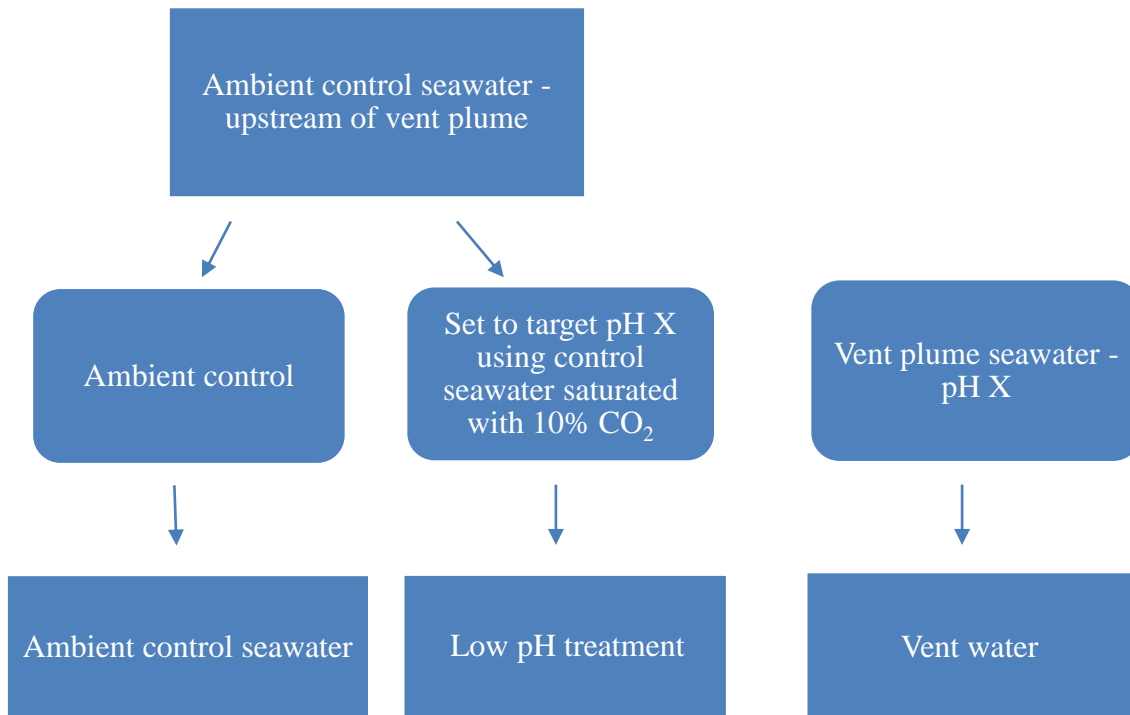


Fig. 6.3. Experimental design

Both incubations 8 and 9 were conducted inside a temperature controlled container (Fig. 6.4), set to the ambient seawater temperature at each collection site (19.6 and 20.6°C). pH and temperature was measured at selected sampling points throughout each incubation (Appendix A: 6.1). Although light availability was not measured at each seawater collection depth (46.5 and 49 m deep respectively), it was likely to be low (pers. comm. Dr Cliff Law) therefore each incubation was maintained in the dark. Further to this, each cubitainer viewing window was covered with a black polythene bag, to minimise ambient light exposure during sub-sampling. Automated sample mixing followed that described in Section 2.1.



Fig. 6.4. Experimental set-up in the temperature controlled container. Two white incubation chambers are stacked on the right side, the black fluorescent plate reader can be seen raised on the bench, while the pH meter is situated on the container floor

The same parameters were sampled as in previous incubations, with the addition of Transparent Exopolymer Particles (TEP) and Total Carbohydrate (TC) concentration (Table 6.1). Dissolved nutrient, DOC, TEP, TC and total HMW organic compound concentrations were sampled less frequently than the nominated primary parameters (Table 6.1).

Table 6.1. Parameter sampling protocol for incubations 8 and 9. The total number of times a parameter was sampled is indicated, followed by its respective sampling frequency [in square brackets], after an initial time-zero sample is shown. Parameters in **bold** indicate parameters of primary significance

Incubation	8		9	
Duration	07.03.13 – 10.03.13 (84 h)		11.03.13 – 14.03.13 (84 h)	
	Vent	Control	Vent	Control
Location ($^{\circ}$)	37.96 $^{\circ}$ N 176.97 $^{\circ}$ E	37.77 $^{\circ}$ N 176.83 $^{\circ}$ E	37.86 $^{\circ}$ N 176.97 $^{\circ}$ E	37.77 $^{\circ}$ N 176.83 $^{\circ}$ E
Depth (m)	47.5	46.5	47	49
Temperature ($^{\circ}$ C)	20.7	19.6	20.6	20.6
Salinity (psu)	35.54	35.48	35.53	35.58
pH _T at time-zero	7.71	8.03	7.83	8.03
β-glucosidase and α-glucosidase	7 [12 h]		7 [12 h]	
Leu-aminopeptidase and Arg-aminopeptidase	7 [12 h]		7 [12 h]	
Bacterial cell numbers	7 [12 h]		7 [12 h]	
Pico-cyanobacteria spp. cell numbers	7 [12 h]		7 [12 h]	
Total eukaryotic phytoplankton cell numbers	7 [12 h]		7 [12 h]	
BSP DNA synthesis	7 [12 h]		7 [12 h]	
BSP protein synthesis	7 [12 h]		7 [12 h]	
Dissolved nutrients	1 [84 h]		1 [84 h]	
DOC	1 [84 h]		1 [84 h]	
Total HMW organic compound concentration (reducing-sugar & protein)	5 [17 h]		5 [17 h]	
TEP and TC	2 [42 h]		2 [42 h]	

6.3 Results

Comparison of time-zero conditions

Due to single sample collection for enzyme activity determination at time-zero, insufficient data were available for statistical interpretation in incubations 8 and 9. As anticipated, time-zero conditions differed in the vent water from the low pH treatment and ambient control (Table. 6.2). In incubation 8, time-zero Leu-aminopeptidase activity was higher in the vent water than the ambient control, while total HMW protein substrate concentration, bacterial and phytoplankton cell numbers were also significantly higher. In contrast, time-zero protein synthesis was significantly lower in the vent water than the ambient control (Table. 6.2). Time-zero DRSi and dissolved ammonium concentrations were significantly higher in the vent water than the ambient control, while dissolved nitrate concentrations were significantly lower (Table. 6.2). In incubation 9, time-zero Leu-aminopeptidase activity was higher in the vent water than the ambient control, while activity was lower in the low pH treatment than the ambient control (Table. 6.2). Time-zero total eukaryotic phytoplankton cell numbers, DRSi and dissolved ammonium concentrations were all significantly higher in the vent water when compared to the ambient control, but nitrate concentrations were significantly lower (Table. 6.2). In contrast to incubation 8, *Prochlorococcus* spp. cell numbers were significantly lower in the time-zero vent water when compared to the ambient control, while TEP concentrations were significantly higher (Table. 6.2).

Table 6.2. Average time-zero value for each parameter per treatment in incubations 8 and 9 (\pm SE). Samples were analysed following methodology in Chapter 2. *: indicates the parameter was significantly different from the ambient control ($p < 0.05$)

Parameter	Incubation 8			Incubation 9		
	Vent	Low pH	Control	Vent	Low pH	Control
β -glucosidase (nmol l ⁻¹ h ⁻¹)	1.07	1.33	0.77	0.40	0.45	0.53
α -glucosidase (nmol l ⁻¹ h ⁻¹)	0.29	0.75	0.24	0.06	0.09	0.10
Arg-aminopeptidase (nmol l ⁻¹ h ⁻¹)	0.00	0.00	43.77	57.56	8.94	22.80
Leu-aminopeptidase (nmol l ⁻¹ h ⁻¹)	104.81	63.08	61.65	42.41	40.41	30.17
Bacterial numbers (cells ml ⁻¹) (n=3)	1.8 x 10 ⁶ ($\pm 1.8 \times 10^4$) *	1.0 x 10 ⁶ ($\pm 1.8 \times 10^4$)	1.1 x 10 ⁶ ($\pm 3.4 \times 10^4$)	7.6 x 10 ⁵ ($\pm 1.0 \times 10^5$)	6.2 x 10 ⁵ ($\pm 1.0 \times 10^5$)	7.1 x 10 ⁵ ($\pm 5.0 \times 10^4$)
<i>Synechococcus</i> spp. numbers (cells ml ⁻¹) (n=3)	5.3 x 10 ⁴ ($\pm 1.1 \times 10^3$) *	1.7 x 10 ⁴ ($\pm 8.8 \times 10^2$)	1.7 x 10 ⁴ ($\pm 1.0 \times 10^3$)	1.0 x 10 ⁴ ($\pm 8.0 \times 10^2$)	1.2 x 10 ⁴ ($\pm 3.8 \times 10^2$)	1.2 x 10 ⁴ ($\pm 5.1 \times 10^2$)
<i>Prochlorococcus</i> spp. numbers (cells ml ⁻¹) (n=3)	7.1 x 10 ⁴ ($\pm 4.9 \times 10^2$) *	3.2 x 10 ⁴ ($\pm 5.0 \times 10^3$)	3.1 x 10 ⁴ ($\pm 2.1 \times 10^3$)	2.5 x 10 ⁴ ($\pm 1.4 \times 10^3$) *	4.6 x 10 ⁴ ($\pm 2.3 \times 10^3$)	4.7 x 10 ⁴ ($\pm 2.9 \times 10^3$)
Total eukaryotic phytoplankton numbers (cells ml ⁻¹) (n=3)	1.7 x 10 ⁴ ($\pm 7.4 \times 10^2$) *	1.0 x 10 ⁴ ($\pm 7.9 \times 10^2$)	1.2 x 10 ⁴ ($\pm 8.0 \times 10^2$)	2.4 x 10 ⁴ ($\pm 6.0 \times 10^1$) *	1.1 x 10 ⁴ ($\pm 2.0 \times 10^2$)	1.1 x 10 ⁴ ($\pm 2.7 \times 10^2$)
BSP DNA synthesis (μ g C l ⁻¹ day) (n=3)	65.25 (± 6.50)	63.25 (± 1.50)	54.44 (± 5.20)	118.67 (± 9.30)	91.12 (± 7.60)	83.19 (± 3.50)
BSP protein synthesis (μ g C l ⁻¹ day) (n=3)	0.47 (± 0.00) *	1.49 (± 0.09)	1.56 (± 0.11)	0.98 (± 0.03)	0.82 (± 0.05)	0.86 (± 0.03)
Nitrate (μ g l ⁻¹) (n=3)	1.50 (± 0.00) *	8.75 (± 0.25)	8.53 (± 0.12)	0.50 (± 0.00) *	1.05 (± 0.05)	1.20 (± 0.00)
DRP (μ g l ⁻¹) (n=3)	7.45 (± 0.45)	7.85 (± 0.25)	7.93 (± 0.35)	4.60 (± 0.11)	3.70 (± 0.00)	3.95 (± 0.15)
DRSi (μ g l ⁻¹) (n=3)	145.50 (± 0.50) *	130.00 (± 5.32)	120.00 (± 1.25)	114.00 (± 0.00) *	74.45 (± 2.75)	78.10 (± 0.80)
Ammonium (μ g l ⁻¹) (n=3)	22.95 (± 0.45) *	12.30 (± 0.30)	12.00 (± 0.65)	11.45 (± 0.35) *	6.65 (± 0.25)	7.70 (± 0.00)
DOC (μ g ml ⁻¹) (n=2)	1.55 (± 0.43)	1.39 (± 0.34)	0.86 (± 0.06)	1.33 (± 0.30)	1.18 (± 0.02)	1.16 (± 0.05)
Total HMW reducing-sugar (μ g ml ⁻¹ gluc eq.) (n=3)	0.00	0.00	0.00	0.01 (± 0.003)	0.01 (± 0.001)	0.01 (± 0.001)
Total HMW protein (μ g ml ⁻¹ BSA eq.) (n=3)	1.20 (± 0.01) *	0.53 (± 0.03)	0.36 (± 0.03)	0.54 (± 0.03)	0.44 (± 0.05)	0.44 (± 0.02)
TEP (μ g l ⁻¹ xant eq.) (n=2)	126.66 (± 10.1)	81.56 (± 3.7)	88.55 (± 4.4)	105.50 (± 10.5) *	54.99 (± 6.9)	47.50 (± 2.5)
TC (μ g l ⁻¹ gluc eq.) (n=2)	97.07 (± 52.2)	77.90 (± 7.5)	29.00 (± 2.6)	42.00 (± 11.6)	43.30 (± 3.2)	65.50 (± 7.6)

6.3.1 Extracellular enzyme activity

6.3.1.1 Incubation 8

During incubation 8, time-zero β -glucosidase activity was similar between vent water, the low pH treatment and the ambient control (Fig. 6.5). The β -glucosidase activity increased more than ten-fold in the vent water from time-zero ($1.06 \text{ nmol l}^{-1} \text{ h}^{-1}$) to 84 h ($13.90 \text{ nmol l}^{-1} \text{ h}^{-1}$), while activity increased five-fold in the low pH treatment across the same period (1.33 to $6.72 \text{ nmol l}^{-1} \text{ h}^{-1}$ respectively). Activity in the ambient control only doubled from time-zero to 84 h (0.76 to $2.15 \text{ nmol l}^{-1} \text{ h}^{-1}$ respectively) and consequently β -glucosidase activity was significantly higher in the vent water and low pH treatment at each sampling point from 24 h to 84 h (Fig. 6.5, p-values in Appendix E: 6.1). Similarly, activity increased at a faster rate in the vent water when compared to the low pH treatment from 24 h to 84 h (Fig. 6.5 & Appendix E: 6.1). A similar overall response was measured for α -glucosidase, with activity in vent water increasing more than fifteen-fold from time-zero ($0.28 \text{ nmol l}^{-1} \text{ h}^{-1}$) to 84 h ($4.78 \text{ nmol l}^{-1} \text{ h}^{-1}$), reflecting a significantly higher activity than both the low pH treatment and ambient control from 36 h to 84 h (Fig. 6.5 & Appendix E: 6.1). Activity in the low pH treatment was significantly higher than the ambient control from 36 h to 84 h (Fig. 6.5 & Appendix E: 6.1). Although overall treatment trends were similar between β -glucosidase and α -glucosidase activity, average β -glucosidase activity was approximately three times higher than α -glucosidase activity in each treatment.

Time-zero Arg-aminopeptidase activity was below detection in the vent water and low pH treatment during incubation 8 (Fig. 6.5), however activity was detected in the ambient control and declined from time-zero ($43.77 \text{ nmol l}^{-1} \text{ h}^{-1}$) to 84 h ($4.79 \text{ nmol l}^{-1} \text{ h}^{-1}$, Fig. 6.5). Time-zero Leu-aminopeptidase activity was higher in the vent water than the low pH treatment and ambient control, and then declined from 48 h ($110.46 \text{ nmol l}^{-1} \text{ h}^{-1}$) to 84 h ($38.31 \text{ nmol l}^{-1} \text{ h}^{-1}$). Despite this negative trend, Leu-aminopeptidase activity was significantly higher in the vent water than the low pH treatment and ambient control from 24 h to 72 h, with activity ranging from 68.52 to $110.46 \text{ nmol l}^{-1} \text{ h}^{-1}$ (Fig. 6.5 & Appendix E: 6.1). Time-zero Leu-aminopeptidase activity was very similar between the low pH treatment and ambient control but deviated after 24 h (Fig. 6.5). Activity in the low pH treatment increased rapidly from 24 h relative to the ambient control, resulting in a significantly higher activity at each sampling point from 36 h to

84 h (Fig. 6.5 & Appendix E: 6.1). Although activity was significantly higher in the vent seawater, it declined at a faster rate from 48 h to 84 h, almost three-fold faster than the low pH treatment which declined two-fold (Fig. 6.5).

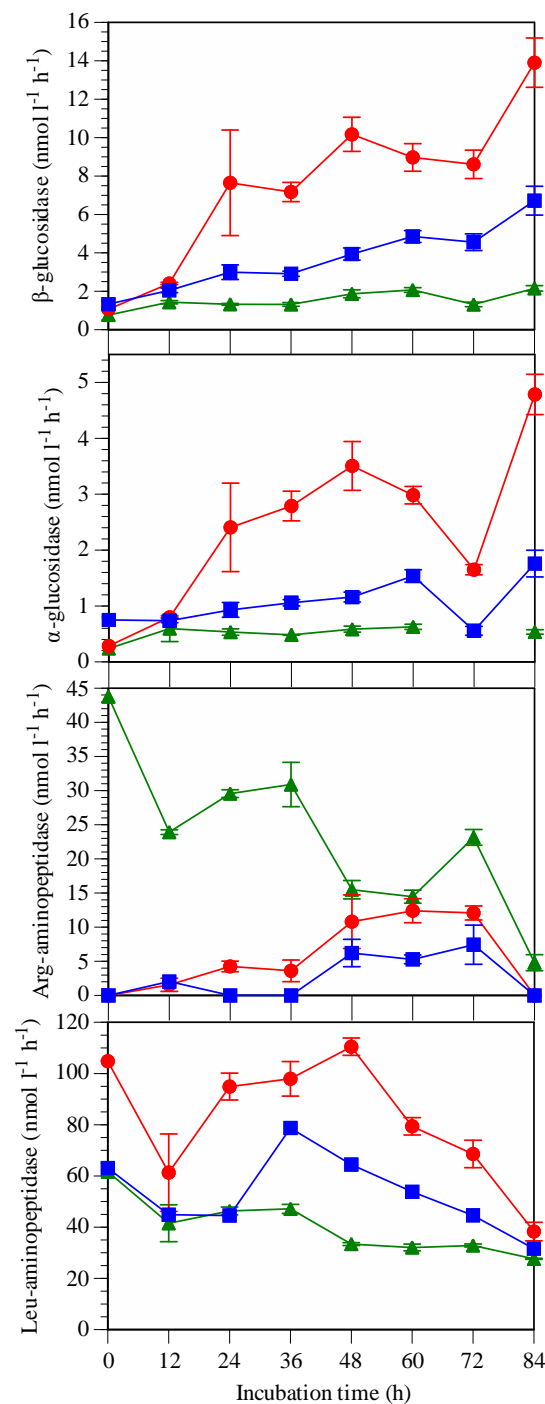


Fig. 6.5. Extracellular enzyme activities in incubation 8 (mean \pm SE, n=3). No value indicates sample was lost. Treatment legend – vent: red circles; low pH: blue squares; ambient control: green triangles

Time-zero cell-specific β -glucosidase activity was higher in the low pH treatment than in the vent water and ambient control (Fig. 6.6), with cell-specific activity increasing in each treatment from time-zero to 84 h (Fig. 6.6). Cell-specific β -glucosidase activity increased five-fold in the vent water from time-zero ($0.60 \text{ amol cell}^{-1} \text{ h}^{-1}$) to 24 h ($2.93 \text{ amol cell}^{-1} \text{ h}^{-1}$, Fig. 6.6). A significantly higher cell-specific β -glucosidase activity was detected in the vent water and low pH treatment when compared to the ambient control at every sampling point from 12 h to 84 h (ANOVA $F_{1,3}$, $p < 0.05$, Fig. 6.6). Cell-specific Leu-aminopeptidase activity peaked in the vent water at 24 h ($64.51 \text{ amol cell}^{-1} \text{ h}^{-1}$) and then declined to 84 h ($14.38 \text{ amol cell}^{-1} \text{ h}^{-1}$); activity in the low pH treatment peaked later at 36 h ($64.83 \text{ amol cell}^{-1} \text{ h}^{-1}$) and then followed a similar declining trend to 84 h ($14.66 \text{ amol cell}^{-1} \text{ h}^{-1}$, Fig. 6.6). Cell-specific Leu-aminopeptidase activity was lowest in the ambient control at time-zero ($54.72 \text{ amol cell}^{-1} \text{ h}^{-1}$) and continuously declined to 84 h ($16.44 \text{ amol cell}^{-1} \text{ h}^{-1}$, Fig. 6.6); as a result, cell-specific activity was significantly higher in the vent water and low pH treatment when compared to the ambient control at each sampling point from 24 h to 60 h (ANOVA $F_{1,3}$, $p < 0.05$, Fig. 6.6).

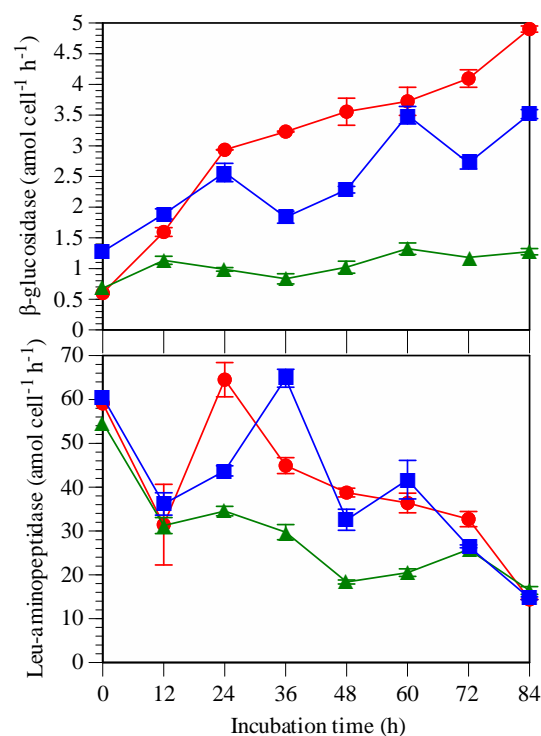


Fig. 6.6. Cell-specific extracellular enzyme activities in incubation 8 (mean \pm SE, $n=3$). Treatment legend – vent: red circles; low pH: blue squares; ambient control: green triangles

6.3.1.2 Incubation 9

Time-zero β -glucosidase activity was very similar between vent water, the low pH treatment and the ambient control (Fig. 6.7). The β -glucosidase activity increased three-fold in the vent water from 12 h to 24 h (1.68 to $5.35 \text{ nmol l}^{-1} \text{ h}^{-1}$) with activity significantly higher when compared to the low pH treatment and ambient control to 72 h (ANOVA $F_{1,3}$, $p < 0.05$, Fig. 6.7). The β -glucosidase activity in the low pH treatment followed a similar activity profile as the ambient control, both increasing from time-zero to 84 h (Fig. 6.7). Time-zero α -glucosidase activities were also very similar between the vent water, the low pH treatment and the ambient control (Fig. 6.7). Each treatment followed a similar α -glucosidase activity profile throughout the incubation, however activity increased at a faster rate in the vent water from time-zero to 24 h, reflecting a 28-fold increase in activity (Fig. 6.7). Vent water activity was higher relative to both the low pH treatment and ambient control from 24 h to 84 h (Fig. 6.7). The α -glucosidase activity in the low pH treatment peaked at 36 h ($1.32 \text{ nmol l}^{-1} \text{ h}^{-1}$) and was significantly higher than the ambient control at 60 h ($0.69 \text{ nmol l}^{-1} \text{ h}^{-1}$) and 84 h ($1.20 \text{ nmol l}^{-1} \text{ h}^{-1}$, Fig. 6.7 & Appendix E: 6.1).

Arg-aminopeptidase displayed variable activity in incubation 9 (Fig. 6.7), similar to that measured in incubation 8. Time-zero Arg-aminopeptidase activity was higher in the vent water than in the low pH treatment and ambient control (Fig. 6.7), while time-zero activity in the low pH treatment was lower than in the ambient control (Fig. 6.7). The Arg-aminopeptidase activity in the ambient control remained relatively constant from time-zero ($22.69 \text{ nmol l}^{-1} \text{ h}^{-1}$) to 60 h ($16.38 \text{ nmol l}^{-1} \text{ h}^{-1}$), while activity in the vent treatment and the low pH treatment peaked at 36 h, with a significantly higher activity than in the ambient control (Fig. 6.7 & Appendix E: 6.1). Time-zero Leu-aminopeptidase activity was higher in the vent water and low pH treatment when compared to the ambient control, with activity in both treatments following a similar activity profile (Fig. 6.7). The Leu-aminopeptidase activity increased at a faster rate in the vent water from 36 h to 72 h (increasing seven-fold) compared to the low pH treatment (activity increased five-fold). Consequently the vent water contained a significantly higher activity at 60 h and 72 h (ANOVA $F_{1,3}$, $p < 0.05$, Fig. 6.7).

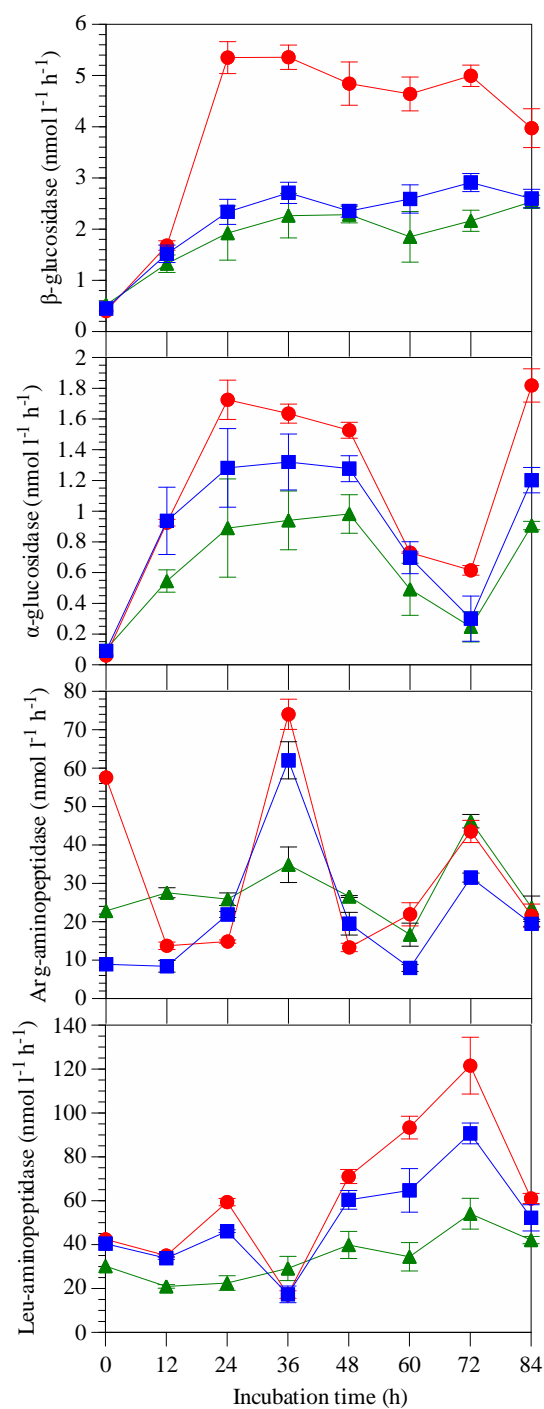


Fig. 6.7. Extracellular enzyme activities in incubation 9 (mean \pm SE, n=3). Treatment legend – vent: red circles; low pH: blue squares; ambient control: green triangles

Time-zero cell-specific β -glucosidase activity was lower in the vent water than in both the low pH treatment and ambient control during incubation 9 (Fig. 6.8). Cell-specific β -glucosidase activity increased in each treatment from time-zero to 24 h (Fig. 6.8). While activity in the ambient control and low pH treatment plateaued at 24 h, activity in the vent water continued to increase to 36 h ($3.83 \text{ amol cell}^{-1} \text{ h}^{-1}$), when activity was significantly higher than in both the ambient control and low pH treatment (ANOVA $F_{1, 3}$, $p < 0.05$, Fig. 6.8). Cell-specific β -glucosidase activity was significantly higher in the vent water than the ambient control from 36 h to 84 h, with a respective activity ranging from 3.48 to $3.83 \text{ amol cell}^{-1} \text{ h}^{-1}$ (ANOVA $F_{1, 3}$, $p < 0.05$, Fig. 6.8). Time-zero cell-specific Leu-aminopeptidase activity was higher in the low pH treatment and vent water compared to the ambient control, and showed a similar trend from time-zero to 60 h (Fig. 6.8). Except for a sharp decline at 36 h, cell-specific activity was higher in the vent water and low pH treatment than in the ambient control. Cell-specific activity increased in the low pH treatment from 60 h to 84 h, with activity significantly higher than the vent water and ambient control (ANOVA $F_{1, 2}$, $p < 0.05$, Fig. 6.8).

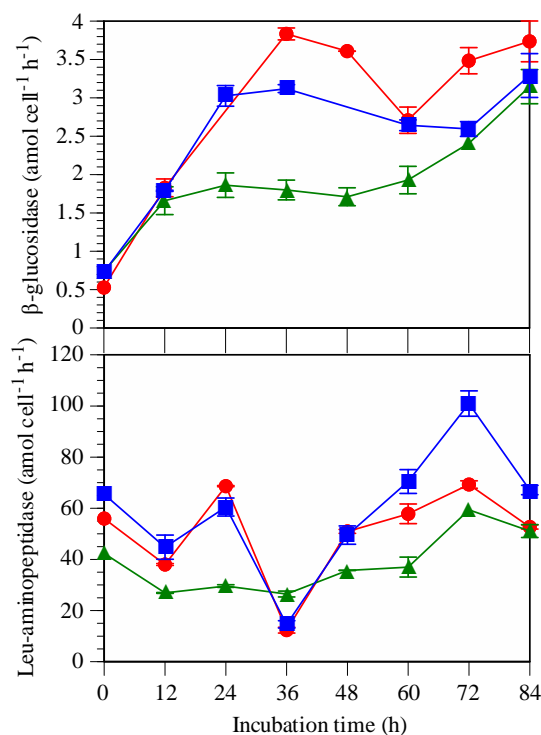


Fig. 6.8. Cell-specific extracellular enzyme activities in incubation 9 (mean \pm SE, $n=3$). Treatment legend – vent: red circles; low pH: blue squares; ambient control: green triangles

Summary of results

Overall, β - and α -glucosidase activity increased in the vent water relative to the ambient control in incubations 8 and 9 (Table 6.3), while the activity also increased in the low pH treatment in incubation 8 (Table 6.3). The response of Arg- and Leu-aminopeptidase activity to vent water varied between incubations (Table 6.3), while Leu-aminopeptidase activity increased in the low pH treatment relative to the ambient control in both incubations (Table 6.3).

Table 6.3. Summary of extracellular enzyme activity changes in each treatment relative to the ambient control over 84 h. \uparrow : indicates an increase relative to the control; \downarrow : decrease; empty cell: no change; $<$: time-zero value was lower than the control; $>$: time-zero value was higher than the control

Parameter	Incubation 8		Incubation 9	
	Vent	Low pH	Vent	Low pH
β -glucosidase	\uparrow	\uparrow	\uparrow	
α -glucosidase	\uparrow	$>\uparrow$	\uparrow	\uparrow
Arg-aminopeptidase			$>\downarrow$	$<\uparrow$
Leu-aminopeptidase	$>\downarrow$	\uparrow	$>\uparrow$	$>\uparrow$

6.3.2 Cell numbers

6.3.2.1 Incubation 8

Time-zero bacterial cell numbers were statistically higher in the vent water when compared to the low pH treatment and ambient control (Fig. 6.9). Vent water bacterial cell numbers remained higher than the ambient control for the duration of the incubation (ANOVA $F_{1, 4}$, $p < 0.01$), while following a similar temporal response to the low pH treatment and ambient control (Fig. 6.9). Bacterial cell numbers increased significantly in the low pH treatment relative to the ambient control from 72 h (ANOVA $F_{1, 4}$, $p < 0.01$, Fig. 6.9). Time-zero *Synechococcus* spp., *Prochlorococcus* spp. and total eukaryotic phytoplankton cell numbers were also significantly higher in the vent water than the ambient control (ANOVA $F_{1, 4}$, $p < 0.05$, Fig. 6.9), whereas time-zero phytoplankton cell numbers were not significantly different between the low pH treatment and ambient control (Fig. 6.9). *Synechococcus* spp., *Prochlorococcus* spp. and total eukaryotic phytoplankton numbers declined from time-zero to 72 h at similar rates in all treatments (Fig. 6.9). Total phytoplankton cell numbers did not change significantly relative to the ambient control throughout incubation 8 (Fig. 6.9, p-values in Appendix E: 6.2).

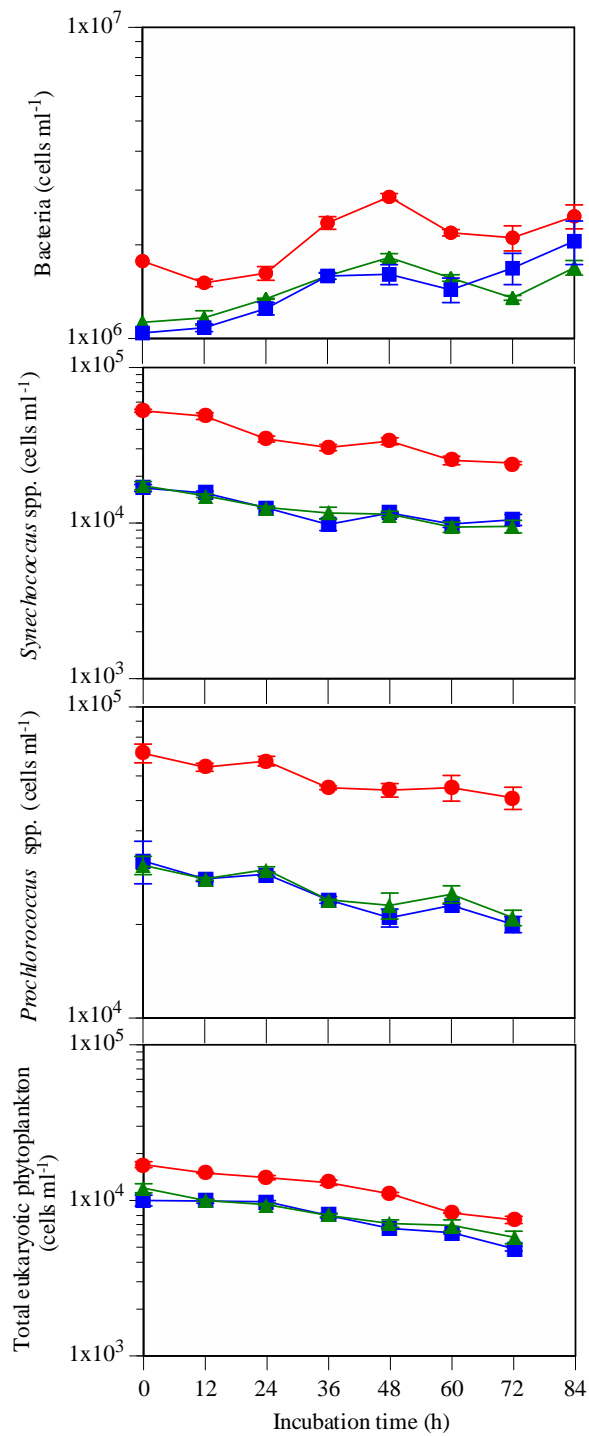


Fig. 6.9. Bacteria, *Synechococcus* spp., *Prochlorococcus* spp. and total eukaryotic phytoplankton cell numbers (log scale) in incubation 8 (mean \pm SE, n=3). Missing value indicates sample was lost. Treatment legend – vent: red circles; low pH: blue squares; ambient control: green triangles

6.3.2.2 Incubation 9

In contrast to incubation 8, time-zero bacterial cell numbers were not significantly higher in the vent water when compared to the low pH treatment and ambient control in incubation 9 (Fig. 6.10). Bacterial cell numbers were similar in each treatment from time-zero to 48 h, with numbers increasing in the vent water relative to the low pH treatment and ambient control from 60 h to 84 h (ANOVA $F_{1,4}$, $p < 0.05$, Fig. 6.10). There was no significant difference in bacterial cell numbers between the low pH treatment and ambient control at any sampling point throughout incubation 9 (Fig 6.10 & Appendix E: 6.2). Time-zero *Synechococcus* spp. cell numbers were not significantly higher in the vent water when compared to the low pH treatment or ambient control (Fig. 6.10), and there was no significant difference in *Synechococcus* spp. numbers between the low pH treatment and the ambient control at any sampling point throughout incubation 9 (Fig 6.10 & Appendix E: 6.2). Time-zero vent water *Prochlorococcus* spp. cell numbers were lower, and remained significantly lower than the low pH treatment and ambient control until 48 h, when cell numbers declined rapidly in the low pH treatment and ambient control (Fig 6.10 & Appendix E: 6.2). Similar to incubation 8, time-zero total eukaryotic phytoplankton cells were significantly higher in the vent water than in the low pH treatment and ambient control (Fig. 6.10) and remained constant throughout the incubation (ANOVA $F_{1,4}$, $p < 0.05$, Fig. 6.10). There was no significant difference in time-zero total eukaryotic phytoplankton cell numbers between the low pH treatment and ambient control (Fig. 6.10).

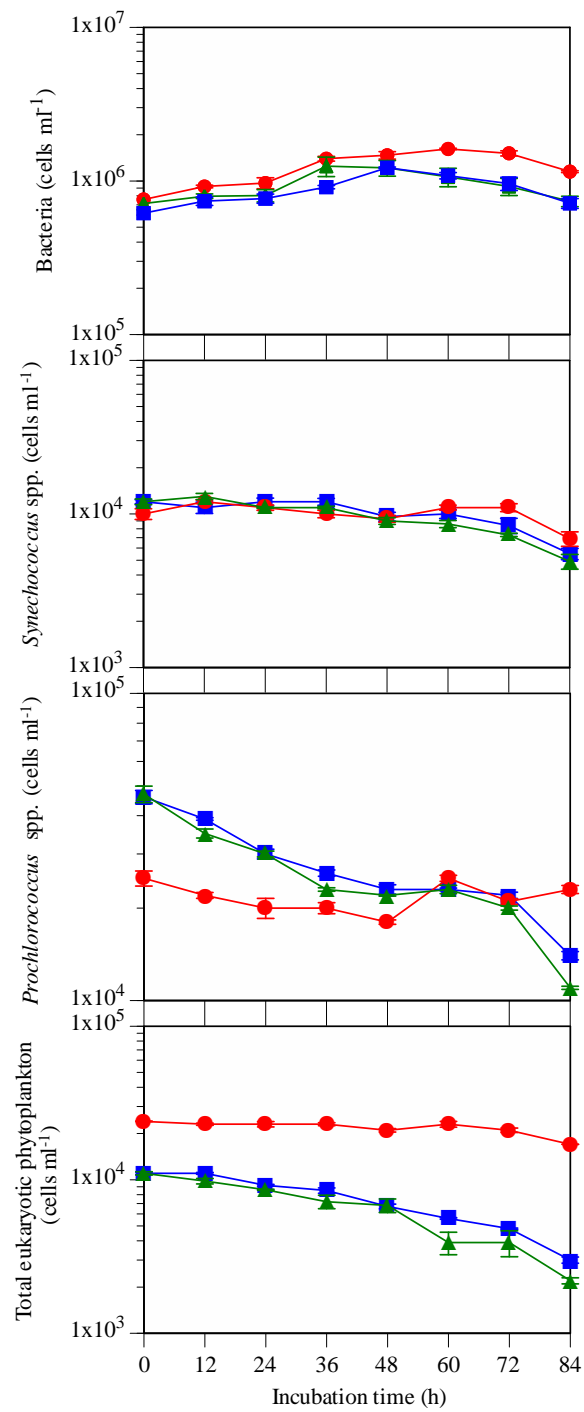


Fig. 6.10. Bacteria, *Synechococcus* spp., *Prochlorococcus* spp. and total eukaryotic phytoplankton cell numbers (log scale) in incubation 9 (mean \pm SE, n=3). Treatment legend – vent: red circles; low pH: blue squares; ambient control: green triangles

Summary of results

Overall, although bacterial, *Synechococcus* spp., *Prochlorococcus* spp. and total eukaryotic phytoplankton cell numbers were highest in the vent water throughout incubation 8, numbers did not change relative to the ambient control (Table 6.4). In contrast, bacterial, *Prochlorococcus* spp. and total eukaryotic phytoplankton numbers increased relative to the ambient control in incubation 9 (Table 6.4). Bacterial, *Synechococcus* spp., *Prochlorococcus* spp. and total eukaryotic phytoplankton cell numbers in the low pH treatment did not differ from the ambient control in either incubation (Table 6.4).

Table 6.4. Summary of cell number changes in each treatment relative to the ambient control over 84 h. ↑: indicates an increase relative to the control; ↓: decrease; empty cell: no change; <: time-zero value was lower than the control; >: time-zero value was higher than the control

Parameter	Incubation 8		Incubation 9	
	Vent	Low pH	Vent	Low pH
Bacterial			↑	
<i>Synechococcus</i> spp.				
<i>Prochlorococcus</i> spp.			<↑	
Total eukaryotic phytoplankton cells			>↑	

6.3.3 Bacterial secondary production

6.3.3.1 Incubation 8

There was no significant difference in time-zero DNA synthesis rates between each treatment in incubation 8 (Fig. 6.11, p-values in Appendix E: 6.3). DNA synthesis rates increased three-fold in the low pH treatment and ambient control from time-zero ($63.25 \mu\text{g C l}^{-1} \text{d}^{-1}$ and $54.44 \mu\text{g C l}^{-1} \text{d}^{-1}$ respectively) to 12 h ($224.22 \mu\text{g C l}^{-1} \text{d}^{-1}$ and $200.30 \mu\text{g C l}^{-1} \text{d}^{-1}$ respectively), but then plateaued at $\sim 120 \mu\text{g C l}^{-1} \text{d}^{-1}$ (Fig. 6.11). In contrast, DNA synthesis in the vent water increased at a slower rate to 84 h ($224.05 \mu\text{g C l}^{-1} \text{d}^{-1}$, Fig. 6.11). Time-zero protein synthesis was significantly lower in the vent water when compared to the low pH treatment and ambient control in incubation 8 (Fig. 6.11 & Appendix E: 6.3); but increased 10-fold to 36 h ($14.76 \mu\text{g C l}^{-1} \text{d}^{-1}$), after which synthesis remained constant at a significantly higher rate than the low pH treatment and ambient control (ANOVA $F_{1,3}$, $p < 0.01$, Fig. 6.11). Protein synthesis rates in the low pH treatment and ambient control followed a similar response profile throughout incubation 8, increasing steadily from time-zero (Fig. 6.11).

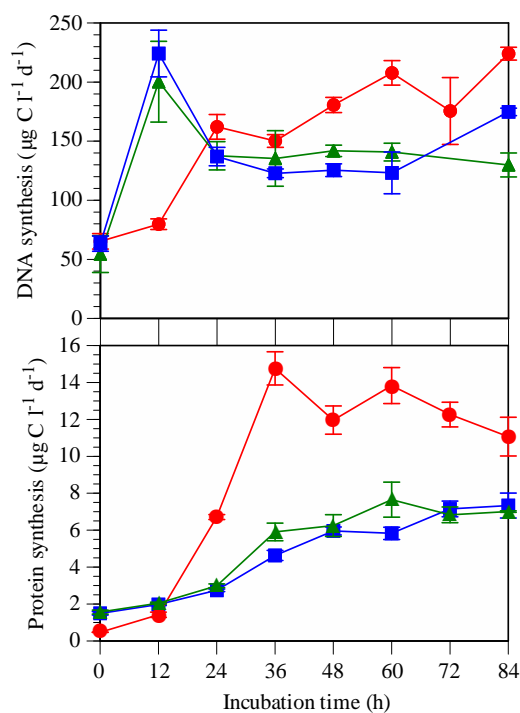


Fig. 6.11. BSP throughout incubation 8 (mean \pm SE, $n=3$). Treatment legend – vent: red circles; low pH: blue squares; ambient control: green triangles

Cell-specific protein synthesis rates followed a very similar trend to potential protein synthesis during incubation 8. Time-zero vent water cell-specific protein synthesis rates were significantly lower than both the low pH treatment and ambient control (ANOVA $F_{1,4} = 146.36$, $p < 0.05$, Fig. 6.12); but increased six-fold from 12 h ($0.94 \text{ fg C cell}^{-1} \text{ d}^{-1}$) to 36 h ($6.30 \text{ fg C cell}^{-1} \text{ d}^{-1}$) and maintained an elevated rate until 84 h (Fig. 6.12). Cell-specific protein synthesis rates in the low pH treatment and ambient control followed a similar response, increasing steadily from time-zero (Fig. 6.12).

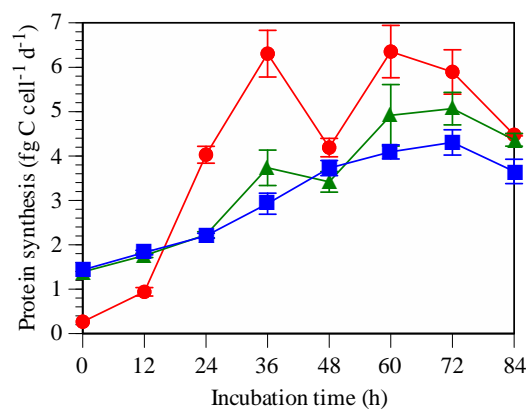


Fig. 6.12. Cell-specific protein synthesis throughout incubation 8 (mean \pm SE, $n=3$). Treatment legend – vent: red circles; low pH: blue squares; ambient control: green triangles

6.3.3.2 Incubation 9

There was no significant difference in time-zero DNA synthesis rates between each treatment in incubation 9 (Fig. 6.13 & Appendix E: 6.3). DNA synthesis increased in each treatment from time-zero to 36 - 48 h; with synthesis in the vent water increasing at a faster rate (Fig. 6.13). DNA synthesis rates declined in each treatment from 60 h, with synthesis highest in the vent water at 84 h ($192.99 \mu\text{g C l}^{-1} \text{ d}^{-1}$, Fig. 6.13). There was no significant difference in time-zero protein synthesis rates between each treatment (Fig. 6.13 & Appendix E: 6.3). Protein synthesis increased eight-fold in each treatment from time-zero to 24 h (ANOVA $F_{1,3}$, $p < 0.01$, Fig. 6.13), but protein synthesis in the vent water increased at a slightly faster rate and remained significantly higher from 24 h to 84 h (ANOVA $F_{1,3}$, $p < 0.05$, Fig. 6.13).

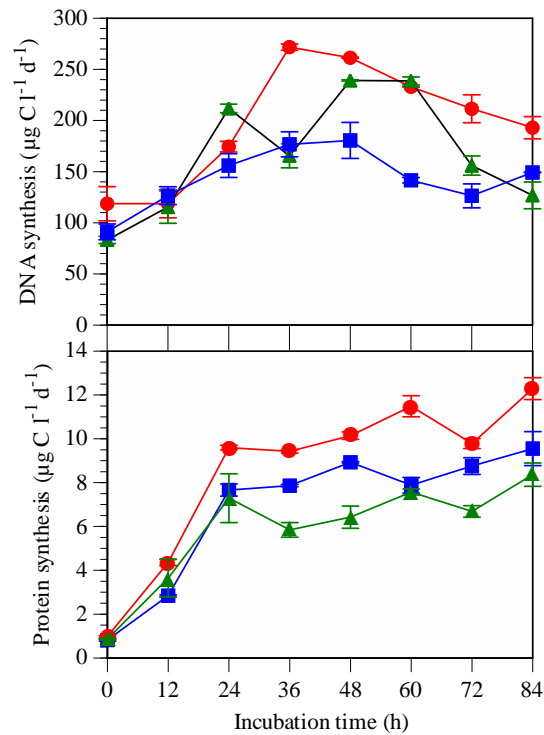


Fig. 6.13. BSP throughout incubation 9 (mean \pm SE, n=3). Treatment legend – vent: red circles; low pH: blue squares; ambient control: green triangles

Cell-specific protein synthesis rates increased rapidly across all treatments from time-zero to 24 h (Fig. 6.14). Overall, there was a consistent trend in cell-specific synthesis with no significant difference between treatments from 48 h to 84 h (Fig. 6.14).

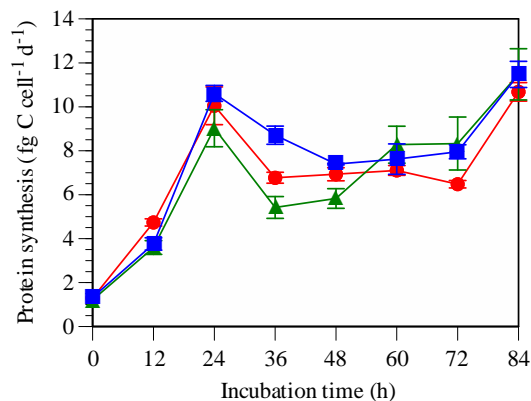


Fig. 6.14. Cell-specific protein synthesis throughout incubation 9 (mean \pm SE, n=3). Treatment legend – vent: red circles; low pH: blue squares; ambient control: green triangles

Summary of results

Overall, DNA and protein synthesis rates increased in the vent water relative to the ambient control in incubations 8 and 9 (Table 6.5). The low pH treatment also had a positive effect on protein synthesis relative to the ambient control, however this was only detected in incubation 9 (Table 6.5).

Table 6.5. Summary of DNA and protein synthesis rate changes in each treatment relative to the ambient control over 84 h. \uparrow : indicates an increase relative to the control; \downarrow : decrease; empty cell: no change; <: time-zero value was lower than the control; >: time-zero value was higher than the control

Parameter	Incubation 8		Incubation 9	
	Vent	Low pH	Vent	Low pH
BSP DNA synthesis	\uparrow		$>\uparrow$	
BSP protein synthesis	$<\uparrow$		\uparrow	\uparrow

6.3.4 Dissolved nutrient concentration

6.3.4.1 Incubation 8

Time-zero DRSi and ammonium concentrations were significantly higher in the vent water than the ambient control, while dissolved nitrate concentrations were significantly lower (Table 6.6). Dissolved nitrate concentrations were also significantly lower in the vent water at 84 h ($1.50 \mu\text{g l}^{-1}$) when compared to the low pH treatment ($8.75 \mu\text{g l}^{-1}$) and ambient control ($8.53 \mu\text{g l}^{-1}$, ANOVA $F_{1,3}$, $p < 0.05$, Table 6.6). DRP concentrations declined in each treatment from time-zero, resulting in similar concentrations at 84 h (Table 6.6). In contrast, DRSi concentrations remained relatively stable in each treatment from time-zero to 84 h (Table 6.6). Dissolved ammonium concentrations declined in each treatment from time-zero to 84 h, however a significantly higher concentration was measured in vent water when compared to the low pH treatment and ambient control at 84 h (Table 6.6).

Table 6.6. Average dissolved nutrient concentrations in each treatment at time-zero and 84 h in incubation 8 (\pm SE, n=3). T0: time-zero; Δ : change; *: indicates the parameter was significantly different from the ambient control ($p < 0.05$)

Incubation 8									
	Control			Vent			Low pH		
	T0	84 h	Δ from T0 to 84 h	T0	84 h	Δ from T0 to 84 h	T0	84 h	Δ from T0 to 84 h
Nitrate ($\mu\text{g l}^{-1}$)	9.25 (± 0.1)	2.55 (± 0.2)	- 6.70	1.50 (± 0.0) *	1.06 (± 0.0) *	- 0.44	8.75 (± 0.2)	1.90 (± 0.0)	- 6.85
DRP ($\mu\text{g l}^{-1}$)	7.93 (± 0.3)	5.75 (± 0.1)	- 2.18	7.45 (± 0.4)	5.40 (± 0.1)	- 2.05	7.85 (± 0.2)	5.43 (± 0.2)	- 2.42
DRSi ($\mu\text{g l}^{-1}$)	112 (± 2.4)	145 (± 0.8)	+ 33.0	145.50 (± 0.5) *	146.33 (± 0.3)	+ 0.83	130.00 (± 0.3)	143.00 (± 1.1)	+ 13.00
Ammonium ($\mu\text{g l}^{-1}$)	10.75 (± 0.6)	2.20 (± 0.5)	- 8.55	22.95 (± 0.4) *	5.40 (± 0.4) *	- 17.55	12.30 (± 0.3)	0.96 (± 0.2) *	- 11.34

6.3.4.2 Incubation 9

Time-zero DRSi and ammonium concentrations were significantly higher in the vent water when compared to the ambient control, while dissolved nitrate concentrations were significantly lower (Table 6.7), as was measured in incubation 8. Dissolved nitrate concentrations in the vent water remained constant from time-zero to 84 h (Table 6.7), while concentrations declined in the low pH treatment and ambient control (Table 6.7). DRP concentrations declined in each treatment from time-zero to 84 h, when vent water concentrations were significantly lower relative to the ambient control (Table 6.7). In contrast, DRSi concentrations were higher in the vent water when compared to the low pH treatment and ambient control from time-zero to 84 h, with only minor changes in concentration occurring throughout the incubation (Table 6.7). Dissolved ammonium concentrations declined in each treatment from time-zero to 84 h, reflecting statistically similar concentrations at 84 h (Table 6.7).

Table 6.7. Average dissolved nutrient concentrations in each treatment at time-zero and 84 h in incubation 9 (\pm SE, n=3). T0: time-zero; Δ : change; *: indicates the parameter was significantly different from the ambient control ($p < 0.05$)

Incubation 9									
	Control			Vent			Low pH		
	T0	84 h	Δ from T0 to 84 h	T0	84 h	Δ from T0 to 84 h	T0	84 h	Δ from T0 to 84 h
Nitrate ($\mu\text{g l}^{-1}$)	1.20 (± 0.2)	0.00	- 1.20	0.50 (± 0.0) *	0.50 (± 0.0)	0.00	1.05 (± 0.0)	0.50 (± 0.0)	- 0.55
DRP ($\mu\text{g l}^{-1}$)	3.95 (± 0.1)	3.63 (± 0.1)	- 0.32	4.60 (± 0.1)	3.23 (± 0.2) *	- 1.37	3.70 (± 0.0)	3.33 (± 0.2)	- 0.37
DRSi ($\mu\text{g l}^{-1}$)	7.81 (± 0.8)	83.00 (± 1.1)	+ 75.19	114.00 (± 0.0) *	113.00 (± 0.5) *	- 1.00	74.45 (± 2.0)	77.23 (± 0.1)	+ 2.78
Ammonium ($\mu\text{g l}^{-1}$)	8.40 (± 0.0)	1.93 (± 0.7)	- 6.47	11.45 (± 0.3) *	2.56 (± 0.0)	- 8.89	6.65 (± 0.2)	0.90 (± 0.2)	- 5.75

6.3.5 Dissolved organic carbon concentration

Time-zero dissolved organic carbon (DOC) concentrations were not significantly different between the vent water ($1.55 \mu\text{g ml}^{-1}$), low pH treatment ($1.39 \mu\text{g ml}^{-1}$) or ambient control ($0.85 \mu\text{g ml}^{-1}$), and did not change significantly throughout incubation 8. Similarly, time-zero DOC concentrations in incubation 9 were not significantly different between the vent water ($1.33 \mu\text{g ml}^{-1}$), low pH treatment ($1.18 \mu\text{g ml}^{-1}$) or ambient control ($1.16 \mu\text{g ml}^{-1}$), and did not change significantly throughout the incubation.

6.3.6 Total high molecular weight organic compound concentration

6.3.6.1 Incubation 8

Total high molecular weight (HMW) reducing-sugar concentrations were first detected at 36 h during incubation 8, with high variability recorded in the vent water at each sampling point (Fig. 6.15). Total HMW reducing-sugar concentrations were significantly lower in the low pH treatment when compared to the vent water and ambient control at 36 h (Fig. 6.15, p-values in Appendix E: 6.4), and also significantly lower in the low pH treatment than the ambient control at 72 h (Fig. 6.15 & Appendix E: 6.4). At 84 h, total HMW reducing-sugar concentrations were significantly higher in the vent water than the ambient control (Fig. 6.15 & Appendix E: 6.4). Total HMW protein concentrations in the vent water declined from time-zero to 84 h, but remained higher than in both the low pH treatment and ambient control (Fig. 6.15 & Appendix E: 6.4). Total HMW protein concentrations in the low pH treatment did not change relative to the ambient control throughout incubation 8 (Fig. 6.15).

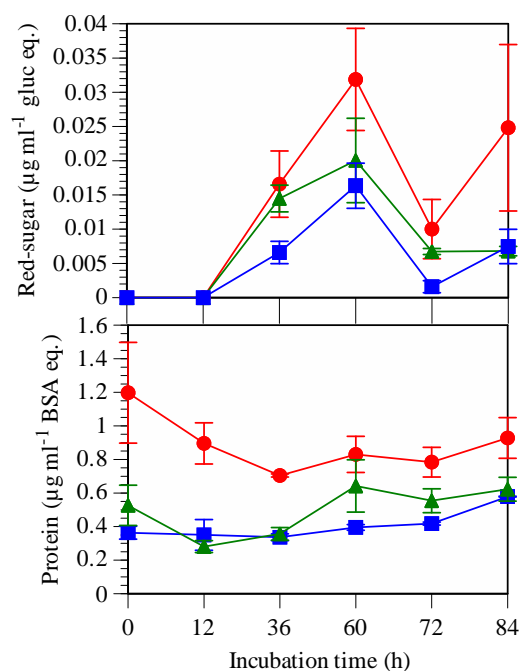


Fig. 6.15. Total HMW organic compound concentrations throughout incubation 8 (mean \pm SE, $n=3$). Treatment legend – vent: red circles; low pH: blue squares; ambient control: green triangles

6.3.6.2 Incubation 9

Total HMW reducing-sugar concentrations were higher in the vent water than the low pH treatment and ambient control, with each following a similar trend throughout incubation 9 (Fig. 6.16). Total HMW reducing-sugar concentrations in the vent water were significantly different from the ambient control throughout incubation 9, whereas concentrations in the low pH treatment only differed from the ambient control at 72 h (Fig. 6.16 & Appendix E: 6.4). Total HMW protein concentrations were higher in the vent water than in the low pH treatment and ambient control throughout incubation 9 (Fig. 6.16), while concentrations were significantly higher than the ambient control throughout, with respective concentrations ranging from 0.46 to 0.91 $\mu\text{g ml}^{-1}$ BSA eq. (Fig. 6.16 & Appendix E: 6.4). Total HMW protein concentrations in the low pH treatment and ambient control were similar and also increased throughout incubation 9 (Fig. 6.16).

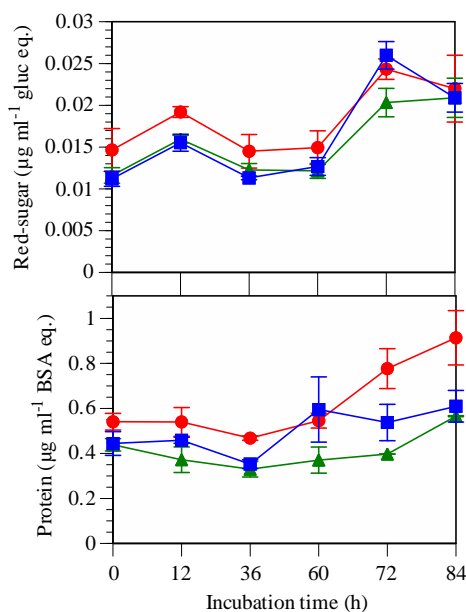


Fig. 6.16. Total HMW organic compound concentrations throughout incubation 9 (mean \pm SE, n=3). Treatment legend – vent: red circles; low pH: blue squares; ambient control: green triangles

Summary of results

Overall, total HMW reducing-sugar concentrations increased in the vent water relative to the ambient control in incubation 8, however the same trend was not measured in incubation 9 (Table 6.8). Total HMW protein concentrations declined in the vent water relative to the ambient control in incubation 8, but increased in incubation 9 (Table 6.8). Total HMW organic compound concentrations in the low pH treatment did not change relative to the ambient control in incubations 8 or 9 (Table 6.8).

Table 6.8. Summary of total HMW organic compound concentration changes in each treatment relative to the ambient control over 84 h. \uparrow : indicates an increase relative to the control; \downarrow : decrease; empty cell: no change; <: time-zero value was lower than the control; >: time-zero value was higher than the control

Parameter	Incubation 8		Incubation 9	
	Vent	Low pH	Vent	Low pH
Total HMW reducing-sugar	\uparrow			
Total HMW protein	$>\downarrow$		$>\uparrow$	

6.3.7 TEP & TC

6.3.7.1 Incubation 8

Transparent Exopolymer Polysaccharide (TEP) concentrations in the vent water were higher when compared to the low pH treatment and ambient control from time-zero to 84 h (Fig. 6.17), and significantly higher than the ambient control at 36 h ($155.21 \mu\text{g l}^{-1}$ xant eq.) and 84 h ($147.66 \mu\text{g l}^{-1}$ xant eq., ANOVA $F_{1,4}$, $p < 0.05$, Fig. 6.17). TEP concentrations in the low pH treatment and ambient control were similar throughout incubation 8, increasing only slightly from time-zero to 84 h (Fig. 6.17). Total Carbohydrate (TC) concentrations in the vent water declined from time-zero to 36 h, and then increased to 84 h ($110.48 \mu\text{g l}^{-1}$ gluc eq.). The TC concentrations in the vent water were significantly higher than in the low pH treatment ($64.15 \mu\text{g l}^{-1}$ gluc eq.) and ambient control at 84 h ($55.33 \mu\text{g l}^{-1}$ gluc eq., ANOVA $F_{1,4}$, $p < 0.05$, Fig. 6.17). TC concentrations declined in the low pH treatment from time-zero ($78 \mu\text{g l}^{-1}$ gluc eq.) to 84 h ($64.84 \mu\text{g l}^{-1}$ gluc eq.), while concentrations in the ambient control peaked at 36 h ($101.00 \mu\text{g l}^{-1}$ gluc eq.) and then also declined to 84 h (Fig. 6.17).

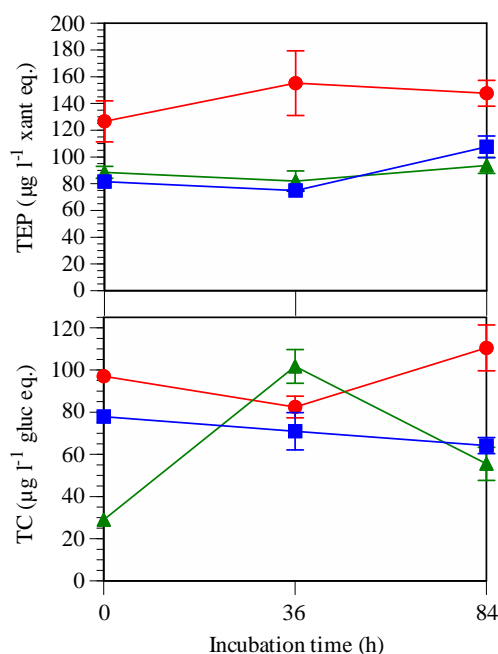


Fig. 6.17. TEP and TC concentrations throughout incubation 8 (mean \pm SE, $n=3$). Treatment legend – vent: red circles; low pH: blue squares; ambient control: green triangles

6.3.7.2 Incubation 9

The TEP concentration in the vent water declined from time-zero to 84 h, and was increasingly similar to the ambient control concentration (Fig. 6.18). TEP concentrations increased in the ambient control from time-zero to 36 h ($72.81 \mu\text{g l}^{-1} \text{ xant eq.}$) relative to the low pH treatment ($40.52 \mu\text{g l}^{-1} \text{ xant eq.}$), resulting in a significantly lower concentration in the low pH treatment (ANOVA $F_{1,4} = 8.93$, $p < 0.05$, Fig. 6.18). TEP concentrations in the vent water and low pH treatment were not significantly different from in the ambient control at 84 h (Fig. 6.18, p-values in Appendix E: 6.5). In contrast to incubation 8, TC concentrations declined in the vent water, low pH treatment and ambient control from time-zero to 84 h (Fig. 6.18). However, due to high sample variability, concentrations were not significantly different at 36 h or 84 h (Fig. 6.18).

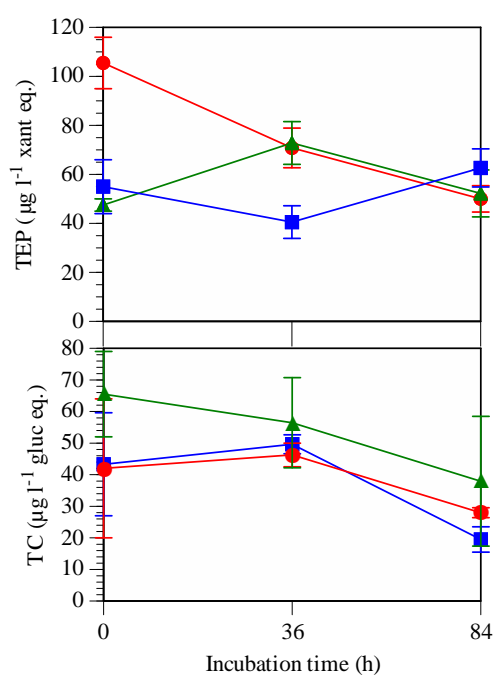


Fig. 6.18. TEP and TC concentrations throughout incubation 9 (mean \pm SE, $n=3$). Treatment legend – vent: red circles; low pH: blue squares; ambient control: green triangles

Summary of results

Overall, TEP concentrations varied in response to vent water and the low pH treatment when compared to the ambient control in incubations 8 and 9 (Table 6.9). TEP concentrations increased in both the vent water and low pH treatment relative to the ambient control during incubation 8, however vent water concentrations declined in incubation 9 (Table 6.9).

Table 6.9. Summary of TEP concentration changes in each treatment relative to the ambient control over 84 h. \uparrow : indicates an increase relative to the control; \downarrow : decrease; empty cell: no change; <: time-zero value was lower than the control; >: time-zero value was higher than the control

Parameter	Incubation 8		Incubation 9	
	Vent	Low pH	Vent	Low pH
TEP	> \uparrow	< \uparrow	> \downarrow	

6.3.8 Multivariate data analysis

The following section will investigate similarity and dissimilarity of multivariate data from each incubated treatment simultaneously. Multivariate data will be presented visually allowing identification of treatment variation at selected sampling times. Statistical difference is based on a SIMPROF analysis at 5% significance. Both incubation MDS plots have a stress coefficient ≤ 0.1 which indicates that the multivariate matrices are well represented by the 2D ordination plot (Section 2.11).

6.3.8.1 Incubation 8

Multivariate analysis of incubation 8 data showed all treatments changed from time-zero to 84 h (Fig. 6.19). Vent water was significantly different from the ambient control and low pH treatment at every sampling point, except 12 h (broken line cluster, Fig. 6.19); while there was no significant difference between the ambient control and low pH treatment at any sampling point. There was no significant difference between vent water from 36 h to 72 h (solid line cluster, Fig. 6.19).

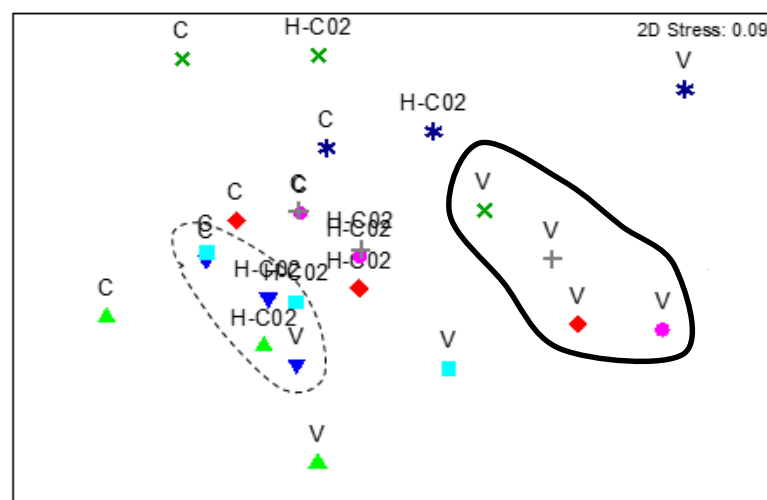


Fig. 6.19. MDS plot of eight sampled biotic and abiotic parameters collected during incubation 8. Abbreviations – V: vent; H-CO₂: low pH; C: ambient control. Highlighted clusters are based on SIMPROF analysis at 5% significance. Incubation treatments are labelled per sampling point - 0 h: ▲; 12 h: ▼; 24 h: ■; 36 h: ◆; 48 h: ●; 60 h: +; 72 h: ×; 84 h: *

6.3.8.2 Incubation 9

Multivariate analysis of incubation 9 data showed that vent water was significantly different from the ambient control and low pH treatment at time-zero and every sampling point after 24 h (Fig. 6.20). There was, however, no significant difference between the ambient control and low pH treatment at time-zero (broken line cluster, Fig. 6.20) or at any other sampling point thereafter, except 36 h. The vent water did not change significantly from 24 h to 84 h (solid line cluster, Fig. 6.20), excepting the 36 h sample point which did not cluster with the other vent water samples and was significantly different (Fig. 6.20).

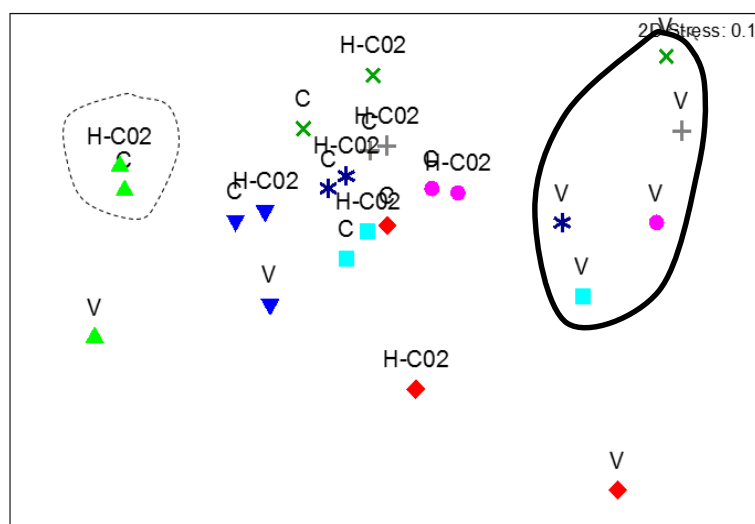


Fig. 6.20. MDS plot of eight sampled biotic and abiotic parameters collected during incubation 9. Highlighted clusters are based on SIMPROF analysis at 5% significance. Abbreviations – V: vent; H-CO₂: low pH; C: ambient control. Incubation treatments are labelled per sampling point - 0 h: ▲; 12 h: ▼; 24 h: ■; 36 h: ◆; 48 h: ●; 60 h: +; 72 h: ×; 84 h: *

6.4 Discussion

The following section will first discuss the response of the primary sampled parameters (Table 6.1) to artificially acidified coastal seawater, and compare the trends to those determined from open ocean seawater (Chapters 4 & 5). The discussion will then focus on the response of the primary sampled parameters from the naturally low pH vent compared to ambient coastal seawater, and whether pH was the key driver of the measured variation. The interpretation of the results will also consider the possibility that the low pH coastal vent water was only recently acidified as currents passed through the active vent region.

6.4.1 Coastal water response to low pH

The coastal ocean is characterised by different abiotic and biotic factors when compared to the open ocean environment (Kaiser et al. 2011). For example, coastal oceans experience large fluctuations in pH on seasonal scales (Hofmann et al. 2011) and higher inorganic nutrient and organic carbon concentrations due to localised river input and land runoff (Morris & Foster 1971, Gattuso et al. 1998, Hopkinson et al. 1998, Retamal et al. 2007) contributing to high turbidity and sediment resuspension (Gray et al. 2002, Thrush et al. 2004). Coastal waters are also characterised by different primary producers when compared to the open ocean, such as macrophytes (seagrasses and macroalgae) and mangroves (Gattuso et al. 1998 and references therein). These factors contribute to coastal environments containing a distinct bacterial community, and organic matter composition and concentration when compared to the open ocean (Du et al. 2013), and therefore the response of coastal bacterial extracellular enzymes to low pH conditions may differ from those determined in the open ocean (Chapters 4 & 5). These incubation experiments provide the opportunity to examine this possibility. Measured trends throughout incubations 8 and 9 show that extracellular enzyme activities were the only sampled parameter to consistently respond to the low pH treatment (Table 6.10).

Table 6.10. Summary of each parameter response from incubations 8 and 9 relative to the ambient control over 84 h. \uparrow : indicates an increase relative to the control; \downarrow : decrease; empty cell: no change; $<$: time-zero value was lower than the control; $>$: time-zero value was higher than the control

Parameter	Incubation 8		Incubation 9	
	Vent	Low pH	Vent	Low pH
β -glucosidase	\uparrow	\uparrow	\uparrow	
α -glucosidase	\uparrow	$>\uparrow$	\uparrow	\uparrow
Arg-aminopeptidase			$>\downarrow$	$<\uparrow$
Leu-aminopeptidase	$>\downarrow$	\uparrow	$>\uparrow$	$>\uparrow$
Bacterial numbers			\uparrow	
<i>Synechococcus</i> spp. numbers				
<i>Prochlorococcus</i> spp. numbers			$<\uparrow$	
Total eukaryotic phytoplankton numbers			$>\uparrow$	
BSP DNA synthesis	\uparrow		$>\uparrow$	
BSP protein synthesis	$<\uparrow$		\uparrow	\uparrow
Total HMW reducing-sugar	\uparrow			
Total HMW protein	$>\downarrow$		$>\uparrow$	
TEP	$>\uparrow$	$<\uparrow$	$>\downarrow$	
TC	$>\uparrow$	$>\downarrow$		

Elevated time-zero β - and α -glucosidase activities during incubation 8 support results from the short-term acidification trial (Section 3.2) as well as those reported by Piontek et al. (2013), suggesting a direct pH affect. A direct effect could result from a shift toward the enzymes' optimal pH, a change in the charge of the enzyme active site or a change in the tertiary or quaternary protein structure (Section 1.7). A similar direct pH effect on β - and α -glucosidase was not measured during incubation 9, which may reflect the response of a different group of

glucosidases, or alternatively, may show variation in the response of the same group of enzymes within the coastal environment.

During incubations 8 and 9, coastal β - and α -glucosidase activity followed very similar trends in each treatment, which contrasts to the open ocean. Coastal β - and α -glucosidase activity responded positively to low pH conditions (Table 6.10), as reported by several researchers (Grossart et al. 2006, Piontek et al. 2010, 2013, Maas et al. 2013). The β -glucosidase Δ hydrolysis potential integrated to 72 h was 12.54 nmol^{-1} in incubation 8, and 2.53 nmol^{-1} in incubation 9. These positive Δ hydrolysis values show that β -glucosidase activity was enhanced in the low pH treatment relative to the ambient control. A similar positive β -glucosidase response to low pH was recorded in some of the near-surface open ocean phytoplankton communities (Section 4.3), but not in the subsurface open ocean (Section 5.3). Moreover, the positive α -glucosidase response to low pH in coastal waters was not measured in either the near-surface or subsurface open ocean. This confirms that the response of glucosidase to low pH conditions varies between different seawater environments and may reflect a different coastal β - and α -glucosidase synthesis relative to the open ocean, potentially a result of different bacterial groups. Bacterial diversity was assessed by terminal-restriction fragment length polymorphism (T-RFLP) analysis of the 16S rRNA gene (method as per Maas et al. 2013). The resulting terminal restriction fragments (T-RFs) correspond approximately to genetic variants that were metabolically active and can be used as an index for bacterial community diversity (Liu et al. 1997, Osborn et al. 2000). The coastal time-zero control water from incubations 8 and 9 had the highest average number of T-RFs (282) when compared to the near-surface open ocean control water (253: average across incubations 1 to 4) and subsurface open ocean control water (238: average across incubations 6 and 7). Arrieta & Herndl (2002) observed a positive correlation between β -glucosidase diversity and bacterial species richness, detecting up to eight different types of β -glucosidases at the peak of a coastal *Phaeocystis* phytoplankton bloom. High coastal bacterial diversity could have resulted in an increase in the number of glucosidase types, assuming that different glucosidases have different kinetic parameters and pH optima (Tipton & Dixon 1979). This could explain the variation in response to low pH between the seawater environments. Existing research conducted in soils using the same enzyme activity methodology (Section 2.3) suggests that the pH optima of β - and α -glucosidase can differ among different soil types (Turner 2010). The different glucosidase response between ocean environments may also reflect variation in organic matter

substrate composition; for example, coastal-derived organic matter can contain higher concentrations of lipids, amino acids and humic substances (Hedges et al. 1997 and references therein) which could alter the type of glucosidase synthesised by the bacteria, or change the bacterial community and consequently the glucosidase produced. Although time-zero coastal-derived total HMW reducing-sugar concentrations were below methodology detection, it is possible that a labile fraction of the total substrate was not detected, but still affected glucosidase activity. The coastal waters may have contained a higher concentration of terminal linked 1-4 alpha-glucose residues when compared to the open ocean, with the low pH conditions stimulating α -glucosidase activity. A significant increase in coastal β - and α -glucosidase activity could increase bacterial respiration and inorganic carbon production, potentially resulting in a positive CO₂ feedback in coastal regions. Depending on rainfall and tidal movements, coastal environments also export significant quantities of organic matter to open ocean environments (Gattuso et al. 1998 and references therein). Consequently, an increase in coastal glucosidase activity in future low pH conditions could affect the concentration of HMW carbohydrate substrate transported to open ocean environments (Bianchi 2011).

Time-zero Leu-aminopeptidase activity was higher in the low pH treatment than the ambient control in incubation 9, while time-zero cell-specific Leu-aminopeptidase activity showed the same response in both incubations, providing evidence for a direct pH effect as discussed in Section 1.7. In contrast to this, and also findings reported by Piontek et al. (2013), time-zero Leu-aminopeptidase activity in incubation 8 did not display a direct pH effect, and neither did the short-term acidification trial (Section 3.2.4). This difference in response may reflect a high diversity in aminopeptidase (Matsui et al. 2006) and the response of a different enzyme to low pH conditions. The Leu-aminopeptidase activity showed a significant positive indirect response to low pH coastal conditions from 36 h onward in both incubations (Table 6.10). This is supported by the positive Leu-aminopeptidase Δ hydrolysis values integrated to 72 h for incubation 8 (99.09 nmol l⁻¹) and incubation 9 (122.34 nmol l⁻¹). Both values suggest an enhanced Leu-aminopeptidase activity over 72 h in the low pH treatment relative to the ambient control. The enhanced protein substrate turnover is likely to result from an increased number of enzymes synthesised under low pH, possibly in response to a change in cellular membrane fluidity (Jacobs 1940, Ray et al. 1971), or an increase in the number of active bacteria in the coastal seawater (Hoppe 1978).

Furthermore, Leu-aminopeptidase activity was much higher than glucosidase activity in the low pH treatment during incubation 8, with a Leu-aminopeptidase to β -glucosidase ratio of 21.73, indicating a low nutritional carbon pool (Christian & Karl 1992). This activity ratio indicates a preferential degradation of protein based substrate relative to carbohydrate, however the ratio is lower than expected for typical coastal water, reflecting similar values to the subsurface open ocean (Chapter 5) but lower values than the near-surface open ocean (Chapter 4). Comparison of substrate remineralisation ratios between ocean environments also suggests that coastal carbohydrate substrate has a higher nutritional quality than near surface open ocean substrate, potentially resulting from high terrestrial input of fresh labile carbohydrates (Gattuso et al. 1998 and references therein).

Similar to glucosidase, the increase in Leu-aminopeptidase activity after 36 h was not directly correlated with a significant increase or decrease in total HMW protein substrate concentration in either incubation. This result may indicate that the measured total HMW protein substrate, which includes potential bacterial and phytoplankton substrate, was not the only substrate remineralised by Leu-aminopeptidase in coastal water. Alternately, the enzyme may have remineralised the labile fraction of the substrate which only made up a small proportion of the total HMW substrate. In contrast to Leu-aminopeptidase activity in incubation 9, time-zero Arg-aminopeptidase activity was lower in the low pH treatment than the ambient control, while no activity was detected in the low pH treatment at time-zero in incubation 8. The variation in the aminopeptidase responses to low pH may reflect a high enzyme diversity and therefore enzyme specific responses. A positive Leu-aminopeptidase response to low pH was also detected in the near-surface open ocean (Section 4.3.1), as well as the subsurface open ocean at selected sampling points only (Section 5.3.1). The uniform Leu-aminopeptidase response to low pH in the coastal and open ocean environments contrasts with that of glucosidase. While several different Leu-aminopeptidases may be active in the different ocean environments (Matsui et al. 2006), they may all have a similar indirect response to low pH conditions. The different responses of Leu- and Arg-aminopeptidase, however suggest that Leu-aminopeptidase may be more susceptible to changes in ocean pH and substrate availability.

As Leu-aminopeptidase activity was not significantly different from the ambient control at the final sampling point (84 h) in either coastal incubation, the significant increase in Leu-aminopeptidase activity in response to low pH may be temporary. A similar temporary

Leu-aminopeptidase response was also apparent in two of the four near-surface phytoplankton community incubations (Section 4.3.1) and one of the subsurface open-ocean seawater incubations (Section 5.3.1). DNA synthesis rates and total HMW protein substrate concentrations in the low pH coastal water and near-surface open ocean seawater were all similar to their respective ambient controls at the final sampling point, potentially explaining the temporary response. In contrast, cell-specific Leu-aminopeptidase in incubation 9 was significantly higher in the low pH treatment than the ambient control at the final sampling point, while a similar trend was obvious in both acidified subsurface incubations (Section 5.3.1). Grossart et al. (2007) reported variation in cell-specific protease activities between different bacterial strains, because time-zero bacterial diversity was significantly different between the coastal and open ocean environments (Maas E, unpublished data). This could explain the variation in cell-specific activity measured. It is therefore clear that, although a uniform Leu-aminopeptidase response to low pH was detected in the coastal and open ocean environments, variability may exist in the longevity of the response.

A significant temporary increase in coastal Leu-aminopeptidase and glucosidase activity could temporarily increase the concentration of LMW substrate, thereby increasing BSP and bacterial cell numbers. This is supported by Rosso & Azam (1987) who reported a strong relationship between extracellular enzyme activity, BSP and bacterial cell numbers in coastal waters. During this thesis research, a similar positive correlation was measured between BSP and bacterial cell numbers in both incubations, however unlike enzyme activity, they were not significantly affected by low pH (Table 6.10). This suggests that in the low pH treatment, bacteria did not significantly increase DNA or protein synthesis in response to elevated glucosidase or protease activity. One possible explanation is that the increase in enzyme activity was in direct response to low pH, resulting in the production of excess LMW labile substrate over that required by the bacteria, and hence BSP did not significantly increase. This uncoupled hydrolysis has also been reported under ambient conditions by other researchers (Cho & Azam 1988, Smith et al. 1992, Grossart & Ploug 2001). As in the coastal ocean, DNA and protein synthesis rates and bacterial cell numbers were not significantly affected by low pH in the near-surface open ocean (Section 5.3.2), whereas a negative effect was measured for DNA and protein synthesis in the subsurface open ocean (Section 5.4.2). Although total BSP was not significantly affected by low pH in the coastal ocean, average time-zero DNA synthesis was approximately 15-fold higher in the ambient control coastal

water when compared to near-surface open ocean synthesis, while protein synthesis in the coastal water was similar to the near-surface open ocean (Chapter 4). Moreover, average time-zero DNA synthesis was approximately 100-fold higher in the ambient control coastal water than in the subsurface open ocean, while protein synthesis was ten-fold higher (Chapter 5). Not unexpectedly, these findings show that the coastal environment had a higher overall DNA and protein synthesis than both open ocean environments, especially the subsurface ocean (Ducklow & Carlson 1992 and references therein). Average time-zero cell-specific protein synthesis was three-fold higher in the ambient control coastal water when compared to the subsurface ocean, and 4.5 times higher in the near-surface ocean. This shows a similar declining cell-specific protein synthesis with depth, however the near-surface open ocean had a slightly higher cell specific protein synthesis than the coastal water.

Although a significant increase in enzyme activity under low pH was not correlated with a significant increase in BSP during these incubations, the overall higher BSP in coastal water is likely in response to increased enzyme activity producing elevated concentrations of LMW substrate for bacterial assimilation (Rosso & Azam 1987, Riemann et al. 2000). This hypothesis is supported by time-zero ambient control coastal glucosidase values which were at least ten-fold higher than the near-surface open ocean values, while time-zero protease activities were also approximately ten-fold higher than the near-surface and subsurface open ocean ambient activities. The large discrepancy in DNA and protein synthesis between coastal and open ocean environments suggests that coastal bacteria were synthesising significantly more DNA relative to protein than open ocean bacteria. This trend could be explained by a faster bacterial growth rate in coastal environments when compared to the open ocean (del Giorgio et al. 2011). This is further supported by the fact that time-zero bacterial cell numbers were higher in coastal water than the near-surface open ocean (Table 4.2) and almost a log higher than those determined from the subsurface (Table 5.2). The measured spatial variation in enzyme activity, BSP and bacterial numbers under ambient condition is supported by additional studies (Davey et al. 2001, Baltar et al. 2009, 2010, del Giorgio et al. 2011).

Overall, this study suggests that the responses of extracellular enzymes in a future low pH coastal environment will have some similarities to those expected in the open ocean, although an increase in α -glucosidase activity may only occur in the coastal ocean. These results suggest

that LMW labile substrate concentrations may increase in the coastal environment, however may not be directly assimilated by bacteria.

6.4.2 Vent seawater response

The aim of the vent study was to investigate the response of a bacterial community exposed to low pH for an extended period of time and compare this with ambient coastal seawater recently exposed to low pH. However, sampling showed that the low pH effect of the vent was extremely localised, with low pH (< 7.9) only obtained when water was sampled immediately over the centre of the vent (pers. comm. Dr Cliff Law, NIWA), suggesting that the water had a low residence time in the vicinity of the vent. Consequently, the vent water sampled was only exposed to high CO_2 (and other vent biogeochemistry) for a short period of time (hours) before sampling and therefore cannot be used to examine responses in a long-term low pH adapted community. This being the case, the time-zero parameter values should be similar between the low pH treatment and the vent water if pH is the sole driver of change. This study is different from others vent studies because it focuses on a localised low pH area rather than a larger affected area.

Time-zero vent water β - and α -glucosidase activity was similar to the ambient control in both incubations (Table 6.2). However, time-zero Leu-aminopeptidase activity was higher in the vent water than the ambient control and low pH treatment in both incubations, as was Arg-aminopeptidase activity in incubation 9 (Table 6.2). Time-zero cell-specific Leu-aminopeptidase activity was also higher in the vent water than the ambient control in both incubations. This shows that the elevated vent activity was not due to elevated bacterial cell numbers and may suggest a direct vent affect. Vent waters surrounding Whale Island have a different biogeochemical composition when compared to the surrounding non-vent water, resulting from gas and liquid discharged from the volcanic vents (Tarasov 2006). For example, dissolved iron concentrations at the Whale Island vent site were four-times higher (2150 nM) than control coastal seawater (530 nM, samples collected and analysed by Dr Sylvia Sander - University of Otago pers. comm.). A diversity of trace metals is also known to be discharged from vent plumes (Goff et al. 1998) and could act as enzyme cofactors, assisting in enzyme activity (King 1986, Morel & Price 2003). Because Leu- and Arg-aminopeptidase are

metalloenzymes (Burley et al. 1990, Bogra et al. 2009), enzymes in which metal ions may assist in activity (McCall et al. 2000), a higher concentration of enzyme cofactors in the vent water may explain the elevated time-zero protease activity. Many of the glucosidase group are not dependent on metal ions for catalysis (Naumoff 2011) which could explain the different time-zero activities when compared to protease.

An alternative explanation for the elevated time-zero protease activity could be the physical effect of vent bubbling. The vent plume may transport organic matter from the sediment into the water column and concentrate it through particle collisions and coagulation (Kepkay & Johnson 1989, Woolf 2001), thereby increasing the concentration of hydrolysable substrate. The physical effect of bubbling could explain the high time-zero total HMW protein and TEP concentrations measured in the vent water in incubations 8 and 9, and also the increase in enzyme activity following short-term CO₂ bubbling in the acidification experiment (Section 3.3). Although time-zero total HMW reducing-sugar concentrations were higher in the vent water than the ambient control in incubation 9 (Table 6.2), the vent water bacterial community in each incubation showed a preferential degradation of peptide based substrate over glucose relative to the ambient control (incubation 8 time-zero vent water Leu-aminopeptidase to β -glucosidase ratio was 98.40 and the ambient control ratio was 80.58, incubation 9 time-zero vent water Leu-aminopeptidase to β -glucosidase ratio was 106.01 and the ambient control ratio was 57.45). The vent plume may also transport bacteria from the sediment and concentrate free-living and particle attached bacteria within the water column, potentially explaining the elevated time-zero vent water bacterial cell numbers in incubation 8 (Table 6.2). Importantly, this same trend was not detected during incubation 9 and could indicate vent variability. Vent activity and bubble emissions were highly localised and spatially variable (pers. comm. Dr Cliff Law, NIWA), potentially creating large variability within the vent plume water biogeochemistry. Time-zero phytoplankton cell numbers were typically higher in the vent water than in the ambient control in both incubations 8 and 9 (Table 6.2). Although time-zero vent water dissolved nitrate concentrations were lower than in the ambient control (Table 6.2), providing evidence for high nutrient drawdown and a potential explanation for the elevated phytoplankton cell numbers, this is unlikely to be the driving factor behind the high time-zero cell numbers in the vent water due to the low photosynthetic active radiation expected at each sampling depth, as well as the short residence time in the vent environment. One possible explanation for this trend is that coastal planktonic cells were transported from high light

seawater surrounding the vent and concentrated in the turbid vent bubble plume as described for particulate organic matter (Bayona et al. 2002). This could explain the high time-zero planktonic cell numbers and also the overall declining cell numbers in each incubation.

Vent water β - and α -glucosidase activity increased rapidly within the first 24 h and remained significantly higher relative to the low pH treatment and ambient control throughout incubations 8 and 9 (Table. 6.10). This significant vent response is supported by the MDS plots which show clear divergence away from the ambient control and Low pH treatment (Section 6.3.8). Vent water β -glucosidase Δ hydrolysis integrated to 72 h was higher than the low pH treatment in incubation 8 (35.95 nmol l⁻¹ and 12.54 nmol l⁻¹ respectively), and incubation 9 (14.93 nmol l⁻¹ and 2.53 nmol l⁻¹ respectively). Vent water cell-specific β -glucosidase activity was also elevated indicating that the activity response was not in response to an increase in bacterial numbers, but instead may be explained by the higher total HMW reducing-sugar concentration in incubation 8, potentially providing bacteria with more labile HMW substrate for hydrolysis. This qualitative interpretation is based on an increase in HMW substrate concentration independent of an increase in bacterial and total eukaryotic phytoplankton cell numbers (Table. 6.10). Reports also suggest that bacteria attached to a particulate substrate have a higher relative hydrolysis rate when compared to free-living bacteria (Decho 1990, Verdugo et al. 2004, Grossart et al. 2007, Engel et al. 2014). The increased concentration of TEP detected in vent water during incubation 8 may have provided bacteria with more physical attachment sites and, because TEP primarily consists of carbohydrate components (Passow 2002), may also explain the increased total glucosidase activity. Because attached bacteria are typically found in high density colonies (Passow 2002 and references therein), this hypothesis could explain the significantly higher bacterial cell abundance and BSP in the vent water in incubation 8, and the late increase in bacterial numbers during incubation 9. Furthermore, TEP is also reported to induce aggregate formation due to its 'sticky' nature (Mari 2008, Engel et al. 2014) and may have contributed to the elevated vent water HMW organic compound concentrations.

The Leu-aminopeptidase activity was higher in the vent water than in the low pH treatment and ambient control throughout both incubations, potentially reflecting the higher total HMW protein concentrations, or a higher concentration of trace metal enzyme cofactors. Importantly, Leu-aminopeptidase activity in the vent water was not significantly different from the low pH

treatment or ambient control at 84 h, as measured in the coastal low pH treatment. So although the vent water did have a significant short-term effect on Leu-aminopeptidase activity, it may not have a long-term (> 84 h) effect. As vent water glucosidase and Leu-aminopeptidase activity followed a similar trend to the low pH treatment, but a different trend to the ambient control, this suggests that pH was a factor in the increased enzyme activity. However, because activity in the vent water was significantly higher than in the low pH treatment, pH was not the only factor affecting enzyme activity in vent water.

Molecular fingerprinting of the microbial communities using rRNA provides evidence that an unknown factor in vent water has an effect on more than just enzyme activities. For example, the time-zero bacterial community diversity was similar between the vent water (296 T-RFs) and low pH treatment (298 T-RFs) relative to the ambient control in incubation 8 (254 T-RFs), however by 84 h, T-RFs in the low pH treatment community had decreased (238 T-RFs) to a similar number to the ambient control community (237 T-RFs), while the vent water community T-RFs did not decrease as significantly (254 T-RFs), so maintaining a more diverse community relative to the control (samples analysed by Dr Els Maas and Debbie Hulston, NIWA). The change in bacterial diversity between treatments may have resulted from exposure to different biogeochemical environments. For example, dissolved methane concentrations at the Whale Island vent site from 50 m depth (3500 nM) were more than 150 times higher than the surrounding coastal surface seawater concentrations (3 to 20 nM; samples analysed by Andrew Marriner, NIWA). A high concentration of methane in vent water may have shifted the bacterial community composition towards methanotrophs, which oxidise methane as their primary carbon and energy source (Hanson & Hanson 1996 and references therein). A different biogeochemical environment could also explain the high time-zero vent water bacterial and plankton cell numbers in incubation 8, as well as the high DRSi and ammonium concentrations measured in both incubations (Table 6.2).

Based on the significant increase in total BSP rates (DNA & protein synthesis) in both incubations, a significant increase in vent water glucosidase and protease activity may have led to a significant increase in the assimilation of LMW substrate. However, the increase in total BSP was not correlated to the increase in bacterial cell numbers in incubation 8. This may reflect a temporal lag between bacterial substrate assimilation and cellular growth (Rolfe et al. 2012) and would explain the delayed increase in bacterial cell numbers recorded in

incubation 9. As time-zero vent water BSP values and bacterial cell numbers were not significantly higher than in the ambient control and low pH treatment, the measured BSP response in vent water resulted from an inferred increase in LMW substrate availability and not a direct vent water response.

This study has demonstrated clear differences in the response of extracellular enzymes between naturally low pH vent water and ambient coastal seawater. These results suggest pH has a significant effect on extracellular enzyme activity but also that other factors in vent water such as bubble-induced changes in organic matter form and availability, and elevated concentrations of dissolved nutrient and trace metal ions may influence bacterial processes. This suggests that naturally low pH environments may not be ideal analogies for a future ocean, although this needs to be examined in similar studies by characterising the vent liquid and gas discharge. Not only is an understanding of the individual vent important, but knowledge of water movements and residence time in the region of the vent is required to determine whether water at the site represents a long-term low pH environment. Active vent sites can provide unique insight into bacterial community processes under pH levels similar to those predicted in a future low pH environment, and represent a powerful natural observatory if well-characterised.

6.5 Summary

The responses of glucosidase and Leu-aminopeptidase to low pH conditions may differ between coastal and open ocean environments. It was determined that extracellular enzyme activities in a naturally low pH vent environment are significantly different from those of an ambient upstream coastal control site. By comparing responses from the vent water and low pH treatment, it was hypothesised that the significantly higher vent water glucosidase and Leu-aminopeptidase activities may reflect a higher organic matter concentration and the production of more enzymes, potentially in response to particle coagulation, in addition to higher concentrations of dissolved nutrients and trace metal ions.

Chapter 7 : Concluding discussion

The following chapter will summarise the findings of the previous chapters and discuss the potential implications for the flux of organic matter in a coastal and open ocean context. The effects of low pH in a future ocean will be discussed first, followed by the effects of elevated temperature and then the combined effects of low pH and elevated temperature. Finally, this chapter will close by providing directions for possible future research.

7.1 Influence of low pH

The decline in ocean pH predicted by the end of the century will have a significant effect on the structure and functioning of coastal and open ocean ecosystems (Doney et al. 2012 and references therein). One example of this is the response of phytoplankton and bacteria to low pH and the implications for the cycling of carbon throughout the water column (Raven et al. 2005, Doney et al. 2012, Passow & Carlson 2012). Existing research has shown that low pH conditions may affect phytoplankton community composition (Engel et al. 2008, Finkel et al. 2010, Endo et al. 2013), with a possible increase in smaller sized species and a decline in marine calcifiers (Riebesell 2004, Delille et al. 2005, Egge et al. 2009). A change to smaller sized phytoplankton could reduce surface ocean dissolved organic matter production, as well as active and passive carbon export (Finkel et al. 2010, Passow & Carlson 2012, Endo et al. 2013). Although the response of the phytoplankton community to low pH was not the main focus of this research, the incubation results showed that phytoplankton cell numbers, including *Synechococcus* spp. and *Prochlorococcus* spp., did not change significantly under low pH conditions in near-surface open ocean or coastal seawater, contrasting with other researchers' results (Tortell et al. 2008, Lomas et al. 2012, Endo et al. 2013). Research to date has also shown that future low pH may increase phytoplankton-derived dissolved organic matter production (Wolf-Gladrow et al. 1999, Riebesell 2004, Egge et al. 2009, Engel et al. 2014), promoting particle coagulation and high molecular weight substrate formation (Chin et al. 1998, Engel et al. 2014).

Temporal variation in the response of extracellular enzyme activities to low pH conditions was apparent in incubations from different environments. For example, low pH did not have a direct effect on protease activity in the short-term acidification trial (Section 3.2), or in open ocean seawater (Chapters 4 & 5). In contrast, a direct effect was evident in the coastal seawater incubations (Section 6.3.1), similar to Piontek et al. (2013) who reported a positive direct pH effect on Leu-aminopeptidase activity in Arctic fjord coastal seawater. The absence of a direct protease effect in specific ocean environments could indicate protease diversity and consequently different pH optima. A change in H^+ concentration may have affected the protein tertiary and quaternary structures differently, as well as altered different key residues in the enzymes' active sites. Low pH also had a positive indirect effect on protease activity that was independent of the dominant phytoplankton community in the open ocean (Table 4.3 & 4.4), and also a positive effect in coastal waters (Table 6.10), consistent with observations reported from an Arctic fjord (Piontek et al. 2013), Norwegian fjord (Grossart et al. 2006) and the Bay of Biscay (Piontek et al. 2010). The Leu-aminopeptidase Δ hydrolysis potential was highest in the low pH treatment in all surface open ocean incubations (Table 4.3), while a positive Leu-aminopeptidase Δ hydrolysis potential was also measured in low pH conditions in both coastal water incubations. Despite not observing a direct protease response in open ocean seawater, the consistent indirect protease response in coastal and open ocean environments adds to the body of knowledge that protease, potentially synthesised by different bacterial communities, is sensitive to low pH.

A significant increase in protease activity in response to future low pH conditions could strengthen the microbial loop, increasing the availability of low molecular weight labile organic matter for bacterial assimilation and secondary production in the surface ocean (Grossart et al. 2006, Piontek et al. 2010, Doney et al. 2012, Passow & Carlson 2012). However, further results contradict this hypothesis, in that low pH did not have a significant effect on bacterial secondary production rates or bacterial cell numbers in coastal or near-surface open ocean seawater. This result extends our current knowledge that low pH has no definitive effect on bacterial secondary production (Arnosti et al. 2011, Teira et al. 2012) or bacterial cell numbers (Yoshimura et al. 2009, Arnosti 2011, Krause et al. 2012, Teira et al. 2012, Newbold et al. 2012, Roy et al. 2013). Therefore an increase in low molecular weight substrate arising from increased hydrolytic activity under low pH may not necessarily result in a subsequent increase in bacterial substrate assimilation and productivity in the surface ocean. This response may

instead indicate a change in the efficiency of active substrate transport and passive enzyme transport pathways (Jacobs 1940), thereby reducing the efficiency with which substrate actively enters the cell, but not affecting passive enzyme transport through porin channels. Alternatively, loss processes such as grazing and viral lysis may have inhibited the detection of a significant bacterial secondary production response. In contrast to coastal and near-surface open ocean seawater, subsurface results indicate that protein synthesis rates may decline in low pH conditions, with a concurrent decline in bacterial numbers. The major difference between these two ocean environments is the availability of labile organic substrate. Average subsurface cell-specific Leu-aminopeptidase activity was lower than two near-surface open ocean incubations, and half the cell-specific activity detected in the coastal ocean. This contrasting response to low pH in subsurface water may signify a change in bacterial cellular transport mechanisms, as well as a reduction in the availability of labile organic substrate with depth.

In contrast to Leu-aminopeptidase activity, low pH had a direct positive effect on β -glucosidase activity in the short-term acidification trial (Section 3.2), similar to that reported by Piontek et al. (2013) and consistent with the positive indirect response measured in the coastal seawater incubations (Table 6.10). A positive indirect β -glucosidase response was also detected in some of the surface open ocean phytoplankton communities (Table 4.9) with Δ hydrolysis potential ranging from 0.04 to 0.99 nmol l⁻¹, but was not detected in the subsurface open ocean (Table 5.8). Moreover, a direct positive α -glucosidase response to low pH was only measured in coastal seawater, with Δ hydrolysis potential ranging from 0.25 to 0.54 nmol l⁻¹. The positive surface ocean glucosidase response is thought to reflect greater availability of terminal-linked glucose residues relative to the subsurface ocean (Simon et al. 2002). In contrast to the consistent positive protease response between the coastal and subsurface open ocean, these results have shown for the first time that glucosidase activities are likely to vary in response to low pH between different ocean environments with variable substrate concentrations.

Bacteria preferentially remineralise protein-based substrate over carbohydrate under ambient conditions, a trend which has been reported by other researchers (Smith et al. 1992, Skoog & Benner 1997, Baltar et al. 2009). My work extends this current body of knowledge with the discovery that the preferential remineralisation of protein substrate increased under low pH relative to the ambient control in two near-surface open ocean incubations and one coastal incubation. Although dissolved nutrient concentrations were not affected by low pH, this

uncoupling of nitrogen (protein) remineralisation from carbon (glucose) could alter the concentration and availability of dissolved inorganic and organic nitrogen in different ocean environments. As phytoplankton and bacteria require dissolved inorganic nitrogen (Falkowski 2000, Liu et al. 2010), an increased turnover of proteins and amino acids in open ocean and coastal waters could lead to an increased frequency of bloom events and the early onset of nitrogen limitation. If the trend of increased protease activity also occurs in the sub-tropical and tropical waters, this may exacerbate the expansion of the oligotrophic ocean that is predicted to occur due to ocean warming (Bopp et al. 2005, Polovina et al. 2008).

7.2 Influence of elevated temperature

Ocean warming has a positive effect on biological metabolic activity (Doney et al. 2012 and references therein) which affects bacterial community carbon demand (Vázquez-Domínguez et al. 2007), bacterial community respiration (Pomeroy & Deibel 1986, Lomas et al. 2002, Vázquez-Domínguez et al. 2007, Hoppe et al. 2008), bacterial cell numbers (Li & Dickie 1987, Vázquez-Domínguez et al. 2012), community composition (Rose et al. 2009) and bacterial extracellular enzyme activity (Hollibaugh & Azam 1983, Hoppe 1983, Zeebe & Wolf-Gladrow 2001, Piontek et al. 2009, 2010). However, ocean warming also influences larger scale oceanographic properties which may affect future biogeochemical cycling. A review by Bijma et al. (2013) showed that ocean warming will increase ocean stratification, reduce the surface ocean mixed layer depth and restrict the upwelling of nutrient rich deep-water containing inorganic nitrogen and phosphorus. A reduction in surface ocean inorganic nutrients may reduce the frequency and duration of phytoplankton bloom events (Finkel et al. 2010, Bijma et al. 2013). Episodic phytoplankton blooms are important sources of organic matter into the subsurface ocean (Passow & Carlson 2012) and a future reduction in bloom events could weaken the biological carbon pump. A reduction in export of organic substrate into the ocean interior (Denman et al. 2007, Sarmiento et al. 2010, Joint et al. 2011) will have significant implications for the balance of inorganic and organic carbon in the ocean (Doney et al. 2012, Passow & Carlson 2012). Surface ocean warming may also increase the frequency of storm events in which strong surface winds temporally deepen the surface mixed layer and oxygen minimum zone in spatially localised areas (Babin et al. 2004). This wind driven surface mixing

would oxygenate the surface ocean and could deposit limiting trace nutrients for phytoplankton growth such as iron dust from terrestrial sources. This scenario may counter the effects of surface ocean stratification and increase the frequency of phytoplankton bloom events in spatially localised areas (Babin et al. 2004).

Existing research shows that phytoplankton communities have species specific sensitivities to ocean warming, with community compositions expected to change in future ocean conditions (Bopp et al. 2005, Chen et al. 2011, Huertas et al. 2011, Doney et al. 2012). Results from the near-surface open ocean incubations support this finding with *Synechococcus* spp. showing variable responses across different phytoplankton communities, and *Prochlorococcus* spp. showing no clear response (Section 4.3.2). Overall, different phytoplankton communities had different responses to elevated temperature which could have implications for inorganic carbon uptake, affecting organic matter production and its eventual flux (Engel et al. 2008, Finkel et al. 2010, Endo et al. 2013).

Each near-surface seawater incubation showed the same positive protease activity response to elevated temperature regardless of the phytoplankton composition (Table 4.3). This is consistent with that reported by Piontek et al. (2009) from Kiel Fjord (Baltic Sea) seawater, and with predictions made by Hoppe et al. (2008). Surprisingly, protease activities in the elevated temperature treatments (+3⁰C) were at least 10-times higher than those predicted by the Q₁₀ coefficient, suggesting that temperature is not the only factor influencing enzyme activity. An increase in substrate remineralisation would strengthen the microbial loop, increasing the availability of labile substrate for heterotrophic assimilation (Doney et al. 2012 and references therein). This hypothesis is supported by the increase in bacterial secondary production rates in three of the four near-surface ocean phytoplankton communities, and is consistent with other observations from coastal Mediterranean seawater (Vázquez-Domínguez et al. 2007, 2012), Chesapeake Bay seawater (Lomas et al. 2002) and Antarctic lake water (Nedwell & Rutter 1994). In two of the mixed phytoplankton communities, the increase in bacterial secondary production rates was also strongly correlated with an increase in bacterial cell numbers, indicating that bacterial abundance may increase in the surface ocean under future elevated temperatures, as reported by Vázquez-Domínguez et al. (2012). In addition, total high molecular weight protein substrate concentrations increased in two of the four near-surface open ocean incubations following considerations for bacteria and phytoplankton

cellular substrate (Table 4.9). This substrate could stimulate an extended temporal pulse of protease activity (days-weeks), providing bacteria with labile low molecular weight substrate for secondary production and further stimulating an increase in bacterial cell numbers. In contrast, elevated subsurface ocean temperatures did not have an effect on protease or glucosidase activity, bacterial secondary production rates showed a variable response, and bacterial cell numbers declined (Table 5.8). This result may signify a unique subsurface bacterial community, a different set of extracellular enzymes or lower substrate concentrations (Section 5.4).

Overall, this research shows for the first time that while bacterial extracellular enzyme activity and growth may increase in the future surface ocean, bacterial growth and abundance may decline in the subsurface ocean. This scenario would reduce labile organic matter export to the subsurface ocean, thereby influencing the vertical depth profile of substrate remineralisation. Increased nutrient recycling in surface waters and a reduction in the mid-water oxygen minimum will further impact on subsurface bacterial communities.

7.3 Influence of low pH and elevated temperature combined

The global oceans are declining in pH and warming simultaneously (Riebesell et al. 2010, IPCC 2013), so a bacterial community response examined under low pH and elevated temperature represents the most realistic scenario predicted by the end of the century. The interaction of these two factors may also result in additive, synergistic or antagonistic responses (Boyd 2011, Joint et al. 2011) over those measured when tested individually.

Existing research shows that phytoplankton community composition may change under future low pH and elevated temperature conditions (Tortell et al. 2002, Lindh et al. 2013). A significant change in community composition could indirectly affect the cycling of carbon, altering the composition, size or amount of organic carbon produced (Hellebust 1965, Williams 1975, Engel et al. 2008, Tada et al. 2011). Although determining the phytoplankton response to elevated temperature and low pH was not the primary aim of this thesis, open ocean *Synechococcus* spp. and *Prochlorococcus* spp. showed no clear response. This trend is supported by Law et al. (2012) who also failed to detect a significant *Synechococcus* spp.

response in seawater collected from the northern Tasman Sea, but contrasts culture studies by Fu et al. (2007). Elevated temperature and low pH did however affect bacterial community diversity in the near-surface and subsurface open ocean (pers. comm. Dr Els Maas, NIWA). This response is supported by Lindh et al. (2013) who recorded an increasing dominance of Betaproteobacteria, and a decline in Bacteroidetes indicating a shift in bacterial community diversity during a Baltic Sea mesocosm experiment. Different heterotrophic bacteria have varying remineralisation capabilities (Fukami et al. 1981), so a significant change in bacterial community diversity could indirectly affect high molecular weight substrate remineralisation rates, influencing the strength of the microbial loop and the vertical flux of carbon throughout the water column (Aristegui et al. 2009, Doney et al. 2012, Passow & Carlson 2012, Endo et al. 2013).

Glucosidase activity increased significantly in only one mixed phytoplankton community under elevated temperature and low pH conditions (Table 4.9), while protease activity increased in all phytoplankton communities, as well as in the subsurface open ocean (Table 5.8). Moreover, based on Leu-aminopeptidase to β -glucosidase ratios, protein-based substrate was preferential remineralised in two of the four near-surface incubations and both subsurface open ocean incubations relative to the ambient control. This variable enzyme response may indicate differences in substrate composition between different phytoplankton communities, and the characteristics of the constituent particles such as polymer length and the presence of microgels may influence the susceptibility of the substrate to coagulate in selected phytoplankton communities (Riebesell 1991, Chin et al. 1998). The near-surface ocean protease activity response was similar between the combined elevated temperature and low pH treatment and the elevated temperature treatment in three of the four phytoplankton communities, however protease activity was highest in the low pH treatment in each near-surface phytoplankton community (Table 4.3). This trend shows that changes in protease activity in the near-surface open ocean were primarily driven by low pH, however no additive or synergistic response was detected in the elevated temperature and low pH treatment. In the subsurface open ocean, an additive response was detected in protease activity. These findings show for the first time that when elevated temperature and low pH conditions are combined, they do not affect protease activity equally in the near-surface or subsurface ocean. It is not clear why an additive enzyme response was not detected in the surface ocean as enzyme activity, bacterial cell numbers and bacterial secondary production were positively affected by

elevated temperature, while no clear response was detected in the subsurface ocean. This imbalance between the two driving factors could reflect the synthesis of different extracellular proteases by surface and subsurface bacteria, depth related changes in the sensitivity of the same protease group, or indirect effects on substrate availability.

In order to conceptualise the open ocean bacterial responses in the elevated temperature and low pH treatments, a simplified model of the biological carbon pump is proposed (Fig. 7.1).

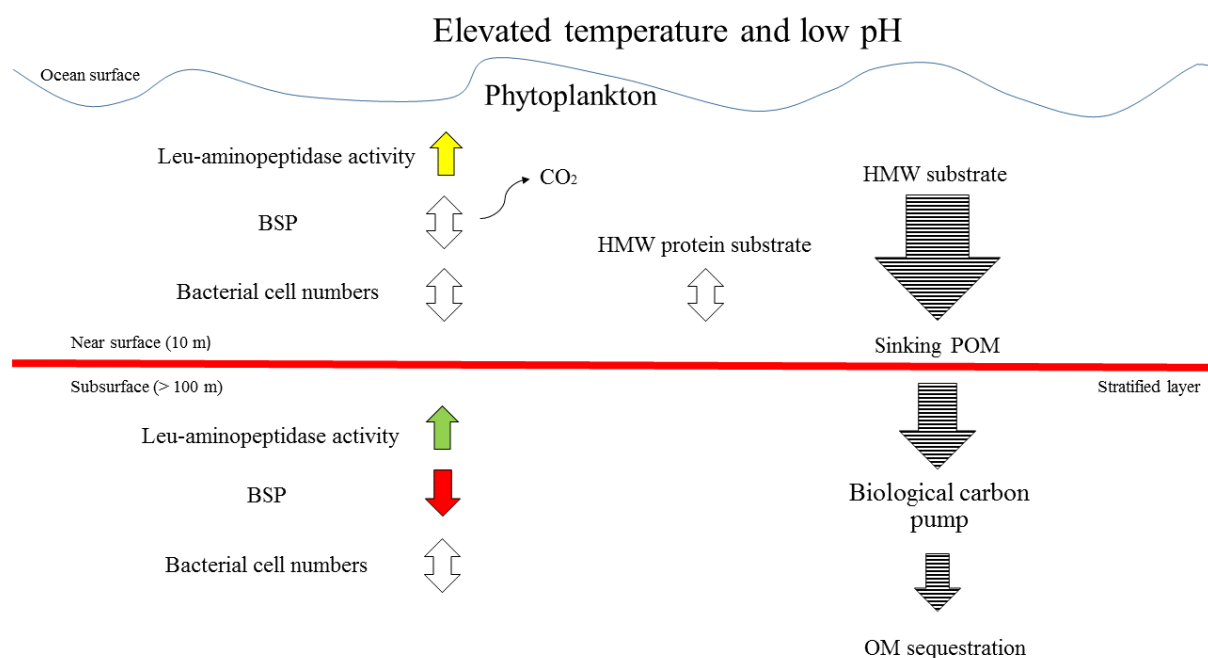


Fig. 7.1. Conceptual diagram of bacterial mediated biological processes in the near-surface and subsurface open ocean under elevated temperature and low pH conditions predicted for the end of the century. Arrows represent measured response and the orientation indicates the direction of change. Yellow: significant increase (antagonistic response relative to the ambient control, $p < 0.05$); red: significant decrease (antagonistic response relative to the ambient control); green: significant additive response (total effect is equal to the sum of the individual effects). Double headed arrows indicate the response was significantly different from the control but varied between incubations. Arrows filled with horizontal lines were not measured and reflect observations reported elsewhere. BSP: bacterial secondary production. Parameters not identified did not show a significant response

This model will be used to further discuss the implications of the measured responses and their potential effects on the flux of organic matter in a future open ocean. Existing research shows that elevated temperature and low pH will increase heterotrophic metabolic activity (Doney et al. 2012 and references therein). This thesis research showed variable responses in bacterial secondary production rates (DNA and protein synthesis) and bacterial cell numbers in different near-surface phytoplankton communities, with three of the four mixed phytoplankton communities showing an increase in DNA synthesis rates, and two of the four showing an increase in protein synthesis rates under elevated temperature and low pH conditions (Fig. 7.1). Analysis of individual treatment responses suggest that bacterial secondary production and bacterial cell numbers were primarily driven by elevated temperature and not low pH. This increase in surface ocean bacterial secondary production is consistent with the increase in protease activity and could result in an increase in metabolic respiration, potentially contributing to positive inorganic carbon feedback (Piontek et al. 2009, Wohlers et al. 2009, Borges & Gypens 2010, Fig. 7.1). In contrast, subsurface bacterial secondary production rates decreased under elevated temperature and low pH (Fig. 7.1), while bacterial cell numbers showed a variable response (Fig. 7.1). There are two potential explanations for this variation between the near-surface and subsurface ocean. Firstly, the near-surface bacterial community had a significantly different diversity to the subsurface bacterial community (pers. comm. Dr Els Maas, NIWA), and so the measured response may be bacterial species specific. Alternatively, if subsurface bacteria are closely related to deep-sea bacteria, elevated temperature and low pH may affect membrane fluidity and cellular transport mechanisms differently as deep-sea bacteria are more adapted to low temperature environments (DeLong & Yayanos 1986, Bartlett 2002); this could reduce low molecular weight substrate uptake and hence bacterial secondary production rates in the subsurface ocean.

Overall, the incubation results show that under conditions predicted for the end of the century, protease activity will increase in open ocean waters which could accelerate and strengthen the heterotrophic microbial loop (Fig. 7.1). The resulting increase in surface ocean protease activity could increase heterotrophic metabolic respiration and reduce organic matter export, weaken the biological carbon pump and diminish long-term carbon sequestration (Fig. 7.1). An increased turnover of proteins and amino acids could lead to nitrogen limitation and contribute to the development of oligotrophic waters surrounding New Zealand. This future scenario may create a positive inorganic carbon feedback that would further exacerbate

acidification of the open ocean. Moreover, experiments conducted using seawater from a naturally low pH vent environment showed that pH is not the only factor influencing bacterial extracellular enzyme activities (Chapter 6). Additional factors such as nutrient concentrations and metal ion availability will also influence bacterial processes in a future ocean. From these incubations, it was also concluded that without basic characterisation of vent biogeochemistry, naturally low pH environments are not ideal analogues for future low pH oceans.

7.4 Final statement and future research recommendations

The series of short-term perturbation incubations conducted in this thesis provide insight into an extremely complex ecosystem of interacting biological processes and communities in three distinct ocean environments surrounding New Zealand. Although an increase in protease activity was measured in response to elevated temperature and low pH conditions in each environment tested, clear variation in bacterial secondary production was detected (Fig. 7.1). To better understand the significance of this variation in a future ocean, the following research could be conducted to substantiate the findings of this thesis:

- Future research would benefit from analysing the compositional change in high molecular weight substrate throughout a perturbation incubation. Using high performance anion exchange chromatography (HPAEC) coupled with pulsed amperometric detection (PAD), Engel & Händel (2011) were able to determine neutral, amino and acidic sugar content of combined carbohydrates in high molecular weight organic matter. This technique, or similar, would provide insight into treatment effects on substrate composition and therefore possible changes in bioavailability.
- While research in this thesis focused on community response, future research might investigate changes in phytoplankton and bacterial species composition in multiple environments. Furthermore, information gained from comparative studies using different bacterial communities would provide information on possible species-specific responses, providing data for improved modelling of inorganic and organic nutrient cycling.

- Investigating how grazers and viruses influence the response of bacterial and phytoplankton communities to future ocean conditions could help explain some of the variation observed within and between different ocean environments.
- Future work focused on longer-term responses will be important to determine adaptive evolutionary change in different microbial communities. This research has indicated that bacterial processes will significantly change in the short-term under future ocean conditions, however, it is also important to determine whether this change will be maintained over months to years.
- Finally, further investigation into the significance of vent drivers (nutrients, trace metals and particles) relative to climate drivers (low pH and elevated temperature) could help explain similar trends measured in other ocean environments which experience localised changes in ocean biogeochemistry.

Bibliography

- Abdullahi A, Underwood G, Gretz M (2006) Extracellular matrix assembly in diatoms (Bacillariophyceae). Environmental effects on polysaccharide synthesis in the model diatom, *Phaeodactylum tricornutum*. J Phycol 378:363–378
- Albertson N, Nyström T, Kjelleberg S (1990) Exoprotease activity of two marine bacteria during starvation. Appl Environ Microbiol 56:218–223
- Alderkamp A, Rijssel M van, Bolhuis H (2007) Characterisation of marine bacteria and the activity of their enzyme systems involved in degradation of the algal storage glucan laminarin. FEMS Microbiol Ecol 59:108–117
- Allredge A (1998) The carbon, nitrogen and mass content of marine snow as a function of aggregate size. Deep-Sea Res I 45:529–541
- Allredge A, Passow U, Logan B (1993) The abundance and significance of a class of large, transparent organic particles in the ocean. Deep-Sea Res I 40:1131–1140
- Allers E, Gómez-Consarnau L, Pinhassi J, Gasol J, Simek K, Pernthaler J (2007) Response of *Alteromonadaceae* and *Rhodobacteriaceae* to glucose and phosphorus manipulation in marine mesocosms. Environ Microbiol 9:2417–2429
- Allgaier M, Riebesell U, Vogt M, Thyraug R, Grossart H (2008) Coupling of heterotrophic bacteria to phytoplankton bloom development at different pCO₂ levels: a mesocosm study. Biogeosciences 5:317–359
- Allison S, Martiny J (2008) Resistance, resilience, and redundancy in microbial communities. P Natl Acad Sci USA 105:11512–11519
- Alonso C, Pernthaler J (2006) Roseobacter and SAR11 dominate microbial glucose uptake in coastal North Sea waters. Environ Microbiol 8:2022–2030
- American Society for Testing & Materials (1994) Standard test method for total and organic carbon in water by high temperature oxidation and by coulometric detection. American Soc. Testing & Materials, Philadelphia
- Amon R, Benner R (1994) Rapid cycling of high molecular weight dissolved organic matter in the ocean. Nature 369:549–552
- Amon R, Benner R (1996) Bacterial utilisation of different size classes of dissolved organic matter. Limnol Oceanogr 41:41–51
- Amon R, Fitznar H, Benner R (2001) Linkages among the bioreactivity, chemical composition, and diagenetic state of marine dissolved organic matter. Limnol Oceanogr 46:287–297
- Andrews P, Williams PL (1971) Heterotrophic utilisation of dissolved organic compounds in the sea. J Mar Biol Ass UK 51:111–125
- Applebury M, Coleman J (1969) *Escherichia coli* alkaline phosphatase: Metal binding, protein conformation, and quaternary structure. J Biol Chem 244:308–318

- Arístegui J, Gasol J, Duarte C, Herndl G (2009) Microbial oceanography of the dark ocean's pelagic realm. *Limnol Oceanogr* 54:1501–1529
- Arnosti C (2003) Microbial extracellular enzymes and their role in dissolved organic matter cycling. In: Findlay S, Sinsabaugh R (eds) *Aquatic ecosystems: Interactivity of dissolved organic matter*. Academic Press, p 315–342
- Arnosti C (2011) Microbial extracellular enzymes and the marine carbon cycle. (CAGSJ Carlson, Ed.). *Annu Rev Mar Sci* 3:401–425
- Arnosti C, Jørgensen B (2003) High activity and low temperature optima of extracellular enzymes in Arctic sediments: implications for carbon cycling by heterotrophic microbial communities. *Mar Ecol Prog Ser* 249:15–24
- Arnosti C, Jørgensen B, Sagemann J, Thamdrup B (1998) Temperature dependence of microbial degradation of organic matter in marine sediments: polysaccharide hydrolysis, oxygen consumption, and sulfate reduction. *Mar Ecol Prog Ser* 165:59–70
- Arnosti C, Grossart H, Mühling M, Joint I, Passow U (2011) Dynamics of extracellular enzyme activities in seawater under changed atmospheric pCO₂: a mesocosm investigation. *Aquat Microb Ecol* 64:285–298
- Arrieta J, Herndl G (2002) Changes in bacterial β -glucosidase diversity during a coastal phytoplankton bloom. *Limnol Oceanogr* 47:594–599
- Arrigo K (2007) Carbon cycle: marine manipulations. *Nature* 450:491–492
- Arruda Fatibello S, Henriques Vieira A, Fatibello-Filho O (2004) A rapid spectrophotometric method for the determination of transparent exopolymer particles (TEP) in freshwater. *Talanta* 62:81–85
- Azam F, Hodson R (1977) Size distribution and activity of marine microheterotrophs. *Limnol Oceanogr* 22:492–501
- Azam F, Fenché T, Field J, Gray J, Meyer-Reil L, Thingstad F (1983) The ecological role of water-column microbes in the sea. *Mar Ecol Prog Ser* 10:257–263
- Azam F, Ammerman W (1984) Cycling of organic matter by bacterioplankton in pelagic marine ecosystems: microenvironmental considerations. In: Fasham MJR (ed) *Microenvironmental considerations, flows of energy and materials in marine ecosystems*. Plenum Publishing Company, New York, p 345–360
- Azam F, Cho B (1987) Bacterial utilisation of organic matter in the sea. *Symp Soci Gen Microb* 41:261–281
- Azam F, Smith D, Steward G, Hagstrom A (1994) Bacteria-organic matter coupling and its significance for oceanic carbon cycling. *Microb Ecol* 28:167–179
- Azam F (1998) Microbial control of oceanic carbon flux: the plot thickens. *Science* 280:694–696

- Azam F, Malfatti F (2007) Microbial structuring of marine ecosystems. *Nat Rev Microb* 5:782–791
- Babin S, Carton J, Dickey T, Wiggert J (2004) Satellite evidence of hurricane-induced phytoplankton blooms in an oceanic desert. *J Geophys Res* 109:1–21
- Baines S, Pace M (1991) The production of dissolved organic matter by phytoplankton and its importance to bacteria: patterns across marine and fresh water systems. *Limnol Oceanogr* 36:1078–1090
- Baltar F, Arístegui J, Sintes E, Aken H van, Gasol J, Herndl G (2009) Prokaryotic extracellular enzymatic activity in relation to biomass production and respiration in the meso-and bathypelagic waters of the (sub) tropical Atlantic. *Environ Microbiol* 11:1998–2014
- Baltar F, Arístegui J, Gasol J, Sintes E, Aken H van, Herndl G (2010) High dissolved extracellular enzymatic activity in the deep central Atlantic Ocean. *Aquat Microb Ecol* 58:287–302
- Bayona J, Monjonell A, Miquel J (2002) Biogeochemical characterisation of particulate organic matter from a coastal hydrothermal vent zone in the Aegean Sea. *Org Geochem* 33:1609–1620
- Beguin P (1990) Molecular biology of cellulose degradation. *Annu Rev Microbiol* 44:219–248
- Bell W, Mitchell R (1972) Chemotactic and growth responses of marine bacteria to algal extracellular products. *Biol Bull* 143:265–277
- Benner R, Pakulski J, McCarthy M, Hedges JI, Hatcher PG (1992) Bulk chemical characteristics of dissolved organic matter in the ocean. *Science* 255:1561–1564
- Benner R, Biddanda B, Black B, McCarthy M (1997) Abundance, size distribution, and stable carbon and nitrogen isotopic compositions of marine organic matter isolated by tangential-flow ultrafiltration. *Mar Chem* 57:243–263
- Benner R (2002) Chemical composition and reactivity. In: Hansell D, Carlson C (eds) *Biogeochemistry of marine dissolved organic matter*. Academic Press, p 59–91
- Ben-Yaakov S, Kaplan I (1968) pH-temperature profiles in ocean and lakes using an *in situ* probe. *Limnol Oceanogr* 670:688–693
- Berg J, Tymoczko J, Stryer L (2002) The biosynthesis of amino acids. In: *Biochemistry*, 6th ed., p 697–698
- Bhaskar PV, Bhosle NB (2005) Microbial extracellular polymeric substances in marine biogeochemical processes. *Curr Sci* 88:45–53
- Bianchi T (2011) The role of terrestrially derived organic carbon in the coastal ocean: A changing paradigm and the priming effect. *Proc Natl Acad Sci USA* 108:19473–19481
- Bijma J, Pörtner H-O, Yesson C, Rogers A (2013) Climate change and the oceans-What does the future hold? *Mar Pollut Bull* 74:495–505

- Billen G, Joiris C, Wijnant J, Gillain G (1980) Concentration and microbiological utilisation of small organic molecules in the Scheldt estuary, the Belgian coastal zone of the North Sea and the English Channel. *Estuar Coast Shelf Sci* 11:279–294
- Bindoff N, Willebrand J, Artale V, Cazenave A, Gregory J, Gulev S, Hanawa K, Quéré C Le, Levitus S, Nojiri Y, Shum C, Talley L, Unnikrishnan A (2007) Observations: oceanic climate change and sea level. In: Labeyrie L and Wratt D (eds). Cambridge University Press, Cambridge, United Kingdom and New York, USA
- Bird D, Kalff J (1984) Empirical relationships between bacterial abundance and chlorophyll concentration in fresh and marine waters. *Can J Fish Aquat Sci* 41:1015–1023
- Boetius A (1995) Microbial hydrolytic enzyme activities in deep-sea sediments. *Helgolander Meeresunters* 49:177–187
- Bogra P, Singh J, Singh H (2009) Purification and characterisation of aminopeptidase B from goat brain. *Process Biochem* 44:776–780
- Bopp L, Monfray P, Aumont O, Dufresne J, Treut H Le, Madec G, Terray L, Orr J (2001) Potential impact of climate change on marine export production. *Glob Biogeochem Cy* 15:81–99
- Bopp L, Aumont O, Cadule P, Alvain S, Gehlen M (2005) Response of diatoms distribution to global warming and potential implications: A global model study. *Geophys Res Lett* 32: 1–4
- Borch N, Kirchman D (1997) Concentration and composition of dissolved combined neutral sugars (polysaccharides) in seawater determined by HPLC-PAD. *Mar Chem* 57:85–95
- Botz R, Wehner H, Schmitt M, Worthington T, Schmidt M, Stoffers P (2002) Thermogenic hydrocarbons from the offshore Calypso hydrothermal field, Bay of Plenty, New Zealand. *Chem Geol* 186:235–248
- Bowler C, Karl D, Colwell R (2009) Microbial oceanography in a sea of opportunity. *Nature* 459:180–184
- Boyd PW (2011) Beyond ocean acidification. *Nat Geosci* 4:273–274
- Brewer PG (2009) A changing ocean seen with clarity. *P Natl Acad Sci USA* 106:12213–12214
- Brown S, Kelly R (1993) Characterisation of amylolytic enzymes, having both α -1,4 and α -1,6 hydrolytic activity, from the Thermophilic Archaea *Pyrococcus furiosus* and *Thermococcus litoralis*. *Appl Environ Microbiol* 59:2614–2621
- Brown J, Gillooly J, Allen A, Savage V, West G (2004) Toward a metabolic theory of ecology. *Ecology* 85:1771–1789
- Buck K, Barry J, Simpson A (2000) Monterey Bay cold seep biota: Euglenozoa with chemoautotrophic bacterial epibionts. *Eur J Protistol* 36:117–126
- Burley S, David P, Taylor A, Lipscomb W (1990) Molecular structure of leucine aminopeptidase at 2.7-Å resolution. *Proc Natl Acad Sci USA* 87:6878–6882

- Button D, Robertson B (1989) Kinetics of bacterial processes in natural aquatic systems based on biomass as determined by high-resolution flow cytometry. *Cytometry* 10:558–563
- Calosi P, Rastrick S, Lombardi C, Guzman H, Davidson L, Jahnke M, Giangrande A, Hardege J, Schulze A, Spicer J, Gambi M (2013) Adaptation and acclimatisation to ocean acidification in marine ectotherms: an *in situ* transplant experiment with polychaetes at a shallow CO₂ vent system. *Phil Trans R Soc B* 368:1–15
- Campbell N, Reece J (2005) Biology. In: Wilbur B (eds), 7th edi. Benjamin Cummings
- Carlson C, Ducklow H (1995) Dissolved organic carbon in the upper ocean of the central equatorial Pacific Ocean, 1992: Daily and finescale vertical variations. *Deep-Sea Res II* 42:639–656
- Carlson C (2002) Production and removal processes. In: Hansell DA, Carlson CA (eds) *Biogeochemistry of marine dissolved organic matter*. Elsevier Science, USA, p 91–151
- Caron D, Dam H, Kremer P, Lessard E, Madin L, Malone T, Napp J, Peele E, Roman M, Youngblut M (1995) The contribution of microorganisms to particulate carbon and nitrogen in surface waters of the Sargasso Sea near Bermuda. *Deep-Sea Res I* 42:943–972
- Chen C, Durbin E (1994) Effects of pH on the growth and carbon uptake of marine phytoplankton. *Mar Ecol Prog Ser* 109:83–94
- Chen B, Irwin A, Finkel Z (2011) Biogeographic distribution of diversity and size-structure of organic-walled dinoflagellate cysts. *Mar Ecol Prog Ser.* 425:35–45
- Cherrier J, Bauer J, Druffel E (1996) Utilisation and turnover of labile dissolved organic matter by bacterial heterotrophs in eastern North Pacific surface waters. *Mar Ecol Prog Ser* 139:267–279
- Cho B, Azam F (1988) Major role of bacteria in biogeochemical fluxes in the ocean's interior. *Nature* 332:441–443
- Cho B, Azam F (1990) Biogeochemical significance of bacterial biomass in the ocean's euphotic zone. *Mar Ecol Prog Ser* 63:253–259
- Christian J, Karl D (1992) Exocellular enzyme activities in Gerlache Strait, Antarctica. *Antarct J US* 27:170–171
- Christian J, Karl D (1995) Bacterial ectoenzymes in marine waters: Activity ratios and temperature responses in three oceanographic provinces. *Limnol Oceanogr* 40:1042–1049
- Chróst R, Faust M (1983) Organic carbon release by phytoplankton: its composition and utilisation by bacterioplankton. *J Plankton Res* 5:477–493
- Chróst R, Albrecht D, Siuda W, Overbeck J (1986) A method for determining enzymatically hydrolyzable phosphate (EHP) in natural waters. *Limnol Oceanogr* 31:662–667
- Chróst R, Overbeck J (1987) Kinetics of alkaline phosphatase activity and phosphorus availability for phytoplankton and bacterioplankton in lake plusee (North German Eutrophic Lake). *Microb Ecol* 13:229–248

- Chróst R (1989) Characterisation and significance of β -glucosidase activity in lake water. *Limnol Oceanogr* 34:660–672
- Chróst R (1990) Microbial ectoenzymes in aquatic environments. In: Overbeck J, Chróst RJ (eds) *Aquatic microbial ecology - biochemical and molecular approaches*. Springer-Verlag, New York, p 47–78
- Chróst R (1992) Significance of bacterial ectoenzymes in aquatic environments. *Hydrobiologia* 243/244:61–70
- Chróst R, Rai H (1993) Ectoenzyme activity and bacterial secondary production in nutrient-impooverished and nutrient-enriched freshwater mesocosms. *Microb Ecol* 25:131–150
- Chróst R, Siuda W (2006) Microbial production, utilisation, and enzymatic degradation of organic matter in the upper trophogenic layer in the pelagial zone of lakes along a eutrophication gradient. *Limnol Oceanogr* 51:749–762
- Church M (2008) Resource control of bacterial dynamics in the sea. In: *Microbial ecology of the oceans*. Wiley-Blackwell, p 335–382
- Cigliano M, Gambi M, Rodolfo-Metalpa R, Patti F, Hall-Spencer J (2010) Effects of ocean acidification on invertebrate settlement at volcanic CO₂ vents. *Mar Biol* 157:2489–2502
- Clarke K (1993) Non-parametric multivariate analyses of changes in community structure. *Aust J Ecol* 18:117–143
- Clarke K, Gorley N (2006) *PRIMER v6: User Manual/Tutorial*
- Cloern J (1996) Phytoplankton bloom dynamics in coastal ecosystems: a review with some general lessons from sustained investigation of San Francisco Bay, California. *Rev Geophys* 34:127–168
- Coffin R (1989) Bacterial uptake of dissolved free and combined amino acids in estuarine waters. *Limnol Oceanogr* 34:531–542
- Cohen G, Monod J (1957) Bacterial Permeases. *Bacteriol Rev* 21:169–194
- Coleman G, Brown S, Stormonm D (1975) A model for the regulation of bacterial extracellular enzyme and toxin biosynthesis. *J Theor Biol* 52:143–148
- Cullen J (1982) The deep chlorophyll maximum: comparing vertical profiles of chlorophyll *a*. *Can J Fish Aquat Sci* 39:791–803
- Cunha A, Almeida A, Coelho F, Gomes N, Oliveira V, Santos A (2010) Bacterial extracellular enzymatic activity in globally changing aquatic ecosystems. *Appl Microbiol Biot* 13:978–984
- Daniel R, Danson M (2010) A new understanding of how temperature affects the catalytic activity of enzymes. *Trends Biochem Sci* 35:584–591
- Danovaro R, Corinaldesi C, Dell’anno A, Fuhrman J, Middelburg J, Noble R, Suttle C (2010) Marine viruses and global climate change. *FEMS Microbiol Rev* 35:993–1034

- Davey K, Kirby R, Turley C, Weightman A, Fry J (2001) Depth variation of bacterial extracellular enzyme activity and population diversity in the northeastern North Atlantic Ocean. *Deep-Sea Res II* 48:1003–1017
- Davies G, Henrissat B (1995) Structures and mechanisms of glycosyl hydrolases. *Structure* 3:853–859
- Deason E (1980) Grazing of *Acartia hudsonica* (*A. clausi*) on *Skeletonema costatum* in Narragansett Bay (USA): Influence of food concentration and temperature. *Mar Biol* 60:101–113
- Decho A (1990) Microbial exopolymer secretions in ocean environments: Their role(s) in food webs and marine processes. *Ocean Mar Biol* 28:73–153
- Delcour A (2003) Solute uptake through general porins. *Front Biosci* 8:1055–1071
- Delille B, Harlay J, Zondervan I (2005) Response of primary production and calcification to changes of pCO₂ during experimental blooms of the coccolithophorid *Emiliania huxleyi*. *Global Biogeochem Cy* 19:1–37
- Denman K, Brasseur G, Chidthaisong A, Ciais P, Cox P, Dickinson R, Hauglustaine D, Heinze C, Holland E, Jacob D, Lohmann C, Ramachandran S, Silva Dias P da, Wofsy S, Zhang X (2007) Couplings between changes in the climate system and biogeochemistry. In: Solomon S, Qin D, Manning M, Chen Z, Marquis M, Averyt K.B, Tignor M and Miller H.L (eds). Cambridge University Press, Cambridge, United Kingdom and New York, NY, USA
- Descolas-Gros C, Billy Gd (1987) Temperature adaptation of RuBP carboxylase: kinetic properties in marine Antarctic diatoms. *J Exp Mar Biol Ecol* 108:147–158
- Dickson A, Sabine C, Christian J (2007) Guide to best practices for ocean CO₂ measurements
- Dixon M (1953) The effect of pH on the affinities of enzymes for substrates and inhibitors. *Biochem J* 55:161–170
- DOE (1994) Handbook of methods for the analysis of the various parameters of the carbon dioxide system in sea water. In: Dickson AG and Goyet C (eds). U.S. Department of Energy, Special Research Grant Program
- Doney S, Ruckelshaus M, Duffy J, Barry J, Chan F, English C, Galindo H, Grebmeier J, Hollowed A, Knowlton N, Polovina J, Rabalais N, Sydeman W, Talley L (2012) Climate change impacts on marine ecosystems. *Annu Rev Mar Sci* 4:11–37
- Dore J, Lukas R, Sadler D, Church M, Karl D (2009) Physical and biogeochemical modulation of ocean acidification in the central North Pacific. *P Natl Acad Sci USA* 106:12235–12240
- Du J, Xiao K, Li L, Ding X, Liu H, Lu Y, Zhou S (2013) Temporal and spatial diversity of bacterial communities in coastal waters of the South China Sea. *PLoS One* 8:1–14

- DuBois M, Gilles K, Hamilton J, Rebers P, Smith F (1956) Colorimetric method for determination of sugars and related substances. *Anal Chem* 28:350–356
- Ducklow H (2000) Bacterial production and biomass in the oceans. In: Kirchman D (ed) *Microbial ecology of the oceans*. Wiley, New York, p 1–47
- Ducklow H, Carlson C (1992) Oceanic bacterial production. *Adv Microb Ecol* 12:113–181
- Ducklow H, Steinberg D, Buesseler K (2001) Upper ocean carbon export and the biological pump. *Oceanography* 14:50–58
- Duncan A, Pantin H (1969) Evidence for submarine geothermal activity in the bay of plenty. *NZ J Mar Freshw Res* 3:602–606
- Egge J, Thingstad T, Larsen A, Engel A, Wohlers J, Bellerby R, Riebesell U (2009) Primary production during nutrient-induced blooms at elevated CO₂ concentrations. *Biogeosciences* 6:877–885
- Emerson S, Hedges J (2007) Carbonate chemistry. In: *Chemical oceanography and the marine carbon cycle*, p 103–132
- Endo H, Yoshimura T, Kataoka T, Suzuki K (2013) Effects of CO₂ and iron availability on phytoplankton and eubacterial community compositions in the northwest subarctic Pacific. *J Exp Mar Biol Ecol* 439:160–175
- Endres S, Galgani L, Riebesell U, Schulz K-G, Engel A (2014) Stimulated bacterial growth under elevated pCO₂: results from an off-shore mesocosm study. *PLoS One* 9:1–8
- Engel A (2002) Direct relationship between CO₂ uptake and transparent exopolymer particles production in natural phytoplankton. *J Plankton Res* 24:49–53
- Engel A, Delille B, Jacquet S, Riebesell U, Rochelle-Newall E, Terbruggen A, Zondervan I (2004) Transparent exopolymer particles and dissolved organic carbon production by *Emiliania huxleyi* exposed to different CO₂ concentrations: a mesocosm experiment. *Aquat Microb Ecol* 34:93–104
- Engel A, Schulz K, Riebesell U, Bellerby R, Delille B, Schartau M (2008) Effects of CO₂ on particle size distribution and phytoplankton abundance during a mesocosm bloom experiment (PeECE II). *Biogeosciences* 5:509–521
- Engel A, Händel N (2011) A novel protocol for determining the concentration and composition of sugars in particulate and in high molecular weight dissolved organic matter (HMW-DOM) in seawater. *Mar Chem.* 127:180–191
- Engel A, Händel N, Wohlers J, Lunau M, Grossart H, Sommer U, Riebesell U (2011) Effects of sea surface warming on the production and composition of dissolved organic matter during phytoplankton blooms: results from a mesocosm study. *J Plankton Res* 33:357–372
- Engel A, Piontek J, Grossart H-P, Riebesell U, Schulz K, Sperling M (2014) Impact of CO₂ enrichment on organic matter dynamics during nutrient induced coastal phytoplankton blooms. *J Plankton Res* 0:1–17

- Eppley R (1972) Temperature and phytoplankton growth in the sea. *Fish B* 70:1063–1085
- Eppley RW, Peterson BJ (1979) Particulate organic matter flux and planktonic new production in the deep ocean. *Nature* 282:677–680
- Falkowski P (2000) Rationalising elemental ratios in unicellular algae. *J Phycol* 36:3–6
- Fehling J, Davidson K, Bolch C, Brand T, Narayanaswamy B (2012) The relationship between phytoplankton distribution and water column characteristics in North West European shelf sea waters. *PLoS One* 7:1–16
- Feng Y, Hare C, Leblanc K, Rose J, Zhang Y, DiTullio G, Lee P, Wilhelm S, Rowe J, Sun J, Nemcek N, Gueguen C, Passow U, Benner I, Brown C, Hutchins D (2009) Effects of increased pCO₂ and temperature on the North Atlantic spring bloom. I. The phytoplankton community and biogeochemical response. *Mar Ecol Prog Ser* 388:13–25
- Field K, Gordon D, Wright T, Urback E, Vergin K, Giovannoni S (1997) Diversity and depth-specific distribution of SAR11 cluster rRNA genes from marine planktonic bacteria. *App Environ Microbiol* 63:63–70
- Finkel Z, Beardall J, Flynn K, Quigg A, Rees T, Raven J (2010) Phytoplankton in a changing world: cell size and elemental stoichiometry. *J Plankton Res* 32:119–137
- Form A, Riebesell U (2012) Acclimation to ocean acidification during long-term CO₂ exposure in the cold-water coral *Lophelia pertusa*. *Glob Chang Biol* 18:843–853
- Fry B, Hopkinson C, Nolin A, Jr C (1996) Long-term decomposition of DOC from experimental diatom blooms. *Limnol Oceanogr* 41:1344–1347
- Fu F, Warner M, Zhang Y, Feng Y, Hutchins D (2007) Effects of increased temperature and CO₂ on photosynthesis, growth, and elemental ratios in marine *Synechococcus* and *Prochlorococcus* (Cyanobacteria). *J Phycol* 43:485–496
- Fuhrman J, Azam F (1982) Thymidine incorporation as a measure of heterotrophic bacterioplankton production in marine surface waters: evaluation and field results. *Mar Biol* 66:109–120
- Fuhrman J, Ferguson R (1986) Nanomolar concentrations and rapid turnover of dissolved free amino acids in seawater: agreement between chemical and microbiological measurements. *Mar Ecol Prog Ser* 33:237–242
- Fukami K, Simidu U, Taga N (1981) Fluctuation of the communities of heterotrophic bacteria during the decomposition process of phytoplankton. *J Exp Mar Biol Ecol* 55:171–184
- Garcia-Viloca M, Gao J, Karplus M, Truhlar D (2004) How enzymes work: analysis by modern rate theory and computer simulations. *Science* 303:186–195
- Gasol J, Giorgio P, Duarte C (1997) Biomass distribution in marine planktonic communities. *Limnol Oceanogr* 42:1353–1363
- Gattuso J, Lavigne H (2009) Technical Note: Approaches and software tools to investigate the impact of ocean acidification. *Biogeosciences* 6:2121–2133

- Gattuso J, Hansson L (2011) Ocean acidification: background and history. In: Gattuso J, Hansson L (eds) Ocean Acidification. Oxford University Press, New York, p 1–17
- Ghiglione J, Galand P, Pommier T, Pedrós-Alió C, Maas E, Bakker K, Bertilson S, Kirchman J D, Lovejoy C, Yager P, Murray A (2012) Pole-to-pole biogeography of surface and deep marine bacterial communities. *Proc Natl Acad Sci USA* 109:17633–17638
- Giorgio P del, Cole J (1998) Bacterial growth efficiency in natural aquatic systems. *Annu Rev Ecol Syst* 29:503–541
- Giorgio P del, Condon R, Bouvier T, Longnecker K, Bouvier C, Sherr E, Gasol J (2011) Coherent patterns in bacterial growth, growth efficiency, and leucine metabolism along a northeastern Pacific inshore-offshore transect. *Limnol Oceanogr* 56:1–16
- Glasby G (1971) Direct observations of columnar scattering associated with geothermal gas bubbling in the Bay of Plenty, New Zealand. *New Zeal J Mar Fresh* 5:483–496
- Goff F, Janik C, Delgado H, Werner C, Counce D, Stimac J, Siebe C, Love S, Williams S, Fischer T, Johnson L (1998) Geochemical surveillance of magmatic volatiles at Popocatepetl Volcano, Mexico. *Geol Soc Am Bull* 110:695–710
- Gottschalk G (1985) Regulation of bacterial metabolism. In: Gottschalk G (ed) *Bacterial Metabolism*, Second edi. Springer-Verlag, New York, p 178–207
- Gould A, May B, Elliott W (1975) Release of extracellular enzymes from *Bacillus amyloliquefaciens*. *J Bacteriol* 122:34–40
- Grossart H, Allgaier M, Passow U, Riebesell U (2006) Testing the effect of CO₂ concentration on dynamics of marine heterotrophic bacterioplankton. *Limnol Oceanogr* 51:1–11
- Grossart H, Tang K, Kiorboe T, Ploug H (2007) Comparison of cell-specific activity between free-living and attached bacteria using isolates and natural assemblages. *FEMS Microbiol Lett* 266:194–200
- Gruber N, Gloor M, Fletcher Mikaloff S, Doney S, Dutkiewicz S, Follows M, Gerber M, Jacobson A, Joos F, Lindsay K, Menemenlis D, Mouchet A, Müller S, Sarmiento J, Takahashi T (2009) Oceanic sources, sinks, and transport of atmospheric CO₂. *Glob Biogeochem Cy* 23:1–21
- Haake B, Ittekkot V, Honjo S, Manganini S (1993) Amino acid, hexosamine and carbohydrate fluxes to the deep Subarctic Pacific (Station P). *Deep-Sea Res I* 40:547–560
- Haight RD, Morita RY (1966) Thermally induced leakage from *Vibrio marinus*, an obligately psychrophilic marine bacterium. *J Bacteriol* 92:1388–1393
- Hall J, Safi K, Cumming A (2004) Role of microzooplankton grazers in the subtropical and subantarctic waters to the east of New Zealand. *New Zeal J Mar Fresh* 38:91–101
- Hannah L (2011) *Climate change biology*. Elsevier Ltd
- Hansell D, Carlson C (2001) Marine dissolved organic matter and the carbon cycle. *J Oceanogr* 14:41–49

- Hansell D (2002) DOC in the global ocean carbon cycle. In: Hansell DA, Carlson CA (eds) Biogeochemistry of marine dissolved organic matter. Elsevier Science, USA, p 685–716
- Hansell D, Carlson C, Repeta D, Schlitzer R (2009) Dissolved organic matter in the ocean: A controversy stimulates new insights. *J Oceanogr* 22:202–211
- Hansell D (2013) Recalcitrant dissolved organic carbon fractions. *Annu Rev Mar Sci* 5:421–445
- Hanson R, Hanson T (1996) Methanotrophic bacteria. *Microbiol Rev* 60:439–471
- Hardy JA, Lam J, Nguyen JT, O'Brien T, Wells JA (2004) Discovery of an allosteric site in the caspases. *PNAS* 34:12461–12466
- Hartree E (1972) Determination of protein: A modification of the Lowry method that gives a linear photometric response. *Anal Biochem* 48:422–427
- Hedges J (1992) Global biogeochemical cycles: progress and problems. *Mar Chem* 39:67–93
- Hedges J, Keil R, Benner R (1997) What happens to terrestrial organic matter in the ocean? *Org Geochem* 27:195–212
- Hein M, Sand-Jensen K (1997) CO₂ increases oceanic primary production. *Nature* 388:526–527
- Hellebust J (1965) Excretion of some organic compounds by marine phytoplankton. *Limnol Oceanogr* 10:192–206
- Hendriks I, Duarte C, Alvarez M (2010) Vulnerability of marine biodiversity to ocean acidification: a meta-analysis. *Estuar Coast Shelf Sci* 86:157–164
- Hewson I, Steele J, Capone D, Fuhrman J (2006) Remarkable heterogeneity in meso- and bathypelagic bacterioplankton assemblage composition. *Limnol Oceanogr* 51:1274–1283
- Hildebrand D, Schroth M (1964) β -Glucosidase activity in phytopathogenic bacteria. *Appl Microb* 12:487–491
- Hinga K (2002) Effects of pH on coastal marine phytoplankton. *Mar Ecol Prog Ser* 238:281–300
- Hocking M, Hannington M, Percival J, Stoffers P, Schwarz-Schampera U, Ronde C de (2010) Clay alteration of volcanoclastic material in a submarine geothermal system, Bay of Plenty, New Zealand. *J Volcanol Geoth Res* 191:180–192
- Hofmann G, Smith J, Johnson K, Send U, Levin L, Micheli F, Paytan A, Price N, Peterson B, Takeshita Y, Matson P, Crook E, Kroeker K, Gambi M, Rivest E, Frieder C, Yu P, Martz T (2011) High-frequency dynamics of ocean pH: a multi-ecosystem comparison. *PLoS One* 6:1–11
- Hoffmann L, Breitbarth E, McGraw C, Law C, Currie K, Hunter K (2013) A trace-metal clean, pH-controlled incubator system for ocean acidification incubation studies. *Limnol Oceanogr* 11:53–61

- Hollibaugh J, Azam F (1983) Microbial degradation of dissolved proteins in seawater. *Limnol Oceanogr* 28:1104–1116
- Hopkinson C, Buffam I, Hobbie J, Vallino J (1998) Terrestrial inputs of organic matter to coastal ecosystems: An intercomparison of chemical characteristics and bioavailability. *Biogeochemistry* 43:211–234
- Hopkinson C, Vallino J (2005) Efficient export of carbon to the deep ocean through dissolved organic matter. *Nature* 433:142–145
- Hoppe H (1976) Determination and properties of actively metabolising heterotrophic bacteria in the sea, investigated by means of micro-autoradiography. *Mar Biol* 36:291–302
- Hoppe H (1978) Relations between active bacteria and heterotrophic potential in the sea. *Netherlands J Sea Res* 12:78–98
- Hoppe H (1983) Significance of exoenzymatic activities in the ecology of brackish water: measurements by means of methylumbelliferyl-substrates. *Mar Ecol Progr Ser* 11:299–308
- Hoppe H (1984) Relations between bacterial extracellular enzyme activities and heterotrophic substrate uptake in a brackishwater environment. In: *Colloq Int Bacteriol Mar Brest (France)*, p 119–128
- Hoppe H, Kim S, Gocke K (1988) Microbial decomposition in aquatic environments: combined process of extracellular enzyme activity and substrate uptake. *Appl Environ Microbiol* 54:784–790
- Hoppe H (1993) Use of fluorogenic model substrates for extracellular enzyme activity (EEA) measurement of bacteria. In: Kemp PF, Sherr BF, Sherr EB, Cole JJ (eds) *Handbook of methods in aquatic microbial ecology*. Lewis Publ. Boca Raton, p 423–431
- Hoppe H, Ullrich S (1999) Profiles of ectoenzymes in the Indian Ocean: phenomena of phosphatase activity in the mesopelagic zone. *Aquat Microb Ecol* 19:139–148
- Hoppe H, Arnosti C, Herndl G (2002) Ecological significance of bacterial enzymes in the marine environment. In: Burns RG, Dick RP (eds) *Enzymes in the environment: activity, ecology, and applications*. Marcel Dekker Inc, New York, p 73–107
- Hoppe H, Breithaupt P, Walther K, Koppe R, Bleck S, Sommer U, Juergens K (2008) Climate warming in winter affects the coupling between phytoplankton and bacteria during the spring bloom: a mesocosm study. *Aquat Microb Ecol* 51:105–115
- Hoppe C, Langer G, Rost B (2011) *Emiliania huxleyi* shows identical responses to elevated pCO₂ in TA and DIC manipulations. *J Exp Mar Biol Ecol* 406:54–62
- Huertas IE, Rouco M, López-Rodas V, Costas E (2011) Warming will affect phytoplankton differently: evidence through a mechanistic approach. *Proc Biol Sci/R Soc* 278:3534–3543
- Hunter K (2007) SWCO₂: computes equilibrium composition of carbon dioxide in seawater. http://neon.otago.ac.nz/research/mfc/people/keith_hunter/software/software.htm

- Hurd C, Hepburn C, Currie K, Raven J, Hunter K (2009) Testing the effects of ocean acidification on algal metabolism: considerations for experimental designs. *J Phycol* 45:1236–1251
- IGBP-IOC-SCOR (2013) Ocean Acidification summary for policymakers - third symposium on the ocean in a high CO₂ world
- Iglesias-Rodriguez M, Buitenhuis E, Raven J, Schofield O, Poulton A, Gibbs S, Halloran P, Baar HJwd (2008) Response to comment on “phytoplankton calcification in a high CO₂ world”. *Science* 322:15–16
- IPCC (2001) Climate Change 2001: The scientific basis. Contribution of working group 1 to the third assessment report of the Intergovernmental Panel on Climate Change. Intergovernmental Panel on Climate Change 2001, United Kingdom and New York, NY, USA
- IPCC (2007) Climate Change 2007 : Synthesis Report. An assessment of the Intergovernmental Panel on Climate Change
- IPCC (2013) Summary for policymakers. In: Stocker TF, Qin D, Plattner GK, Tignor M, Allen SK, Boschung J, Nauels A, Xia Y, Bex V, Midgley P (eds) Climate change 2013: The physical science basis. Contribution of working group 1 to the fifth assessment report of the intergovernmental panel on climate change, p 1–33
- Ittekkot V, Deuser W, Degens E (1984) Seasonality in the fluxes of sugars, amino acids, and amino sugars to the deep ocean: Sargasso Sea. *Deep-Sea Res I* 31:1057–1069
- Iturriaga R, Hoppe H-G (1977) Observations of heterotrophic activity on photoassimilated organic matter. *Mar Biol* 40:101–108
- Iwashita K, Todoroki K, Kimura H, Shimoi H (1998) Purification and characterisation of extracellular and cell wall bound β -glucosidase from *Aspergillus kawachii*. *Biosci Biotechnol Biochem* 62:1938–1946
- Jacobs M (1940) Some aspects of cell permeability to weak electrolytes. *Cold Spring Harb Symp Quant Biol* 8:30–39
- Jacobsen T, Azam F (1984) Role of bacteria in copepod fecal pellet decomposition: colonisation, growth rates and mineralisation. *B Mar Sci* 35:495–502
- Jensen L (1983) Phytoplankton release of extracellular organic carbon, molecular weight composition, and bacterial assimilation. *Mar Ecol Progr Ser* 11:39–48
- Jiao N, Herndl G, Hansell D, Benner R, Kattner G, Wilhelm S, Kirchman D, Weinbauer M, Luo T, Chen F, Azam F (2010) Microbial production of recalcitrant dissolved organic matter: long-term carbon storage in the global ocean. *Nat Rev Microb* 8:593–599
- Johnson V, Brownlee C, Rickaby R, Graziano M, Milazzo M, Hall-Spencer J (2013) Responses of marine benthic microalgae to elevated CO₂. *Mar Biol* 160:1813–1824

- Joint I, Karl D, Doney S, Armbrust E, Balch W, Beman M, Bowler C, Church M, Dickson A, Heidelberg J, Iglesias-Rodriguez D, Kirchman D, Kolber Z, Letelier R, Lupp C, Maberly S, Park S, Raven J, Repeta D, Riebesell U, Steward G, Tortell P, Zeebe R, Zehr J (2009) Consequences of high CO₂ and ocean acidification for microbes in the global ocean. In: Rising CO₂, ocean acidification, and their impacts on marine microbes. Hawaii, USA, p 1–23
- Joint I, Doney S, Karl D (2011) Will ocean acidification affect marine microbes? *Int Soc Microb Ecol* 5:1–7
- Jorgensen N, Kroer N, Coffin R, Yang X, Lee C (1993) Dissolved free amino acids, combined amino acids, and DNA as sources of carbon and nitrogen to marine bacteria. *Mar Ecol Prog Ser* 98:135–148
- Jumars P, Penry D, Baross J, Perry M, Frost B (1989) Closing the microbial loop: dissolved carbon pathway to heterotrophic bacteria from incomplete ingestion, digestion and absorption in animals. *Deep-Sea Res II* 36:483–495
- Kaiser M, Attrill M, Jennings S, Thomas D, Barnes D, Brierley A, Hiddink J, Kaartokallio H, Polunin N, Raffaelli D (2011) *Marine ecology: processes, systems, and impacts.*, 2nd edn. Oxford University Press
- Kamimura K, Fuse H, Takimura O, Yamaoka Y, Ohwada K, Hashimoto J (1992) Pressure-induced alteration in fatty acid composition of barotolerant deep-sea bacterium. *J Oceanogr* 48:93–104
- Kaplan A, Reinhold L (1999) CO₂ concentrating mechanisms in photosynthetic microorganisms. *Annu Rev Plant Biol* 50:539–570
- Karl D, Hebel D, Bjorkman K, Letelier R (1998) The role of dissolved organic matter release in the productivity of the oligotrophic North Pacific Ocean. *Limnol Oceanogr* 43:1270–1286
- Karner M, Rassoulzadegan F (1995) Extracellular enzyme activity: indications for high short-term variability in a coastal marine ecosystem. *Microb Ecol* 30:143–156
- Kawasaki N, Benner R (2006) Bacterial release of dissolved organic matter during cell growth and decline: Molecular origin and composition. *Limnol Oceanogr* 51:2170–2180
- Kennelly P, Krebs E (1991) Consensus sequences as substrate specificity determinants for protein kinases and protein phosphatases. *J Biol Chem* 266:15555–15558
- Kepkay P, Johnson B (1989) Coagulation on bubbles allows microbial respiration of oceanic dissolved organic-carbon. *Nature* 338:63–65
- Kim S, Hoppe H (1984) Microbial extracellular enzyme detection on agar plates by means of fluorogenic methylumbelliferyl-substrates. In: *Colloq Int Bacteriol Mar Brest (France)* 1-8:175–183

- Kim J-M, Lee K, Shin K, Yang E, Engel A, Karl D, Kim H-C (2011) Shifts in biogenic carbon flow from particulate to dissolved forms under high carbon dioxide and warm ocean conditions. *Geophys Res Lett* 38:1–5
- King G (1986) Characterisation of β -glucosidase activity in intertidal marine sediments. *Appl Environ Microbiol* 51:373–380
- Kjørboe T, Ploug H, Thygesen U (2001) Fluid motion and solute distribution around sinking aggregates I: Small-scale fluxes and heterogeneity of nutrients in the pelagic environment. *Mar Ecol Prog Ser* 211:1–13
- Kirchman D, Mitchell R (1982) Contribution of particle-bound bacteria to total microheterotrophic activity in five ponds and two marshes. *Appl Environ Microbiol* 43:200–209
- Kirchman D (2001) Measuring bacterial biomass production and growth rates from leucine incorporation in natural aquatic environments. *Method Microbiol* 30:227–237
- Kirchman D (2008) Introduction and overview. In: *Microbial ecology of the oceans*. Wiley-Blackwell, p 1–26
- Kjelleberg S, Hermansson M, Marden P (1987) The transient phase between growth and nongrowth of heterotrophic bacteria, with emphasis on the marine environment. *Annu Rev Microbiol* 41:25–49
- Krause E, Wichels A, Gimenez L, Lunau M, Schilhabel M, Gerdt G (2012) Small changes in pH have direct effects on marine bacterial community composition: A microcosm approach. *PLoS One* 7:1–12
- Kujawinski E (2011) The impact of microbial metabolism on marine dissolved organic matter. *Annu Rev Mar Sci* 3:567–599
- Laidler K, Peterman B (1979) Temperature effects in enzyme kinetics. *Method Enzym* 63:234–257
- Lancelot C, Billen G (1985) Carbon-nitrogen relationships in nutrient metabolism of coastal marine ecosystems. *Adv Aquat Microbiol* 3:263–321
- Larsson U, Hagström A (1979) Phytoplankton exudate release as an energy source for the growth of pelagic bacteria. *Mar Biol* 52:199–206
- Larsson U, Hagstrom A (1982) Fractionated phytoplankton primary production, exudate release and bacterial production in a Baltic eutrophication gradient. *Mar Biol* 67:57–70
- Law B (1980) Transport and utilisation of proteins by bacteria. In: Payne JW (ed) *Microorganisms and nitrogen sources : transport and utilisation of amino acids, peptides, proteins, and related substrates*. John Wiley & Sons Ltd, New York, p 381–409
- Law C, Breitbarth E, Hoffmann L, McGraw C, Langlois R, LaRoche J, Marriner A, Safi K (2012) No stimulation of nitrogen fixation by non-filamentous diazotrophs under elevated CO₂ in the South Pacific. *Glob Chang Biol* 18:3004–3014

- Laws E, Falkowski P, Smith Jr W, Ducklow H, McCarthy J (2000) Temperature effects on export production in the open ocean. *Glob Biogeochem Cy* 14:1231–1246
- Lebaron P, Parthuisot N, Catala P (1998) Comparison of blue nucleic acid dyes for flow cytometric enumeration of bacteria in aquatic systems. *Appl Environ Microbiol* 64:1725–1730
- Lee K, Tong L, Millero F, Sabine C, Dickson A, Goyet C, Park G-H, Wanninkhof R, Feely R, Key R (2006) Global relationships of total alkalinity with salinity and temperature in surface waters of the world's oceans. *Geophys Res Lett* 33:1–5
- Lee C, Watanabe T, Fujita Y, Asakawa S, Kimura M (2012) Heterotrophic growth of cyanobacteria and phage-mediated microbial loop in soil: Examination by stable isotope probing (SIP) method. *Soil Sci Plant Nutr* 58:161–168
- Lefevre D, Denis M, Lambert C, Miquel J (1996) Is DOC the main source of organic matter remineralisation the ocean water column? *J Mar Syst* 7:281–291
- Legendre L, Fèvre J (1995) Microbial food webs and the export of biogenic carbon in oceans. *Aquat Microb Ecol* 9:69–77
- Lenhart J, Schroeder J, Walsh B, Simmons L (2012) DNA repair and genome maintenance in *Bacillus subtilis*. *Microbiol Mol Biol Rev* 76:530–564
- Levy M, Bopp L, Karleskind P, Resplandy L, Ethe C, Pinsard F (2013) Physical pathways for carbon transfers between the surface mixed layer and the ocean interior. *Global Biogeochem Cycles* 27:1001–1012
- Li W, Dickie P (1987) Temperature characteristics of photosynthetic and heterotrophic activities: Seasonal variations in temperate microbial plankton. *Appl Environ Microbiol* 53:2282–2295
- Lindh M, Riemann L, Baltar F, Romero-Oliva C, Salomon P, Granéli E, Pinhassi J (2013) Consequences of increased temperature and acidification on bacterioplankton community composition during a mesocosm spring bloom in the Baltic Sea. *Environ Microbiol Rep* 5:252–262
- Liu W, Marsh T, Cheng H, Forney L (1997) Characterisation of microbial diversity by determining terminal restriction fragment length polymorphisms of genes encoding 16S rRNA. *Appl Environ Microbiol* 63:4516–4522
- Liu J, Curry J (2010) Accelerated warming of the Southern Ocean and its impacts on the hydrological cycle and sea ice. *P Natl Acad Sci USA* 107:14987–14992
- Liu J, Weinbauer M, Maier C, Dai M, Gattuso J (2010) Effect of ocean acidification on microbial diversity and on microbe-driven biogeochemistry and ecosystem functioning. *Aquat Microb Ecol* 61:291–305
- Lomas M, Glibert P, Shiah F, Smith E (2002) Microbial processes and temperature in Chesapeake Bay: current relationships and potential impacts of regional warming. *Glob Chang Biol* 8:51–70

- Lomas M, Steinberg D, Dickey T, Carlson C, Nelson N, Condon R, Bates N (2010) Increased ocean carbon export in the Sargasso Sea linked to climate variability is countered by its enhanced mesopelagic attenuation. *Biogeosciences* 7:57–70
- Lomas M, Hopkinson B, Losh J, Ryan D, Shi D, Xu Y, Morel F (2012) Effect of ocean acidification on cyanobacteria in the subtropical North Atlantic. *Aquat Microb Ecol* 66:211–222
- Lowry O, Rosebrough N, Farr A, Randall R (1951) Protein measurement with the Folin Phenol reagent. *J Biol Chem* 193:265–275
- Maas E, Law C, Hall J, Pickmere S, Currie K, Chang F, Voyles K, Caird D (2013) Effect of ocean acidification on bacterial abundance, activity and diversity in the Ross Sea, Antarctica. *Aquat Microb Ecol* 70:1–15
- McCall K, Huang C, Fierke C (2000) Function and mechanism of zinc metalloenzymes. *J Nutr* 130:1437–1446
- McGraw C, Cornwall C, Reid M, Currie K, Hepburn C, Boyd P, Hurd C, Hunter K (2010) An automated pH-controlled culture system for laboratory-based ocean acidification experiments. *Limnol Oceanogr* 8:686–694
- McManus M, Woodson C (2012) Plankton distribution and ocean dispersal. *J Experi Biol* 215:1008–1016
- Madigan M, Martinko J, Parker J (2000) Brock biology of microorganisms. 9th edi. Prentice-Hall, USA, p 1-991
- Mari X (2008) Does ocean acidification induce an upward flux of marine aggregates? *Biogeosciences Discuss* 5:1631–1654
- Marra J (1978) Phytoplankton photosynthetic response to vertical movement in a mixed layer. *Mar Biol* 208:203–208
- Martin J, Knauer G, Karl D, Broenkow W (1987) VERTEX: carbon cycling in the northeast Pacific. *Deep-Sea Res I* 34:267–285
- Martín-Cuadrado A-B, López-García P, Alba J-C, Moreira D, Monticelli L, Strittmatter A, Gottschalk G, Rodríguez-Valera F (2007) Metagenomics of the deep Mediterranean, a warm bathypelagic habitat. *PLoS One* 2:1–15
- Martinez J, Smith D, Steward G, Azam F (1996) Variability in ectohydrolytic enzyme activities of pelagic marine bacteria and its significance for substrate processing in the sea. *Aquat Microb Ecol* 10:223–230
- Martin-Jézéquel V, Hildebrand M, Brzezinski M (2000) Silicon metabolism in diatoms: implications for growth. *J Phycol* 36:821–840
- Matsui M, Fowler J, Walling L (2006) Leucine aminopeptidases: diversity in structure and function. *Biol Chem* 387:1535–1544

- Mayer L, Schick L, Sawyer T, Plante C, Jumars P, Self R (1995) Bioavailable amino-acids in sediments: A biomimetic, kinetics-based approach. *Limnol Oceanogr* 40:511–520
- Miller D, Agard D (1999) Enzyme specificity under dynamic control: A normal mode analysis of α -Lytic Protease. *J Mol Biol* 286:267–278
- Moran X, Sebastia M, Pedro C, Estrada M, Morán X, Sebastián M (2006) Response of Southern Ocean phytoplankton and bacterioplankton production to short-term experimental warming. *Limnol Oceanogr* 51:1791–1800
- Morel F, Price N (2003) The biogeochemical cycles of trace metals in the oceans. *Science* 300:944–947
- Morris A, Foster P (1971) The seasonal variation of dissolved organic carbon in the inshore waters of the Menai Strait in relation to primary production. *Limnol Oceanogr* 16:987–989
- Munday P, Cheal A, Dixson D (2014) Behavioural impairment in reef fishes caused by ocean acidification at CO₂ seeps. *Nat Clim Ch*, p 1–6
- Münster U (1991) Extracellular enzyme activity in eutrophic and polyhumic lakes. In: *Microbial enzymes in aquatic environments*, p 96–122
- Münster U, Chrost R (1990) Origin, composition, and microbial utilisation of dissolved organic matter. In: Overbeck J, Chrost RJ (eds) *Aquatic microbial ecology*. Springer-Verlag, New York, p 8–46
- Murray A, Arnosti C, La Rocha C De, Grossart H-P, Passow U (2007) Microbial dynamics in autotrophic and heterotrophic seawater mesocosms. II. Bacterioplankton community structure and hydrolytic enzyme activities. *Aquat Microb Ecol* 49:123–141
- Myklestad S (2000) Dissolved organic carbon from phytoplankton. In: *Marine Chemistry*, p 112–144
- Nagata T (2008) Organic matter–bacteria interactions in seawater. In: Kirchman DL (eds) *Microbial Ecology of the Oceans*. Second Edition, p 207–241
- Nagata T, Fukuda H, Fukuda R, Koike I (2000) Bacterioplankton distribution and production in deep Pacific waters: Large-scale geographic variations and possible coupling with sinking particle fluxes. *Limnol Oceanogr* 45:426–435
- Nausch M, Pollehne F, Kerstan E (1998) Extracellular enzyme activities in relation to hydrodynamics in the Pomeranian Bight (Southern Baltic Sea). *Microb Ecol* 36:251–258
- Nedwell D, Rutter M (1994) Influence of temperature on growth rate and competition between two psychrotolerant Antarctic bacteria: low temperature diminishes affinity for substrate uptake. *Appl Environ Microbiol* 60:1984–1992
- Nedwell D (1999) Effect of low temperature on microbial growth: lowered affinity for substrates limits growth at low temperature. *FEMS Microbiol Ecol* 30:101–111

- Nelson N (1944) A photometric adaptation of the Somogyi method for the determination of glucose. *J Biol Chem* 153:375–380
- Nelson N, Siegel D (2002) Chromophoric DOM in the open ocean. In: Hansell DA, Carlson CA (eds) *Biogeochemistry of marine dissolved organic matter*. Elsevier Science, USA, p 547–578
- Neu T, Lawrence J (1999) *In situ* characterisation of Extracellular Polymeric Substances (EPS) in biofilm systems. In: Wingender J, Neu TR, Flemming C (eds) *Microbial extracellular polymeric substances*. Springer-Verlag, Germany, p 21–42
- Newbold L, Oliver A, Booth T, Tiwari B, Desantis T, Maguire M, Andersen G, Gast C van der, Whiteley A (2012) The response of marine picoplankton to ocean acidification. *Environ Microbiol* 14:2293–22307
- Nikaido H, Vaara M (1985) Molecular basis of bacterial outer membrane permeability. *Microbiol Rev* 49:1–32
- Nikaido H (2003) Molecular basis of bacterial outer membrane permeability revisited. *Microbiol Mol Biol R* 67:593–656
- Ogawa H, Tanoue E (2003) Dissolved organic matter in oceanic waters. *J Oceanogr* 59:129–147
- Orr J (2011) Recent and future changes in ocean carbonate chemistry. In: Gattuso JP, Hansson L (eds) *Ocean Acidification*. Oxford University Press, New York, p 41–79
- Orsi B, Tipton K (1979) Kinetic analysis of progress curves. *Method Enzym* 63:159–183
- Osborn A, Moore E, Timmis K (2000) An evaluation of terminal-restriction fragment length polymorphism (T-RFLP) analysis for the study of microbial community structure and dynamics. *Env Microbiol* 2:39–50
- Pakulski J, Benner R (1994) Abundance and distribution of carbohydrate in the ocean. *Limnol Oceanogr* 39:930–940
- Parham J, Deng S (2000) Detection, quantification and characterisation of β -glucosaminidase activity in soil. *Soil Biol Biochem* 32:1183–1190
- Passow U, Alldredge A (1994) Distribution, size and bacterial colonisation of transparent exopolymer particles (TEP) in the ocean. *Mar Ecol Prog Ser* 113:185–198
- Passow U (2002) Transparent Exopolymer Particles (TEP) in aquatic environments. *Prog Ocean* 55:287–333
- Passow U, Christina L, Arnosti C, Grossart H-P, Murray A, Engel A (2007) Microbial dynamics in autotrophic and heterotrophic seawater mesocosms. I. Effect of phytoplankton on the microbial loop. *Aquat Microb Ecol* 49:109–121
- Passow U, Carlson C (2012) The biological pump in a high CO₂ world. *Mar Ecol Progr Ser* 470:249–271

- Pearson P, Palmer M (2000) Atmospheric carbon dioxide concentrations over the past 60 million years. *Nature* 406:695–699
- Piontek J, Händel N, Langer G, Wohlers J, Riebesell U, Engel A (2009) Effects of rising temperature on the formation and microbial degradation of marine diatom aggregates. *Aquat Microb Ecol* 54:305–318
- Piontek J, Lunau M, Händel N, Borchard C, Wurst M, Engel A (2010) Acidification increases microbial polysaccharide degradation in the ocean. *Biogeosciences* 7:1615–1624
- Piontek J, Borchard C, Sperling M, Schulz K, Riebesell U, Engel A (2013) Response of bacterioplankton activity in an Arctic fjord system to elevated pCO₂: results from a mesocosm perturbation study. *Biogeosciences* 10:297–314
- Pollock M (1962) Exoenzymes. In: Gunsalus I, Stainer R (eds) *The bacteria*. Academic Press Inc, p 121–178
- Polovina J, Howell E, Abecassis M (2008) Ocean's least productive waters are expanding. *Geophys Res Lett* 35:1–5
- Pomeroy L (1974) The ocean's food web, a changing paradigm. *Bioscience* 24:499–504
- Pomeroy L, Deibel D (1986) Temperature regulation of bacterial activity during the spring bloom in newfoundland coastal waters. *Science* 233:359–361
- Pomeroy L, Wiebe W (1988) Energetics of microbial food webs. *Hydrobiologia* 159:7–18
- Pomeroy L, Wiebe W (2001) Temperature and substrates as interactive limiting factors for marine heterotrophic bacteria. *Aquat Microb Ecol* 23:187–204
- Poretsky R, Sun S, Mou X, Moran M (2010) Transporter genes expressed by coastal bacterioplankton in response to dissolved organic carbon. *Environ Microbiol* 12:616–627
- Porzio L, Garrard S, Buia M (2013) The effect of ocean acidification on early algal colonisation stages at natural CO₂ vents. *Mar Biol* 160:2247–2259
- Post W, Peng T, Emanuel W (1990) The global carbon cycle. *Am Sci* 78:310–326
- Price P, Sowers T (2004) Temperature dependence of metabolic rates for microbial growth, maintenance, and survival. *P Natl Acad Sci USA* 101:4631–4636
- Proctor L, Fuhrman J (1990) Viral mortality of marine bacteria and cyanobacteria. *Nature* 343:60–62
- Pukate Y, Rim-Rukeh A (2008) Variability with depth of some physico-chemical and biological parameters of Atlantic Ocean water in part of the coastal area of Nigeria. *J Appl Env Manag* 12:87–91
- Raven J (1991) Physiology of inorganic C acquisition and implications for resource use efficiency by marine phytoplankton: relation to increased CO₂ and temperature. *Plant, Cell Env* 14:779–794

- Raven J, Caldeira K, Elderfield H (2005) Ocean acidification due to increasing atmospheric carbon dioxide. (PD 12/05. R Society, Ed.), Royal Soci. London
- Ray P, White D, Brock T (1971) Effect of growth temperature on the lipid composition of *Thermus aquaticus*. J Bacteriol 108:227–235
- Retamal L, Vincent W, Martineau C, Osburn C (2007) Comparison of the optical properties of dissolved organic matter in two river-influenced coastal regions of the Canadian Arctic. Estuar Coast Shelf Sci 72:261–272
- Rich J, Ducklow H, Kirchman D (1996) Concentrations and uptake of neutral monosaccharides along 140 degrees W in the equatorial Pacific: Contribution of glucose to heterotrophic bacterial activity and the DOM flux. Limnol Oceanogr 41:595–604
- Riebesell U (1991) Particle aggregation during a diatom bloom; biological aspects. Mar Ecol Progr Ser 69:281–291
- Riebesell U, Wolf-Gladrow D, Smetacek V (1993) Carbon dioxide limitation of marine phytoplankton growth rates. Nature 361:249–251
- Riebesell U (2004) Effects of CO₂ enrichment on marine phytoplankton. J Oceanogr 60:719–729
- Riebesell U, Koertzing A, Oeschies A (2009) Sensitivities of marine carbon fluxes to ocean change. P Natl Acad Sci USA 106:20602–20609
- Riebesell U, Fabry V, Hansson L, Gattuso J (2010) Guide to best practices for ocean acidification research and data reporting. In: Riebesell U, Fabry VJ, Hansson L, and Gattuso J-P (eds). European Commission, Luxembourg
- Riebesell U, Tortell P (2011) Effects of ocean acidification on pelagic organisms and ecosystems. In: Gattuso JP, Hansson L (eds) Ocean Acidification: background and history. Oxford University Press., New York, p 99–121
- Riemann L, Steward G, Azam F (2000) Dynamics of bacterial community composition and activity during a mesocosm diatom bloom. Appl Environ Microbiol 66:578–587
- Rivkin R (1991) Seasonal patterns of planktonic production in McMurdo Sound, Antarctica. Am Zool 31:5–16
- Rivkin R, Legendre L (2001) Biogenic carbon cycling in the upper ocean: effects of microbial respiration. Science 291:2398–2400
- Rochelle-Newall E, Fisher T, Fan C, Glibert P (1999) Dynamics of chromophoric dissolved organic matter and dissolved organic carbon in experimental mesocosms. Int J Remote Sens 20:627–641
- Rodolfo-Metalpa R, Lombardi C, Cocito S, Hall-Spencer J, Gambi M (2010) Effects of ocean acidification and high temperatures on the bryozoan *Myriapora truncata* at natural CO₂ vents. Mar Ecol 31:447–456

- Rogers H (1961) The dissimilation of high molecular weight substances. In: The bacteria, p 257–318
- Rolfe M, Rice J, Lucchini S, Pin C, Thompson A, Cameron A, Alston M, Stringer M, Betts R, Baranyi J, Peck M, Hinton J (2012) Lag phase is a distinct growth phase that prepares bacteria for exponential growth and involves transient metal accumulation. *J Bacteriol* 194:686–701
- Romankevich E (1984) Geochemisrty of organic matter in the ocean. Springer-Verlag, Moscow
- Rose J, Feng Y, Gobler C, Gutierrez R, Hare C, Leblanc K, Hutchins D (2009) Effects of increased pCO₂ and temperature on the North Atlantic spring bloom. II. Microzooplankton abundance and grazing. *Mar Ecol Prog Ser* 388:27–40
- Roslev P, Larsen M, Jorgensen D, Hesselsoe M (2004) Use of heterotrophic CO₂ assimilation as a measure of metabolic activity in planktonic and sessile bacteria. *J Microbiol Methods* 59:381–393
- Rosso A, Azam F (1987) Proteolytic activity in coastal oceanic waters: depth distribution and relationship to bacterial populations. *Mar Ecol Prog Ser.* 41:231–240
- Rost B, Zondervan I, Wolf-Gladrow D (2008) Sensitivity of phytoplankton to future changes in ocean carbonate chemistry: current knowledge, contradictions and research directions. *Mar Ecol Prog Ser* 373:227–237
- Roy A, Gibbons S, Schunck H, Owens S, Caporaso J, Sperling M, Nissimov J, Romac S, Bittner L, Mühling M, Riebesell U, LaRoche J, Gilbert J (2013) Ocean acidification shows negligible impacts on high-latitude bacterial community structure in coastal pelagic mesocosms. *Biogeosciences* 10:555–566
- Rudolph F, Fromm H (1979) Plotting methods for analysing enzyme rate data. *Method Enzym* 63:138–159
- Sabine C, Feely R, Gruber N, Key R, Lee K, Bullister J, Wanninkhof R, Wong C, Wallace D, Tilbrook B, Millero F, Peng T-H, Kozyr A, Ono T, Rios A (2004) The oceanic sink for anthropogenic CO₂. *Science* 305:367–371
- Saha B, Bothast R (1996) Production, purification, and characterisation of a highly glucose-tolerant novel β -glucosidase from *Candida peltata*. *Appl Environ Microbiol* 62:3165–3170
- Saijo S, Tanoue E (2004) Characterisation of particulate proteins in Pacific surface waters. *Limnol Oceanogr* 49:953–963
- Sala M, Gude H (1996) Influence of algae and crustacean zooplankton on patterns of microbial hydrolytic enzyme activities - an experimental approach. *Adv Limnol* 48:143–154
- Sarano F, Murphy R, Houghton B, Hedenquist J (1989) Preliminary observations of submarine geothermal activity in the vicinity of White Island volcano, Taupo Volcanic Zone, New Zealand. *J R Soc NZ* 19:449–459

- Sarmiento H, Montoya J, Vazquez-Dominguez E, Vaquer D, Gasol J (2010) Warming effects on marine microbial food web processes: how far can we go when it comes to predictions? *Phil Trans R Soc B* 365:2137–2149
- Saunders G (1972) The kinetics of extracellular release of soluble organic matter by plankton. *Verh Internat Verein Limnol* 18:140–146
- Schulz K, Barcelos e Ramos J, Zeebe R, Riebesell U (2009) CO₂ perturbation experiments: similarities and differences between dissolved inorganic carbon and total alkalinity manipulations. *Biogeosciences* 6:2145–2153
- Schulz K, Bellerby R, Brussaard C, Büdenbender J, Czerny J, Engel A, Fischer M, Koch-Klavnsen S, Krug S, Lischka S, Ludwig A, Meyerhöfer M, Nondal G, Silyakova A, Stühr A, Riebesell U (2013) Temporal biomass dynamics of an Arctic plankton bloom in response to increasing levels of atmospheric carbon dioxide. *Biogeosciences* 10:161–180
- Segschneider J, Bendtsen J (2013) Temperature-dependent remineralisation in a warming ocean increases surface pCO₂ through changes in marine ecosystem composition. *Global Biogeochem Cy* 27:1214–1225
- Sharp J (1977) Excretion of organic matter by marine phytoplankton: Do healthy cells do it? *Limnol Oceanogr* 22:381–399
- Sherr B, Sherr E, Fallon R (1987) Use of monodispersed, fluorescently labeled bacteria to estimate *in situ* protozoan bacterivory. *Appl Environ Microbiol* 53:958–965
- Sherr E, Sherr B (1996) Temporal offset in oceanic production and respiration processes implied by seasonal changes in atmospheric oxygen: The role of heterotrophic microbes. *Aquat Microb Ecol* 11:91–100
- Shi D, Xu Y, Morel F (2009) Effects of the pH/pCO₂ control method on medium chemistry and phytoplankton growth. *Biogeosciences* 6:1199–1207
- Shiah F, Ducklow H (1997) Bacterioplankton growth responses to temperature and chlorophyll variations in estuaries measured by thymidine:leucine incorporation ratio. *Aquat Microb Ecol* 13:151–159
- Simon M, Azam F (1989) Protein content and protein synthesis rates of planktonic marine bacteria. *Mar Ecol Prog Ser* 51:201–213
- Simon M, Grossart H, Schweitzer B, Ploug H (2002) Microbial ecology of organic aggregates in aquatic ecosystems. *Aquat Microb Ecol* 28:175–211
- Siu N, Apple J, Moyer C (2014) The effects of ocean acidity and elevated temperature on bacterioplankton community structure and metabolism. *Open J Ecol* 4:434–455
- Skoog A, Benner R (1997) Aldoses in various size fractions of marine organic matter: Implications for carbon cycling. *Limnol Oceanogr* 42:1803–1813
- Smayda T (1969) Some measurements of the sinking rate of fecal pellets. *Limnol Oceanogr* 14:621–625

- Smith D, Azam F (1992) A simple, economical method for measuring bacterial protein synthesis rates in seawater using ^3H -leucine. *Mar Microb Food Webs* 6:107–114
- Smith D, Simon M, Alldredge A, Azam F (1992) Intense hydrolytic enzyme activity on marine aggregates and implications for rapid particle dissolution. *Nature* 359:139–142
- Smith E, Spackman D (1955) Leucine aminopeptidase V. Activation, specificity, and mechanism of action. *J Biol Chem* 212:271–299
- Smith R, Hall J (1997) Bacterial abundance and production in different water masses around South Island, New Zealand. *NZ J Mar Freshw Res* 31:515–524
- Somville M (1984) Measurement and study of substrate specificity of exoglucosidase activity in eutrophic water. *Appl Env Microbiol* 48:1181–1185
- Somogyi M (1926) Notes on sugar determination. *J Biol Chem* 70:599–612
- Somogyi M (1952) Notes on sugar determination. *J Biol Chem* 195:19–23
- Sorokin Y, Sorokin P, Zakuskina O (1998) Microplankton and its functional activity in zones of shallow hydrotherms in the Western Pacific. *J Plankt Res* 20:1015–1031
- Steele J (1974) The structure of marine ecosystems. Harvard University Press, Cambridge, Massachusetts, p 128
- Stewart R (2008) Introduction to physical oceanography. Texas A & M University, p 313
- Stoffers P, Hannington M, Wright I, Herzig P, Ronde C (1999) Elemental mercury at submarine hydrothermal vents in the Bay of Plenty, Taupo Volcanic Zone, New Zealand. *Geology* 27:931–934
- Straube W, Deming J, Somerville C, Colwell R, Baross J (1990) Particulate DNA in smoker fluids: evidence for existence of microbial populations in hot hydrothermal systems. *Appl Environ Microbiol* 56:1440–1447
- Strickland J, Parsons T (1968) A practical manual of sea water analysis., 167th edi. Fish Res Board Can Bull
- Stumm W, Morgan J (1981) Aquatic chemistry an introduction emphasising chemical equilibria in natural waters., 2nd edn. John Wiley & Sons, Inc
- Sutherland I (1972) Bacterial exopolysaccharides. In: Rose AH, Tempest DW (eds) *Advances in microbial physiology*. Academic Press, London; New York, p 143–213
- Suttle C (2007) Marine viruses - major players in the global ecosystem. *Nat Rev Microb* 5:801–812
- Suzuki Y, Kishigami T, Abe S (1976) Production of extracellular α -glucosidase by a thermophilic *Bacillus* species. *Appl Environ Microbiol* 31:807–812
- Suzuki Y, Carini M, Butterfield D (2010) Protein carbonylation. *Antioxid Redox Signal* 12:323–325

- Sverdrup H, Johnson M, Fleming R (1942a) Phytoplankton in relation to physical-chemical properties of the environment. In: *The oceans their physics, chemistry, and general biology*. Prentice-Hall, Inc., New York, p 762–798
- Sverdrup H, Johnson M, Fleming R (1942b) Organisms and the composition of sea water. In: *The oceans their physics, chemistry, and general biology*. Prentice-Hall, Inc., New York, p 228–266
- Sverdrup H, Johnson M, Fleming R (1942c) Marine bacteria and their role in the biological and chemical cycles in the sea. In: *The oceans their physics, chemistry, and general biology*. Prentice-Hall, Inc., New York, p 879–924
- Tada Y, Taniguchi A, Nagao I, Miki T, Uematsu M, Tsuda A, Hamasaki K (2011) Differing growth responses of major phylogenetic groups of marine bacteria to natural phytoplankton blooms in the Western North Pacific Ocean. *Appl Environ Microbiol* 77:4055–4065
- Takata N, Hamamoto T, Horikoshi K (1995) Low-temperature active lipase of deep-sea psychrophilic bacteria and effect of hydrostatic pressure on enzyme activity. *Jamstec* 31:87–92
- Takeuchi K, Fujioka Y, Kawasaki Y, Shirayama Y (1997) Impacts of high concentration of CO₂ on marine organisms; a modification of CO₂ ocean sequestration. *Energy Convers Mgmt* 38:337–341
- Tamburini C, Garcin J, Ragot M, Bianchi A (2002) Biopolymer hydrolysis and bacterial production under ambient hydrostatic pressure through a 2000 m water column in the NW Mediterranean. *Deep-Sea Res II* 49:2109–2123
- Tamburini C, Garcin J, Bianchi A (2003) Role of deep-sea bacteria in organic matter mineralisation and adaptation to hydrostatic pressure conditions in the NW Mediterranean Sea. *Aquat Microb Ecol* 32:209–218
- Tanoue E, Nishiyama S, Kamo M, Tsugita A (1995) Bacterial membranes: possible source of a major dissolved protein in seawater. *Geochim Cosmochim Acta* 59:2643–2648
- Tanoue E (1996) Characterisation of the particulate protein in Pacific surface waters. *J Mar Res* 54:967–990
- Tarasov V (2006) Effects of shallow-water hydrothermal venting on biological communities of coastal marine ecosystems of the western Pacific. *Adv Mar Biol* 50:267–421
- Taylor G (1995) Microbial degradation of sorbed and dissolved protein in seawater. *Limnol Oceanogr* 40:875–885
- Teira E, Fernández A, Álvarez-Salgado X, García-Martín E, Serret P, Sobrino C (2012) Response of two marine bacterial isolates to high CO₂ concentration. *Mar Ecol Prog Ser* 36:27–36
- Thermo-FisherScientific (2010) Thermo Scientific Pierce protein assay technical handbook

- Thingstad T, Martinussen I (1991) Are bacteria active in the cold pelagic ecosystem of the Barents Sea? *Polar Res* 10:255–266
- Thrush S, Hewitt J, Cummings V, Ellis J, Hatton C, Lohrer A, Norkko A (2004) Muddy waters: elevating sediment input to coastal and estuarine habitats. *Front Ecol Env* 2:299–306
- Thornton D (2014) Dissolved organic matter (DOM) release by phytoplankton in the contemporary and future ocean. *Eur J Phycol* 49:20–46
- Tibbles B (1996) Effects of temperature on the incorporation of leucine and thymidine by bacterioplankton and bacterial isolates. *Aquat Microb Ecol* 11:239–250
- Tipton K, Dixon H (1979) Effects of pH on enzymes. In: *Enzyme kinetics and mechanism, Part A: Initial rate and inhibitor methods*. Academic Press, New York, p 183–234
- Tortell P, DiTullio G, Sigman D, Morel F (2002) CO₂ effects on taxonomic composition and nutrient utilisation in an Equatorial Pacific phytoplankton assemblage. *Mar Ecol Prog Ser* 236:37–43
- Tortell P, Payne C, Li Y, Trimborn S, Rost B, Smith W, Riesselman C, Dunbar R, Sedwick P, DiTullio G (2008) CO₂ sensitivity of Southern Ocean phytoplankton. *Geophys Res Lett* 35:1–5
- Turner B (2010) Variation in pH optima of hydrolytic enzyme activities in tropical rain forest soils. *Appl Env Microbiol* 76:6485–6493
- Varrot A, Yip V, Li Y, Rajan S, Yang X, Anderson W, Thompson J, Withers S, Davies G (2005) NAD⁺ and metal-ion dependent hydrolysis by family 4 glycosidases: structural insight into specificity for phospho- β -D-glucosides. *J Mol Biol* 346:423–435
- Vázquez-Domínguez E, Vaqué D, Gasol J (2007) Ocean warming enhances respiration and carbon demand of coastal microbial plankton. *Glob Chang Biol* 13:1327–1334
- Vázquez-Domínguez E, Vaqué D, Gasol J (2012) Temperature effects on the heterotrophic bacteria, heterotrophic nanoflagellates, and microbial top predators of the NW Mediterranean. *Aquat Microb Ecol* 67:107–121
- Verdugo P, Alldredge A, Azam F, Kirchman D, Passow U, Santschi P (2004) The oceanic gel phase: a bridge in the DOM-POM continuum. *Mar Chem* 92:67–85
- Vetter Y, Deming J (1994) Extracellular enzyme activity in the Arctic Northeast Water polynya. *Mar Ecol Prog Ser* 114:23–34
- Volk T, Hoffert M (1985) Ocean carbon pumps: Analysis of relative strengths and efficiencies in ocean-driven atmospheric CO₂ changes. In: Sunquist ET, Broecker WS (eds) *The carbon cycle and atmospheric CO₂: natural variations archean to present*. American Geophysical Union, Washington, DC, p 99–110
- Vrba J, Nedoma J, Simex K, Seda J (1992) Microbial decomposition of polymer organic matter related to plankton development in a reservoir: activity of α -, β -glucosidase, and β -N-acetylglucosaminidase and uptake of N-acetylglucosamine. *Arch Hydrobiol* 126:193–211

- Vrba J, Callier C, Bittl T, Simek K, Bertoni R, Filandr P, Hartman P, Hejzlar J, Macek M, Nedoma J (2004) Are bacteria the major producers of extracellular glycolytic enzymes in aquatic environments? *Int Rev Hydrobiol* 89:102–117
- Waksman S, Carey C (1935) Decomposition of organic matter in sea water by bacteria I. Bacterial multiplication in stored sea water. *J Bacteriol* 29:531–543
- Wassenaar TM (2012) Marine Microbiology. In: *Bacteria: The benign, the bad, and the beautiful*, 1st edn. Wiley & Sons, Inc., p 87–94
- Weinbauer M, Chen F, Wilhelm S (2011) Virus-mediated redistribution and partitioning of carbon in the global oceans. In: *Microbial carbon pump in the ocean*, p 54–56
- Weinbauer M, Mari X, Gattuso J (2011) Effects of ocean acidification on the diversity and activity of heterotrophic marine microorganisms. In: Gattuso J, Hansson L (eds) *Ocean Acidification*. Oxford University Press, New York, p 83–95
- Weiss M, Abele U, Weckesser J, Welte W, Schiltz E, Schulz G (1991) Molecular architecture and electrostatic properties of a bacterial porin. *Science* 254:1627–1630
- Weitz J, Wilhelm S (2012) Ocean viruses and their effects on microbial communities and biogeochemical cycles. *F1000 Biol Rep* 4:1–8
- White D (1986) Quantitative physiochemical characterisation of bacterial habitats. In: Poindexter JS, Leadbetter ER (eds) *Bacteria in nature; methods and special applications in bacterial ecology*. Plenum Press, New York, p 177–203
- Whitman W, Coleman D, Wiebe W (1998) Prokaryotes: the unseen majority. *P Natl Acad Sci USA* 95:6578–6583
- Wiebe W, Sheldon W, Pomeroy L (1992) Bacterial growth in the cold: evidence for an enhanced substrate requirement. *Appl Environ Microbiol* 58:359–364
- Williams PL (1975) Biological and chemical aspects of dissolved organic material in sea water. In: *Chemical Oceanography*, p 301–363
- Williams PL (1981) Incorporation of microheterotrophic processes into the classical paradigm of the planktonic food web. *Kieler Meeresforschungen*, p 1–28
- Wingender J, Neu T, Flemming C (1999) What are bacterial extracellular polymeric substances? In: Wingender J, Neu TR, Flemming C (eds) *Microbial extracellular polymeric substances; characterisation, structure and function*. Springer-Verlag, Germany, p 1–15
- Witt V, Wild C, Anthony K, Diaz-Pulido G, Uthicke S (2011) Effects of ocean acidification on microbial community composition of, and oxygen fluxes through, biofilms from the Great Barrier Reef. *Environ Microbiol* 13:2976–2989
- Wohlers J, Engel A, Zöllner E, Breithaupt P, Jürgens K, Hoppe H, Sommer U, Riebesell U, Zöllner E, Jürgens K (2009) Changes in biogenic carbon flow in response to sea surface warming. *P Natl Acad Sci USA* 106:7067–7072

- Wohlers-Zöllner J, Breithaupt P, Walther K, Jürgens K, Riebesell U (2011) Temperature and nutrient stoichiometry interactively modulate organic matter cycling in a pelagic algal-bacterial community. *Limnol Oceanogr* 56:599–610
- Wolf-Gladrow D, Riebesell U, Burkhardt S, Bijma J (1999) Direct effects of CO₂ concentration on growth and isotopic composition of marine plankton. *Tellus* 51:461–476
- Woolf D (2001) Bubbles. In: Steele J, Thorpe S, Turekian K (eds) *Encyclopedia of Ocean Sciences*. Academic Press, p 352–357
- Wright R, Hobbie J (1966) Use of glucose and acetate by bacteria and algae in aquatic ecosystems. *Ecology* 47:447–464
- Wurl O, Min Sin T (2009) Analysis of dissolved and particulate organic carbon with the HTCO technique. In: Wurl O (ed) *Practical guidelines for the analysis of seawater*. CRC Press, p 33–48
- Wurl O, Miller L, Vagle S (2011) Production and fate of transparent exopolymer particles in the ocean. *J Geophys Res* 116:1–16
- Yague E, Estevez M (1988) Purification and characterisation of a β -glucosidase from *Evernia prunastri*. *Eur J Biochem* 175:627–632
- Yoshimura T, Nishioka J, Suzuki K, Hattori H, Kiyosawa H, Watanabe Y (2009) Impacts of elevated CO₂ on phytoplankton community composition and organic carbon dynamics in nutrient-depleted Okhotsk Sea surface waters. *Biogeosciences Discuss* 6:4143–4163
- Yoshimura T, Nishioka J, Suzuki K, Hattori H, Kiyosawa H, Watanabe Y (2010) Impacts of elevated CO₂ on organic carbon dynamics in nutrient depleted Okhotsk Sea surface waters. *J Exp Mar Biol Ecol* 395:191–198
- Yoshimura T, Suzuki K, Kiyosawa H, Ono T, Hattori H, Kuma K, Nishioka J (2013) Impacts of elevated CO₂ on particulate and dissolved organic matter production: microcosm experiments using iron-deficient plankton communities in open subarctic waters. *J Oceanogr* 69:601–618
- Zeebe R, Wolf-Gladrow D (2001) CO₂ in seawater: equilibrium, kinetics, isotopes. Halpern D (eds). Elsevier Science
- Zhou J, Mopper K, Passow U (1998) The role of surface-active carbohydrates in the formation of transparent exopolymer particles by bubble adsorption of seawater. *Limnol Oceanogr* 43:1860–1871
- Ziveri P, Passaro M, Incarbona A, Milazzo M, Rodolfo-Metalpa R, Hall-spencer J (2014) Decline in Coccolithophore diversity and impact on Coccolith Morphogenesis along a natural CO₂ gradient. *Biol Bull* 226:282–290
- Zobell C (1943) The effect of solid surfaces upon bacterial activity. *J Bacteriol* 46:39–56

Appendix A: Supplementary material

2.1. Glass fibre filter retention of reducing-sugars and proteins

As described in Section 2.6, total HMW reducing-sugar and protein samples were obtained by filtering a known sample volume through 25 mm GF/Fs (Whatman; nominal pore size 0.7 μm). Throughout this research, it was of interest to determine the physical size of the trapped substrate. To investigate this, 10 ml of reducing-sugar or protein solution of known concentration and substrate size was filtered through a 25 mm GF/F in triplicate. Both sample filter and filtrate was collected and analysed using the respective detection methodology (Section 2.6). The resulting filter retention ratios highlight the substrate size predominantly trapped on 25 mm GF/F.

During the reducing-sugar retention trial, both maltotriose, a trisaccharide (Sigma-Aldrich, 100-600 dalton), and maltotetraose, a tetrasaccharide (Pure Science, ~1231 dalton) were filtered, while the tripeptide glutathione (Sigma-Aldrich) was trailed for protein retention. Approximately 30% of the total maltotriose trisaccharide reducing-sugar detected was retained on the 25 mm GF/Fs, while the remaining 70% passed through and remained as filtrate. Similarly, approximately 25% of the detected total glutathione tripeptide protein solution was retained on the 25 mm GF/F. Following filtration of maltotetraose tetrasaccharide, a larger HMW reducing-sugar, 52.3% of the total detected substrate was retained while 47.7% was lost as filtrate. It is therefore clear that each respective methodology was able to detect three chain monomer sized substrates (trisaccharide or tripeptide).

Overall, substrate trapped on GF/Fs is likely to consist of tetrasaccharide or tetrapeptide sized substrate (> 1000 daltons), consisting of four monomeric units or larger. Importantly, as substrate accumulates on the filter and blocks filter pores, smaller di- and tri- sized particles will also become trapped and therefore contribute to the total concentration measured.

Oral presentations and posters

- Burrell T, Maas E, Teesdale-Spittle P, Cliff L. Ocean Acidification and its effect on Bacterial Extracellular Enzymes. *Poster presentation* of research proposal. 5th New Zealand Ocean Acidification workshop. 22.08.11. NIWA, Wellington
- Burrell T, Maas E, Teesdale-Spittle P, Cliff L. Ocean Acidification and its effect on Bacterial Extracellular Enzymes. *Oral presentation*. New Zealand Microbiological Society Conference. 26-29.11.12. University of Otago Dunedin
- Burrell T, Maas E, Teesdale-Spittle P, Cliff L. Ocean Acidification and its effect on Bacterial Extracellular Enzymes. *Oral presentation*. 6th New Zealand Ocean Acidification workshop. 07-08.09.13. University of Otago Dunedin
- Burrell T, Maas E, Teesdale-Spittle P, Cliff L. Bacterial extracellular enzyme activity in response to ocean pH and temperature conditions predicted at the end of the century. *Oral presentation*. VUW Post-Graduate Seminar Series. 04.10.13. Victoria University of Wellington
- Burrell T, Maas E, Teesdale-Spittle P, Cliff L. Ocean Acidification and its effect on Bacterial Extracellular Enzymes. *Poster presentation*. First EMBO Conference on Aquatic Microbial Ecology - SAME13. 08-13.09.13. Stresa, Italy
- Burrell T, Maas E, Teesdale-Spittle P, Cliff L. Bacterial extracellular enzyme activity in high-CO₂ vent waters. *Oral presentation*. 7th New Zealand Ocean Acidification workshop. 11-12.02.14. NIWA, Wellington
- Burrell T, Maas E, Teesdale-Spittle P, Cliff L. Bacterial extracellular enzyme activity in high-CO₂ vent waters. *Oral presentation*. New Zealand Microbiological Ecology Conference. 20-21.02.14. University of Auckland
- Burrell T, Maas E, Teesdale-Spittle P, Cliff L. Bacterial extracellular enzyme activity in high-CO₂ vent waters. *Oral presentation*. Center for Microbial Oceanography: Research and Education (C-MORE) Summer Course on Microbial Oceanography. 27.05.14-27.06.14. University of Hawaii at Mānoa

4.1. pH and temperature at selected sampling points in incubations 1, 2 and 3 (mean \pm SE, n=3). Treatment abbreviations – HT: high temperature; GH: greenhouse; C: control; OA: ocean acidification

Incubation	1				2				3			
pH _T	T0	24 h	84 h	144 h	T0	24 h	84 h	144 h	T0	24 h	84 h	144 h
HT	8.00	8.00	7.95	7.95	8.13	8.13	7.82	7.80	8.05	8.05	8.04	8.00
GH	7.83	7.83	7.82	7.80	7.86	7.87	7.87	7.82	7.80	7.80	7.79	7.94
C	8.01	8.01	8.00	7.99	8.13	8.13	7.94	7.94	8.08	8.08	8.07	8.04
OA	7.82	7.82	7.82	7.82	7.86	7.87	7.86	7.85	7.83	7.83	7.83	7.89
Temperature (°C)												
HT	17.0	16.2	17.0	17.8	17.6	17.5	16.5	17.9	16.5	17.5	16.8	17.6
GH	17.5	16.8	18.2	18.2	17.6	17.7	17.6	18.3	16.7	17.5	18.1	18.2
C	14.9	13.2	13.9	15.0	14.5	14.8	13.0	16.2	14.8	15.0	14.8	14.3
OA	15.1	13.8	12.4	14.8	15.8	15.6	13.6	15.5	14.6	15.1	14.7	13.4

4.1. continued. pH and temperature at selected sampling points in incubation 4 (mean \pm SE, n=3). Treatment abbreviations – HT: high temperature; GH: greenhouse; C: control; OA: ocean acidification

Incubation	4			
pH _T	T0	24 h	60 h	120 h
HT	8.16	8.16	8.16	8.18
GH	7.85	7.85	7.84	7.80
C	8.18	8.18	8.18	8.22
OA	7.89	7.89	7.88	7.88
Temperature (°C)				
HT	17.3	17.0	16.6	17.8
GH	16.8	17.5	17.0	17.9
C	13.9	14.9	12.8	14.6
OA	13.8	13.1	13.8	14.3

5.1. pH and temperature at selected sampling points in incubations 5, 6 and 7 (mean \pm SE, n=3). Treatment abbreviations – HT: high temperature; GH: greenhouse; C: control; OA: ocean acidification

Incubation	5					6					7				
pH _T	T0	24 h	48 h	72 h	96 h	T0	24 h	48 h	72 h	96 h	T0	24 h	48 h	72 h	96 h
HT	8.12	8.09	8.10	8.10	8.09	8.08	8.07	8.06	8.05	8.05	8.06	8.08	8.09	8.08	8.08
GH	7.81	7.89	7.92	7.89	7.92	7.80	7.80	7.79	7.79	7.80	7.82	7.84	7.82	7.81	7.81
C	8.12	8.12	8.12	8.12	8.11	8.09	8.08	8.07	8.06	8.06	8.05	8.08	8.09	8.09	8.08
OA	7.81	7.84	7.86	7.85	7.90	7.80	7.80	7.80	7.80	7.81	7.79	7.79	7.79	7.79	7.80
Temperature (°C)															
HT	15.8	15.5	16.0	16.8	16.0	16.4	16.2	16.5	16.1	16.5	16.4	16.3	16.5	16.1	16.7
GH	15.4	14.9	16.0	16.5	16.2	16.5	16.4	16.5	16.4	16.7	16.1	16.5	16.4	16.4	16.6
C	13.9	13.4	13.3	13.3	13.1	13.3	13.5	13.5	13.4	13.1	13.3	13.2	13.5	13.4	13.6
OA	13.5	13.3	12.9	13.3	13.3	13.4	13.4	13.5	13.5	13.2	13.1	12.9	13.2	13.4	13.5

6.1. pH and temperature at selected sampling points in incubations 8 and 9 (mean \pm SE, n=3). Treatment abbreviations – Vent: vent water; C: ambient control; Low pH: acidified ambient seawater

Incubation	8							9						
pH _T	T0	12 h	24 h	36 h	48 h	72 h	84 h	T0	12 h	24 h	36 h	48 h	72 h	84 h
Vent	7.71	7.65	7.82	7.81	7.77	7.74	7.85	7.83	7.77	7.76	7.83	7.76	7.76	7.76
C	8.03	80.5	8.11	8.09	8.11	8.07	8.08	8.03	8.03	8.02	8.10	8.01	8.01	8.04
Low pH	7.79	7.79	7.82	7.80	7.81	7.76	7.83	7.80	7.78	7.88	7.79	7.80	7.79	7.79
Temperature (°C)														
V	20.1	20.2	20.9	19.8	19.8	19.8	21.1	20.6	20.4	20.7	19.7	20.2	19.9	19.9
C	19.6	20.3	21.0	20.5	20.1	21.0	20.6	20.6	20.1	20.8	20.3	20.1	20.3	19.9
Low pH	20.1	20.1	21.26	20.2	20.7	21.2	20.8	20.2	19.9	20.9	19.8	20.2	20.4	20.0

Appendix B: Chapter 3 seawater acidification methodology statistical summary tables

3.1. Statistical comparison of average extracellular enzyme activity in each treatment when compared to the ambient control at selected sampling points during trial 1. Log(x+1) transformed potential activity. *: $p < 0.05$; **: $p < 0.01$; insignificant comparisons are not shown. Treatment abbreviations – Perm: perm-tubing; Air: airstone; Acid: acid treatment; C: ambient control

Trial 1	T0				24 h				48 h				72 h				96 h			
β -glucosidase	Perm	Air	Acid	C	Perm	Air	Acid	C	Perm	Air	Acid	C	Perm	Air	Acid	C	Perm	Air	Acid	C
Perm				**		**	**	**		**	*	*		*		*		*		
Air				**	**			**	**		*	**	*		*	**			*	*
Acid				**	**			**	*	*		**		*		**		*		
C	**	**	**		**	**	**		*	**	**		*	**	**			*		
α -glucosidase																				
Perm		**		**		**	*	*		**	**	*			*			*	**	
Air	**			**	**			**	**			**				*	*			
Acid					*			*	**			**	**			**	**			*
C	**	**			*	**	*		*	**	**			*	**				*	

3.1. continued. Statistical comparison of average extracellular enzyme activity in each treatment when compared to the ambient control at selected sampling points during trial 1. Log(x+1) transformed potential activity. *: $p < 0.05$; **: $p < 0.01$; insignificant comparisons are not shown. Treatment abbreviations – Perm: perm-tubing; Air: airstone; Acid: acid treatment; C: ambient control

Trial 1	T0				24 h				48 h				72 h				96 h			
Leu-aminopeptidase	Perm	Air	Acid	C	Perm	Air	Acid	C	Perm	Air	Acid	C	Perm	Air	Acid	C	Perm	Air	Acid	C
Perm		*		*		*				*	**	**				**				
Air	*		*		*			**	*		**	**				*			*	**
Acid		*		*				**	**	**		**				**		*		**
C	*		*			**	**		**	**	**		**	*	**		**	**	**	
Arg-aminopeptidase																				
Perm			**				*				**				**	**			**	*
Air			*				**				**				**	*			*	
Acid	**	*		*	*	**		**	**	**		**	**	**		**	**	*		**
C			*				**				**		**	*	**		*		**	

3.1. continued. Statistical comparison of average extracellular enzyme activity in each treatment when compared to the ambient control at selected sampling points during trial 2. Log(x+1) transformed potential activity. *: p < 0.05; **: p < 0.01; insignificant comparisons are not shown. Treatment abbreviations – Perm: perm-tubing; Air: airstone; Acid: acid treatment; C: ambient control

Trial 2	T0				24 h				48 h				72 h				96 h			
β-glucosidase	Perm	Air	Acid	C	Perm	Air	Acid	C	Perm	Air	Acid	C	Perm	Air	Acid	C	Perm	Air	Acid	C
Perm						*	*	*		*				*		*				
Air					*			*	*			*	*			*			**	**
Acid					*	*		*										**		
C						*	*			*			*	*				**		
α-glucosidase																				
Perm																				
Air																				
Acid																				
C																				

3.1. continued. Statistical comparison of average extracellular enzyme activity in each treatment when compared to the ambient control at selected sampling points during trial 2. Log(x+1) transformed potential activity. *: $p < 0.05$; **: $p < 0.01$; insignificant comparisons are not shown. Treatment abbreviations – Perm: perm-tubing; Air: airstone; Acid: acid treatment; C: ambient control

Trial 2	T0				24 h				48 h				72 h				96 h			
Leu-aminopeptidase	Perm	Air	Acid	C	Perm	Air	Acid	C	Perm	Air	Acid	C	Perm	Air	Acid	C	Perm	Air	Acid	C
Perm								**				*		*		*		*		**
Air				*				*					*			*	*		*	**
Acid				*												*		*		*
C		*	*		**	*			*				*	*	*		**	**	*	
Arg-aminopeptidase																				
Perm		**	*	**		*	**							*	**					
Air	**			**	*		**								*					
Acid	**			**	**	**		*				*			**	**				
C	**	**	**				*						**	*	**					

3.2. Statistical comparison of average cell numbers in each treatment when compared to the ambient control at selected sampling points during trial 1. Log(x+1) transformed potential activity. *: p < 0.05; **: p < 0.01; insignificant comparisons are not shown. Treatment abbreviations – Perm: perm-tubing; Air: airstone; Acid: acid treatment; C: ambient control

Trial 1	T0				24 h				48 h				72 h				96 h			
Bacteria	Perm	Air	Acid	C	Perm	Air	Acid	C	Perm	Air	Acid	C	Perm	Air	Acid	C	Perm	Air	Acid	C
Perm											*					*		*	*	
Air																	*			*
Acid									*								*			*
C													*					*	*	
<i>Synechococcus</i> spp.																				
Perm			*	**																
Air				*																
Acid	*																			
C	**	*																		

3.2. continued. Statistical comparison of average total eukaryotic phytoplankton numbers in each treatment when compared to the ambient control at selected sampling points during trial 1. Log(x+1) transformed potential activity. *: p < 0.05; **: p < 0.01; insignificant comparisons are not shown. Treatment abbreviations – Perm: perm-tubing; Air: airstone; Acid: acid treatment; C: ambient control

Trial 1	T0				24 h				48 h				72 h				96 h			
	Perm	Air	Acid	C	Perm	Air	Acid	C	Perm	Air	Acid	C	Perm	Air	Acid	C	Perm	Air	Acid	C
Perm			**	**		*	*				*	*		*					**	
Air			**	**	*								*		**	**			*	
Acid	**	**			*			*	*					**			**	*		*
C	**	**					*		*					**					*	

3.2. continued. Statistical comparison of average microbial cell numbers in each treatment when compared to the ambient control at selected sampling points during trial 2. Log(x+1) transformed potential activity. *: p < 0.05; **: p < 0.01; insignificant comparisons are not shown. Treatment abbreviations – Perm: perm-tubing; Air: airstone; Acid: acid treatment; C: ambient control

Trial 2	T0				24 h				48 h				72 h				96 h			
Bacteria	Perm	Air	Acid	C	Perm	Air	Acid	C	Perm	Air	Acid	C	Perm	Air	Acid	C	Perm	Air	Acid	C
Perm		*	**	**						*	**	**		**						**
Air	*							*	*				**			*				*
Acid	**								**											*
C	**					*			**					*			**	*	*	
<i>Synechococcus</i> spp.																				
Perm				*								*						**		
Air			**														**			**
Acid		**		**							*									
C	*		**						*		*							**		

3.2. continued. Statistical comparison of average total eukaryotic phytoplankton numbers in each treatment when compared to the ambient control at selected sampling points during trial 2. Log(x+1) transformed potential activity. *: p < 0.05; **: p < 0.01; insignificant comparisons are not shown. Treatment abbreviations – Perm: perm-tubing; Air: airstone; Acid: acid treatment; C: ambient control

Trial 2	T0				24 h				48 h				72 h				96 h			
	Perm	Air	Acid	C	Perm	Air	Acid	C	Perm	Air	Acid	C	Perm	Air	Acid	C	Perm	Air	Acid	C
Perm				*		**	**			**	**			**	**	**		**	*	**
Air			*	**	**		*	**	**		*	**	**				**		*	**
Acid		*			**	*		**	**	*			**			*	*	*		
C	*	**				**	*			**			**		*		**	**		

3.3. Statistical comparison of average DNA and protein synthesis rates in each treatment when compared to the ambient control at selected sampling points during trial 1. Log(x+1) transformed potential activity. *: $p < 0.05$; **: $p < 0.01$; insignificant comparisons are not shown. Treatment abbreviations – Perm: perm-tubing; Air: airstone; Acid: acid treatment; C: ambient control

Trial 1	T0				24 h				48 h				72 h				96 h			
DNA	Perm	Air	Acid	C	Perm	Air	Acid	C	Perm	Air	Acid	C	Perm	Air	Acid	C	Perm	Air	Acid	C
Perm								*			*	*						*		*
Air			*	*				*				*				*	*		**	**
Acid		*						*	*									**		
C		*			*	*	*		*	*				*			*	**		
Protein																				
Perm				**												*				*
Air				**																
Acid											*									*
C	**	**									*		*				*		*	

3.3. continued. Statistical comparison of average DNA and protein synthesis rates in each treatment when compared to the ambient control at selected sampling points during trial 2. Log(x+1) transformed potential activity. *: p < 0.05; **: p < 0.01; insignificant comparisons are not shown. Treatment abbreviations – Perm: perm-tubing; Air: airstone; Acid: acid treatment; C: ambient control

Trial 2	T0				24 h				48 h				72 h				96 h			
DNA	Perm	Air	Acid	C	Perm	Air	Acid	C	Perm	Air	Acid	C	Perm	Air	Acid	C	Perm	Air	Acid	C
Perm							*			*				*	**				*	
Air							**	**	*				*		**				*	
Acid					*	**		*					**	**		*	*	*		**
C						**	*								*				**	
Protein																				
Perm			**			**	**			**	**			**	**			**	**	
Air					**		**	*	**		*		**		*		**			
Acid	**			*	**	**		*	**	*		*	**	*			**			*
C			*			*	*				*								*	

Appendix C: Chapter 4 sampled parameter statistical summary tables

4.1. Statistical comparison of average extracellular enzyme activity in each treatment when compared to the ambient control at selected sampling points in incubations 1-3. Log(x+1) transformed potential activity. *: $p < 0.05$; **: $p < 0.01$; insignificant comparisons are not shown. Treatment abbreviations – HT: high temperature; GH: greenhouse; OA: ocean acidification

Incubation	Parameter	48 h			72 h			108 h			144 h		
		HT	GH	OA	HT	GH	OA	HT	GH	OA	HT	GH	OA
1	β -glucosidase									**			
1	α -glucosidase												
1	Leu-aminopeptidase			**			*				*	**	
1	Arg-aminopeptidase											**	**
2	β -glucosidase		**	*	*	**	**			**			
2	α -glucosidase												
2	Leu-aminopeptidase	**	*	*	**	*	**						
2	Arg-aminopeptidase		**	*		**	**						
3	β -glucosidase							**	**	*			
3	α -glucosidase							*	**				**
3	Leu-aminopeptidase	*	*	**	*	**	**	**	**	**			
3	Arg-aminopeptidase			**	**	*	**	*	*	**		*	*

4.1. continued. Statistical comparison of average extracellular enzyme activity in each treatment when compared to the ambient control at selected sampling points in incubation 4. Log(x+1) transformed potential activity. *: $p < 0.05$; **: $p < 0.01$; insignificant comparisons are not shown. Treatment abbreviations – HT: high temperature; GH: greenhouse; OA: ocean acidification

Incubation	Parameter	36 h			60 h			96 h			120 h		
		HT	GH	OA	HT	GH	OA	HT	GH	OA	HT	GH	OA
4	β -glucosidase	*	*					**	*		**		
4	α -glucosidase	*				*		**	**		**	**	
4	Leu-aminopeptidase	**	*	*				**	**		**		*
4	Arg-aminopeptidase							**					

4.2. Statistical comparison of average cell numbers in each treatment when compared to the ambient control at selected sampling points in incubations 1-3. Log(x+1) transformed data. *: $p < 0.05$; **: $p < 0.01$; insignificant comparisons are not shown; n.d: not determined; blue shaded cell: parameter not sampled. Treatment abbreviations – HT: high temperature; GH: greenhouse; OA: ocean acidification

Incubation	Parameter	48 h			72 h			108 h			144 h		
		HT	GH	OA	HT	GH	OA	HT	GH	OA	HT	GH	OA
1	Bacterial numbers				*	**	**	n.d	n.d	n.d	*	*	
1	<i>Synechococcus</i> spp. numbers				**		*				*	*	*
1	<i>Prochlorococcus</i> spp. numbers												**
1	Total eukaryotic phytoplankton numbers										*		
2	Bacterial numbers							*			*	*	
2	<i>Synechococcus</i> spp. numbers						**				*		*
2	<i>Prochlorococcus</i> spp. numbers												*
2	Total eukaryotic phytoplankton numbers										*	*	
3	Bacterial numbers				*								
3	<i>Synechococcus</i> spp. numbers				*						*		
3	<i>Prochlorococcus</i> spp. numbers												
3	Total eukaryotic phytoplankton numbers										*		

4.2. continued. Statistical comparison of average cell numbers in each treatment when compared to the ambient control at selected sampling points in incubation 4. Log(x+1) transformed data. *: $p < 0.05$; **: $p < 0.01$; insignificant comparisons are not shown; blue shaded cell: parameter not sampled. Treatment abbreviations – HT: high temperature; GH: greenhouse; OA: ocean acidification

Incubation	Parameter	36 h			60 h			96 h			120 h		
		HT	GH	OA	HT	GH	OA	HT	GH	OA	HT	GH	OA
4	Bacterial numbers	**	**	*	*	*		**	**		**	**	
4	<i>Synechococcus</i> spp. numbers										**	*	
4	<i>Prochlorococcus</i> spp. numbers												
4	Total eukaryotic phytoplankton numbers										**	**	

4.3. Statistical comparison of average DNA and protein synthesis rates in each treatment when compared to the ambient control at selected sampling points in incubations 1-3. Log(x+1) transformed data. *: $p < 0.05$; **: $p < 0.01$; insignificant comparisons are not shown; blue shaded cell: parameter not sampled. Treatment abbreviations – HT: high temperature; GH: greenhouse; OA: ocean acidification

Incubation	Parameter	36 h			72 h			108 h			144 h		
		HT	GH	OA	HT	GH	OA	HT	GH	OA	HT	GH	OA
1	DNA synthesis	*	**			**	*	*	*		*		
1	Protein synthesis						*				*		
2	DNA synthesis	**	*		*	**	*						
2	Protein synthesis				*	*	*						
3	DNA synthesis	**	*		**	**		**	**		**		**
3	Protein synthesis				**	**					*		

4.3. continued. Statistical comparison of average DNA and protein synthesis rates in each treatment when compared to the ambient control at selected sampling points in incubation 4. Log(x+1) transformed data. *: p < 0.05; **: p < 0.01; insignificant comparisons are not shown; blue shaded cell: parameter not sampled. Treatment abbreviations – HT: high temperature; GH: greenhouse; OA: ocean acidification

Incubation	Parameter	36 h			60 h			96 h			120 h		
		HT	GH	OA	HT	GH	OA	HT	GH	OA	HT	GH	OA
4	DNA synthesis	**	**		**	**			*			*	**
4	Protein synthesis										*	*	

4.4. Statistical comparison of average total high molecular weight organic compounds in each treatment when compared to the ambient control at selected sampling points in incubations 1-3. Log(x+1) transformed data. *: $p < 0.05$; **: $p < 0.01$; insignificant comparisons are not shown. Treatment abbreviations – HT: high temperature; GH: greenhouse; OA: ocean acidification

Incubation	Parameter	72 h			144 h		
		HT	GH	OA	HT	GH	OA
1	Total HMW reducing-sugar						*
1	Total HMW protein				*	**	
2	Total HMW reducing-sugar				*		
2	Total HMW protein		**	*	*		
3	Total HMW reducing-sugar				*		**
3	Total HMW protein		**	**	*		*

4.4. continued. Statistical comparison of average total high molecular weight organic compounds in each treatment when compared to the ambient control at selected sampling points in incubation 4. Log(x+1) transformed data. *: $p < 0.05$; insignificant comparisons are not shown. Treatment abbreviations – HT: high temperature; GH: greenhouse; OA: ocean acidification

Incubation	Parameter	60 h			120 h		
		HT	GH	OA	HT	GH	OA
4	Total HMW reducing-sugar				*		
4	Total HMW protein				*	*	

Appendix D: Chapter 5 sampled parameter statistical summary tables

5.1. Statistical comparison of average extracellular enzyme activity in each treatment when compared to the ambient control at selected sampling points in incubations 6 & 7. Log(x+1) transformed data. *: $p < 0.05$; **: $p < 0.01$; insignificant comparisons are not shown. Treatment abbreviations – HT: high temperature; GH: greenhouse; OA: ocean acidification

Incubation	Parameter	24 h			48 h			72 h			96 h		
		HT	GH	OA	HT	GH	OA	HT	GH	OA	HT	GH	OA
6	β -glucosidase										**		*
6	α -glucosidase												
6	Leu-aminopeptidase	*	**	**		*						*	
6	Arg-aminopeptidase					**	**		*	**			
7	β -glucosidase							*					
7	α -glucosidase						**			**			**
7	Leu-aminopeptidase		*		*								**
7	Arg-aminopeptidase						**					**	**

5.2. Statistical comparison of average cell numbers in each treatment when compared to the ambient control at selected sampling points in incubations 6 & 7. Log(x+1) transformed data. *: $p < 0.05$; **: $p < 0.01$; insignificant comparisons are not shown; blue shaded cell: parameter not sampled. Treatment abbreviations – HT: high temperature; GH: greenhouse; OA: ocean acidification

Incubation	Parameter	24 h			48 h			72 h			96 h		
		HT	GH	OA	HT	GH	OA	HT	GH	OA	HT	GH	OA
6	Bacterial numbers					**					**	**	**
6	<i>Synechococcus</i> spp. numbers											**	
6	Total eukaryotic phytoplankton numbers											*	*
7	Bacterial numbers	*				*	*						
7	<i>Synechococcus</i> spp. numbers												
7	Total eukaryotic phytoplankton numbers						*						

5.3. Statistical comparison of average DNA and protein synthesis rates in each treatment when compared to the ambient control at selected sampling points in incubations 6 & 7. Log(x+1) transformed data. *: $p < 0.05$; **: $p < 0.01$; insignificant comparisons are not shown; blue shaded cell: parameter not sampled. Treatment abbreviations – HT: high temperature; GH: greenhouse; OA: ocean acidification

Incubation	Parameter	24 h			48 h			72 h			96 h		
		HT	GH	OA	HT	GH	OA	HT	GH	OA	HT	GH	OA
6	DNA synthesis	*			*					*		**	*
6	Protein synthesis						*				**	**	**
7	DNA synthesis	*	*	**		*	**						*
7	Protein synthesis				**	*	**						**

5.4. Statistical comparison of average total high molecular weight organic compounds in each treatment when compared to the ambient control at selected sampling points in incubations 6 & 7. Log(x+1) transformed data. *: $p < 0.05$; **: $p < 0.01$; insignificant comparisons are not shown. Treatment abbreviations – HT: high temperature; GH: greenhouse; OA: ocean acidification

Incubation	Parameter	48 h			72 h			96 h		
		HT	GH	OA	HT	GH	OA	HT	GH	OA
6	Total HMW reducing-sugar									
6	Total HMW protein									
7	Total HMW reducing-sugar		**	*						
7	Total HMW protein									

Appendix E: Chapter 6 sampled parameter statistical summary tables

6.1. Statistical comparison of average extracellular enzyme activity in each treatment when compared to the ambient control at selected sampling points in incubations 8 & 9. Log(x+1) transformed data. *: $p < 0.05$; **: $p < 0.01$; insignificant comparisons are not shown

Incubation	Parameter	12 h		36 h		60 h		84 h	
		Vent	Low pH	Vent	Low pH	Vent	Low pH	Vent	Low pH
8	β -glucosidase	**	*	**	**	**	**	**	**
8	α -glucosidase	*	*	**	**	**	**	**	**
8	Leu-aminopeptidase	*	*	**	**	**	*	**	**
8	Arg-aminopeptidase	**	**	*	**		**	**	**
9	β -glucosidase	*		**	**	**	*	**	*
9	α -glucosidase	**	*	**	*	**	**	**	*
9	Leu-aminopeptidase	*	**			**		**	
9	Arg-aminopeptidase	**	**	**	*		*		

6.2. Statistical comparison of average cell numbers in each treatment when compared to the ambient control at selected sampling points in incubations 8 & 9. Log(x+1) transformed data. *: $p < 0.05$; **: $p < 0.01$; insignificant comparisons are not shown

Incubation	Parameter	12 h		36 h		60 h		84 h	
		Vent	Low pH	Vent	Low pH	Vent	Low pH	Vent	Low pH
8	Bacterial numbers	*	**	**	**	**	*	*	
8	<i>Synechococcus</i> spp. numbers	**		**		**			
8	<i>Prochlorococcus</i> spp. numbers	**		**		**			
8	Total eukaryotic phytoplankton numbers	*		**					
9	Bacterial numbers	*				*		**	
9	<i>Synechococcus</i> spp. numbers					*			
9	<i>Prochlorococcus</i> spp. numbers	**		*		*		*	
9	Total eukaryotic phytoplankton numbers	**		**		**		**	

6.3. Statistical comparison of average DNA and protein synthesis rates in each treatment when compared to the ambient control at selected sampling points in incubations 8 & 9. Log(x+1) transformed data. *: $p < 0.05$; **: $p < 0.01$; insignificant comparisons are not shown

Incubation	Parameter	12 h		36 h		60 h		84 h	
		Vent	Low pH	Vent	Low pH	Vent	Low pH	Vent	Low pH
8	DNA synthesis	*	**		*			*	
8	Protein synthesis	*		**		*		*	
9	DNA synthesis			*			**	*	
9	Protein synthesis	*		**	*	*		**	

6.4. Statistical comparison of average total high molecular weight organic compounds in each treatment when compared to the ambient control at selected sampling points in incubations 8 & 9. Log(x+1) transformed data. *: $p < 0.05$; **: $p < 0.01$; insignificant comparisons are not shown

Incubation	Parameter	12 h		36 h		60 h		72 h		84 h	
		Vent	Low pH	Vent	Low pH	Vent	Low pH	Vent	Low pH	Vent	Low pH
8	Total HMW reducing-sugar				*				**	*	**
8	Total HMW protein	*		**		*		*		*	
9	Total HMW reducing-sugar	*				*					
9	Total HMW protein			*		*		*	**	*	

6.5. Statistical comparison of average TEP and TC in each treatment when compared to the ambient control at selected sampling points in incubations 8 & 9. Log(x+1) transformed data. *: $p < 0.05$; **: $p < 0.01$; insignificant comparisons are not shown

Incubation	Parameter	36 h		84 h	
		Vent	Low pH	Vent	Low pH
8	TEP	*		**	
8	TC			*	
9	TEP		*		
9	TC				